



UNIVERSITÀ DEL PIEMONTE ORIENTALE

Department of Sciences and Technological Innovation

PhD Program in Chemistry & Biology

XXXIII Cycle (2018-2021)

Evaluation of Contaminants of Emerging Concern and Their Transformation Products in Water

Ph.D. Thesis

SSD: CHIM/01

Candidate: Masho Hilawie Belay

Tutor: Prof. Elisa Robotti

PhD Program Coordinator: Prof. Gian Cesare Tron

February 2022





UNIVERSITÀ DEL PIEMONTE ORIENTALE

Department of Sciences and Technological Innovation

PhD Program in Chemistry & Biology

XXXIII Cycle (2018-2021)

Evaluation of Contaminants of Emerging Concern and Their Transformation Products in Water

Ph.D. Thesis

SSD: CHIM/01

Candidate:

Masho Hilawie Belay

Signature..... MASHO HILAWIE

Tutor:

Prof. Elisa Robotti

Signature.....





UNIVERSITÀ DEL PIEMONTE ORIENTALE
DOTTORATO DI RICERCA
IN CHEMISTRY & BIOLOGY

Via Duomo, 6
13100 – Vercelli (ITALY)

DECLARATION AND AUTHORISATION TO ANTIPLAGIARISM DETECTION


The undersignedMasho Hilawie Belay.....student of the Chemistry & Biology
Ph.D. course (XXXIII...Cycle)

declares:

- to be aware that the University has adopted a web-based service to detect plagiarism through a software system called “Turnit.in”,
- his/her Ph.D. thesis was submitted to Turnit.in scan and reasonably it resulted an original document, which correctly cites the literature.

acknowledges:

- his/her Ph.D. thesis can be verified by his/her Ph.D. tutor and/or Ph.D Coordinator in order to confirm its originality.

Date:02/01/2022..... Signature:  MASHO HILAWIE.....

ACKNOWLEDGEMENTS

My heartfelt gratitude goes to my supervisor, Prof. Elisa Robotti, for guiding me through this PhD with her insight and subject expertise. I thank Dr. Fabio Gosetti (currently at the University of Milano-Bicocca, Milan, Italy) for his advice and assistance throughout the first year of my PhD. I also thank Prof. Emilio Marengo for making himself available to me whenever I needed assistance. Thank you to everyone at the Department of Chemistry of the University of Piemonte Orientale. In addition, I would like to thank Dr. Marcello Manfredi and Dr. Sara Timo for coordinating and collaborating on the sample analysis for non-target screening and robustness studies at ISALIT in Novara, Italy.

This PhD Thesis would not have been realized without the financing of the AQUALity project (funded by the European Union under the Marie Skłodowska-Curie Actions – Innovative Training Networks, call: H2020-MSCA-ITN-2017, project N° 765860). Working within the framework of this project has allowed me to realize one of my greatest ambitions, which is to conduct high-quality research in collaboration with other Early Stage Researchers and scientists in an interdisciplinary program. Furthermore, I attended (in presence or remotely) several international conferences and secondments. I would like to thank everyone involved in the project for making this possible. Special thanks to the Early-Stage Researchers Nuno, Cristina, Zsuzsanna, Dimitra, Alice, Bethel, Ivan, Davide, and Ilaria, with whom I have had the privilege of establishing strong friendships and sharing wonderful experiences.

One of the most valuable experiences I developed while pursuing this PhD is working with a diverse group of scholars, especially during my secondments in Turkey, Greece, Denmark, and Italy. I would like to thank the people listed below for their assistance, in one way or another, in completing my secondment research: Prof. Emin Backasiz and Dr. Ilknur Altin from the Karadeniz Technical University, Trabzon, Turkey; Dr. Peter Mortensen, Dr. Ulrich Precht, Pia Nielsen, and Jorgen Andersen from Eurofins Environment Denmark A/S, Vejen, Denmark; Dr. Vasilis Sakkas from the University of Ioannina; Prof. Claudio Medana, Dr. Federica Dal Bello, Alberto Asteggiano, and Enrica Mecarelli from the University of Turin, Turin, Italy.

There have been multiple challenging periods throughout this PhD, but the most significant ones were the disruptions caused by the COVID-19 pandemic and the civil war in Tigray (Ethiopia). My mother and father would have been overjoyed to learn that I am completing this PhD; however, all communication tools have been blocked for more than 16 months, and there is no way they would know. I would like to dedicate my thesis to my mother, my father, my wife, and all my friends and colleagues who have supported me directly or indirectly throughout these tough times.

ABSTRACT

Most of the products that we see or use today have been touched by or involved in a chemical process at some point in time. When we think about it, chemicals have grown more pervasive in our daily lives than ever before. Many people find it hard to think of a home free of plastics, furniture that doesn't have flame-retardants in it, health care that doesn't use pharmaceuticals, and beauty care devoid of cosmetics. These chemicals, together with others, form a group of environmental contaminants often called emerging contaminants of concern (CECs). Their existence in the environment may be harmful to both the ecosystem and humans if they get into the food chain, for example, or if they enter the environment through other ways. As a result, there has been a growing concern and scientific interest in the occurrence, fate, and effects of CECs in the environment in recent years.

In recent decades, pharmaceutical compounds have emerged as a significant new group of CECs. Due to their inefficient removal by conventional wastewater treatment plants (WWTPs), a significant amount of these drugs enters the aquatic environment via municipal sewage systems. Pharmaceutical substances are intended to produce specific effects in the human body, but the effects of many of these substances on other creatures in the environment, as well as their indirect effect on human health, remain largely unknown. Additionally, pharmaceuticals may generate transformation products (TPs) that are potentially more hazardous than the parent drugs. Despite the recent consumption trend, which is projected to continue in the future due to rising incidence of health issues requiring pharmaceutical treatment, little is known about the occurrence and fate of many pharmaceutical compounds in the aquatic environment. Anticancer, antidepressant, and antihypertensive compounds are among the drugs for which there is a considerable lack of data concerning their environmental occurrence and fate. With advances in analytical instrumentation, it is now possible to identify and quantify the occurrence and risk of these substances at extremely low levels. As a result, it is vital to develop rapid, robust, and economical multiresidue methods in order to identify these compounds and their TPs in various aqueous compartments. In this thesis, four works are presented to evaluate the occurrence and fate of pharmaceuticals in different water matrices by exploiting the potential of targeted, semi-targeted, and non-target screening workflows.

Photodegradation is an important factor in the environmental fate of pharmaceutical compounds, as it can result in the formation of a spectrum of unknown TPs. We studied the photodegradation of two drugs (irinotecan and aliskiren) in water. Both drugs are extensively used medications, but their environmental incidence and fate are largely unknown. Our

research involved degrading irinotecan and aliskiren under simulated solar radiation, identifying TPs in ultrapure water, and replicating in real water (e.g., river water). The TPs were identified using mass spectrometry (MS) techniques. Thus, 8 irinotecan TPs were identified with QTRAP MS, while 6 aliskiren TPs were identified using LTQ-Orbitrap MS. Finally, two rapid and sensitive UHPLC-MS/MS methods for irinotecan and its 8 TPs, as well as aliskiren and its 6 TPs, were developed and validated. The methods were applied to analyze nine real water samples from ground, surface, and wastewater sources. Irinotecan and aliskiren were found in hospital effluents, along with one TP each. Additionally, aliskiren and two of its TPs were detected in many wastewater effluents following a retrospective study of several water samples.

We also developed and validated a multiresidue approach based on on-line SPE HPLC-MS/MS for the detection and quantification of ten pharmaceuticals in aqueous samples. Among the target analytes were anticancer, antidepressant, and antihypertensive drugs. On-line SPE cartridges, chromatographic separation, and mass spectrometry parameters were optimized, resulting in a quick and sensitive analytical method. Six hospital effluent samples were analyzed using this method, and maprotiline and methotrexate were detected in five of them. Although this exercise was time consuming and required competence, we successfully demonstrated the critical nature of automating the extraction, separation, and detection procedures in order to develop a rapid and highly sensitive method for ultratrace analysis of multi-class pharmaceuticals in wastewater.

While targeted water analysis methods are well established, current research shows that they cannot explain why known contaminant concentrations are insufficient to account for toxic effects reported in some samples. In fact, there are several reasons to assume that unknown chemical concentrations often exceed known chemical concentrations. Non-target screening approaches can be used to comprehensively address data gaps regarding the presence of emerging contaminants in the environment. We used LC-HRMS based on offline SPE extraction protocols combined with open-source LC-MS/MS data processing tools and public databases to perform non-target screening of 17 water samples (surface waters and wastewater effluents) from France, Greece, and Italy. We identified 264 compounds from the pharmaceutical, personal care product, hormone, pesticide, fluorinated substance, and transformation product families. This work contributed to the advancement of current knowledge regarding emerging contaminants in the aquatic environment by enriching the NORMAN databases via the suspect list exchange and digital sample freezing platform.

Finally, we optimized and investigated the robustness of CECs' abatement methods using experimental design (DOE) methodologies. The aim of this work was to develop guidelines for

the successful implementation of the CECs' abatement technologies in wastewater treatment plants (WWTPs). The guidelines are meant to provide information on parameters that have no effect on the process being examined, or on those that must be strictly controlled, as even tiny alterations can result in decreased efficiency. The photodegradation of irinotecan in the presence of sunlight was studied by a full factorial design, whereas fractional factorial designs were used to investigate the photocatalytic degradation of maprotiline in the presence of Ce-ZnO or Ce/Cu-ZnO photocatalysts. Along with a minimum of three replicate runs in the domain center, all DOE applications included star points to investigate factor interactions and quadratic effects. We constructed regression models that could reliably predict the degradation efficiency of the systems and determine their best operating settings. Furthermore, for the case of maprotiline photocatalysis, four WWTPs were proposed based on observed effect terms and their practicality in actual plants, and response surface methodology was used to establish the robust regions where the processes can operate at their maximum efficiency.

Additionally, as described in **Appendix II**, my secondment at KTU was focused on the development of efficient photocatalysts for the degradation of CECs. The first study investigated a CuWO_4 doped TiO_2 photocatalyst, and the second study focused on a graphitic C_3N_4 doped ZnWO_4 photocatalyst. The sol-gel method was used to synthesize TiO_2 , whereas CuWO_4 and ZnWO_4 were synthesized from precursor salts using the co-precipitation assisted hydrothermal method. All produced materials were characterized structurally and morphologically using X-ray diffraction (XRD), Fourier transform infra-red (FTIR) spectroscopy, Brunauer–Emmett–Teller (BET) N_2 adsorption–desorption analysis, scanning electron microscopy-energy dispersive X-ray spectroscopy (SEM-EDS), transmission electron microscopy (TEM), X-ray photoelectron spectroscopy (XPS), and UV-Vis diffuse reflectance spectroscopy (UV-vis DRS) for optical characterization. Finally, the photocatalytic activities of $\text{CuWO}_4/\text{TiO}_2$ and $\text{g-C}_3\text{N}_4/\text{ZnWO}_4$ catalysts were investigated over carbamazepine (CBZ) and ibuprofen (IBF), respectively. The results indicated that the doped TiO_2 and ZnWO_4 were more efficient than their pure counterparts, degrading nearly 100% of CBZ and IBF after two hours of irradiation. In the case of CBZ degradation using CuWO_4 doped TiO_2 , the impacts of pH, chemical scavengers, H_2O_2 , contaminant ion effects (anions and cations), and humic acid (HA) were explored, and their respective effects on the photocatalyst efficiency toward CBZ degradation were highlighted.

PREFACE

This PhD is part of the AQUALity project, an Innovative Training Network funded by the European Union under the Marie Skłodowska-Curie Actions (call: H2020-MSCA-ITN-2017, grant agreement N^o. 765860). The project was devoted to developing an interdisciplinary cross-sectoral approach for effectively addressing the removal of contaminants of emerging concern (CECs) from water. Working more closely with work package 2 (WP2) of the project, my PhD research activities focused on developing advanced analytical methods for determining CECs and their transformation products (TPs), as well as investigating their fate in the aquatic environment.

The research tasks described in this PhD Thesis were carried out in five institutions/companies. The majority of the works were conceptualized, organized, and performed at the host institution, Università del Piemonte Orientale (UPO), under the supervision of Prof. Elisa Robotti in the Department of Science and Technological Innovation (DiSIT) in Alessandria, Italy. The other four institutions where I completed secondments were Karadeniz Technical University (KTU) in Trabzon, Turkey, Eurofins Environment A/S (Eurofins) in Vejen, Denmark, University of Ioannina (UOI) in Ioannina, Greece, and University of Turin (UniTO) in Turin, Italy. My secondment research was supervised by Prof. Emin Bacaksiz (KTU), Dr. Peter Mortensen (Eurofins), Prof. Vasilis Sakkas (UOI), and Prof. Claudio Medana (UniTO).

The PhD Thesis has been organized into six chapters. **Chapter 1** begins by providing a brief introduction to emerging contaminants of concern (CECs). Following that, a greater emphasis has been placed on pharmaceutical active chemicals (PhACs) due to their direct connection to this thesis. The occurrence and fate of PhACs in the environment has been summarized, with an emphasis on the aquatic environment. At the end of this chapter, the major objectives achieved are outlined. Then, **Chapter 2** describes the fundamentals behind LC-MS method development and validation, non-target screening approaches, and the application of experimental design (DOE) techniques in robustness studies. The PhD research activities (published, submitted, and recently completed) are detailed in Chapters 3–5. **Chapter 3** presents the aspects related to the development and validation of three LC-MS methods for the analysis of CECs and their TPs. **Chapter 4** describes the methodology and results obtained from non-target screening of European wastewater and surface water samples and **Chapter 5** presents the application of DOE in the optimization and robustness study of photolytic and photocatalytic processes developed for the removal of CECs. Finally, in **Chapter 6**, the overall conclusions are summarized.

Figures and tables mentioned in the manuscript text as additional materials are included in **Appendix I**. Moreover, the research work I conducted during my secondment at the Karadeniz Technical University (KTU) in Turkey is reported in **Appendix II** because the research activity was not directly applicable to my thesis.

Finally, **Appendix III** contains the following details:

- Secondments and the specific research projects completed
- Publications: published, submitted, and in preparation
- Presentations: Oral and poster communications of the PhD research findings in different national and international meetings, workshops, and conferences
- Dissemination and outreach activities
- Participation in co-advising of undergraduate and graduate students
- List of PhD courses and training attended

CONTENTS

ACKNOWLEDGEMENTS -----	i
ABSTRACT -----	iii
PREFACE -----	vii
ABBREVIATIONS -----	4
1. INTRODUCTION -----	3
1.1 Contaminants of emerging concern (CECs) -----	3
1.2 Pharmaceutical Active Compounds (PhACs) -----	3
1.2.1 Sources and pathways of PhACs-----	5
1.2.2 Transformation and degradation of PhACs-----	7
1.3 Occurrence of PhACs in the aquatic environment -----	10
1.3.1 PhACs in wastewaters-----	10
1.3.2 PhACs in Surface and Groundwaters-----	11
1.3.3 PhACs in treated/drinking waters-----	12
1.4 PhACs Studied in this Thesis -----	13
1.4.1 Antineoplastic agents-----	13
1.4.2 Antihypertensive Drugs-----	16
1.4.3 Antidepressant Drugs-----	17
1.5 Objectives -----	18
References -----	19
2. METHODS DEVELOPMENT AND VALIDATION: THEORETICAL AND PRACTICAL CONSIDERATIONS -----	29
2.1 Analysis of PhACs in water samples -----	29
2.2 LC-MS method development and validation -----	29
2.2.1 MS/MS method development-----	31
2.2.2 HPLC method development-----	34
2.2.2.1 Optimization of sample preparation-----	34
2.2.2.2 Solid phase extraction (SPE)-----	35
2.2.3 LC-MS/MS Method Validation-----	36
2.3 Nontarget screening of water samples -----	39
2.4 Experimental design techniques -----	43
2.4.1 Optimization and robustness study-----	46
2.4.1.1 Full and Fractional Factorial Designs-----	46
2.4.1.2 Response Surface Methodology-----	49
References -----	51
3. DEVELOPMENT AND VALIDATION OF LC-MS/MS METHODS FOR CECs DETERMINATION -----	59
3.1 Introduction -----	59

3.2	Background of the studies	60
Part I – Irinotecan and Aliskiren		
3.3	Experimental part	65
3.3.1	Photodegradation experiments	65
3.3.2	Solid-phase extraction (SPE) procedure	66
3.3.3	Development of UHPLC-MS/MS methods	66
3.3.4	Identification of Aliskiren TPs using HRMS	67
3.3.5	Real water samples	67
3.4	Results and Discussion	68
3.4.1	Development of UHPLC-MS/MS methods	68
3.4.2	Validation of the UHPLC-MS/MS methods	70
3.4.3	Identification of TPs of irinotecan and aliskiren	72
3.4.3.1	Irinotecan	72
3.4.3.2	Aliskiren	77
3.4.4	Analysis of real samples	84
3.4.5	Retrospective analysis of aliskiren and its TPs	84
3.5	Conclusions	86
PART II – Ten Pharmaceuticals		
Development and Validation of a Fully Automated On-line SPE LC-MS/MS Method		
		87
3.6	Optimization of LC-MS/MS conditions	89
3.6.1	Optimization of the MRM method	89
3.6.2	Selection of on-line SPE cartridges	91
3.6.3	Optimization of LC-dependent conditions	92
3.6.4	Sample collection and preparation	92
3.7	Results and Discussion	93
3.7.1	Optimization of the HPLC-MS/MS	93
3.7.2	Optimization of the on-line SPE	96
3.7.3	The optimized on-line SPE-LC-MS/MS method	97
3.7.4	Method validation	99
3.7.5	Analysis of real water samples	103
3.8	Conclusions	103
3.9	Materials	104
3.9.1	Chemicals	104
3.9.2	Instrumentation	105
References		106
4.	NON-TARGET SCREENING BY LC/MS-BASED TECHNIQUES	113
4.1	Introduction	113
4.2	Background of the study	114
4.3	Experimental approach	117
4.3.1	Apparatus and materials	117
4.3.2	Chemicals and Reagents	117

4.3.3	Sample collection-----	118
4.3.4	LC-HRMS analysis-----	119
4.4	Results and Discussion-----	120
4.4.1	Non-target identification workflow using MS-DIAL-----	120
4.4.2	List of substances and their categorization-----	126
4.5	Improvement of the NORMAN database-----	126
4.5.1	Suspect List Exchange (SLE)-----	126
4.5.2	Digital Sample Freezing Platform (DSFP)-----	126
4.6	Conclusions and forward-----	127
	References-----	139
5.	ROBUSTNESS STUDIES BY EXPERIMENTAL DESIGN-----	143
5.1	Introduction-----	143
5.2	Background of the study-----	143
5.3	The irradiation procedures-----	146
5.3.1	Photodegradation of irinotecan-----	146
5.3.2	Photocatalytic degradation of maprotiline-----	147
5.4	LC-HRMS analyses-----	148
5.4.1	Irinotecan-----	148
5.4.2	Maprotiline-----	149
5.5	The experimental plans adopted-----	151
5.5.1	Photodegradation of irinotecan-----	151
5.5.2	Photocatalytic degradation of maprotiline-----	153
5.6	Results and Discussion-----	156
5.6.1	Irinotecan-----	156
5.6.1.1	Kinetic study-----	156
5.6.1.2	Modelling the response C/Co-----	157
5.6.2	Maprotiline-----	161
5.6.2.1	Kinetic studies-----	161
5.6.2.2	Modelling the response C/Co-----	162
5.6.2.3	Response surface Methodology (RSM)-----	166
5.7	Conclusions and forward-----	175
5.8	Materials and safety-----	175
5.8.1	Chemicals-----	175
5.8.2	Instrumentation-----	176
5.8.3	Safety-----	176
	References-----	177
6.	CONCLUSIONS-----	181
	Appendices-----	185
	Appendix I-----	187
	Appendix II-----	203
	Appendix III-----	219

ABBREVIATIONS

ACN	Acetonitrile
ALK	Aliskiren
ANOVA	Analysis of Variance
AOP(s)	Advanced Oxidation Process(es)
APCI	Atmospheric Pressure Chemical Ionization
ATC	Anatomical Therapeutic Chemical Classification System
BET	Brunauer-Emmett-Teller (BET)
CCD	Central Composite Design
CE	Collision Energy
Ce/Cu-ZnO	Cerium and Copper co-doped Zinc Oxide
CEC(s)	Contaminant(s) of Emerging Concern
CEP	Collision Entrance Potential
CES	Collision Energy Spread
Ce-ZnO	Cerium doped Zinc Oxide
CID	Collision Induced Dissociation
CTX	Cabazitaxel
CXP	Collision eXit Potential
DDA	Data Dependent Acquisition
dMRM	dynamic Multiple Reaction Monitoring
DOE	Design of Experiments
DOX	Doxorubicin
DP	Declustering Potential
DSFP	Digital Sample Freezing Platform
DTX	Docetaxel
DWTP	Drinking Water Treatment Plant
EDC(s)	Endocrine Disrupting Compound(s)
EI	Electron Impact (Ionization)
EMS	Enhanced Mass Spectrometry
EP	Entrance Potential
EPI	Enhanced Product Ion
ER	Enhanced Resolution
ESI	Electrospray Ionization
ETP	Etoposide
EU	European Union
FT-ICR	Fourier-Transform Ion Cyclotron Resonance
FT-IR	Fourier Transform Infrared Spectroscopy
FWHM	Full Width at Half Maximum
GC	Gas Chromatography
HCD	High Energy Collision Dissociation
HESI	Heated Electrospray Ionization
HILIC	Hydrophilic Interaction Liquid Chromatography
HPLC	High Performance Liquid Chromatography
HRMS	High-Resolution Mass Spectrometry
ICH	International Conference on Harmonization
IDA	Information Dependent Acquisition

IRI	Irinotecan
IS	Internal Standard
IUPAC	International Union of Pure and Applied Chemistry
LC	Liquid Chromatography
LC-MS	Liquid Chromatography - Mass Spectrometry
LLE	Liquid-Liquid Extraction
LOD	Limit of Detection
LOQ	Limit of Quantification
LTQ	Linear Trap Quadrupole
MAP	Maprotiline
MDL	Method Detection Limit
ME	Matrix Effect
MeOH	Methanol
MQL	Method Quantification Limit
MRM	Multiple Reaction Monitoring
MS	Mass Spectrometry
MS/MS	Tandem Mass Spectrometry
MTX	Methotrexate
NIST	National Institute of Standards and Technology
NORMAN	European Network of Laboratories for Monitoring Emerging Pollutants
NSAID(s)	Non-Steroidal Anti-Inflammatory Drug(s)
OFAT	One Factor At-a Time
PBDE(s)	Polybrominated Diphenyl Ether(s)
PCA	Principal Component Analysis
PCP(s)	Personal Care Product(s)
PDP	Photodegradation Product
PEC	Predicted Environmental Concentration
PhAC(s)	Pharmaceutical Active Compound(s)
PI	Positive Ion
POP(s)	Persistent Organic Pollutants
PPCP(s)	Pharmaceuticals and Personal Care Products
PTFE	Polytetrafluoroethylene
PTX	Paclitaxel
QA	Quality Assurance
QC	Quality Control
Q-LIT	Quadrupole Linear Ion Trap
QQQ	Triple Quadrupole
QTRAP	Quadrupole Ion Trap
RDB	Ring Double Bond
RPLC	Reversed Phase Liquid Chromatography
RSD	Relative Standard Deviation
RSM	Response Surface Methodology
RT	Retention Time
RTI	Retention Time Index
SD	Standard Deviation
SEM	Scanning Electron Microscopy
SLE	Suspect List Exchange
SM	Supplementary Material

SNCE	Stepped Normalized Collision Energy
SPE	Solid Phase Extraction
SRM	Selected Reaction Monitoring
STP	Sewage Treatment Plant
TEM	Transmission Electron Microscopy
TIC	Total Ion Chromatogram
TIS	Turbo Ion Spray
TOC	Total Organic Carbon
TOF	Time-of-Flight
TOP	Topotecan
TP(s)	Transformation Product(s)
UHPLC	Ultra-High Performance Liquid Chromatography
UK	United Kingdom
USA	United States of America
USEPA	United States Environmental Protection Agency
UV	Ultraviolet
UV-Vis	Ultraviolet-Visible
WFD	Water Framework Directive
WHO	World Health Organization
WWTP	Wastewater Treatment Plant
XIC	eXtracted Ion Chromatogram
XPS	X-ray Photoelectron Spectroscopy
XRD	X-Ray Diffraction

CHAPTER 1

Introduction

1. INTRODUCTION

1.1 Contaminants of emerging concern (CECs)

Recent advances in the development of robust and sensitive analytical methods and techniques have enabled the detection and quantification of a wide range of contaminants originating from anthropogenic sources. Because their existence in water bodies is usually at trace levels ranging from some ng/L to few µg/L, the pollutants are commonly referred to as micropollutants [1]. They may be classified as either legacy contaminants with well-established hazardous effects and control mechanisms, or as contaminants of emerging concern (CECs) [2]. Over the last few years, there has been a growing scientific interest about the presence and effects of CECs in the environment [1, 2]. CECs are characterized as naturally occurring and man-made compounds that are not regulated by current environmental legislations but may be candidates for regulation in the future, depending on inputs such as presence in the environment, ecotoxicity, potential health impacts and public perception. CECs are not necessarily brand-new chemicals, but they include chemicals that have been recently “discovered” in the environment, often due to improved detection levels of analytical methods [3]. Thus, pollutants that have long been present in the environment but are only now being assessed for their presence and relevance. This category of contaminants includes a wide spectrum of compounds, including Pharmaceuticals and Personal Care Products (PPCPs) such as human prescribed drugs (e.g., antidepressants, blood pressure) and over-the-counter medications (e.g., antidepressants, blood pressure); Persistent Organic Pollutants (POPs) such as polybrominated diphenyl ethers (PBDEs) used in flame retardants, furniture foam, and plastics, and other global organic contaminants such as per-fluorinated organic acids; Endocrine Disrupting Compounds (EDCs) such as synthetic and natural estrogens (e.g., 17-ethynylestradiol, 17β-estradiol, testosterone) and androgens (e.g., trenbolone), and many others (e.g., organochlorine pesticides); Veterinary drugs such antimicrobials, antibiotics, antifungals, growth promoters, and hormones; and Nanomaterials including carbon nanotubes and nano-scale particulate titanium dioxide.

1.2 Pharmaceutical Active Compounds (PhACs)

Pharmaceutical active compounds (PhACs) are one of the most common types of CECs found in the aquatic environment, with their occurrence attributed to a variety of sources, including hospital effluents, landfill leachates, and largely industrial and domestic wastewater due to poor treatment processes [4, 5]. The discovery of PhACs in the aquatic environment dates to the 1980s, and a wide variety of them have been detected since then. The ineffectiveness of

conventional water treatment methods in removing PhACs has been widely documented in the literature [6, 7], and these contaminants pose a concern to the receiving environment.

Pharmaceuticals are divided into various groups according to their physicochemical properties or intended use. Various pharmaceutical classes can be defined based on their mode of action, physiological effect, or chemical structure [8]. Based on these different classification systems, certain drugs may be classified together in one system but not in another. Certain others may have multiple applications (e.g., finasteride is used to regenerate hair as well as treatment of enlarged prostate) and can be categorized in different drug classes under a single classification system. Also, some medications are used for purposes other than those for which they were approved. Examples include levothyroxine, a medicine for hypothyroidism, which is also used off-label for depression treatment [9]. As more and more complex pharmaceuticals enter the market each year, the classification of drugs is likely to become increasingly diverse. Analgesics, anesthetics, antibacterial, antidepressants, antifungals, anti-inflammatory drugs, antineoplastics, antipsychotics, cardiovascular medications such as beta-blockers and ACE inhibitors, and hormonal agents are among the major classes [2]. Even though over 3000 pharmaceuticals are already on the market and their use is expanding, most of these drugs are not being monitored under current environmental regulations [3]. Concerning the aquatic environment, the EU Directive 2008/105/EU requires Member States to establish a 'watch list' of compounds for monitoring in a wide range of freshwater bodies. The first watch list, comprising ten compounds, was established in 2015 [10], and it was amended in 2018 [11] by eliminating five substances and adding three, bringing the total to eight substances. The most recent EU Water Framework Directive (WFD) "watch list" of nineteen priority pharmaceuticals for EU-wide monitoring includes Ciprofloxacin, Sulfamethoxazole, Trimethoprim, Venlafaxine, O-desmethylvenlafaxine, and Amoxicillin [12]. In addition to the watch list compounds, each Member State may choose compounds of national or local concern.

Due to the presence of multiple knowledge gaps regarding their occurrence, contamination caused by the release of PhACs in the environment is still a complex growing problem. Even though PhACs have been known to exist in the environment for more than four decades, their accurate consumption data and environmental concentrations are still lacking [13]. Furthermore, these compounds can undergo biological or chemical transformations, resulting in unknown transformation products (TPs) that are potentially more toxic than the parent compounds.

1.2.1 Sources and pathways of PhACs

PhACs are released into the environment at some juncture during the life cycle of a pharmaceutical (Fig. 1.1). In the context of PhACs evaluation in aqueous systems, understanding the potential sources and routes of PhACs release depicted in Fig. 1.1 is essential. The drug discovery and development processes are substantial contributors of pharmaceutical pollution in the environment through, for example, leaks and manufacturing waste [14]. Emission of pharmaceuticals can occur during the R&D of Pharmaceutically Active Ingredients (APIs) and preparation of the finished drug products. Once the drugs are administered to humans, they are excreted together with their APIs and metabolites, which may or may not be biologically active. Improper waste management and disposal is another significant source of PhACs release. Any leftover medication improperly disposed of may be flushed down the drain and enter the sewage system where it will be treated and disposed of at a wastewater treatment plant. For certain PhACs, such treatments are not adequate to eliminate them completely [15]. Thus, part of the drug, as well as the metabolites and transformation products (TPs), reach the receiving body of water. Furthermore, when sewage effluent and/or sludge are used in agriculture, the compounds in the effluent and/or sludge can enter terrestrial systems and pollute the environment. As a result, PhACs have been detected in practically every environmental matrix around the globe, including wastewater treatment plant influents and effluents, sludge, surface water (rivers, streams, lakes, estuaries, and seawater), and groundwater [3].

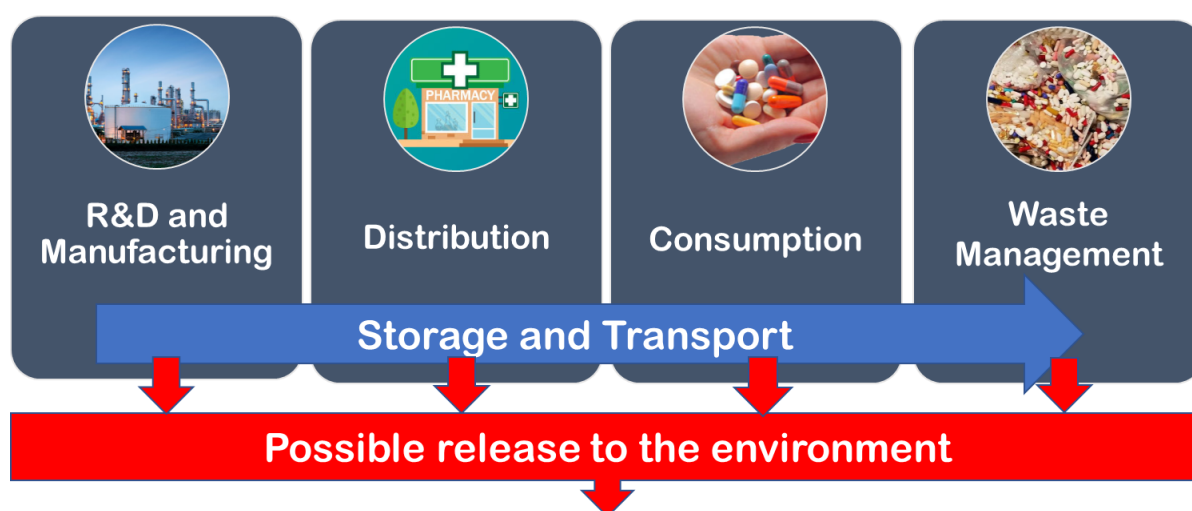


Figure 1.1. The basic life cycle of medicinal products (adapted from [16])

Due to advancements in analytical methods and instruments that allow for high accuracy and sensitivity measurements, trace quantification of a wide range of these substances in aqueous systems is becoming a common practice. The occurrence and distribution of PhACs in water

are influenced by their rate of consumption or prescription, excretion of the unmetabolized drug, physico-chemical properties, and environmental fate. The schematic design in Fig. 1.2 depicts the known emission pathways associated with the use-phase of pharmaceutical products for humans. While excretion is the primary route of drugs into the environment [16], significant amounts of pharmaceuticals (e.g., anti-inflammatory gels) can also be washed off the skin during bathing. As a result, drugs with a higher rate of consumption or prescription have frequently been found in wastewater, surface water, and even in drinking water [17], raising concerns about their potential effects on human health, especially after a long-term exposure to low level concentrations. In general, PhACs of various classes have been commonly detected in aqueous systems at very low concentrations ranging from some ng/L to few $\mu\text{g/L}$ [18, 19]. However, recent reports indicated that pharmaceutical levels in urban wastewaters are rising due to population aging and increased density [20]. Antibiotics and analgesics are the two most abundant classes of PhACs in the aquatic environment, but results may vary by country, region, consumption pattern, and manufacturing industry location [21].

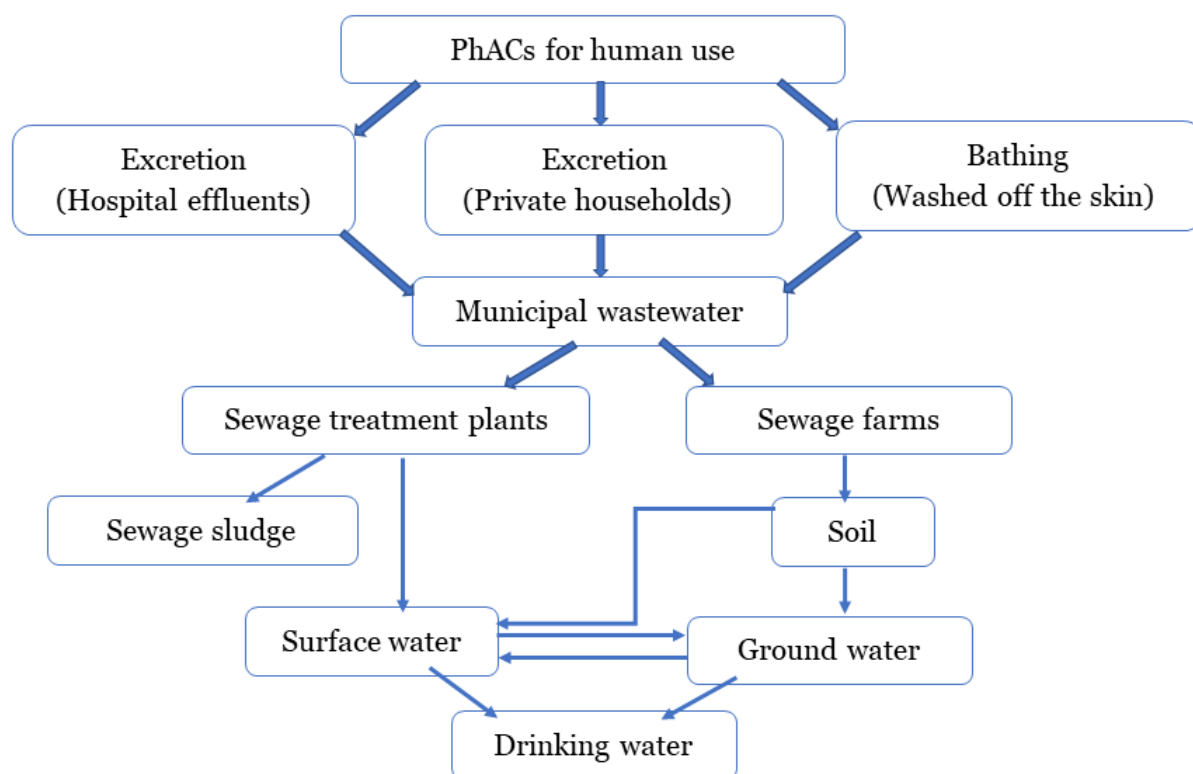


Figure 1.2. Routes of PhACs use-phase release and contamination.

1.2.2 Transformation and degradation of PhACs

Once PhACs reach into the aquatic environment, the parent chemicals may undergo a variety of physicochemical processes, including absorption/adsorption, sorption, desorption, oxidation, biodegradation, hydrolysis, and photodegradation (Fig. 1.3). Chemical properties such as hydrophobicity and biodegradability of the pharmaceutical, as well as WWTP's operational conditions such as pH and temperature can affect the removal process. As a result, the roles of biodegradation, hydrolysis, sorption, and photodegradation in the removal of pharmaceuticals vary significantly between treatment plants. Pharmaceuticals that enter a WWTP are initially removed during the biological treatment stage. Several studies reported that biodegradation is the most important and prevalent transformation pathway for pharmaceuticals [22]. However, it is important to emphasize that abiotic degradation mechanisms such as hydrolysis, oxidation, and photolysis play an important role. Under certain circumstances (e.g., deep soils or deep surface conditions) where biodegradation is limited by low microbial activity [23], the abiotic mechanism may be the primary mode of degradation. The principal abiotic degradation processes include hydrolysis, oxidation, and photolysis. According to several studies, the two most important pharmaceutical abiotic degradation processes are photolysis and hydrolysis [24].

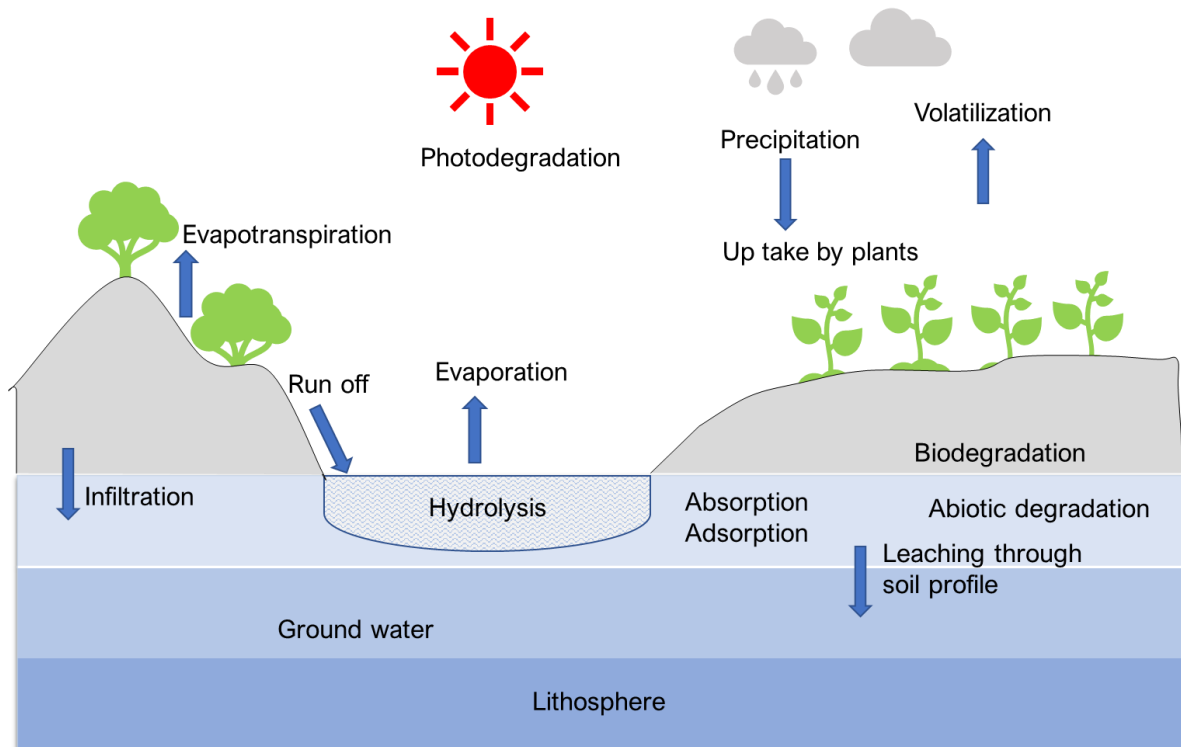


Figure 1.3. An overview of the environmental fate and mobility of PhACs

In surface waters, photochemical processes play a significant role in the transformation of pharmaceuticals, in which a drug may be entirely mineralized to carbon dioxide and water or transformed to degradation products. Photodegradation becomes a key degradation mechanism when ultraviolet (UV) radiation levels are high. When a drug molecule receives energy and becomes excited, the process of photodegradation begins, and the molecule either breaks up or generates less stable bonds that can be readily broken later. The molecules can receive photo energy in two ways: directly when exposed to UV light within the range of the sunlight spectrum, or indirectly when dissolved organic matter (DOM) such as nitrates, nitrites, and carbonates absorb photoenergy and generate reactive species that react with the CECs [25, 26].

The interaction of pharmaceuticals with solar radiation has both beneficial and detrimental environmental consequences. On the good side, UV light can be absorbed by certain molecules and triggers their removal through photodegradation, as demonstrated by several studies focusing on the direct photolysis [27] and indirect photolysis via, for example, carbonate radicals [28], resulting in effective removal of some photolabile PhACs discharged into the environment and eventually reduction in their toxicity. On the contrary, photochemistry may result in the production of transformation products that are more toxic than the parent compound [29, 30]. Additionally, studies [31] have demonstrated that the concurrent persistence of parent chemicals and their TPs has a mixed effect on organisms, increasing or decreasing the total toxicity. Therefore, to compile comprehensive data on the occurrence and eco(toxicity) of PhACs in the aquatic environment, studies on their fate under solar radiation exposure, as well as the potential toxicity of their TPs and interactions with other chemicals, must be integrated into environmental monitoring and risk assessment programs. Notably, CECs may include not only the parent drugs but also their metabolites and TPs.

In general, the radiation sources most frequently employed in research involving the photo-transformation of CECs are efficient UVA and UVC lamps. Although these lamps can usually provide a high CEC breakdown rate [32], utilizing a xenon lamp to replicate natural solar radiation may be the most environmentally friendly option [33]. More than 250 pharmaceuticals that have been approved by the European Pharmacopoeia are photolabile, which means that studies of their interaction with solar radiation can help researchers better understand the environmental fate of these drugs and devise new methods for removing them.

Many researchers have studied the interaction of pharmaceuticals in surface waters with solar radiation [33-35]. A study conducted by Mathon et al. [35], for example, used simulated solar radiation (Xe lamp) and studied the photodegradation of 36 pharmaceuticals belonging to different families and found half-times ranging between 0.05 to 118 h. They also reported that

compounds which contained OH-C=O, C=N-O-, =N-OH, -CH=N, -O-P=O, -C=C- functional groups in their structure were more sensitive to photodegradation, while those containing -O-R and -Cl had low sensitivity. Trawinski et al. [33] studied the direct photolytic and photocatalytic (H₂O₂ and TiO₂) degradation of the antipsychotic drug asenapine applying simulated solar radiation and detected 18 TPs as a result of direct photolysis, out of a total of 19 TPs identified using photocatalysis. According to in-silico toxicity studies, most TPs were found to be comparable or less toxic to aquatic organisms; however, all TPs had higher developmental toxicity than the parent molecule. It is important to note that many pharmaceuticals have little to no absorbance of UV light within the sunlight spectrum, for example the anticancer drug cyclophosphamide [27, 36], and thus are extremely resistant to direct photolysis.

For a variety of reasons, including a lack of occurrence data, a lack of acceptable analytical techniques, and, in certain cases, a lack of attention, many pharmaceuticals are not included in current targeted environmental monitoring programs. Specifically, lack of sufficient information on the environmental fate and behavior of lesser-known PhACs leads to inadequate exposure data, putting them at risk of being omitted from environmental monitoring programs. In fact, it is common to see widely prescribed drugs being excluded in routine environmental monitoring. Indeed, the Matthew effect [37] could have an impact on substances chosen for routine environmental monitoring. Among these are numerous widely used antineoplastic and antihypertensive drugs, the presence of which has been reported in a variety of wastewater effluents and surface waters [38]. Despite their widespread identification in a variety of aquatic matrices and the rising concern about their potential adverse effects on human health and the environment, little to no information exists on the potential TPs produced during photodegradation driven by solar light.

In line with the above discussion, two pharmaceuticals were selected for this thesis due to their widespread prescription, reported environmental presence, relatively high rate of excretion, and a lack of literature on their environmental fate when exposed to sunlight. These were irinotecan, an anticancer agent, and aliskiren, an antihypertensive drug. We used simulated sun irradiation to evaluate the photodegradation fate of both chemicals and developed UHPLC-MS/MS methods for identifying their distinct transformation products. The two studies on irinotecan and aliskiren are discussed in Chapters 3 under Part I.

1.3 Occurrence of PhACs in the aquatic environment

The increasing presence of PhACs in the environment has been related to their widespread applications for both human and veterinary uses. PhACs such as antibiotics, analgesics, and psychiatric medications pose a major concern to water quality due to their bioactivity even at low concentrations and accumulation in the environment. Indeed, PhACs have been detected in surface waters, wastewaters, soils, sludge, and even living organisms, with some PhACs exhibiting the tendency to bioaccumulate [39]. The rising public awareness and concern in recent years has resulted in an increase in the number and quality of research aimed at establishing relevant information regarding their occurrence, fate, and detrimental effects. Such findings will undoubtedly influence future water policies, as they can be used in improving regulatory enforcements to limit PhACs release into the environment and provide a set of best water quality management practices. The establishment and ongoing updating of the EU's 'watch list' of priority substances for Union-wide monitoring of surface waters in accordance with Directive 2008/105/EC [12] highlights the importance of ongoing research efforts to include more compounds determined to pose risk to the ecosystem on a priority substances list.

1.3.1 PhACs in wastewaters

Several detailed studies have been conducted on the removal of PhACs from WWTPs. While modern biological treatment systems are reported to be quite effective at eliminating easily biodegradable PhACs such as ibuprofen, with a removal rate of over 90%, conventional wastewater treatment plants, on the other hand, are less efficient in degrading moderately persistent PhACs such as diclofenac, sulfonamide and macrolide antibiotics, or beta blockers, with removal rates typically ranging from 20% to 80% [40]. A study by Gros et al. [41] spanning four sampling periods over three years, analyzed a total of 84 samples, including influent and effluent samples from seven Spanish WWTPs located along the Ebro River Basin and the receiving river waters, to determine the presence of 73 pharmaceuticals representing several drug classes. The compounds detected with high concentrations were Ketoprofen (2980 µg/L), Ibuprofen (2400 µg/L), Diclofenac (1090 µg/L), and Naproxen (1740 µg/L). The study also found that absolute removal efficiencies ranged from 20% to 100%, indicating that conventional wastewater treatment processes used at the seven WWTPs were unable to entirely remove most of the pharmaceuticals under consideration and that PhACs constitute a significant source of pollution in the aquatic environment. Another long-term monitoring program conducted for nearly two-years by Bueno et al. [42] evaluated 100 organic micropollutants from diverse chemical groups, including pharmaceuticals, in five WWTPs

located in the south-east, center, and north of Spain. The average efficiencies of removal ranged from 20% (erythromycin) to 99% (acetaminophen), with several compounds found at mean range concentrations of 0.007–59.495 µg/L (influent) and 0.005–32.720 µg/L (effluent). Moreover, they found 20 persistent chemicals that are frequently detected in wastewater effluents, including atenolol, galaxolide, hydrochlorothiazide, and gemfibrozil. A large-scale EU-wide study [43] analyzed effluents from 90 WWTPs for 156 polar organic micropollutants, 42 of which were pharmaceuticals. Maximum pharmaceutical concentrations ranged from 0.01 to 4.60 µg/L, with Triclosan (4.60 µg/L), Carbamazepine (4.26 µg/L), Gemfibrozil (3.62 µg/L), and Ibuprofen (2.13 µg/L) recording the highest values.

A recent study carried out by Vieno et al. [44] on municipal WWTPs located in Sweden, Germany, Denmark, Finland, Estonia, and Russia, reported that only nine out of 118 drugs were eliminated efficiently (> 95%) during the wastewater treatment process, and almost half of the compounds had removal efficiencies below 50%. In general, inefficient WWTPs have been shown to significantly contribute to the release of PhACs into the aquatic environment. Additionally, untreated domestic, industrial and hospital effluents may directly discharge PhACs into various receiving water bodies due to, for example, sewer failure [45]. Untreated hospital effluents are another significant source of PhACs in the aquatic environment. Even though no explicit guidelines or instructions exist for the management of hospital wastewater [13], their direct discharge to surface water is prohibited. Several studies [46, 47] discovered substantial amounts of PhACs (on the order of µg/L) in hospital effluents discharged into surface water.

1.3.2 PhACs in Surface and Groundwaters

The occurrence of PhACs in surface and ground water has been documented by various studies, with antibiotics and analgesics being the most frequently detected compounds in Europe and Asia, and estrogens being the most prevalent in Latin America, the Caribbean, and Africa [21]. Concerning surface waters, a large screening study conducted by Kondor et al. [48] assessed the occurrence of 111 PhACs along the Hungarian section of the Danube River Basin and revealed the occurrence of alkaloids (0.18-3400 ng/L), antipsychotics/antidepressants (0.16-64.7 ng/L), antiepileptics (0.81-498 ng/L), anxiolytics (0.02-45.07 ng/L), cardiovascular drugs (0.06-233 ng/L), hormones (0.10-9.82 ng/L), NSAID's (1.71-115 ng/L) and local anesthetics (0.11-298 ng/L). Another study carried out by Jameel et al. [49] evaluated 112 PhACs across 64 rivers located in 22 European, Asian, and North American countries. The study identified 22 PhACs with high detection rates, many of which were also among the most widely consumed in several European countries, the USA, and the UK [50, 51], implying that these compounds were present widespread in all the studied rivers. The

identified PhACs were analgesics, antibiotics, estrogens, and beta-blockers. Additionally, recent global pharmaceutical evaluations of surface waters reported similar findings [52, 53]. Similarly, high concentrations of various pharmaceuticals were found in Poland's surface waters [54, 55]. On the other hand, a study conducted by Pereira et al. [56] revealed that the range of PhACs concentrations observed in Portuguese rivers was significantly lower than those observed elsewhere in Europe, with detection frequencies of 27.8% and an average (7.78–39.21 ng/L) and maximum (69.15 ng/L) concentration in the low ng/L range. Several studies have also indicated that the quality of ground water [57] and catchments [58] is increasingly compromised because of PhACs contamination caused by, for example, storm water infiltration.

Another factor that can influence the concentrations of PhACs in the environment is the pandemics, as they increase the use of specific drugs for specific time periods. After the COVID-19 pandemic, various studies reported a sharp increase of pharmaceuticals' concentrations around the world. For instance, a study conducted by Chen et al. [59] showed that five categories of drugs used against COVID-19 were detected in surface water (lakes and WWTP river estuary system) near hospitals in the city of Wuhan (China), in concentrations between 2.61 and 1122 ng/L as a sum of them. Another study [60] demonstrated that the COVID-19 pandemic will also have an effect on the prevalence of antidepressants in the environment, as it globally increases depression and anxiety cases, thereby increasing the use of medications to alleviate their symptoms.

1.3.3 PhACs in treated/drinking waters

Most countries rely on surface and groundwater for their drinking water needs. However, distribution of safe drinking water becomes a complex issue, as these sources are often contaminated with a variety of pollutants. Occurrence of PhACs has been reported in tap water around the world [61-66], raising concerns about the health risks that these compounds can pose to humans after a lifelong exposure to contaminated water. It is considered that their presence in treated water is due to inadequate treatment in Drinking Water Treatment Plants (DWTPs) [63]. Wu et al. [67] reported the occurrence of carbamazepine, amitriptyline, diazepam, tetrazepam and alprazolam in treated samples but in concentrations significantly lower than those found in raw samples. The same findings were corroborated by a study conducted in Portugal [56], which demonstrated that even when medicines were discovered in treated samples, their amounts were less than their respective MDLs. Another study [63] reported the presence of 12 PPCPs in treated water from a DWTP in China, with caffeine and ketoprofen being the most abundant, results evidenced also in a study by Papagiannaki et al. [68], which reported their detection alongside with ibuprofen and carbamazepine in treated

samples from a DWTP in Italy. In the majority of the studies reporting occurrence of pharmaceuticals in drinking water, the detected concentrations are at trace level (few ng/L). In general, different studies indicate that PhACs occurrence in drinking water is primarily due to the consumption trends in a particular region and the hydrophilic character of the compounds, which enables them to readily flow through the various stages of DWTPs [68].

1.4 PhACs Studied in this Thesis

In this thesis, a total of ten PhACs were studied (Fig. 1.4). These target compounds were chosen based on current and predicted consumption trends in Europe, the rate of excretion of the unmodified drug, the frequency of detection in wastewaters (where data was available), and suitability for analysis using LC-MS/MS. The sections that follow will discuss the descriptions and current knowledge regarding their occurrence in the aquatic environment.

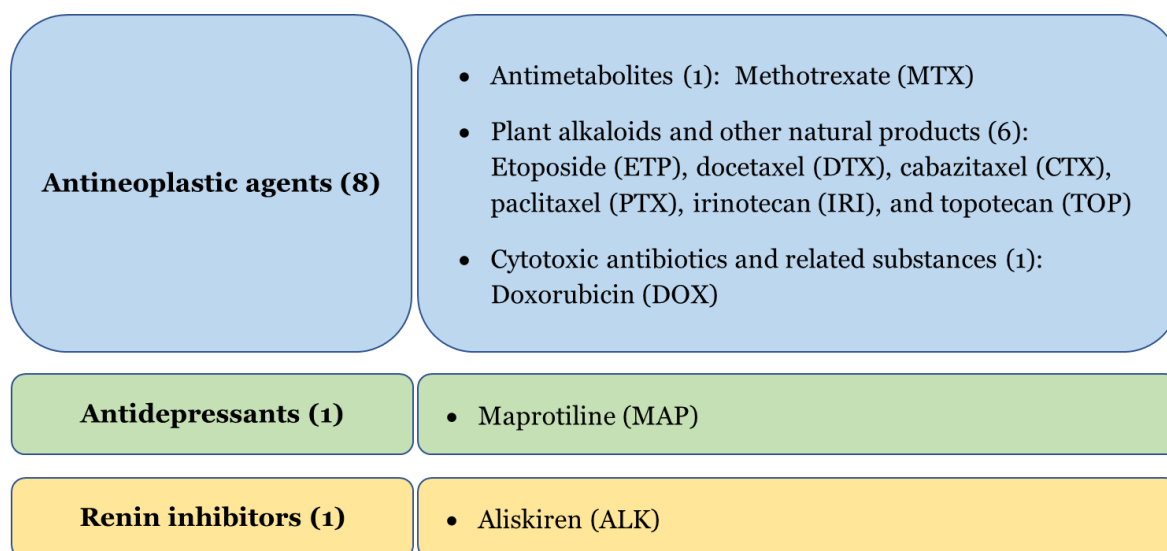


Figure 1.4. List of PhACs studied in this thesis

1.4.1 Antineoplastic agents

According to recent WHO reports, cancer is the second biggest cause of mortality worldwide, after cardiovascular illnesses. In 2017, the globe registered more than 9.5 million cancer deaths [69] showing a significant increase compared to, for example, 8.2 million deaths in 2012 [70]. As the number of cancer cases increases, so does the use of antineoplastic drugs. The annual number of new cancer cases is predicted to reach 22 million by 2032, implying that the use of anticancer medications would rise [71, 72]. Anticancer drug usage trends in countries such as France, Spain, Portugal, the United Kingdom, and Sweden are practically constant or increasing [73-77]. With the increasing number of cancer cases, consumption of

anticancer drugs has increased in recent years, and this trend is likely to continue for the years to come.

The WHO adopted the Anatomical Therapeutic Chemical Classification System (ATC), a drug classification system maintained by the Norwegian Institute of Public Health's WHO Collaborating Centre for Drug Statistics Methodology [73, 78]. The ATC system classifies drugs according to their target organ, mode of action, and chemical and therapeutic properties. Anticancer agents are found in the group of antineoplastic and immunomodulating agents, with the class L01 – antineoplastic agents. Fig. 1.5 displays the various subclasses of L01 (antineoplastic agents), with representative drugs listed in each class.

Typically, anticancer medications are delivered in hospitals. Thus, hospital wastewater is among the significant pathways for these substances to enter the aquatic environment. Furthermore, since most cancer patients leave the hospital after undergoing treatment, residential wastewater and, eventually, wastewater treatment plants (WWTPs) are important channels. Even though consumption varies by country, some of the most widely used anticancer drugs in chemotherapy are cyclophosphamide, ifosfamide, 5-fluorouracil, methotrexate, gemcitabine, azathioprine, doxorubicin, tamoxifen, etoposide, vincristine, chlorambucil, docetaxel, irinotecan, and paclitaxel [73, 74, 79]. Various reports have demonstrated that antineoplastics may be cytotoxic, genotoxic, mutagenic, carcinogenic, or teratogenic to aquatic species [80]. Additionally, studies have shown that antineoplastics degrade poorly in standard wastewater treatment processes [31, 36]. As a result, parent drugs, as well as their metabolites and transformation products, are frequently detected in surface waters. In agreement with this, a growing number of studies on the presence of antineoplastics in wastewater effluents and influents [81-84] have been published, with some studies also measuring them in surface and ground waters [38, 85, 86].

Out of the ten PhACs studied in this thesis (Fig. 1.4), eight were antineoplastics belonging to various ATC families (shown in blue in Fig. 1.5). As is the case with other medications, some anticancer agents are insufficiently absorbed and digested by the human body and are thus eliminated in the urine or feces and discharged into wastewater treatment plants (WWTPs). Another factor to consider is the amount of these chemicals that are eliminated in their original form. The unmetabolized forms of these eight antineoplastic compounds were reported to be excreted in quite large amounts. Specifically, 60–95% methotrexate; 25–45% etoposide and topotecan; 15–25% irinotecan; and 5–15% paclitaxel, docetaxel, cabazitaxel, and doxorubicin [82]. Due to the low biodegradability of most anticancer drugs, their elimination in conventional WWTPs is minimal, and as a result, they may be constantly released into the aquatic environment.

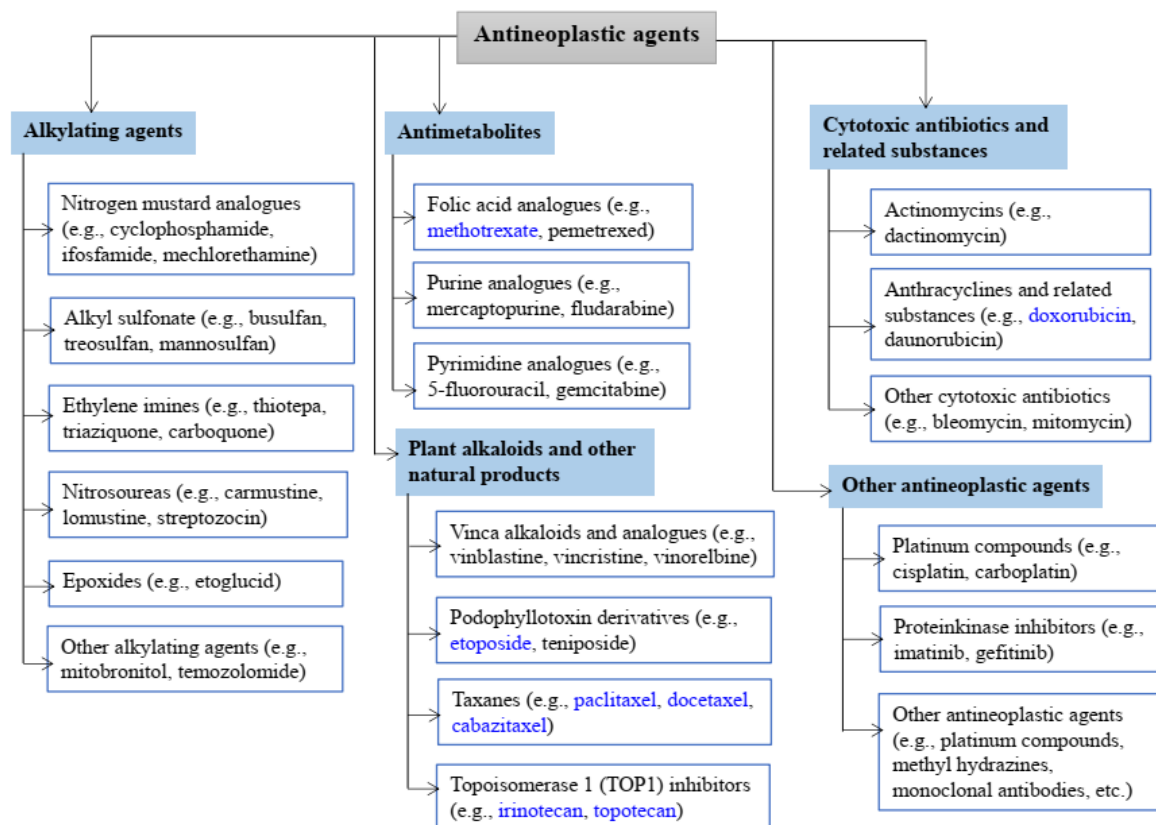


Figure 1.5. Classification of antineoplastic agents (adopted from [78])

Interestingly, the antineoplastic compounds studied in this thesis and lots of their metabolites have been determined in ng/L levels in hospital and residential wastewater effluents, as well as surface waters [20]. For example, 1.6–300 ng/L MTX [38, 79, 82, 87], 18.5–100 ng/L PTX [38, 88], 9.0–10 ng/L MAP [44, 89], 2.5–2.7 ng/L DOX [38], 0.4–60 ng/L IRI [38, 83, 87, 90], 3.4–15 ng/L ETP [83], 0.4–1900 ng/L ALK [91], and 97.7–175.1 ng/L DTX [88] have been reported, which supports the notion that standard WWTPs may only remove these drugs in part. However, information on the environmental occurrence of all the selected compounds is currently scarce. Moreover, when these substances enter the aquatic environment, they can produce transformation products with unknown effects [92]. As a result, developing highly sensitive and robust analytical methods capable of determining trace levels of these compounds is critical in order to gain a better understanding of their presence in aquatic systems so that, when necessary, appropriate treatment methods can be implemented to avoid the release of these chemicals into surface waters.

Due to the large number and variety of anticancer compounds delivered to patients, it is impracticable to analyze all of them because of time and cost constraints. It is also worth noting that pharmaceuticals fall into a variety of chemical classes, making the development of

multi-residue methods capable of simultaneously analyzing large groups of them, a difficult analytical task. Prior to implementing a monitoring program, it is often common to develop a system, such as the one developed by the European Medicines Agency, for determining predicted environmental concentration (PEC) values and identifying the anticancer compounds that are more likely to be found in aquatic environments. As per this approach, an antineoplastic with PEC value greater than 10 ng/L should undergo further investigation on its environmental presence, fate, and toxic effects. Even though this approach has been widely employed in the study of PhACs [73], there are certain limitations. For example, for most pharmaceuticals, there is a difference between the amount sold and the amount used by patients, resulting in an overestimation of PEC values. Moreover, prioritizing methods often overlook the potential effects of some compounds at even extremely low concentrations. Given the relatively high consumption and excretion rates of the unmetabolized forms of the anticancer agents discussed above, we believe that research focusing on the environmental occurrence and fate of less investigated anticancer agents that may have a detrimental effect on the aquatic environment is still necessary to establish exhaustive scientific evidence.

1.4.2 Antihypertensive Drugs

Psychoactive drugs are another important class of pharmaceuticals that have been widely identified in the aquatic environment with reports of adverse effects to aquatic life [93]. The five major classes of antihypertensive drugs are beta-blockers, diuretics, angiotensin converting enzyme inhibitors, angiotensin II receptor antagonists, and calcium channel blockers [94]. The global trend indicates that antihypertensive drugs usage nearly doubled in Europe between 2000 and 2017 [69]. Due to the increased consumption and incomplete removal in WWTPs, the antihypertensive drugs most frequently detected include beta-blockers (e.g., atenolol, metoprolol, propranolol, and sotalol) and diuretics (e.g., hydrochlorothiazide and furosemide). For instance, a study by Bueno et al. [42] detected the diuretics furosemide and hydrochlorothiazide in higher concentrations in wastewater influent, between 0.7–2 µg/L and 2.5–14 µg/L, respectively, with a detection frequency greater than 85% in all cases. Moreover, atenolol was the most abundant beta-blocker detected at the highest concentration levels of 0.7–25 µg/L for wastewater influent and 1.1–15 µg/L for effluent. In a study involving the assessment of 156 pharmaceuticals and two metabolites [44], furosemide was found with the highest concentration of 1,300 µg/l in municipal WWTPs effluents from Denmark. Two important antihypertensive drugs frequently detected in European surface waters are irbesartan and valsartan, which were widely reported in concentrations ranging from 5 to 651 ng/L and 11 to 6260 ng/L, respectively [55, 95-97].

Aliskiren, a direct renin inhibitor commonly used since 2009 as a monotherapy or as the main component of up to eight aliskiren-based medication combinations, is one of the numerous antihypertensive pharmaceuticals widely detected in wastewater effluents and surface waters [98]. Nearly 80% of aliskiren is excreted unchanged [99], making it one of the CECs which are constantly released into the aquatic environment, with reports of concentrations ranging from 0.4 to 1.9 µg/L in WWTP effluents [91]. Furthermore, aliskiren concentrations in surface waters (0.4 to 5.0 ng/L) were found to be related to drug consumption trends [100]. While very sensitive analytical approaches capable of quantifying aliskiren at trace levels are still required to gain a clearer understanding of its environmental occurrence, the lack of information regarding its fate is even more striking. As a result, we studied the photoinduced transformation of aliskiren in aqueous systems for the first time and identified six transformation products, two of which were predicted to be more toxic than the parent drug, as described in Chapter 3 of this thesis.

1.4.3 Antidepressant Drugs

Because of their extensive usage and persistence in water, antidepressants are among the emerging contaminants of concern often detected in aqueous systems [101]. Several studies have found evidence of their recalcitrant nature and presence in the aquatic environment. Esteban et al. [102], for example, evaluated the presence of 14 psychoactive drugs in the watersheds of Galicia in Spain and found 7 antidepressants in wastewater samples from five sewage treatment plants, with detection frequencies ranging from 7 to 47 %. Venlafaxine had the highest concentration in both influent and effluent samples, with average concentrations ranging from 16-401 ng/L (influent) to 4-317 ng/L (effluent). Furthermore, multiple studies have demonstrated that antidepressants are harmful to aquatic animals. Yang et al. [103] studied the effects of mianserin, a tetracyclic antidepressant from the same family as maprotiline, on early development of fish embryos at low environmentally relevant concentrations (10-1000 ng/L) and revealed a concentration-dependent inhibition of total antioxidant capacity and cholinesterase activity in exposed fish larvae. Another four-year monitoring project [104] reported the detection of the antidepressant Paroxetine, as well as six common drugs, in marine mussels off the coasts of Italy at a detection rate of 40%.

Maprotiline is a tetracyclic antidepressant authorized in a number of countries for the treatment of depression related to agitation or anxiety [105]. Its average removal rate in WWTP was found to be only 44 % [44]. Due to excretion of the unmetabolized form and improper disposal, maprotiline has been detected in WWTP influent and effluent, as well as surface waters, in concentrations ranging from 0.4-16.5 ng/L [43, 44]. Furthermore, Goncalves et al. [106, 107] found around 30 maprotiline TPs as a result of treatments with

various advanced oxidation processes, where the TPs were estimated to be less toxic than the parent drug. Nonetheless, the combined effects of the TPs and their interactions with other water constituents are unknown, and more evidence is required to obtain a clear picture of maprotiline occurrence and distribution in different aquatic compartments, making it critical to develop highly sensitive analytical methods capable of determining trace levels of drug.

1.5 Objectives

In this Thesis, pharmaceutical compounds that form the group of emerging contaminants of concern (CECs) have been studied, with the following objectives:

- Identification of new transformation products (TPs) of CECs produced in aqueous systems as a result of the interaction with the solar radiation. This was accomplished by combining the potentials of a quadrupole ion trap (QTRAP) and a linear trap quadrupole (LTQ) orbitrap mass spectrometry techniques.
- Selection and development of solid-phase extraction (SPE) sample preparation techniques (offline or on-line) for the extraction of CECs from different aqueous matrices.
- Development and in-house validation of new analytical methods to separate and identify the target CECs and their transformation products in aqueous matrices, using (ultra) high performance liquid chromatography (UHPLC) coupled with tandem mass spectrometry (MS/MS).
- Non-target screening of different aqueous matrices and identification of potential CECs using HPLC coupled with high-resolution mass spectrometry (HRMS) and open-source non-target LC-MS data processing tools.
- Application of experimental design (DOE) techniques to optimize and investigate the robustness of methods/procedures developed for the abatement of CECs from water.

References

1. Souza, D.M., J.F. Reichert, and A.F. Martins, A simultaneous determination of anti-cancer drugs in hospital effluent by DLLME HPLC-FLD, together with a risk assessment. *Chemosphere*, 2018. 201: 178-188.
2. Yang, W., H. Zhou, and N. Cicek, Treatment of organic micropollutants in water and wastewater by UV-based processes: a literature review. *Critical Reviews in Environmental Science and Technology*, 2014. 44(13): p. 1443-1476.
3. Patel, M., Kumar, R., Kishor, K., Mlsna, T., Pittman Jr, C. U., & Mohan, D. Pharmaceuticals of emerging concern in aquatic systems: chemistry, occurrence, effects, and removal methods. *Chemical reviews*, 2019. 119(6), 3510-3673.
4. Richardson, S.D., Water analysis: emerging contaminants and current issues. *Analytical chemistry*, 2009. 81(12): 4645-4677.
5. Stefanakis, A.I. and J.A. Becker, A review of emerging contaminants in water: classification, sources, and potential risks. *Impact of Water Pollution on Human Health and Environmental Sustainability*, 2016: 55-80.
6. Birkett, J. W., & Lester, J. N. (Eds.). *Endocrine disruptors in wastewater and sludge treatment processes*. 2002, IWA Publishing.
7. Song, W., et al., Determination of amprolium, carbadox, monensin, and tylosin in surface water by liquid chromatography/tandem mass spectrometry. *Rapid Communications in Mass Spectrometry: An International Journal Devoted to the Rapid Dissemination of Up-to-the-Minute Research in Mass Spectrometry*, 2007. 21(12): 1944-1950.
8. FDA, U.S. Pharmacologic Class. Available from: <https://www.fda.gov/industry/structured-product-labeling-resources/pharmacologic-class>. Accessed on 03/27/2018.
9. Bauer, M., et al., Levothyroxine effects on depressive symptoms and limbic glucose metabolism in bipolar disorder: a randomized, placebo-controlled positron emission tomography study. *Molecular psychiatry*, 2016. 21(2): 229-236.
10. European Commission, Commission Implementing Decision (EU) 2015/495 of 20 March 2015 establishing a watch list of substances for Union-wide monitoring in the field of water policy pursuant to Directive 2008/105/EC of the European Parliament and of the Council. *Off. J. Eur. Union L*, 2015. 78: 40-42.
11. European Commission, Commission Implementing Decision (EU) 2018/840 of 5 June 2018 establishing a watch list of substances for Union-wide monitoring in the field of water policy pursuant to Directive 2008/105/EC of the European Parliament and of the Council. *Off. J. Eur. Union L*, 2018. 141: 9-12.
12. European Commission, Commission Implementing Decision (EU) 2020/1161 of 4 August 2020 establishing a watch list of substances for Union-wide monitoring in the field of water policy pursuant to Directive 2008/105/EC of the European Parliament and of the Council. *Off. J. Eur. Union L*, 2020. 257: 32-35.
13. Caban, M. and P. Stepnowski, How to decrease pharmaceuticals in the environment? A review. *Environmental Chemistry Letters*, 2021: 1-24.
14. González-Plaza, J. J., Blau, K., Milaković, M., Jurina, T., Smalla, K., & Udiković-Kolić, N. Antibiotic-manufacturing sites are hot-spots for the release and spread of antibiotic resistance genes and mobile genetic elements in receiving aquatic environments. *Environment international*, 2019: 130, 104735.
15. Vystavna, Y., Frkova, Z., Celle-Jeanton, H., Diadin, D., Huneau, F., Steinmann, M., ... & Loup, C., Priority substances and emerging pollutants in urban rivers in Ukraine: occurrence, fluxes and loading to transboundary European Union watersheds. *Science of the Total Environment*, 2018. 637: 1358-1362.
16. Mudgal, S., De Toni, A., Lockwood, S., Salès, K., Backhaus, K., Sorensen, B.H. Study on the environmental risks of medicinal products, Final Report prepared for Executive Agency for Health and Consumers. 2013, *BIO Intelligence Service*.

17. Chander, V., Sharma, B., Negi, V., Aswal, R., Singh, P., Singh, R., & Dobhal, R., Pharmaceutical compounds in drinking water. *Journal of xenobiotics*, 2016. 6(1): 1-7.
18. de Jongh, C. M., Kooij, P. J., de Voogt, P., & ter Laak, T. L., Screening and human health risk assessment of pharmaceuticals and their transformation products in Dutch surface waters and drinking water. *Science of the Total Environment*, 2012. 427: 70-77.
19. Grabicova, K., Lindberg, R. H., Östman, M., Grabic, R., Randak, T., Larsson, D. J., & Fick, J., Tissue-specific bioconcentration of antidepressants in fish exposed to effluent from a municipal sewage treatment plant. *Science of the Total Environment*, 2014. 488: 46-50.
20. Jureczko, M. and J. Kalka, Cytostatic pharmaceuticals as water contaminants. *European journal of pharmacology*, 2020. 866: 172816.
21. aus der Beek, T., Weber, F. A., Bergmann, A., Hickmann, S., Ebert, I., Hein, A., & Küster, A., Pharmaceuticals in the environment—Global occurrences and perspectives. *Environmental toxicology and chemistry*, 2016. 35(4): 823-835.
22. Tiwari, B., Sellamuthu, B., Ouarda, Y., Drogui, P., Tyagi, R. D., & Buelna, G., Review on fate and mechanism of removal of pharmaceutical pollutants from wastewater using biological approach. *Bioresource technology*, 2017. 224: 1-12.
23. Alfonso-Muniozguren, P., Serna-Galvis, E. A., Bussemaker, M., Torres-Palma, R. A., & Lee, J., et al., A review on pharmaceuticals removal from waters by single and combined biological, membrane filtration and ultrasound systems. *Ultrasonics Sonochemistry*, 2021. 76.
24. Jayasiri, H., C. Purushothaman, and A. Vennila, Pharmaceutically active compounds (PhACs): a threat for aquatic environment. National aquatic resources research and development agency, Crow Island, Sri Lanka, 2013.
25. Rathore, H.S. and L.M. Nollet, Pesticides: evaluation of environmental pollution. 2012: CRC press.
26. Tripathi, A. K., David, A., Govil, T., Rauniyar, S., Rathinam, N. K., Goh, K. M., & Sani, R. K., Environmental remediation of antineoplastic drugs: present status, challenges, and future directions. *Processes*, 2020. 8(7): 747.
27. Lin, A.Y.-C., X.-H. Wang, and W.-N. Lee, Phototransformation determines the fate of 5-fluorouracil and cyclophosphamide in natural surface waters. *Environmental science & technology*, 2013. 47(9): 4104-4112.
28. Vione, D., Khanra, S., Man, S. C., Maddigapu, P. R., Das, R., Arsene, C., ... & Minero, C., Inhibition vs. enhancement of the nitrate-induced phototransformation of organic substrates by the •OH scavengers bicarbonate and carbonate. *Water research*, 2009. 43(18): 4718-4728.
29. Gómez, M. J., Sirtori, C., Mezcua, M., Fernández-Alba, A. R., & Agüera, A., Photodegradation study of three dipyrone metabolites in various water systems: Identification and toxicity of their photodegradation products. *Water research*, 2008. 42(10-11): 2698-2706.
30. Gros, M., Williams, M., Llorca, M., Rodriguez-Mozaz, S., Barceló, D., & Kookana, R. S., Photolysis of the antidepressants amisulpride and desipramine in wastewaters: Identification of transformation products formed and their fate. *Science of the Total Environment*, 2015. 530: 434-444.
31. Kümmerer, K., A. Al-Ahmad, and V. Mersch-Sundermann, Biodegradability of some antibiotics, elimination of the genotoxicity and affection of wastewater bacteria in a simple test. *Chemosphere*, 2000. 40(7): 701-710.
32. Osawa, R. A., Barrocas, B. T., Monteiro, O. C., Oliveira, M. C., & Florêncio, M. H., Photocatalytic degradation of cyclophosphamide and ifosfamide: Effects of wastewater matrix, transformation products and in silico toxicity prediction. *Science of The Total Environment*, 2019. 692: 503-510.
33. Trawiński, J. and R. Skibiński, Studies on photodegradation process of psychotropic drugs: a review. *Environmental Science and Pollution Research*, 2017. 24(2): 1152-1199.
34. Trawiński, J., Szpot, P., Zawadzki, M., & Skibiński, R., Photochemical transformation of fentanyl under the simulated solar radiation—Enhancement of the process by heterogeneous photocatalysis and in silico analysis of toxicity. *Science of The Total Environment*, 2021. 791: 148171.

35. Mathon, B., Ferreol, M., Coquery, M., Choubert, J. M., Chovelon, J. M., & Miege, C., Direct photodegradation of 36 organic micropollutants under simulated solar radiation: Comparison with free-water surface constructed wetland and influence of chemical structure. *Journal of Hazardous Materials*, 2021. 407: 124801.
36. Lutterbeck, C. A., Baginska, E., Machado, Ê. L., & Kümmerer, K., Removal of the anti-cancer drug methotrexate from water by advanced oxidation processes: aerobic biodegradation and toxicity studies after treatment. *Chemosphere*, 2015. 141: 290-296.
37. Daughton, C.G., The Matthew Effect and widely prescribed pharmaceuticals lacking environmental monitoring: Case study of an exposure-assessment vulnerability. *Science of the Total Environment*, 2014. 466: 315-325.
38. Negreira, N., M.L. de Alda, and D. Barceló, Cytostatic drugs and metabolites in municipal and hospital wastewaters in Spain: filtration, occurrence, and environmental risk. *Science of the Total Environment*, 2014. 497: 68-77.
39. Silva, S., Rodrigues, J. A., Coelho, M. R., Martins, A., Cardoso, E., Cardoso, V. V., ... & Almeida, C. M., Occurrence of pharmaceutical active compounds in sewage sludge from two urban wastewater treatment plants and their potential behaviour in agricultural soils. *Environmental Science: Water Research & Technology*, 2021. 7(5): 969-982.
40. Hollender, J., Zimmermann, S. G., Koepke, S., Krauss, M., McArdell, C. S., Ort, C., ... & Siegrist, H., Elimination of organic micropollutants in a municipal wastewater treatment plant upgraded with a full-scale post-ozonation followed by sand filtration. *Environmental Science & Technology*, 2009. 43(20): 7862-7869.
41. Gros, M., Petrović, M., Ginebreda, A., & Barceló, D., Removal of pharmaceuticals during wastewater treatment and environmental risk assessment using hazard indexes. *Environment International*, 2010. 36(1): 15-26.
42. Bueno, M. M., Gomez, M. J., Herrera, S., Hernando, M. D., Agüera, A., & Fernández-Alba, A. R., Occurrence and persistence of organic emerging contaminants and priority pollutants in five sewage treatment plants of Spain: two years pilot survey monitoring. *Environmental Pollution*, 2012. 164: 267-273.
43. Loos, R., Carvalho, R., António, D. C., Comero, S., Locoro, G., Tavazzi, S., ... & Gawlik, B. M., EU-wide monitoring survey on emerging polar organic contaminants in wastewater treatment plant effluents. *Water research*, 2013. 47(17): 6475-6487.
44. Vieno, N., Hallgren, P., Wallberg, P., Pyhälä, M., Zandaryaa, S., & Baltic Marine Environment Protection Commission, Pharmaceuticals in the aquatic environment of the Baltic Sea region: a status report. Vol. 1. 2017: UNESCO Publishing.
45. Preisner, M., Surface water pollution by untreated municipal wastewater discharge due to a sewer failure. *Environmental Processes*, 2020. 7(3): 767-780.
46. Wang, Q., P. Wang, and Q. Yang, Occurrence and diversity of antibiotic resistance in untreated hospital wastewater. *Science of the Total Environment*, 2018. 621: 990-999.
47. Azuma, T., Otomo, K., Kunitou, M., Shimizu, M., Hosomaru, K., Mikata, S., ... & Hayashi, T., Environmental fate of pharmaceutical compounds and antimicrobial-resistant bacteria in hospital effluents, and contributions to pollutant loads in the surface waters in Japan. *Science of the Total Environment*, 2019. 657: 476-484.
48. Kondor, A. C., Molnár, É., Vancsik, A., Filep, T., Szeberényi, J., Szabó, L., ... & Szalai, Z., Occurrence, and health risk assessment of pharmaceutically active compounds in riverbank filtrated drinking water. *Journal of Water Process Engineering*, 2021. 41: 102039.
49. Jameel, Y., D. Valle, and P. Kay, Spatial variation in the detection rates of frequently studied pharmaceuticals in Asian, European, and North American rivers. *Science of The Total Environment*, 2020. 724: 137947.
50. Fuentes, A.V., M.D. Pineda, and K.C.N. Venkata, Comprehension of top 200 prescribed drugs in the US as a resource for pharmacy teaching, training, and practice. *Pharmacy*, 2018. 6(2): 43.

51. Letsinger, S. and P. Kay, Comparison of Prioritization Schemes for Human Pharmaceuticals in the Aquatic Environment. *Environmental Science & Pollution Research International*, 2019. 26(4): 3479-3491.
52. Hughes, S.R., P. Kay, and L.E. Brown, Global synthesis and critical evaluation of pharmaceutical data sets collected from river systems. *Environmental Science & Technology*, 2013. 47(2): 661-677.
53. Fekadu, S., Alemayehu, E., Dewil, R., & Van der Bruggen, B., Pharmaceuticals in freshwater aquatic environments: A comparison of the African and European challenge. *Science of the Total Environment*, 2019. 654: 324-337.
54. Kruć, R., K. Dragon, and J. Górski, Migration of pharmaceuticals from the Warta River to the aquifer at a riverbank filtration site in Krajkowo (Poland). *Water*, 2019. 11(11): 2238.
55. Styszko, K., Proctor, K., Castrignanò, E., & Kasprzyk-Hordern, B., Occurrence of pharmaceutical residues, personal care products, lifestyle chemicals, illicit drugs and metabolites in wastewater and receiving surface waters of Krakow agglomeration in South Poland. *Science of the Total Environment*, 2021. 768: 144360.
56. Pereira, A., Silva, L., Laranjeiro, C., & Pena, A., Assessment of Human Pharmaceuticals in Drinking Water Catchments, Tap and Drinking Fountain Waters. *Applied Sciences*, 2021. 11(15): 7062.
57. Pinasseau, L., Wiest, L., Volatier, L., Mermillod-Blondin, F., & Vulliet, E., Emerging polar pollutants in groundwater: Potential impact of urban stormwater infiltration practices. *Environmental Pollution*, 2020. 266: 115387.
58. Chiffre, A., Degiorgi, F., Buleté, A., Spinner, L., & Badot, P. M., Occurrence of pharmaceuticals in WWTP effluents and their impact in a karstic rural catchment of Eastern France. *Environmental Science and Pollution Research*, 2016. 23(24): 25427-25441.
59. Chen, X., Lei, L., Liu, S., Han, J., Li, R., Men, J., ... & Zhu, L., Occurrence and risk assessment of pharmaceuticals and personal care products (PPCPs) against COVID-19 in lakes and WWTP-river-estuary system in Wuhan, China. *Science of The Total Environment*, 2021: 148352.
60. Castillo-Zacarías, C., Barocio, M. E., Hidalgo-Vázquez, E., Sosa-Hernández, J. E., Parra-Arroyo, L., López-Pacheco, I. Y., ... & Parra-Saldívar, R., Antidepressant drugs as emerging contaminants: Occurrence in urban and non-urban waters and analytical methods for their detection. *Science of the Total Environment*, 2021. 757: 143722.
61. Sharma, B. M., Bečanová, J., Scheringer, M., Sharma, A., Bharat, G. K., Whitehead, P. G., ... & Nizzetto, L., Health and ecological risk assessment of emerging contaminants (pharmaceuticals, personal care products, and artificial sweeteners) in surface and groundwater (drinking water) in the Ganges River Basin, India. *Science of the Total Environment*, 2019. 646: 1459-1467.
62. Simazaki, D., Kubota, R., Suzuki, T., Akiba, M., Nishimura, T., & Kunikane, S., Occurrence of selected pharmaceuticals at drinking water purification plants in Japan and implications for human health. *Water research*, 2015. 76: 187-200.
63. Jiang, X., Qu, Y., Liu, L., He, Y., Li, W., Huang, J., ... & Yu, G., PPCPs in a drinking water treatment plant in the Yangtze River Delta of China: Occurrence, removal, and risk assessment. *Frontiers of Environmental Science & Engineering*, 2019. 13(2): 27.
64. Gabarrón, S., Gernjak, W., Valero, F., Barceló, A., Petrovic, M., & Rodríguez-Roda, I., Evaluation of emerging contaminants in a drinking water treatment plant using electro dialysis reversal technology. *Journal of Hazardous Materials*, 2016. 309: 192-201.
65. Ślósarczyk, K., Jakóbczyk-Karpierz, S., Rózkowski, J., & Witkowski, A. J., Occurrence of Pharmaceuticals and Personal Care Products in the Water Environment of Poland: A Review. *Water*, 2021. 13(16): 2283.
66. Aristizabal-Ciro, C., Botero-Coy, A. M., López, F. J., & Peñuela, G. A., Monitoring pharmaceuticals and personal care products in reservoir water used for drinking water supply. *Environmental Science and Pollution Research*, 2017. 24(8): 7335-7347.
67. Wu, M., Xiang, J., Que, C., Chen, F., & Xu, G., Occurrence and fate of psychiatric pharmaceuticals in the urban water system of Shanghai, China. *Chemosphere*, 2015. 138: 486-493.

68. Papagiannaki, D., Morgillo, S., Bocina, G., Calza, P., & Binetti, R., Occurrence and Human Health Risk Assessment of Pharmaceuticals and Hormones in Drinking Water Sources in the Metropolitan Area of Turin in Italy. *Toxics*, 2021. 9(4): 88.
69. González Peña, O.I., M.Á. López Zavala, and H. Cabral Ruelas, Pharmaceuticals Market, Consumption Trends and Disease Incidence Are Not Driving the Pharmaceutical Research on Water and Wastewater. *International Journal of Environmental Research and Public Health*, 2021. 18(5): 2532.
70. Cristóvão, M. B., Janssens, R., Yadav, A., Pandey, S., Luis, P., Van der Bruggen, B., ... & Pereira, V. J., Predicted concentrations of anticancer drugs in the aquatic environment: What should we monitor and where should we treat? *Journal of Hazardous Materials*, 2020. 392: 122330.
71. Ferlay, J., Steliarova-Foucher, E., Lortet-Tieulent, J., Rosso, S., Coebergh, J. W. W., Comber, H., ... & Bray, F., Cancer incidence and mortality patterns in Europe: Estimates for 40 countries in 2012. *European Journal of Cancer*, 2013. 49(6): 1374-1403.
72. Ferlay, J., Colombet, M., Soerjomataram, I., Dyba, T., Randi, G., Bettio, M., ... & Bray, F., Cancer incidence and mortality patterns in Europe: Estimates for 40 countries and 25 major cancers in 2018. *European Journal of Cancer*, 2018. 103: 356-387.
73. Besse, J.-P., J.-F. Latour, and J. Garric, Anticancer drugs in surface waters: what can we say about the occurrence and environmental significance of cytotoxic, cytostatic and endocrine therapy drugs? *Environment International*, 2012. 39(1): 73-86.
74. Booker, V., Halsall, C., Llewellyn, N., Johnson, A., & Williams, R., Prioritising anticancer drugs for environmental monitoring and risk assessment purposes. *Science of the Total Environment*, 2014. 473: 159-170.
75. Santos, M. S., Franquet-Griell, H., Lacorte, S., Madeira, L. M., & Alves, A., Anticancer drugs in Portuguese surface waters—estimation of concentrations and identification of potentially priority drugs. *Chemosphere*, 2017. 184: 1250-1260.
76. Franquet-Griell, H., Gómez-Canela, C., Ventura, F., & Lacorte, S., Anticancer drugs: consumption trends in Spain, prediction of environmental concentrations and potential risks. *Environmental Pollution*, 2017. 229: 505-515.
77. Gustavsson, M., Molander, S., Backhaus, T., & Kristiansson, E., Estimating the release of chemical substances from consumer products, textiles, and pharmaceuticals to wastewater. *Chemosphere*, 2022. 287: 131854.
78. WHO collaborating center for drug statistics methodology. ATC/DDD index 2020. Available from: https://www.whocc.no/atc_ddd_index/. Accessed on 17-12-2020.
79. Nassour, C., Barton, S. J., Nabhani-Gebara, S., Saab, Y., & Barker, J., Occurrence of anticancer drugs in the aquatic environment: a systematic review. *Environmental Science and Pollution Research*, 2020. 27(2): 1339-1347.
80. Santos, L. H., Araújo, A. N., Fachini, A., Pena, A., Delerue-Matos, C., & Montenegro, M. C. B. S. M., Ecotoxicological aspects related to the presence of pharmaceuticals in the aquatic environment. *Journal of Hazardous Materials*, 2010. 175(1-3): 45-95.
81. Kovalova, L., C.S. McArdeall, and J. Hollender, Challenge of high polarity and low concentrations in analysis of cytostatics and metabolites in wastewater by hydrophilic interaction chromatography/tandem mass spectrometry. *Journal of Chromatography A*, 2009. 1216(7): 1100-1108.
82. Yin, J., Shao, B., Zhang, J., & Li, K., A preliminary study on the occurrence of cytostatic drugs in hospital effluents in Beijing, China. *Bulletin of Environmental Contamination and Toxicology*, 2010. 84(1): 39-45.
83. Martín, J., Camacho-Muñoz, D., Santos, J. L., Aparicio, I., & Alonso, E., Simultaneous determination of a selected group of cytostatic drugs in water using high-performance liquid chromatography–triple-quadrupole mass spectrometry. *Journal of Separation Science*, 2011. 34(22): 3166-3177.

84. Rabii, F. W., Segura, P. A., Fayad, P. B., & Sauvé, S., Determination of six chemotherapeutic agents in municipal wastewater using online solid-phase extraction coupled to liquid chromatography-tandem mass spectrometry. *Science of the Total Environment*, 2014. 487: 792-800.
85. Buerge, I. J., Buser, H. R., Poiger, T., & Müller, M. D., Occurrence and fate of the cytostatic drugs cyclophosphamide and ifosfamide in wastewater and surface waters. *Environmental Science & Technology*, 2006. 40(23): 7242-7250.
86. Valcárcel, Y., Alonso, S. G., Rodríguez-Gil, J. L., Gil, A., & Catalá, M., Detection of pharmaceutically active compounds in the rivers and tap water of the Madrid Region (Spain) and potential ecotoxicological risk. *Chemosphere*, 2011. 84(10): 1336-1348.
87. Isidori, M., Lavorgna, M., Russo, C., Kundi, M., Žegura, B., Novak, M., ... & Heath, E., Chemical and toxicological characterisation of anticancer drugs in hospital and municipal wastewaters from Slovenia and Spain. *Environmental Pollution*, 2016. 219: 275-287.
88. Ferrando-Climent, L., S. Rodríguez-Mozaz, and D. Barceló, Development of a UPLC-MS/MS method for the determination of ten anticancer drugs in hospital and urban wastewaters, and its application for the screening of human metabolites assisted by information-dependent acquisition tool (IDA) in sewage samples. *Analytical and Bioanalytical Chemistry*, 2013. 405(18): 5937-5952.
89. Fáberová, M., Bodík, I., Ivanová, L., Grabic, R., & Mackuľak, T., Frequency and use of pharmaceuticals in selected Slovakian town via wastewater analysis. *Monatshefte für Chemie-Chemical Monthly*, 2017. 148(3): 441-448.
90. Negreira, N., M.L. de Alda, and D. Barceló, On-line solid phase extraction-liquid chromatography-tandem mass spectrometry for the determination of 17 cytostatics and metabolites in waste, surface and ground water samples. *Journal of Chromatography A*, 2013. 1280: 64-74.
91. Singer, H. P., Wössner, A. E., Mc Ardell, C. S., & Fenner, K., Rapid screening for exposure to “non-target” pharmaceuticals from wastewater effluents by combining HRMS-based suspect screening and exposure modeling. *Environmental Science & Technology*, 2016. 50(13): 6698-6707.
92. Calza, P., Medana, C., Padovano, E., Giancotti, V., & Minero, C., Fate of selected pharmaceuticals in river waters. *Environmental Science and Pollution Research*, 2013. 20(4): 2262-2270.
93. Lopes, D. G., Duarte, I. A., Antunes, M., & Fonseca, V. F., Effects of antidepressants in the reproduction of aquatic organisms: a meta-analysis. *Aquatic Toxicology*, 2020. 227: 105569.
94. Laurent, S., Antihypertensive drugs. *Pharmacological Research*, 2017. 124: 116-125.
95. Gros, M., S. Rodríguez-Mozaz, and D. Barceló, Fast and comprehensive multi-residue analysis of a broad range of human and veterinary pharmaceuticals and some of their metabolites in surface and treated waters by ultra-high-performance liquid chromatography coupled to quadrupole-linear ion trap tandem mass spectrometry. *Journal of Chromatography A*, 2012. 1248: 104-121.
96. Boix, C., Ibáñez, M., Sancho, J. V., Rambla, J., Aranda, J. L., Ballester, S., & Hernández, F., Fast determination of 40 drugs in water using large volume direct injection liquid chromatography-tandem mass spectrometry. *Talanta*, 2015. 131: 719-727.
97. Petrie, B. and R. Barden, Kasprzyk/Hordern B. A review on emerging contaminants in wastewaters and the environment: Current knowledge, understanding areas and recommendations for future monitoring. *Water research*, 2015. 72: 3-27.
98. Duggan, S., C. Chwieduk, and M. Curran, Erratum to: Aliskiren: a review of its use as monotherapy and as combination therapy in the management of hypertension. *Drugs*, 2011. 71(10): 1280-1280.
99. Waldmeier, F., Glaenzel, U., Wirz, B., Oberer, L., Schmid, D., Seiberling, M., ... & Vaidyanathan, S., Absorption, distribution, metabolism, and elimination of the direct renin inhibitor aliskiren in healthy volunteers. *Drug Metabolism and Disposition*, 2007. 35(8): 1418-1428.
100. Boulard, L., Dierkes, G., Schlüsener, M. P., Wick, A., Koschorreck, J., & Ternes, T. A., Spatial distribution, and temporal trends of pharmaceuticals sorbed to suspended particulate matter of German rivers. *Water research*, 2020. 171: 115366.
101. Cunha, D.L., F.G. de Araujo, and M. Marques, Psychoactive drugs: occurrence in aquatic environment, analytical methods, and ecotoxicity—a review. *Environmental Science and Pollution Research*, 2017. 24(31): 24076-24091.

102. Esteban, S., Valcárcel, Y., Catalá, M., & Castromil, M. G., Psychoactive pharmaceutical residues in the watersheds of Galicia (Spain). *Gaceta Sanitaria*, 2012. 26(5): 457-459.
103. Yang, M., Liu, S., Hu, L., Zhan, J., Lei, P., & Wu, M., Effects of the antidepressant, mianserin, on early development of fish embryos at low environmentally relevant concentrations. *Ecotoxicology and Environmental Safety*, 2018. 150: 144-151.
104. Mezzelani, M., Fattorini, D., Gorbi, S., Nigro, M., & Regoli, F., Human pharmaceuticals in marine mussels: Evidence of sneaky environmental hazard along Italian coasts. *Marine Environmental Research*, 2020. 162: 105137.
105. Aronson, J.K., Meyler's side effects of drugs: the international encyclopedia of adverse drug reactions and interactions. 2015: Elsevier.
106. Gonçalves, N. P., Iezzi, L., Belay, M. H., Dulio, V., Alygizakis, N., Dal Bello, F., ... & Calza, P., Elucidation of the photoinduced transformations of Aliskiren in river water using liquid chromatography high-resolution mass spectrometry. *Science of the Total Environment*, 2021: 149547.
107. Gonçalves, N. P., Varga, Z., Bouchonnet, S., Dulio, V., Alygizakis, N., Dal Bello, F., ... & Calza, P., Study of the photoinduced transformations of maprotiline in river water using liquid chromatography high-resolution mass spectrometry. *Science of the Total Environment*, 2021. 755: 143556.

CHAPTER 2

Methods Development and Validation: Theoretical and Practical Considerations

2. METHODS DEVELOPMENT AND VALIDATION: THEORETICAL AND PRACTICAL CONSIDERATIONS

2.1 Analysis of PhACs in water samples

Analysis of PhACs in aqueous systems involves a wide range of samples, including surface waters (rivers, streams, lakes, reservoirs, ponds, canals, etc.), groundwater, drinking water, rainwater, wastewaters (industrial and municipal), and process water. Sampling, preparation, and analysis of these diverse types of water, which may differ not just in terms of the contaminants present, but also the pollution level, requires careful planning and execution. Surface water and groundwater with low pollution levels generally require less time-consuming sample preparation than more complex samples such as wastewater effluents. Compared to, for example, biological samples, matrix components are less prevalent in aqueous samples, and sample preparation for water samples is often limited to the extraction of specific contaminants from the aqueous sample. Additional cleanup is less important for water analysis and is usually only required for highly polluted samples or in ultra-trace analysis. Many standardized methods of water analysis require the removal of suspended particles through a filtration step using, e.g., a 0.7 μm fiberglass filter, as a first step in the sample preparation procedure. It is important to remember that hydrophobic compounds may be adsorbed onto the suspended phase and that such treatments should be conducted with utmost caution to avoid analyte loss.

In recent years, there has been a greater emphasis on the development and application of generic multi-residue methods that allow simultaneous analysis of multiple-class PhACs in different water matrices [1-3]. In addition to the time and cost savings, these methods provide information on a large number and class of PhACs and help in our understanding of their occurrence, removal, and fate in the aqueous system. Simultaneous analysis of compounds from different groups with varying physicochemical properties, on the other hand, necessitates a compromise in the experimental conditions for sample preparation, chromatographic separation, and mass spectrometric detection.

2.2 LC-MS method development and validation

Since mass spectrometry (MS) gained general acceptance for routine use in the 1950s, it has shown to be a powerful technique for separating organic compounds based on their molecular mass and for detecting and quantifying them with high sensitivity. High performance liquid chromatography (HPLC), which emerged in the 1970s, enables the fast and efficient

separation of compounds from one another as well as from other components of complex matrices. By combining these two techniques, LC-MS offers a unique capacity for fast and efficient quantification of organic compounds for a wide range of applications. Nonetheless, developing effective interfaces to combine these two techniques was not straightforward, and it is only in the last three decades that LC-MS has risen in popularity. Nowadays, LC-MS has gained popularity in many qualitative and quantitative analysis activities thanks to the remarkable achievements over the years such as reduced size and cost of the instrumentation, shorter learning curve for users due to software and automation, and enhanced sensitivity and multiple modes of operation. Recent advancements have also seen LC-MS techniques improve their capabilities, particularly for reliable quantitative analyses of analytes in complex matrices or at trace quantities.

LC-MS is popular in several applications due to the following benefits:

- **Sensitivity:** mass spectrometry is a highly sensitive technique by nature. Moreover, noise reduction as a result of improved selectivity facilitates detection of very low concentrations in the pg/L range.
- **Selectivity:** combining LC and MS in tandem (LC-MSⁿ) enables the analysis of complex mixtures with a reliable selectivity and confidence for isolating a particular compound or group of compounds. MS separates the compounds based on their mass-to-charge ratio (m/z). Compounds that may not separate by LC can be separated by their m/z difference with the help of stable isotopically labelled internal standards, which are also useful for controlling method variability.
- **Speed:** because the MS identifies compounds by their mass, the LC does not need to separate every single component in the sample, allowing for co-elution of non-isobaric compounds. This helps in achieving faster LC analyses and less sample preparation, both of which are important aspects of high throughput method development.

However, LC-MS systems are not for everyone. Despite the remarkable advancements achieved in the last few years, they do have some limitations that prevent them from being acquired and used by everyone. These include: (i) high expenses for purchasing, operating, maintaining the system, (2) increased complexity, particularly in managing the MS ionization, and (3) a limited dynamic range as compared to other quantitative techniques.

The typical workflow for LC-MS/MS is illustrated in Fig. 2.1. The development of an LC-MS/MS method usually involves the development of three interdependent methods separately: sample preparation, LC, and MS. Since modifications in one technique can affect the others, developing an effective LC-MS/MS system integrating these three techniques may

require repeating each optimization step in a cycle. Hence, the method development process begins with multiple repetitions and proceeds with testing and fine-tuning the method until the final optimal version is achieved.

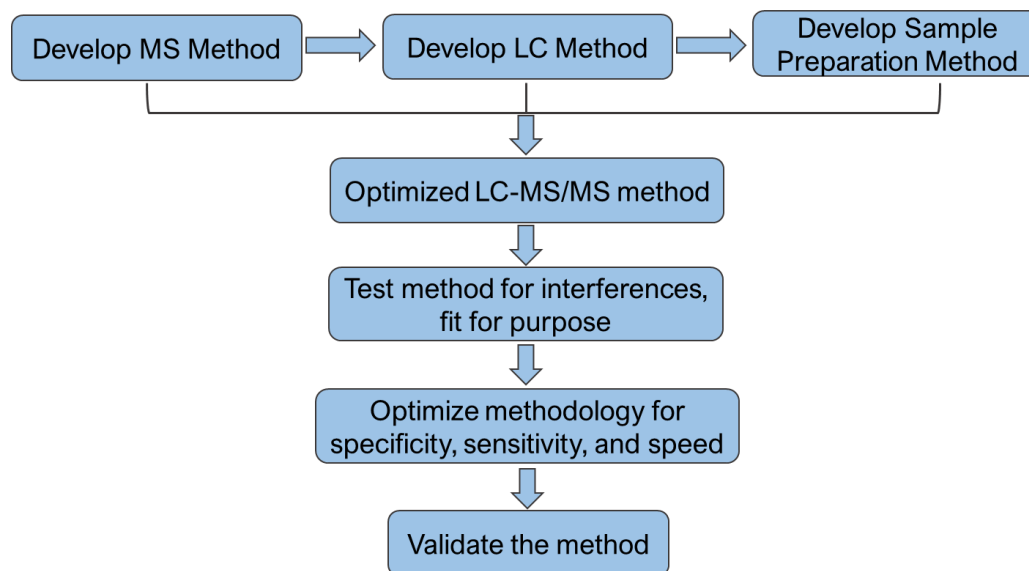


Figure 2.1. Overview of LC-MS/MS method development workflow

2.2.1 MS/MS method development

When developing a new LC-MS/MS method, it starts with the evaluation of the MS response followed by development of a multiple reaction monitoring (MRM) acquisition method that gives the best MS settings for detecting the target compounds. The MRM method can be optimized by injecting individual standards of each target compound and reviewing MS the response manually, automatically, or a combination of both [3]. During the MS optimization process for a target compound, it is important to evaluate: (i) if the molecule of interest is detectable by MS without requiring chemical modification, (ii) the most efficient ionization mode such as electrospray (ESI) or atmospheric pressure chemical (APCI), and (iii) the polarity – positive or negative – that offers the best response. Thus, the MS optimization requires a series of repetitions to arrive at the optimal set of conditions, which is often a time-consuming process. In addition to the ability to execute automatic MRM optimization, modern LC-MS instruments support rapid switching between ionization modes, as well as positive and negative polarity modes.

ESI has grown in popularity over the last three decades, and it is now arguably the most extensively utilized ionization technique in research involving separation with LC. In comparison to other ionization techniques such as electron impact (EI), ESI is a “soft”

ionization technique since it results in little to no fragmentation. ESI has several advantages. It is soft and efficient ionization approach, which results in minimal breakdown of labile analytes and produces only molecular ions in most cases. Additionally, multicharged analytes $[M+zH]^{z+}$ may be easily generated, allowing for the analysis of proteins. Moreover, the simple coupling with liquid chromatography (LC) permits the simultaneous separation of complex mixtures prior to MS, extending its applicability to a broad range of analytes.

Fig. 2.2 illustrates the operational notions of the ESI source. The fundamental concepts underlying the working principles of ESI sources have been discussed in numerous comprehensive reviews [4, 5]. The following is a concise summary of the most frequently used ESI positive ion mode, in which the potential is positive relative to ground. At atmospheric pressure, ESI transforms analyte solution infused into a metal capillary with a potential of several kV to gas-phase ions. Typical infusion rates (up to several hundred $\mu\text{l}/\text{min}$) are well within LC's capability. The fluid is deformed into a Taylor cone at the capillary tip [6], which discharges a fine mist of droplets, which is typically assisted by a coaxial gas flow. Each droplet contains surplus ions such as H^+ , NH_4^+ , Na^+ , and K^+ . Protons frequently account for the majority of the net droplet charge, owing to the acidity of many analyte solutions. The ESI source is analogous to an electrochemical cell where numerous charge-balancing events occur. The circuit is powered by the movement of ions and charged droplets in the gas phase, as well as by electron flow through the wires connecting the ESI capillary (anode) to the mass spectrometer (cathode).

Rapid solvent evaporation occurs in the droplets released by the Taylor cone, which is frequently aided by heating. When aqueous/organic mixes are combined, the organic component often evaporates more quickly, resulting in a progressive increase in the water proportion. The charge density of the shrinking droplets increases until Coulombic repulsion balances the surface tension. At this so-called Rayleigh limit [7], droplets undergo jet fission and create even smaller and more charged daughter droplets. The final creation of ESI droplets with radii of a few nanometers is the result of repeated evaporation/fission operations. These highly charged nanodroplets generate gaseous analyte ions that may be identified by mass spectrometry.

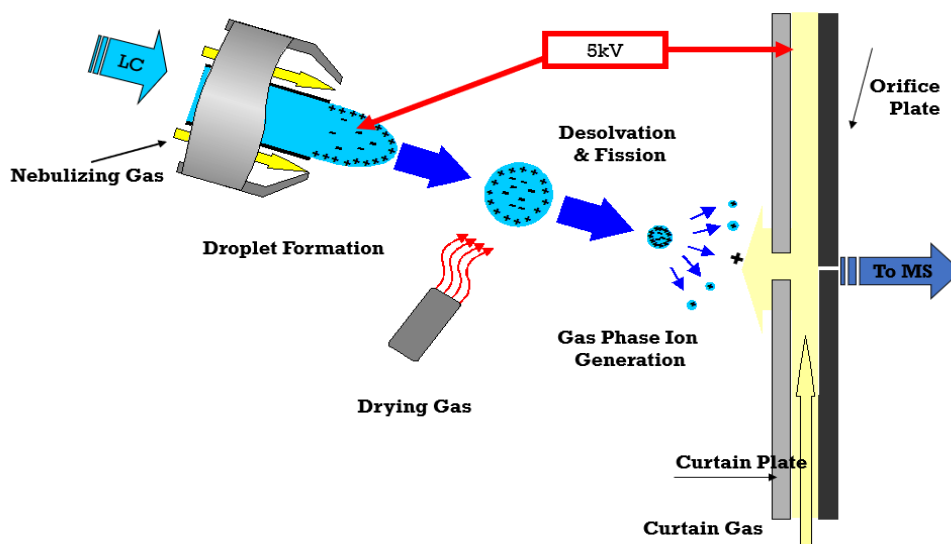


Figure 2.2. Overview of the ESI operational principles

To ensure the development of a highly sensitive and robust MS/MS method, several source and compound-dependent parameters must be optimized. For example, MRM method development on a Sciex 3200 QTRAP LC-MS/MS system (Fig. 2.3) allows the optimization of source parameters including ionization mode, IonSpray Voltage (IS), the nebulizer gas pressure Ion Source Gas 1 (GS1), the heater gas pressure Ion Source Gas 2 (GS2), Temperature (TEMP), Curtain Gas (CUR), and Interface Heater (ihe, ON/OFF). Once the precursor ion is determined, precursor-product (MRM) transitions can be optimized by tuning collision energy. However, it is important to note that other parameters can also be optimized, depending on the instrument type and manufacturer. For the 3200 QTRAP system, additional compound-dependent potentials can be optimized, which include the Declustering Potential (DP), Entrance Potential (EP), Collision Energy (CE), Collision Energy Spread (CES), and Collision Cell Exit Potential (CXP).

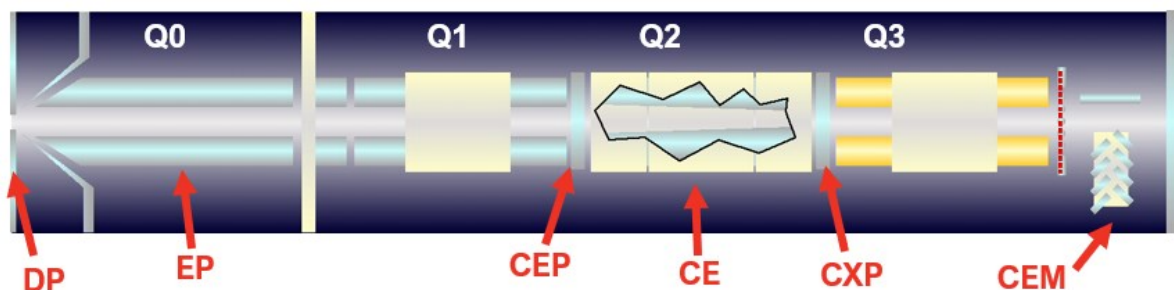


Figure 2.3. Configuration of the hybrid Sciex 3200 QTRAP system

2.2.2 HPLC method development

Developing an HPLC method involves conducting a set of tests to find the optimal separation conditions that fulfill the requirements set for the linearity, range, detection limit, quantitation limit, accuracy, precision, specificity, and robustness. Factors such as the analytical column, mobile phase components, and pH will all have an impact on the process. Thus, a systematic approach to LC method development can significantly simplify the process and allow the realization of optimal separation conditions rapidly.

The first step in LC method development is screening for retention of target compounds by the analytical column. For instance, a 50 x 2 mm C18 column can be used for screening retention of analytes at both low and high pH using methanol and acetonitrile separately with a 5 to 95% organic gradient over 2-4 min. Here, selection of a column suitable for the target compounds is critical. Given their excellent retention and suitability for various applications, C18 columns are generally the most popular, including for the analysis of PhACs in different aqueous matrices [8, 9]. Moreover, studies [10] have shown that using a short column, such as a 50 mm C18 column, permits for a faster run time with adequate resolution for all or most analytes. Often, analyte retention screening is followed by selection of the pH and organic solvent that provides the best retention, sensitivity, and selectivity for the analytes of interest. Optimization of the mobile phase gradient should be performed in order to achieve a rapid analysis time without compromising resolution and sensitivity. Moreover, it is important to evaluate any potential interferences from labware and matrix components. In some circumstances, successful chromatographic separation of all analytes can be challenging and time-consuming because it requires a series of trials.

2.1.1.1 Optimization of sample preparation

The cleanliness of the sample to be analyzed can have a significant influence on the performance of an LC method. The analytical method's reproducibility, repeatability, sensitivity, or throughput may be seriously compromised. Prior to submitting a sample for analysis, it is critical to have a thorough understanding of its nature. While simple sample pretreatment measures may be sufficient for some samples, optimal sample preparation methods will be necessary for the efficient removal of interferences from the sample matrix and concentration of the analytes of interest. Optimal sample preparation is critical when analyzing PhACs in aqueous samples, as they are frequently detected at extremely low concentrations, often requiring preconcentration. The typical challenges that an optimal sample preparation overcomes include complex sample matrices, inadequate recovery and

reproducibility, low sensitivity, ion suppression or enhancement, interfering peaks, the need to concentrate or reconstitute, and limited sample volume.

Extraction of aqueous samples needs to meet requirements such as high analyte enrichment, increased recovery, good accuracy and precision, and low detection limit [11]. However, the most common issue in water analysis is that samples prepared using exhaustive extraction procedures typically contain many matrix components, which may affect the quantitative analysis by interfering with the target analytes. Thus, sample pretreatment is applied to reduce the matrix components and enrich the target compounds. Often these lengthy and laborious extraction and clean-up procedures account for the largest portion of the analysis time. In addition, laboratories that conduct monitoring studies need to use completely automated high-throughput analytical methods to keep up with the frequently large number of samples they must analyze. As a result, much effort is being devoted to the development of low-cost sample handling approaches that benefit from efficiency and simplicity.

Regarding the trends in recent years, four general approaches to LC-MS analysis of PhACs in water samples can be identified: (i) offline SPE extraction of the target analytes followed by LC-MS analysis [12, 13], (ii) coupling the sample preparation units and detection systems to automate the process; the combination of on-line solid phase extraction (SPE) with LC-MS equipment is noteworthy in this second approach [2, 14], (iii) using customized sorbents such as molecular imprinted polymers, immunosorbents, and nanomaterials [15], and (iv) combining several sample preparation steps for simultaneous sampling, extraction, and enrichment [16]. It is worth noting that several recent studies such as those by Ng et. al. [3] Mosekiemang et. al. [17] have successfully implemented direct injection techniques and obtained results that are comparable to, for example, SPE extraction. Additionally, attempts aimed to overcome the drawbacks of the traditional liquid-liquid extraction applying, for example, ultrasound-assisted dispersive liquid-liquid microextraction have also emerged as viable alternatives [18, 19].

2.1.1.2 Solid phase extraction (SPE)

Concerning PhACs in water, the most widely used strategy involves extracting all target analytes simultaneously in a single SPE step, preferably by connecting it on-line to the LC-MS system [11]. The most recent ‘watch list’ of substances for EU-wide monitoring [20] stipulates LC-MS/MS for their analysis in water, with SPE as the sole sample preparation methodology for all compounds except for metaflumizone, which can also be extracted using LLE. In studies focusing PhACs evaluation in water, Oasis HLB cartridge is predominantly used for the extraction of pharmaceuticals with a wide range of polarities and pH values due to its

hydrophilic–lipophilic balance [13, 21]. Furthermore, because of its ability to adsorb neutral, polar, non-polar, and cationic compounds from aqueous media, the mixed-mode cation-exchanger Oasis MCX has also been widely used [12, 22].

The use of automated instruments that combine extraction, purification, and detection steps has become increasingly popular over the past years due to their numerous advantages, including increased accuracy and precision owing to minimal sample handling, low sample volume, and decreased solvent use. When it comes to on-line sample extraction coupled with LC–MS, several generic approaches have been developed using different extraction sorbents such as disposable or reusable cartridges, restricted access materials (RAM), large size particles or monolithic materials [2, 23]. Among these, on-line SPE combined with LC-MS is the most widely applied technique for the analysis of PhACs in water. Some recent applications for the analysis of multi-class PhACs in water samples include the determination of 12 pharmaceuticals together with 25 endocrine-disrupting compounds [14]. After testing various on-line SPE cartridges, the researchers discovered that the Oasis HLB loading column provided the best results, with quantification limits ranging from 0.25 to 10 ng/L. Moreover, the authors reported that their on-line SPE method benefited from little sample handling, minimal solvent use, and high sample throughput, all of which resulted in time and cost savings. Similarly, Anumol and Synder [24] used multi-residue on-line SPE LC-MS method to determine 32 microcontaminants in ground water, surface water and wastewater samples, of which 16 were pharmaceuticals including ibuprofen, carbamazepine, and trimethoprim. During their experiments, they evaluated three commercial on-line SPE columns and an in-house packed column and reported that the PLRP-s cartridge achieved higher recoveries (70–130% for 26 analytes) and method detection limits (MDLs) ranged from 0.1 to 13.1 ng/L. Along with reduced solvent use and increased throughput, their on-line SPE method had the advantage of requiring only a 1.7 mL sample volume and enhanced reproducibility. Another study by Rubirola et. al. [25] on 24 Water Framework Directive priority substances, including diclofenac, erythromycin, and clarithromycin, applied an on-line SPE LC-MS method for the analysis of surface water, drinking water, and wastewater effluents achieving detection limits between 0.1 and 1.4 ng/L. To summarize, while reproducibility varied significantly amongst methods, it was consistently noted that on-line SPE was more time and cost-effective than its offline counterpart.

2.2.3 LC-MS/MS Method Validation

Validation tests must be undertaken prior to applying a method to the analysis of real samples to confirm that its performance characteristics fulfil the requirements for its intended application and that it is scientifically sound under the conditions of use. Several guidance

materials on how to achieve this has been provided by various bodies, including the International Union of Pure and Applied Chemistry (IUPAC) [26], Eurachem [27], the International Council for Harmonization of Technical Requirements for Pharmaceuticals for Human Use (ICH) regulation [28, 29], and regulations such as the Commission Decision 2002/657/EC [30]. While there is consensus on the different validation parameters to be reviewed, there is considerable variation in the validation methods and acceptance criteria used [31]. As a result, different guidelines use different terminologies and recommendations. In fact, the analytical community has yet to reach an agreement on how exactly validation of LC-MS methods should be performed [32]. In the context of LC-MS methods for the determination of PhACs in water, the analytical properties typically evaluated in the method validation process are selectivity, linearity, range, limit of detection, limit of quantification, accuracy, precision, and robustness. The following sections will refer to the IUPAC [26] definitions of these parameters.

Selectivity refers to the method's ability to measure accurately and specifically the analyte of interest without being affected by the presence of other sample matrix components (metabolites, degradation products, etc.). Interferents may affect the measurement results by enhancing or suppressing the analyte signal. Thus, the method should be evaluated using various samples (complex matrices, neat standards) to determine its capacity to distinguish between molecules with nearly related properties. Selectivity is demonstrated by determining the recovery of target analytes and the observed effects of potential interferences. Typically, an MS/MS screening approach [33] is used, by specifying one quantifier MRM transition for each analyte and one or two qualifier (confirmatory) transitions.

The **working range** of a method is obtained by analyzing samples with various analyte concentrations and establishing the concentration range within which the analyte of interest can be determined with a sufficient level of linearity, accuracy, and precision. A working range must be defined for each sample matrix included in the method. **Linearity**, on the other hand, refers to the method's ability to produce measurement responses that are proportional to analyte concentration within a specified range, either directly or through explicit mathematical transformations. Linearity should be established across the entire range of the analytical method using a minimum of five concentrations [30]. Working range and linearity are established by constructing calibration curves that represent the analyte concentration-response relationship, and the formula and goodness-of-fit parameters of the regression line should be reported.

The **limit of detection (LOD)** is defined as the lowest concentration of an analyte that can be detected in a sample at a specified level of confidence, whereas **limit of quantification (LOQ)** refers to the lowest concentration of an analyte in a sample that can be quantified with acceptable accuracy and precision. LOD is an important parameter, particularly in trace level analysis, and the nomenclature used to describe it is quite diverse across sectors. Because LOD is matrix-dependent, it should be estimated with matrix-matched samples, or a blank of similar matrix when finding matrix-matching samples is difficult. In general, LOD can be estimated as a signal-to-noise ratio (S/N) of 3:1, or it can be calculated at levels close to the LOD using the formula: $LOD = 3.3 (SD/S)$, where S is the slope of the calibration curve and SD represents standard deviation of the response based on either the standard deviation of the blank, the residual standard deviation of the regression line, or the standard deviation of y-intercepts of regression lines. Similarly, LOQ can be determined as 10:1 S/N ratio or calculated using the formula: $LOQ = 10(SD/S)$. Given the variety of approaches available for estimating LOD and LOQ, it is always vital to describe and support the procedures used in a specific analytical method. Another widely used technique for estimation of the LOD, and eventually the LOQ, is the regression-based Hubaux-Vos' algorithm [34]. However, this method requires that the residuals from the linear model are homoscedastic, i.e., a distribution that is uniform across the entire calibration range [34, 35]. In practice, heteroscedasticity is frequently encountered in analytical models that span a wide range of concentrations. To overcome this limitation, the Hubaux-Vos' LOD calculation can be performed with a weighted least squares (WLS) calibration model instead of an unweighted model [36].

When the measurement of some property of a sample is performed (e.g., CECs in water), there will be some form of difference between the measured value and the true value, which is expressed as error. When repeated measurements are taken, an error can have different magnitude and sign (random error), or the same or systematically changing magnitude and sign (systematic error). In analytical measurements, we work with the estimates of errors rather than the actual errors because the later cannot be exactly determined. Thus, the estimate of the systematic error is referred to as **trueness**. Trueness, as defined explicitly, is the agreement between the average of an infinite number of replicate measurements and the true value [37]. In practice, reference values are used in place of true values and trueness is determined using a small number of replicate measurements. Trueness can be determined by comparing the results of the current method with the analysis of a standard reference material. Precision is an estimate of the random error, which refers to the degree to which individual test results of the same quantity agree with one another when an analytical procedure is applied repeatedly [38]. There are various forms of precision based on the conditions under which it is calculated, but the approaches most used in analytical method are repeatability

(also known as within-run precision) and intermediate precision (also called between-run precision) [27]. Accuracy encompasses both trueness and precision and is used to describe the total error.

In the absence of certified reference materials, quality control (QC) samples spiked with known concentrations of target analytes and having passed through the complete analytical method from sample preparation through final analysis are used to estimate accuracy and precision. All QCs should be analyzed within each run (within-run) and across runs (between-run). Trueness and precision are usually evaluated using the same runs and data. In general, QCs prepared at three concentration levels within the calibration curve range can be used, i.e., the LOQ (low QC), 30-50% of the calibration curve (medium QC), and 75-80% of the highest level in the calibration curve (high QC). Within-run (intraday) accuracy and precision should be estimated by analyzing at least five replicates of each QC level, while between-run (inter-day) accuracy and precision should be assessed by analyzing each QC in at least three analytical runs over at least two days. Trueness is expressed as the percentage recovery of the added amount of analyte in each QC. Similarly, precision can be estimated by calculating standard deviation or relative standard deviation (%RSD). At each QC level, an overall accuracy of $\pm 15\%$ is acceptable, as is a precision (%RSD) of not more than 15%.

For methods that involve an extraction procedure, the extraction efficiency must be evaluated by performing **recovery** experiments of extracted samples at multiple concentrations; usually at low, medium, and high QC levels. Recovery is calculated as a percentage of the measured quantity of the analyte divided by the fortified level, when certified reference materials are not available. Most guidelines specify that the mean recovery should be between 80 and 120% [37]. According to IUPAC recommendations, it is crucial to have a uniform chemical and/or isotopic ratio between the original and added materials when analyzing recovery using the spike or standard addition approaches [39]. Moreover, the analyte concentration in the spike should be high enough to prevent matrix dilution. In addition, the change in the analyte response caused by the presence of interferences in the sample - **matrix effect** - should be evaluated by analyzing at least three replicates of low and high QCs prepared using matrices from different sources. Each matrix source should have accuracy of $\pm 15\%$ for all QC levels, and the precision (RSD) should not exceed 15% [40].

2.3 Nontarget screening of water samples

A water sample containing unknown substances raises the question of how to identify the contaminants present and those that have undesired effects on the environment and living

organisms. To deal with this, various analytical approaches and strategies based on targeted biological or chemical analyses have been developed over the last years [41].

Depending on the purpose and scope of analysis needed to be achieved, three conceptually different screening approaches of environmental samples can be distinguished: targeted analysis, semi-targeted (suspect) screening, and untargeted (nontarget) screening [42]. A targeted analysis typically involves a quantitative determination of a relatively small number of known compounds with a certainty of identification and using a highly specific (targeted) signal acquisition mode achieved by employing well-established standards of target compounds. It is important to note, however, that suspect and nontarget screening approaches cannot be strictly distinguished from one another. In suspect screening, an evaluation of mass spectral data is typically assisted by information on potentially occurring compounds, whereas real nontarget screening begins without any *a priori* information.

In recent years, there has been a rise in the number and quality of publications regarding the identification of transformation products (TPs) of pharmaceuticals in various water matrices. To this end, different MS methodologies have been used. Performing collision-induced dissociation (CID) on QqQ and ion trap (IT) instruments, for example, allows MS² data acquisition either in space (QqQ) or in time (IT). Hybrid MS instruments such as QqLIT and QqTOF can also similarly utilize CID. For example, Krakstrom et al. [43] used ion trap mass spectrometry with electrospray ionization (ESI) source for the identification of ibuprofen and diclofenac TPs formed as a result of ozonation treatment. MS data was generated in full scan and automatic MS⁵ scan modes, allowing for further fragmentation of the precursor and product-ions, which provided valuable information for elucidation of the TPs. In one of our studies [44] we employed a hybrid QqLIT instrument to identify eight photodegradation products of the antineoplastic drug irinotecan. In this work, data was acquired using Information-Dependent Acquisition (IDA), a type of Data-Dependent Acquisition (DDA). This approach allowed linking a non-targeted “survey scan” with “dependent scans” when pre-defined IDA criteria are met. The Enhanced MS (EMS) was chosen as a survey scan for the nontarget screening, with the Q3 working as an ion trap collecting the ions of interest. The two dependent scans, Enhanced Resolution (ER) and Enhanced Product Ion (EPI), were performed automatically when the EMS detects a signal that exceeds a certain threshold. Each survey-dependent scan is repeated in a cycle of the entire chromatographic run. The ER scan confirms the isotope pattern, while the EPI provides an enhanced MS/MS scan resulting in a greater abundance of the product-ions.

In recent years, the evolution of high-resolution mass spectrometry (HRMS) has sparked a new trend in the analysis of environmental samples. As a result of their high mass resolution,

instruments such as TOF and Orbitrap can produce mass errors in the low ppm range, overcoming one of the limitations of QqQ and QqLIT devices. Moreover, when compared to TOF analyzers, Orbitrap analyzers offer a higher dynamic range of detection and, in general, higher mass resolution (>100 000 FWHM). In addition, Orbitraps can be calibrated externally to achieve superior mass accuracy, the only pitfall being their much slower scanning speed. HRMS instruments are also suitable for elucidating the structure of unknown compounds and have emerged as powerful tools for the nontarget identification of pharmaceuticals and their transformation products in water [45, 46]. Other HRMS instruments such as FTICR-MS have also been used [47] but their application has been limited to their cost and user requirements.

Recent developments in suspect and nontarget screening have enabled the identification of unknown TPs in wastewater [48, 49], surface water [45, 50], and drinking water [51, 52], following various water treatment methods such as ozonation, hydrolysis, filtration, chlorination, photolysis, and advanced oxidation processes. Targeting potential TPs has become an integral part of the recent research in environmental monitoring and assessment of pharmaceuticals. For instance, Stadlmair et al. [53] employed MS-based workflows using both qTOF and QqLIT instruments for the identification of peroxide- and enzyme-catalyzed TPs of diclofenac, mefenamic acid and sotalol. The complementary MS information obtained from both TOF and QqLIT analyzers increased the confidence in the identification of TPs. Another study by Tian et al. [54] applied HRMS for the suspect and nontarget screening of emerging contaminants in a marine environment. Eight of the 87 identified compounds were pharmaceuticals including metoprolol, methamphetamine, and lamotrigine and their TPs.

Evaluation of nontarget data, on the other hand, is not an easy task due to the enormous number of peaks representing potentially relevant CECs, which can be time-intensive and necessitates expertise. When screening large LC-HRMS data in spectral libraries, it is common to get multiple hits for the same exact mass values, which may lead to the detection of false positives. Thus, data pre-processing and cleanup are immensely required to remove/reduce false positives. Furthermore, removal of false positives and minimizing the large data preprocessing work can be achieved by employing a proper suspect list connected to the environmental scenario and regulatory concern. Such suspect lists also allow evaluation of whether the compounds can be detected by the analytical method, hence avoiding false-negative results due to an ineffective analytical methodology. Understandably, when a high degree of certainty is required, the complexity rises dramatically, and the task becomes extremely challenging [42]. Fig. 2.4 depicts the major steps usually employed in non-target data treatment. It is crucial to note that, depending on the data quality and outcomes, several additional steps can be included in addition to those shown in the workflow. Detailed

descriptions of each of the steps indicated in the workflow and possible others can be found elsewhere [55].

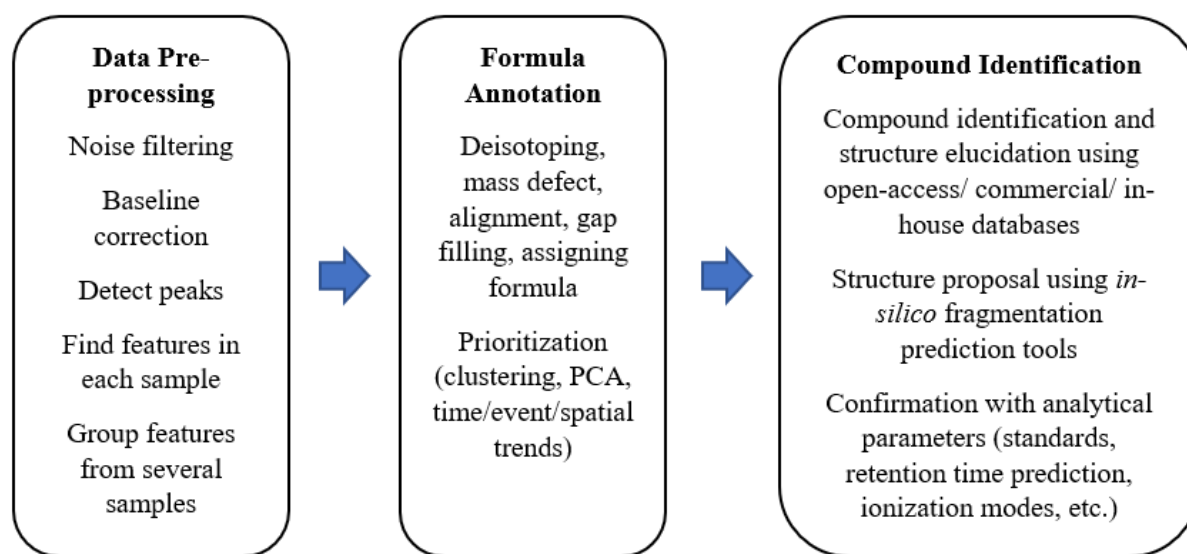


Figure 2.4. Overview of the steps in non-target screening workflow

The first phase in the workflow is peak picking and cleaning up the data, in which false positives and spectra that are assumed to be background ions, in-source fragments, isotopic ions, and others should be removed before annotation. Several studies applied software packages such as MZmine 2 [56], XCMS [57], XCMS Online [58], CAMERA [59] and MS-DIAL [60] for this purpose. There are also software tools, such as SIRIUS [61] and seven golden rules [62], available to support the prediction of the chemical formulas for unknown substances using the accurate mass measurements obtained from HRMS. Many other algorithms have been developed in recent years, which are covered in several publications; for example, more information can be found in the review paper by Blazenovic et al. [63]. Following the data cleanup and prediction of chemical formulas, structure elucidation begins by exploring in-house spectral libraries, open-access databases (e.g., ChemSpider, NORMAN Massbank, Drugbank, HMDB, KEGG), or commercial libraries (e.g., Sciex MS/MS library). For those compound features where no matches were found in any of the available databases, a supplemental strategy most commonly used is to perform *in-silico* fragmentation using tools such as MetFrag [64], MS-FINDER [65] and CFM-ID [66]. However, conclusions based on spectral library matching and *in-silico* fragmentation methods depend on the analyst's judgment as a number of candidates with different scores are returned for each molecule. Moreover, models that predict retention time, such as that used by the NORMAN network - the Retention Time Index (RTI) [67], can also be utilized for compound identification. Such

models are used to confirm the chromatographic behavior of certain features using quantitative structure-retention relationships.

Once the final list of candidates is prepared, they are classified according to the five confidence levels outlined in Schymanski et al. [42]. When an unknown feature of interest is detected and only the exact mass of the compound can be provided, it is confirmed at Level 5 (the lowest level). Consequently, the confirmation proceeds with the unequivocal molecular formula (Level 4), tentative structure or class (Level 3), probable structure from literature/database matching by diagnostic evidence (Level 2), and structure confirmation by reference standard (Level 1).

Another important trend of employing LC-HRMS is the possibility to undertake retrospective screening, which is extremely useful in environmental monitoring programs. Digital Sample Freezing Platforms (DSFP) can be used to store HRMS data [68], allowing for the retrospective screening of various CECs. The realization of DSFPs has shown to be crucial in the screening CECs that were previously unknown [69-71], including TPs [72-74], thanks to the capacity to compare MS data across several environmental matrices such as water, biota, sediment, air and indoor environment. While target analysis is critical in monitoring and exposure assessment, nontarget retrospective screening of digitally archived HRMS data has the potential to be used as a first screening step to improve the environmental risk assessment of CECs by triggering further target analysis.

2.4 Experimental design techniques

In an experiment, we purposely change one or more process factors (or variables) in order to determine the effect on one or more response variables. Traditionally, this is accomplished by the One Factor At-a Time (OFAT) approach, in which only one variable is changed at a time while maintaining all other factors constant. However, it is usually too time-consuming to investigate the exact relationship among factors (particularly when many variables must be evaluated) and this gets even more difficult when there is the possibility of factor interaction. Solving such complex scenarios would require the execution of a huge number of experiments, which is often unrealistic due to time and expense constraints. In fact, the OFAT method is often inadequate in fields like analytical chemistry where complex chemical problems demand an accurate planning of the entire study in order to investigate the experimental domain uniformly and gather maximum information with the least number of experiments possible.

Experimental design (DOE) is a field within statistics which is devoted to the development of methods for conducting experiments in a systematic and methodological manner such that a

maximum of information can be extracted about a system using a minimum of experiments [75]. The first step for establishing a DOE is the so-called analysis of the problem, which consists of four major stages: (i) determining the objectives and evaluating the response(s) under consideration for optimization, (ii) identifying the factors that are likely to affect the experimental results and coding them across the experimental range using a standard mathematical scale, typically +1 for high and -1 for low, (iii) definition of eventual constraints on the responses, and (iv) selecting the experimental domain and designing the experiment in such a way that all factors not included in the experimentation are controlled and/or the effects of uncontrolled factors are minimized. Then, the best DOE approach can be identified, and the experiments can be carried out, applying statistical analysis to separate and evaluate the effects of the studied factors. When we have a large number of variables and are uncertain about their significance, we should first perform screening tests, such as the Plackett Burman design [76], to narrow them down to a small number of truly significant factors. Following that, an in-depth analysis of the effect of the selected parameters is conducted using well-established methods such as factorial design, central composite design, or others, to also include interactions and eventually quadratic effects.

The characteristics of a process model are illustrated in Fig. 2.5. The input factors are values which can be adjusted arbitrarily by the investigator, and one or more output responses are measured. In addition to controllable factors, the study must account for various uncontrollable factors that may influence the response, such as ambient temperature or humidity. The response is something we want to understand – we can use DOE to determine how the different factors influence the observed response(s) – and/or optimize – maximize or minimize the response(s).

Using the experimental data, an empirical model is developed that relates the outputs (y) and inputs (x), which can be represented mathematically as:

$$y = f(X_1, X_2, X_3, \dots, X_k) \quad (2.1)$$

Often, the experimental data fits to first-order (linear) or second-order (quadratic) empirical models. For instance, a linear model with two factors X_1 and X_2 can be written as:

$$y = \beta_0 + \sum \beta_i X_i + \sum \beta_{ij} X_i X_j + \varepsilon \quad (2.2)$$

where the constant β_0 is obtained when all main effects are equal to zero, β_i represents the coefficients of the linear factors (i.e., the main effects), β_{ij} represents the coefficients of the interaction factors, X_i and X_j represents the factors, and ε is the random error to the response.

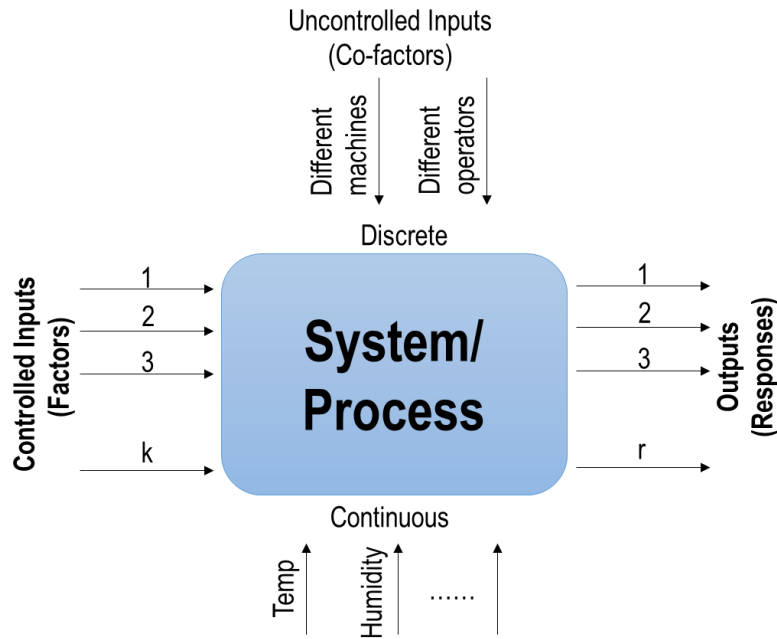


Figure 2.5. A process model (adapted from [77])

The response in Eq. (2.2) contains three main-effects terms (X_1 , X_2 and X_3), three 2-way interaction terms (X_1X_2 , X_1X_3 , and X_2X_3), and one 3-way interaction term ($X_1X_2X_3$). In some cases, the relationship between inputs (X 's) and response (Y) exhibits curvature, rendering a linear model unsuitable to adequately model the experimental data. Experiments at the center of the domain (center points) can be used to statistically determine whether a relationship is linear or not. By comparing the average response at the center point calculated by means of the model and the experimental response in the center of the experimental domain, it is possible to conclude that curvature exists if the p-value is < 0.05 . As a result, quadratic models of the type given in Eq. (2.3) should be used to interpret the experimental data.

$$y = \beta_0 + \sum \beta_i X_i + \sum \beta_{ij} X_i X_j + \sum \beta_{ii} X_i^2 + \varepsilon \quad (2.3)$$

where β_{ii} represents the coefficients of the quadratic terms.

Prior to tackling DOE, it is critical to plan for replicate measurements to average out experimental error. Additionally, the experiments must be executed in a random order to avoid systematic errors. Blocking may also be important, as tests with the least variance should be conducted within a single block. For instance, if a study requires 18 experiments but only six can be conducted daily, the experiments should be organized into three blocks of six each.

The adequacy of a specific model [77] can be evaluated by examining normal probability plots, residuals, main and interaction plots, contour plots, and analysis of variance (ANOVA) statistics (F-test, t-test, R^2 , adjusted- R^2 , and lack-of-fit).

2.4.1 Optimization and robustness study

The experimental design chosen is determined by the objectives of the study and the number of parameters to be explored. DOE can be used to successfully achieve the following tasks: (i) reaching a target, (ii) optimizing (maximizing or minimizing) a response, (iii) ensuring the robustness of a process, and (iv) achieving several goals. If the study involves one or more factors with the primary objective of evaluating whether there is a significant change in the response for various levels of a known significant factor, it is a comparative problem that requires a comparative design, such as performing a one-factor completely randomized design. Another goal of DOE may be to reduce the large number of factors into a few significant ones, which can be accomplished effectively using screening methods such as Full or Fractional Factorial and Plackett-Burman designs. Another important objective is the Response Surface objective, which requires the DOE study to determine interaction and quadratic effects to provide an idea of the local shape of the response surface being investigated. These last approaches are commonly referred to as Response Surface Method (RSM) designs. RSM designs are applied to identify improved or optimal process parameters, to troubleshoot problems of a process, and to make a product or process more robust against small changes in operational parameters.

Sequential and simultaneous optimization procedures are the two most common multivariate optimization approaches [78]. In fact, it is also possible to employ a combination of these approaches. A sequential approach, such as the well-known Simplex method, requires only a few experiments to be run at a time, with the results being used to choose the next experiment. Simultaneous methods, on the other hand, involve performing a series of experiments according to a predetermined plan. The most popular factorial designs are included in the latter category, and they are briefly described in the following sections.

2.4.1.1 Full and Fractional Factorial Designs

After defining the experimental domain, it is necessary to determine the levels of the variables. In general, if there are K factors and n levels, n^K experiments are required to develop a comprehensive factorial design. The graphical illustration of a 2^3 design (a two-level full factorial design for three factors) is shown in Fig. 2.6. As indicated in the table, eight experiments need to be performed without taking into account replications or center points.

The arrows indicate the direction in which the variables increase, and the numbers (from 1 to 8) indicate the standard order of the experiments.

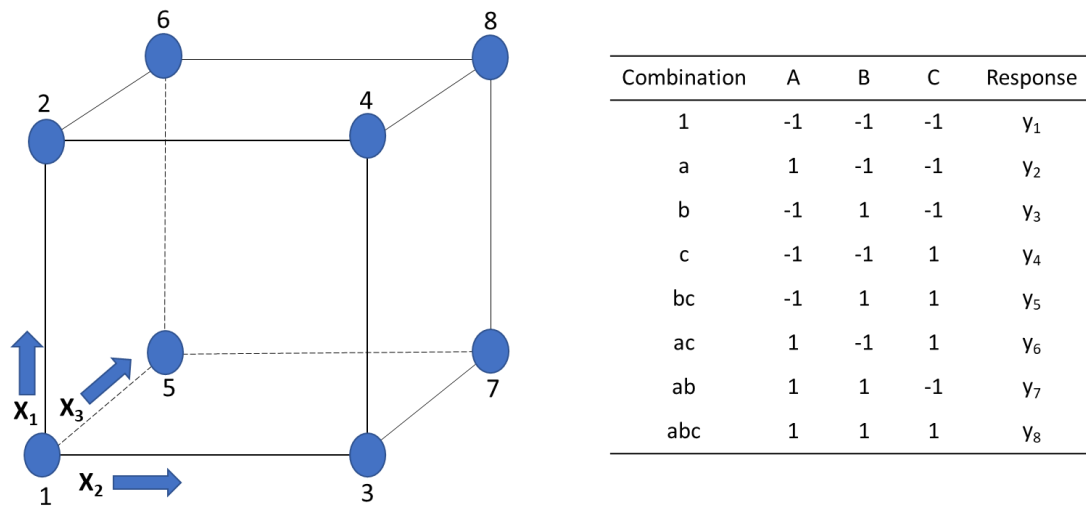


Figure 2.6. A randomized 2^3 full factorial design

The design in Fig. 2.6 must be randomized to ensure that any memory effects (e.g., experimenter training, reagent degradation, instrumental drifts, environmental effects, etc.) are taken into account. The general rule is to randomize the run order to the greatest possible extent. To evaluate variability and detect any quadratic effects, the design should also include at least three center points at the beginning, middle, and end of the experiment. Center points are necessary to evaluate the process's reliability and intrinsic variability and to check for curvature, giving thus, a total of eleven experiments. In three-level designs, the symbols +1, 0 and -1 are often used to denote the high, center, and low levels, respectively.

When the number of variables and levels increases, the number of experiments grows exponentially. The need for such a large number of experiments leads to undesired high-order interactions. For example, 128 experiments are required for a seven factor 2-level full factorial design. However, anything more than two-factor interactions is unlikely to be significant [75]. As a result, 99 of the 128 experiments are redundant and can be discarded. Indeed, by making assumptions about which interaction effects are not important (e.g., we assume that 3-way interaction effects are not important), fractional factorial designs can be used to run fewer experiments. We may only use a portion of the full factorial design (e.g., one-half, one-quarter, or one-eighth of the experiments). In general, for a 2^k full factorial design, we can have a 2^{k-p} fractional factorial design, where p defines how much experiments/information are/is subtracted. A 2^{5-2} design, for example, has just $2^3 = 8$ of the available 32 experiments of the

full factorial design. The designs must be chosen in such a way that the experiments provide the maximum information.

Consider the 2^4 full factorial designs, involving 16 experiments. Experiments for a 2^{4-1} fractional factorial design can be represented as in Table 2.1. This half-factorial design contains information on the main effects of factors A, B, C and D and some information (but not complete) on their interactions. The effect observed in a fractional factorial design may be contaminated by other effects - a situation commonly known as confounding. For example, in the design shown in table 2.1, the main effects are confounded with the three-way interactions. For example, the expression for the three-way interaction between factors A, B, and C (commonly abbreviated as ABC) is identical to the expression for the main effect of D. As a result, the effects of D and ABC are computed using the same formula: $(y_1 + y_3 + y_5 + y_7 - y_2 - y_4 - y_6 - y_8) / 4$. This effect is the sum of D and ABC. These pairs of effects are referred to as aliases. Of course, eliminating experiments from the full factorial design results in a loss of information and, as a result, the capacity to discriminate between the contributions of diverse effects.

Table 2.1. A 2^{4-1} fraction factorial design

Experiment	A	B	C	D=ABC	Response
1	1	1	1	1	y_1
2	1	1	-1	-1	y_2
3	1	-1	1	-1	y_3
4	1	-1	-1	1	y_4
5	-1	1	1	-1	y_5
6	-1	1	-1	1	y_6
7	-1	-1	1	1	y_7
8	-1	-1	-1	-1	y_8

All fractional factorial designs exhibit some degree of confounding. While confounding may be unimportant in some situations, it will always require careful analysis. With four factors, there are four main effects, six two-way interactions, four three-way interactions, and one four-way interaction: it is unreasonable to expect that all of these effects will be resolved entirely in only eight experiments. The magnitude of the confounding effect in any fractional factorial design is determined by the resolution (R), which implies that no confusion exists

between a p-factor effect and an effect comprising $< (R-p)$ factors [79]. In the four-factor example, the resolution is IV (i.e., four), showing that there is no confusion between the main effects and two-way interactions, i.e., $< (4-1)$.

The Plackett–Burman design [76] is one of the simplest and most popular factorial designs; it provides information on the factors' main effects but not on their interactions. A common feature of this strategy is that it relies on performing $4n$ ($n = 1, 2, 3, \text{etc.}$) experiments. Thus, it eliminates the drawbacks associated with factorial and fractional factorial designs. A Plackett–Burman design with $4n$ experiments is appropriate for the investigation of up to $4n-1$ factors. However, these designs are generally advantageous for economically finding large main effects, assuming that all interactions are negligible in comparison to the few significant main effects.

2.4.1.2 Response Surface Methodology

Effective optimization approaches have two characteristics: they either generate a set of experimental settings that results in the optimal solution, or they produce a response that is close to the optimal with the fewest possible experiments. In practice, the simplicity and speed of the optimization strategy are crucial, and in some cases, a method that provides a result near to the true optimum in a few stages may suffice. Suppose we have performed 2-level factorial designs to determine the most important factors and find the optimum. We can then employ Response Surface Methodology (RSM) to study the local model in more detail. The full three-level factorial design (3^k), central composite design (CCD), Doehlert design, and Box-Behnken design are the most commonly used DOEs in RSM [80]. The following discussion will focus on CCD, which was used in this thesis for the robustness evaluation of removal processes of contaminants of emerging concern.

A CCD is composed of an embedded factorial or fractional factorial design that includes center points and star points (axial points) for the purpose of determining the curvature. A CCD design with k factors will always have $2k$ star points. The star points denote new extreme values for each factor (i.e., low and high). The characteristics of the three types of central composite design are depicted in Fig. 2.7.

In general, CCC designs generate high-quality predictions across the whole design space, but they require factor values that are not inside the factorial space. Although CCI designs use only points inside the factor boundaries specified initially, they do not provide the same level of prediction throughout the entire design space as CCC designs. Each factor must have five levels in both CCC and CCI designs. CCF designs use three levels of each factor and produce

reasonably accurate estimates across the whole design space without the need to utilize points outside the initial factor domain. However, they are less precise in predicting pure quadratic coefficients [77].

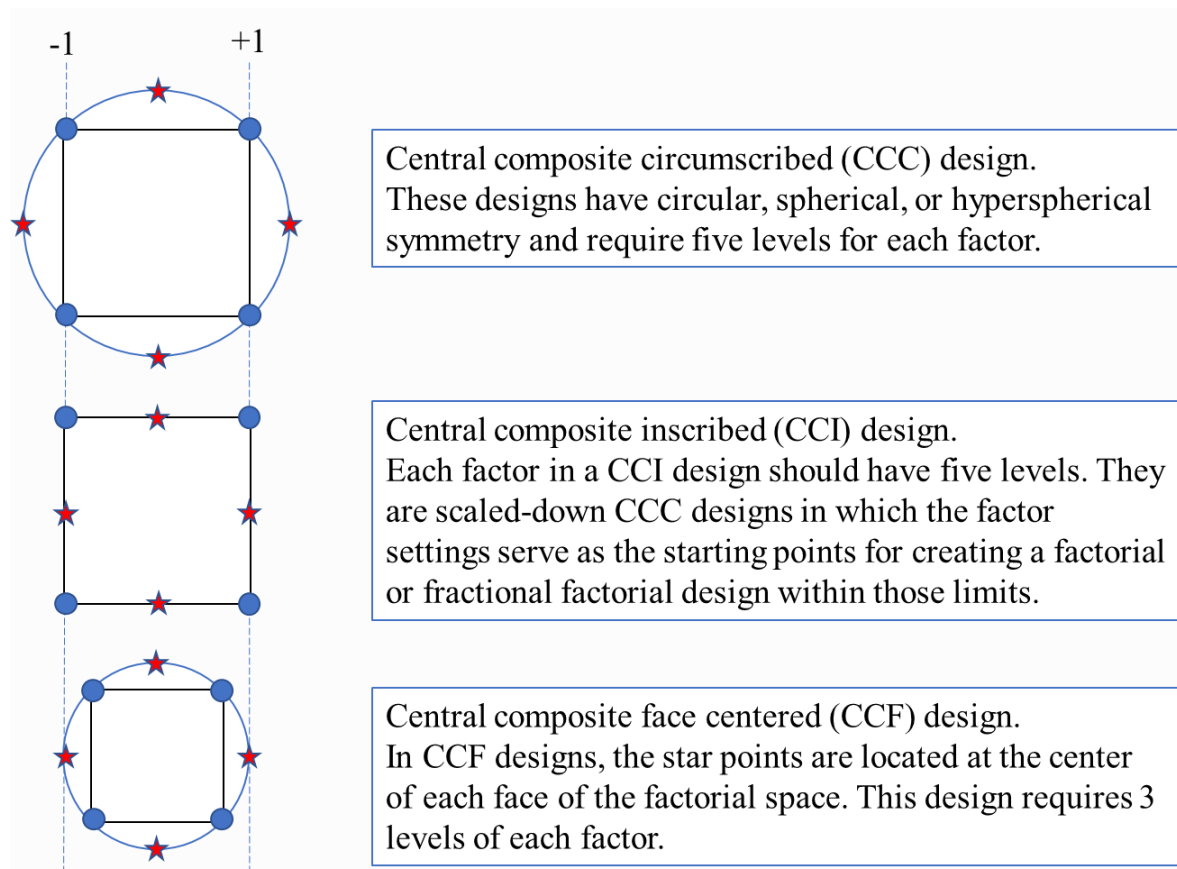


Figure 2.7. The three types of central composite designs

An important application of DOEs is the robustness study of processes, methods, or systems. Robustness refers to a process's ability to stay unaffected by small, intentional changes in process parameters [81]. It is a measure of the reliability of a process. If the outcome of a process is sensitive to changes in process parameters, these elements should be effectively controlled, and a thorough study of the robust region should be provided. The purpose of such a study is to develop guidelines for running the process in such a way that the optimal response is not jeopardized. Fig. 2.8 depicts an RSM example for the photocatalytic degradation of maprotiline (see Chapter 5 for a detailed discussion of the findings related to this process and others). The RSM illustrates that the best results (low C/C_0 , corresponding to the highest degradation rate) were obtained in two situations: (i) when the catalyst dose (K) is low (-1) and the UV irradiance (W) is between 0 (center) and -1 (low), and (ii) when K is high ($+1$) and W is between 0 and 0.6 . In light of the robustness of this specific process, it is shown that the process is robust regardless of the values of K , but only in the range of 0.0 to 0.6 of W . As a

result, UV irradiation must be monitored to ensure that it remains within this range and that the process's abatement efficiency is not significantly affected.

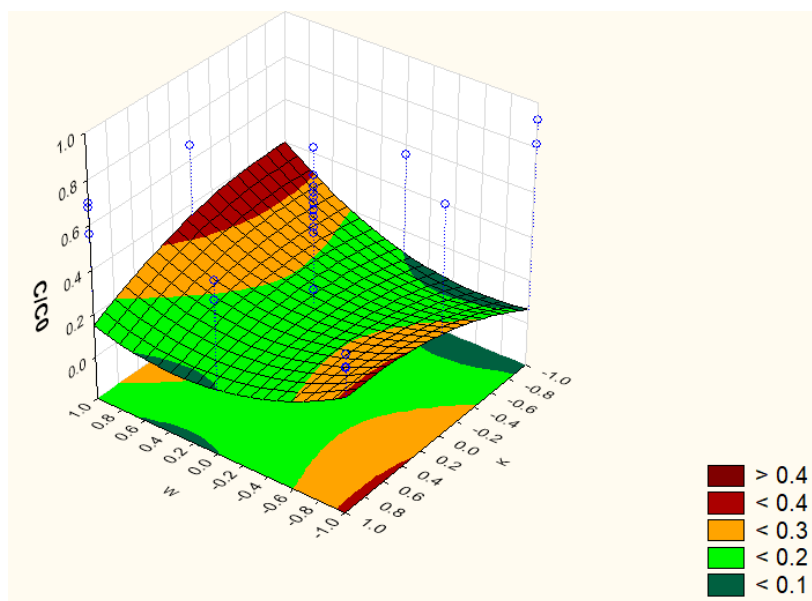


Figure 2.8. RSM example

References

1. Pereira, A., Silva, L., Laranjeiro, C., & Pena, A. (2021). Assessment of Human Pharmaceuticals in Drinking Water Catchments, Tap and Drinking Fountain Waters. *Applied Sciences*, *11*(15), 7062.
2. López-García, E., Mastroianni, N., Postigo, C., Barceló, D., & de Alda, M. L. (2018). A fully automated approach for the analysis of 37 psychoactive substances in raw wastewater based on on-line solid phase extraction-liquid chromatography-tandem mass spectrometry. *Journal of Chromatography A*, *1576*, 80-89.
3. Ng, K. T., Rapp-Wright, H., Egli, M., Hartmann, A., Steele, J. C., Sosa-Hernández, J. E., ... & Barron, L. P. (2020). High-throughput multi-residue quantification of contaminants of emerging concern in wastewaters enabled using direct injection liquid chromatography-tandem mass spectrometry. *Journal of hazardous materials*, *398*, 122933.
4. Fenn, J. B. (2003). Electrospray wings for molecular elephants (Nobel lecture). *Angewandte Chemie International Edition*, *42*(33), 3871-3894.
5. Konermann, L., Ahadi, E., Rodriguez, A. D., & Vahidi, S. (2013). Unraveling the mechanism of electrospray ionization.
6. Wu, X., Oleschuk, R. D., & Cann, N. M. (2012). Characterization of microstructured fibre emitters: in pursuit of improved nano electrospray ionization performance. *Analyst*, *137*(18), 4150-4161.
7. Rayleigh, L. (1882). XX. On the equilibrium of liquid conducting masses charged with electricity. *The London, Edinburgh, and Dublin Philosophical Magazine and Journal of Science*, *14*(87), 184-186.
8. Pinasseau, L., Wiest, L., Volatier, L., Mermillod-Blondin, F., & Vulliet, E. (2020). Emerging polar pollutants in groundwater: Potential impact of urban stormwater infiltration practices. *Environmental Pollution*, *266*, 115387.

9. Petrie, B., Barden, R., & Kasprzyk-Hordern, B. (2015). A review on emerging contaminants in wastewaters and the environment: current knowledge, understudied areas and recommendations for future monitoring. *Water research*, 72, 3-27.
10. Silva, S., Rodrigues, J. A., Coelho, M. R., Martins, A., Cardoso, E., Cardoso, V. V., ... & Almeida, C. M. (2021). Occurrence of pharmaceutical active compounds in sewage sludge from two urban wastewater treatment plants and their potential behaviour in agricultural soils. *Environmental Science: Water Research & Technology*, 7(5), 969-982.
11. Petrovic, M., Farré, M., De Alda, M. L., Perez, S., Postigo, C., Köck, M., ... & Barcelo, D. (2010). Recent trends in the liquid chromatography–mass spectrometry analysis of organic contaminants in environmental samples. *Journal of Chromatography A*, 1217(25), 4004-4017.
12. Christophoridis, C., Veloutsou, S., Mitsika, E., Zacharis, C. K., Christia, C., Raikos, N., & Fytianos, K. (2021). Determination of illicit drugs and psychoactive pharmaceuticals in wastewater from the area of Thessaloniki (Greece) using LC–MS/MS: estimation of drug consumption. *Environmental monitoring and assessment*, 193(5), 1-15.
13. Papagiannaki, D., Morgillo, S., Bocina, G., Calza, P., & Binetti, R. (2021). Occurrence and Human Health Risk Assessment of Pharmaceuticals and Hormones in Drinking Water Sources in the Metropolitan Area of Turin in Italy. *Toxics*, 9(4), 88.
14. Camilleri, J., Baudot, R., Wiest, L., Vulliet, E., Cren-Olivé, C., & Daniele, G. (2015). Multiresidue fully automated online SPE-HPLC-MS/MS method for the quantification of endocrine-disrupting and pharmaceutical compounds at trace level in surface water. *International Journal of Environmental Analytical Chemistry*, 95(1), 67-81.
15. Khulu, S., Ncube, S., Nuapia, Y., Madikizela, L. M., Tutu, H., Richards, H., ... & Chimuka, L. (2022). Multivariate optimization of a two-way technique for extraction of pharmaceuticals in surface water using a combination of membrane assisted solvent extraction and a molecularly imprinted polymer. *Chemosphere*, 286, 131973.
16. Godlewska, K., Stepnowski, P., & Paszkiewicz, M. (2021). Pollutant analysis using passive samplers: principles, sorbents, calibration and applications. A review. *Environmental Chemistry Letters*, 19(1), 465-520.
17. Mosekiemang, T. T., Stander, M. A., & de Villiers, A. (2019). Simultaneous quantification of commonly prescribed antiretroviral drugs and their selected metabolites in aqueous environmental samples by direct injection and solid phase extraction liquid chromatography-tandem mass spectrometry. *Chemosphere*, 220, 983-992.
18. Vázquez, M. P., Vázquez, P. P., Galera, M. M., García, M. G., & Uclés, A. (2013). Ultrasound-assisted ionic liquid dispersive liquid–liquid microextraction coupled with liquid chromatography-quadrupole-linear ion trap-mass spectrometry for simultaneous analysis of pharmaceuticals in wastewaters. *Journal of Chromatography a*, 1291, 19-26.
19. Guan, J., Zhang, C., Wang, Y., Guo, Y., Huang, P., & Zhao, L. (2016). Simultaneous determination of 12 pharmaceuticals in water samples by ultrasound-assisted dispersive liquid–liquid microextraction coupled with ultra-high performance liquid chromatography with tandem mass spectrometry. *Analytical and bioanalytical chemistry*, 408(28), 8099-8109.
20. European Commission, Commission Implementing Decision (EU) 2020/1161 of 4 August 2020 establishing a watch list of substances for Union-wide monitoring in the field of water policy pursuant to Directive 2008/105/EC of the European Parliament and of the Council. *Off. J. Eur. Union L*, 2020. 257: 32-35
21. Kiszkiel-Taudul, I. (2021). Determination of antihistaminic pharmaceuticals in surface water samples by SPE-LC-MS/MS method. *Microchemical Journal*, 162, 105874.
22. Coelho, M. M., Ribeiro, A. R. L., Sousa, J. C., Ribeiro, C., Fernandes, C., Silva, A. M., & Tiritan, M. E. (2019). Dual enantioselective LC–MS/MS method to analyse chiral drugs in surface water: Monitoring in Douro River estuary. *Journal of Pharmaceutical and Biomedical Analysis*, 170, 89-101.
23. de Carvalho Abrão, L. C., de Faria, H. D., Santos, M. G., Barbosa, A. F., & Figueiredo, E. C. (2019). Restricted Access Materials for Sample Preparation. *Handbook of Smart Materials in Analytical Chemistry*, 411-438.

24. Anumol, T., & Snyder, S. A. (2015). Rapid analysis of trace organic compounds in water by automated online solid-phase extraction coupled to liquid chromatography–tandem mass spectrometry. *Talanta*, *132*, 77-86.
25. Rubirola, A., Boleda, M. R., & Galceran, M. T. (2017). Multiresidue analysis of 24 Water Framework Directive priority substances by on-line solid phase extraction-liquid chromatography tandem mass spectrometry in environmental waters. *Journal of Chromatography A*, *1493*, 64-75.
26. Thompson, M., Ellison, S. L., & Wood, R. (2002). Harmonized guidelines for single-laboratory validation of methods of analysis (IUPAC Technical Report). *Pure and applied chemistry*, *74*(5), 835-855.
27. Magnusson, B. (2014). The fitness for purpose of analytical methods: a laboratory guide to method validation and related topics (2014).
28. ICH Harmonized Guideline (2019). Bioanalytical method validation M10. *Draft version*, 26.
29. ICH Harmonized Tripartite Guideline (2005). Validation of analytical procedures: text and methodology. *Q2 (R1)*, 1(20), 05.
30. European Commission, Commission Decision of 12 August 2002 implementing Council Directive 96/23/EC concerning the performance of analytical methods and the interpretation of results (2002/657/EC). *Off. J. Eur. Union L*, 2002. 221: 8-36.
31. Chandran, S., & Singh, R. S. P. (2007). Comparison of various international guidelines for analytical method validation. *Die Pharmazie-An International Journal of Pharmaceutical Sciences*, *62*(1), 4-14.
32. Kruve, A., Rebane, R., Kipper, K., Oldekop, M. L., Evard, H., Herodes, K., ... & Leito, I. (2015). Tutorial review on validation of liquid chromatography–mass spectrometry methods: Part I. *Analytica chimica acta*, *870*, 29-44.
33. Anagnostopoulos, C. J., Aplada Sarli, P., Liapis, K., Haroutounian, S. A., & Miliadis, G. E. (2012). Validation of two variations of the QuEChERS method for the determination of multiclass pesticide residues in cereal-based infant foods by LC–MS/MS. *Food Analytical Methods*, *5*(4), 664-683.
34. Caruso, R., Scordino, M., Traulo, P., & Gagliano, G. (2012). Determination of volatile compounds in wine by gas chromatography–flame ionization detection: comparison between the US Environmental Protection Agency 3 σ approach and Hubaux-Vos calculation of detection limits using ordinary and bivariate least squares. *Journal of AOAC International*, *95*(2), 459-471.
35. Alladio, E., Amante, E., Bozzolino, C., Seganti, F., Salomone, A., Vincenti, M., & Desharnais, B. (2020). Effective validation of chromatographic analytical methods: the illustrative case of androgenic steroids. *Talanta*, *215*, 120867.
36. Sanchez, J. M. (2018). Estimating detection limits in chromatography from calibration data: ordinary least squares regression vs. weighted least squares. *Separations*, *5*(4), 49.
37. Kruve, A., Rebane, R., Kipper, K., Oldekop, M. L., Evard, H., Herodes, K., ... & Leito, I. (2015). Tutorial review on validation of liquid chromatography–mass spectrometry methods: Part II. *Analytica chimica acta*, *870*, 8-28.
38. BiPM, I. E. C., IFCC, I., IUPAC, I., & ISO, O. (2012). The international vocabulary of metrology—basic and general concepts and associated terms (VIM). *JcGM*, *200*, 2012.
39. Burns, D. T., Danzer, K., & Townshend, A. (2002). Use of the term "recovery" and "apparent recovery" in analytical procedures (IUPAC Recommendations 2002). *Pure and applied chemistry*, *74*(11), 2201-2205.
40. Tiwari, G., & Tiwari, R. (2010). Bioanalytical method validation: An updated review. *Pharmaceutical methods*, *1*(1), 25-38.
41. González-Gaya, B., Lopez-Herguedas, N., Bilbao, D., Mijangos, L., Iker, A. M., Etxebarria, N., ... & Zuloaga, O. (2021). Suspect and non-target screening: the last frontier in environmental analysis. *Analytical Methods*, *13*(16), 1876-1904.
42. Schymanski, E. L., Singer, H. P., Slobodnik, J., Ipolyi, I. M., Oswald, P., Krauss, M., ... & Hollender, J. (2015). Non-target screening with high-resolution mass spectrometry: critical review using a collaborative trial on water analysis. *Analytical and bioanalytical chemistry*, *407*(21), 6237-6255.

43. Kråkström, M., Saeid, S., Tolvanen, P., Kumar, N., Salmi, T., Kronberg, L., & Eklund, P. (2021). Identification and Quantification of Transformation Products Formed during the Ozonation of the Non-steroidal Anti-inflammatory Pharmaceuticals Ibuprofen and Diclofenac. *Ozone: Science & Engineering*, 1-15.
44. Gosetti, F., Belay, M. H., Marengo, E., & Robotti, E. (2020). Development and validation of a UHPLC-MS/MS method for the identification of irinotecan photodegradation products in water samples. *Environmental Pollution*, 256, 113370.
45. Gonçalves, N. P., Varga, Z., Bouchonnet, S., Dulio, V., Alygizakis, N., Dal Bello, F., ... & Calza, P. (2021). Study of the photoinduced transformations of maprotiline in river water using liquid chromatography high-resolution mass spectrometry. *Science of the Total Environment*, 755, 143556.
46. Calza, P., Jiménez-Holgado, C., Cocha, M., Chrimatopoulos, C., Dal Bello, F., Medana, C., & Sakkas, V. (2021). Study of the photoinduced transformations of sertraline in aqueous media. *Science of The Total Environment*, 756, 143805.
47. Cazzaniga, N., Varga, Z., Nicol, E., & Bouchonnet, S. (2020). UV-visible photodegradation of naproxen in water—Structural elucidation of photoproducts and potential toxicity. *European Journal of Mass Spectrometry*, 26(6), 400-408.
48. Bergé, A., Buleté, A., Fildier, A., Mailler, R., Gasperi, J., Coquet, Y., ... & Vulliet, E. (2018). Non-target strategies by HRMS to evaluate fluidized micro-grain activated carbon as a tertiary treatment of wastewater. *Chemosphere*, 213, 587-595.
49. Schollée, J. E., Bourgin, M., von Gunten, U., McArdell, C. S., & Hollender, J. (2018). Non-target screening to trace ozonation transformation products in a wastewater treatment train including different post-treatments. *Water research*, 142, 267-278.
50. Zahn, D., Mucha, P., Zilles, V., Touffet, A., Gallard, H., Knepper, T. P., & Frömel, T. (2019). Identification of potentially mobile and persistent transformation products of REACH-registered chemicals and their occurrence in surface waters. *Water research*, 150, 86-96.
51. Brunner, A. M., Vughs, D., Siegers, W., Bertelkamp, C., Hofman-Caris, R., Kolkman, A., & Ter Laak, T. (2019). Monitoring transformation product formation in the drinking water treatments rapid sand filtration and ozonation. *Chemosphere*, 214, 801-811.
52. Di Marcantonio, C., Bertelkamp, C., van Bel, N., Pronk, T. E., Timmers, P. H., van der Wielen, P., & Brunner, A. M. (2020). Organic micropollutant removal in full-scale rapid sand filters used for drinking water treatment in The Netherlands and Belgium. *Chemosphere*, 260, 127630.
53. Stadlmair, L. F., Grosse, S., Letzel, T., Drewes, J. E., & Grassmann, J. (2019). Comprehensive MS-based screening and identification of pharmaceutical transformation products formed during enzymatic conversion. *Analytical and bioanalytical chemistry*, 411(2), 339-351.
54. Tian, Z., Peter, K. T., Gipe, A. D., Zhao, H., Hou, F., Wark, D. A., ... & James, C. A. (2019). Suspect and nontarget screening for contaminants of emerging concern in an urban estuary. *Environmental science & technology*, 54(2), 889-901.
55. Ccancapa-Cartagena, A., Pico, Y., Ortiz, X., & Reiner, E. J. (2019). Suspect, non-target and target screening of emerging pollutants using data independent acquisition: Assessment of a Mediterranean River basin. *Science of the total environment*, 687, 355-368.
56. Pluskal, T., Castillo, S., Villar-Briones, A., & Orešič, M. (2010). MZmine 2: modular framework for processing, visualizing, and analyzing mass spectrometry-based molecular profile data. *BMC bioinformatics*, 11(1), 1-11.
57. Smith, C. A., Want, E. J., O'Maille, G., Abagyan, R., & Siuzdak, G. (2006). XCMS: processing mass spectrometry data for metabolite profiling using nonlinear peak alignment, matching, and identification. *Analytical chemistry*, 78(3), 779-787.
58. Tautenhahn, R., Patti, G. J., Rinehart, D., & Siuzdak, G. (2012). XCMS Online: a web-based platform to process untargeted metabolomic data. *Analytical chemistry*, 84(11), 5035-5039.
59. Kuhl, C., Tautenhahn, R., & Neumann, S. (2010). LC-MS peak annotation and identification with CAMERA. *Anal Chem*, 84, 1-14.

60. Tsugawa, H., Cajka, T., Kind, T., Ma, Y., Higgins, B., Ikeda, K., ... & Arita, M. (2015). MS-DIAL: data-independent MS/MS deconvolution for comprehensive metabolome analysis. *Nature methods*, 12(6), 523-526.
61. Dürrkop, K., Scheubert, K., & Böcker, S. (2013). Molecular formula identification with SIRIUS. *Metabolites*, 3(2), 506-516.
62. Kind, T., & Fiehn, O. (2007). Seven Golden Rules for heuristic filtering of molecular formulas obtained by accurate mass spectrometry. *BMC bioinformatics*, 8(1), 1-20.
63. Blaženović, I., Kind, T., Ji, J., & Fiehn, O. (2018). Software tools and approaches for compound identification of LC-MS/MS data in metabolomics. *Metabolites*, 8(2), 31.
64. Ruttkies, C., Schymanski, E. L., Wolf, S., Hollender, J., & Neumann, S. (2016). MetFrag relaunched: incorporating strategies beyond in silico fragmentation. *Journal of cheminformatics*, 8(1), 1-16.
65. Tsugawa, H., Kind, T., Nakabayashi, R., Yukihiro, D., Tanaka, W., Cajka, T., ... & Arita, M. (2016). Hydrogen rearrangement rules: computational MS/MS fragmentation and structure elucidation using MS-FINDER software. *Analytical chemistry*, 88(16), 7946-7958.
66. Djoumbou-Feunang, Y., Pon, A., Karu, N., Zheng, J., Li, C., Arndt, D., ... & Wishart, D. S. (2019). CFM-ID 3.0: significantly improved ESI-MS/MS prediction and compound identification. *Metabolites*, 9(4), 72.
67. Aalizadeh, R., Alygizakis, N. A., Schymanski, E. L., Krauss, M., Schulze, T., Ibanez, M., ... & Thomaidis, N. S. (2021). Development and application of liquid chromatographic retention time indices in HRMS-based suspect and nontarget screening. *Analytical Chemistry*, 93(33), 11601-11611.
68. Alygizakis, N. A., Oswald, P., Thomaidis, N. S., Schymanski, E. L., Aalizadeh, R., Schulze, T., ... & Slobodnik, J. (2019). NORMAN digital sample freezing platform: A European virtual platform to exchange liquid chromatography high resolution-mass spectrometry data and screen suspects in "digitally frozen" environmental samples. *TrAC Trends in Analytical Chemistry*, 115, 129-137.
69. Angeles, L. F., Islam, S., Aldstadt, J., Saqeeb, K. N., Alam, M., Khan, M. A., ... & Aga, D. S. (2020). Retrospective suspect screening reveals previously ignored antibiotics, antifungal compounds, and metabolites in Bangladesh surface waters. *Science of the Total Environment*, 712, 136285.
70. Creusot, N., Casado-Martinez, C., Chiaia-Hernandez, A., Kiefer, K., Ferrari, B. J., Fu, Q., ... & Hollender, J. (2020). Retrospective screening of high-resolution mass spectrometry archived digital samples can improve environmental risk assessment of emerging contaminants: A case study on antifungal azoles. *Environment International*, 139, 105708.
71. Sabater-Liesa, L., Montemurro, N., Ginebreda, A., Barceló, D., Eichhorn, P., & Pérez, S. (2021). Retrospective mass spectrometric analysis of wastewater-fed mesocosms to assess the degradation of drugs and their human metabolites. *Journal of Hazardous Materials*, 408, 124984.
72. Gonçalves, N. P., Iezzi, L., Belay, M. H., Dulio, V., Alygizakis, N., Dal Bello, F., ... & Calza, P. (2021). Elucidation of the photoinduced transformations of Aliskiren in river water using liquid chromatography high-resolution mass spectrometry. *Science of The Total Environment*, 800, 149547.
73. Freeling, F., Alygizakis, N. A., Peter, C., Slobodnik, J., Oswald, P., Aalizadeh, R., ... & Scheurer, M. (2019). Occurrence and potential environmental risk of surfactants and their transformation products discharged by wastewater treatment plants. *Science of the Total Environment*, 681, 475-487.
74. Ibáñez, M., Borova, V., Boix, C., Aalizadeh, R., Bade, R., Thomaidis, N. S., & Hernandez, F. (2017). UHPLC-QTOF MS screening of pharmaceuticals and their metabolites in treated wastewater samples from Athens. *Journal of hazardous materials*, 323, 26-35.
75. Box, G. E., Hunter, W. H., & Hunter, S. (1978). *Statistics for experimenters* (Vol. 664). New York: John Wiley and sons.
76. Mašković, M., Jančić-Stojanović, B., Malenović, A., Ivanović, D., & Medenica, M. (2010). Assessment of liquid chromatographic method robustness by use of Plackett-Burman design. *Acta Chromatographica*, 22(2), 281-296.

77. Guthrie, W., Filliben, A., & Tarvainen, T. (2013). NIST/SEMATECH e-handbook of statistical methods. *Process Modeling*.
78. Massart, D. L., Vandeginste, B. G., Buydens, L. M. C., De Jong, S., Lewi, P. J., & Smeyers-Verbeke, J. (1998). Handbook of chemometrics and qualimetrics: Part A. *Elsevier Science*.
79. Miller, J., & Miller, J. C. (2018). *Statistics and chemometrics for analytical chemistry*. Pearson education.
80. Sakkas, V. A., Islam, M. A., Stalikas, C., & Albanis, T. A. (2010). Photocatalytic degradation using design of experiments: a review and example of the Congo red degradation. *Journal of hazardous materials*, 175(1-3), 33-44.
81. Ferreira, S. L., Caires, A. O., Borges, T. D. S., Lima, A. M., Silva, L. O., & dos Santos, W. N. (2017). Robustness evaluation in analytical methods optimized using experimental designs. *Microchemical Journal*, 131, 163-169.

CHAPTER 3

Development and Validation of LC-MS/MS Methods for CECs Determination

3. DEVELOPMENT AND VALIDATION OF LC-MS/MS METHODS FOR CECs DETERMINATION

3.1 Introduction

This chapter discusses three LC-MS/MS methods that were developed and validated for analyzing emerging contaminants of concern (CECs) in water. Two of these methods were developed to analyze a specific CEC and its transformation products (TPs), whereas the third method was developed for the determination of ten pharmaceutical compounds consisting of anticancer agents, an antidepressant, and a renin-inhibitor.

Part I describes the LC-MS/MS methods developed for analyzing a particular compound and its TPs. The compounds of interest were irinotecan (an anticancer agent) and aliskiren (a renin-inhibitor). First, the photodegradation fate of each of these compounds in water was studied independently using simulated solar irradiation, and the photodegradation products were identified. Then, two independent UHPLC-MS/MS methods were developed and validated for the analysis of irinotecan and its PDPs, as well as aliskiren and its PDPs, in various matrices (surface waters, ground water, and wastewater effluents). Part I will cover the photodegradation procedures, identification of TPs, and description of the LC-MS/MS method development, validation, and application to real samples. The general workflow was similar for both irinotecan and aliskiren. Thus, the experimental and conclusion sections have been integrated and presented together. However, the results and discussion sections have been treated separately.

The findings of the research reported in Part I have been published in two peer-reviewed open access journals that may be accessed via the following links:

- Irinotecan (<https://doi.org/10.1016/j.envpol.2019.113370>)
- Aliskiren (<https://doi.org/10.1016/j.scitotenv.2021.149547>)

Part II is devoted to the development and validation of an automated on-line SPE LC-MS/MS method for the determination of ten pharmaceuticals in wastewater. The target analytes were from three different drug classes, and this part of the chapter will detail the method development and validation, as well as its application to real wastewater samples.

The findings reported in Part II have also been recently published in a peer-reviewed open access journal which can be accessed via the following link:

- Online SPE LC-MS/MS method <https://www.mdpi.com/2305-6304/10/3/103>.

In general, this chapter is organized as follows: first, a brief BACKGROUND is provided, which is common to both Part I and II and explains the knowledge gap and objectives. Then, for Part I and Part II, the EXPERIMENTAL, RESULTS AND DISCUSSION, and CONCLUSION sections will be described separately. Following that, all the chemicals, reagents, and instrumentation used in the three LC-MS/MS methods are listed under the 'MATERIALS' section. Finally, CONCLUSIONS for the entire chapter has been provided, followed by a list of references.

3.2 Background of the studies

Pharmaceuticals are among the most frequently detected CECs in water, usually at very low concentrations ranging from ultratrace (ng/L) to trace ($\mu\text{g/L}$) levels [1, 2], which are currently regarded as a potential hazard for a variety of living organisms, including humans [3, 4]. Moreover, recent studies have shown that pharmaceuticals levels in urban wastewaters are rising due to population ageing and the increase in population density [5]. The removal efficiency of pharmaceuticals varies greatly among different wastewater treatment systems, and a significant amount of the parent drugs, metabolites, and their transformation products may pass through and enter the aquatic environment [6-9] and wetlands [10]. The occurrence of pharmaceuticals in the environment can be affected by their overall consumption and their fate in the environment. As a result, pharmaceuticals with larger consumption rates have been commonly detected in wastewater, surface water, and even in drinking water [11]. Nowadays, thanks to the advancements in analytical instruments and the increased sensitivity of analytical methods, quantification of a large group of pharmaceuticals in various aqueous matrices is becoming a common practice.

The continuous rise of cancer cases has led to the increased use of anticancer drugs and a further increase of their use in the future is predicted [12, 13]. Anticancer drugs (also known as, antineoplastics) are a group of compounds mainly administered to outpatient and inpatient cancer therapy in hospitals and they represent one of the most toxic compounds used as a medication [14]. Municipal and hospital wastewaters, treated or untreated, are the main routes for anticancer drugs in the aquatic environment. Studies have indicated that anticancer drugs could exert cytotoxic, genotoxic, mutagenic, carcinogenic, or teratogenic effects on aquatic species [15, 16]. Furthermore, other studies [17, 18] have found that antineoplastics have low

degradability by conventional wastewater treatments. As a result, anticancer drugs and their transformation products require greater attention as potential emerging contaminants, and sufficient information regarding their occurrence and concentrations in the aquatic environment should be documented. In agreement with this, a growing number of studies have been published reporting the occurrence of antineoplastics in wastewater effluents and influents [14, 19-22], while some studies have also measured them in surface and ground waters [23-25]. A considerable gap exists in the development of highly sensitive and reliable multi-residue analytical methods capable of measuring anticancer drugs at low concentrations. Furthermore, the environmental fate of many of these compounds has received little to no attention. As a result, there is currently a scarcity of data on the occurrence and fate of most of the approved anticancer drugs in the aquatic environment.

In this thesis, we studied ten pharmaceutical compounds consisting of eight antineoplastics (methotrexate (MTX), docetaxel (DTX), etoposide (ETP), irinotecan (IRI), topotecan (TOP), cabazitaxel (CTX), paclitaxel (PTX), and doxorubicin (DOX)), an antidepressant (maprotiline (MAP)), and an antihypertensive (aliskiren (ALK)). The chemicals were selected based on available consumption data in the EU, excretion percentage of their unchanged forms, and frequency of detection in WWTP influents and effluents [5, 11, 16, 26-28]. Other criteria in their selection were a scarcity of information about their occurrence and fate in the aquatic environment, as well as their suitability for LC-MS/MS analysis (see *Chapter 1* for further info).

Significant amounts of the selected compounds are excreted unmetabolized. For example, 60–95% MTX; 25–45% ETP and TOP; 5–15% PAC, DTX, CTX and DOX; 45–63% IRI; up to 80% ALK [27-29]. Furthermore, most of the selected target analytes were reported to have been detected and quantified in surface waters, and urban and hospital wastewaters (influent and effluent) at low concentrations. This included 1.6–300 ng/L MTX [20, 22, 30, 31], 18.5–100 ng/L PTX [1, 22], 9.0–10 ng/L MAP [32, 33], 2.5–2.7 ng/L DOX [22], 0.4–60 ng/L IRI [21, 22, 25, 30], 3.4–15 ng/L ETP [21], 0.4–1900 ng/L ALK [34], and 97.7–175.1 ng/L DTX [1]. Once they enter the aquatic environment, these compounds can undergo transformations and generate products whose effects are merely known [35-38]. Despite their extensive usage and the relatively higher excretion rates in their unmetabolized forms, CTX and TOP have not been previously detected in the aquatic environment. In general, there is limited information on the occurrence of all of the target compounds in the aquatic environment, which motivated us to develop a fully automated, highly sensitive on-line SPE LC-MS/MS method for determining them in different wastewater samples.

We also investigated the photodegradation fate of irinotecan and aliskiren using simulated solar irradiation. A large amount (45-63%) of unmetabolized irinotecan is excreted [39], an

amount that typically enters the sewerage system in concentrations ranging from 0.015 ng/L to 2.03 µg/L [30, 40-43], ultimately reaching groundwater and surface water. Similarly, aliskiren – a direct renin inhibitor – is mostly eliminated (approximately 80%) in its unmetabolized form [29] and existing wastewater treatment systems are ineffective at removing it, as indicated by a small decrease from 0.27 µg/L (influent) to 0.25 µg/L (effluent) [44]. As a result, aliskiren has been found in wastewater effluents at concentrations ranging from 0.4 to 1.9 µg/L [34] and surface waters in the range 0.4-5.0 ng/L [45]. To the best of our knowledge, despite their presence in environmental matrices, there is very limited information on the photodegradation fate of irinotecan and none on aliskiren. Thus, we investigated the natural photodegradation of irinotecan and aliskiren for the identification of, potentially new, degradation products in water samples. We carried out the degradation experiments under simulated solar irradiation in a Solarbox equipped with a xenon lamp, fixing irradiation intensity and temperature values to reproduce the average conditions of surface water for the period between May and September in Alessandria, Italy. This approach was successfully used in previous studies and allowed the identification of several transformation products of different micropollutants in water [46-49].

The following sections will describe the development and validation of two rapid and sensitive UHPLC-MS/MS methods suitable for the identification of irinotecan, aliskiren and their respective TPs in different real water samples, and a multi-residue on-line SPE LC-MS/MS method developed for the determination of the ten pharmaceuticals described above.

Part I – Irinotecan and Aliskiren

**UHPLC-MS/MS Methods Developed and
Validated for the Identification of Irinotecan,
Aliskiren, and their Transformation Products**

3.3 Experimental part

3.3.1 Photodegradation experiments

Photodegradation experiments were conducted using a simulated solar irradiation in a Solarbox 3000e (CoFoMeGra, Milan, Italy) equipped with a Xenon lamp (2500 W). Experiments for irinotecan and aliskiren were performed separately. A 10.0 mg/L solution of the target compound (i.e., irinotecan or aliskiren) prepared in ultrapure water was transferred into a 28-mL cylindrical quartz cell (Fig. 3.1b) and inserted into the Solarbox (Fig. 3.1a). The simulated solar irradiation was provided by the Xe lamp, which was fixed at irradiation intensity and temperature of 600 W/m² and 35 °C, respectively. Moreover, a UV outdoor filter (<290 nm) was installed to better mimic the natural surface water conditions. The instrumental conditions were chosen based on the average (day and night) solar irradiation and temperature in Alessandria (Piedmont, Italy) as measured by our department's meteorological station from May to September. The irradiation experiments were carried out for a total of 13 days. Sample aliquots (3 mL) were withdrawn after every irradiation at prefixed time intervals (0, 1, 2, 4, 8, 24, 48, 72, 154, 182, 296, and 312 h). The quartz cell was emptied and meticulously cleaned after each sample withdrawal before being refilled with a new fresh solution of the target compound. The degradation progress was initially monitored by analyzing the sample aliquots using a UV-Vis spectrophotometer. Then, the aliquots were stored in amber vials at -20 °C until further analysis by LC-MS/MS.

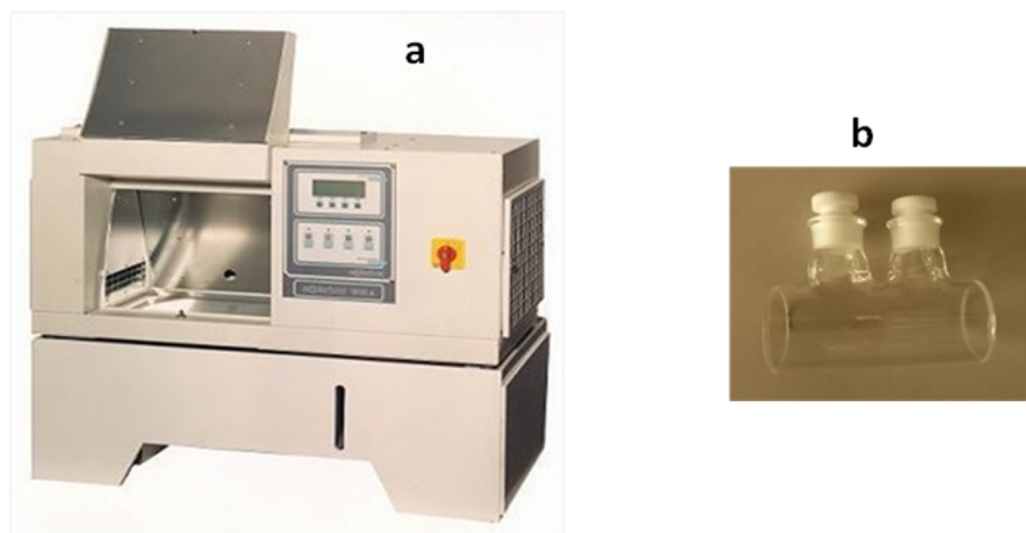


Figure 3.1. Solarbox 3000e (a) and a quartz cuvette (b)

3.3.2 Solid-phase extraction (SPE) procedure

SPE was performed using a VWR (Merck, Darmstadt, Germany) C18 Isolute (100 mg/1 mL) cartridge which had been pre-conditioned with 2.0 mL of methanol and 2.0 mL of ultrapure water. The cartridge was loaded with a 10 mL water sample, washed with 2.0 mL water, and dried for 5 minutes under vacuum. The sample was then eluted with 1.6 mL of methanol, evaporated to dryness with a gentle stream of nitrogen, and reconstituted with 1.0 mL of the mobile phase at the initial gradient conditions (final pre-concentration factor 10x).

3.3.3 Development of UHPLC-MS/MS methods

The chromatographic separation was achieved using a Phenomenex (Bologna, Italy) Kinetex XB-C18 column (3.0 x 100 mm, 1.7 μ m) with a mobile phase mixture of water with the addition of 0.1% formic acid (A) and methanol with the addition of 0.1% formic acid (B), eluting at a flow rate 0.45 mL/min. The injection volume was 5.0 μ L, and the oven temperature was set at 40 °C. The total run time was 10 min and the final gradient conditions for the LC-MS/MS methods working in selected reaction monitoring (SRM) mode were as follows: 10% B at 0.00-0.05 min, 90% B at 8.00 min, 100% B at 8.01 which was maintained until 8.80 min, and equilibrated at the initial conditions of 10% B from 8.81 to 10.00 min.

For both irinotecan and aliskiren, the turbo ion spray (TIS) ionization in positive ion (PI) mode was produced by a Turbo VTM interface. The MS source parameters are summarized in Table 3.1. The collision energy (CE) was set at 10 V in MS experiments and at 65 \pm 20 V collision energy spread (CES) in the Enhanced Product Ion (EPI) experiments. The unit mass resolution was established and maintained in each mass-resolving quadrupole by keeping a full width at half maximum (FWHM) of about 0.7 u.

Table 3.1. MS source parameters for the irinotecan and aliskiren methods

Parameter	IRI method	ALK method
Ion spray voltage (IS)	5300 V	5000 V
Curtain gas (N ₂)	30 psig	30 psig
Nebuliser gas GS1 (N ₂)	70 psig	65 psig
Drying gas GS2 (N ₂)	65 psig	70 psig
Desolvation temperature (TEM)	450 °C	500 °C
Collision activated dissociation gas (CAD)	6 arb	6 arb

To develop a sensitive UHPLC-MS/MS method capable of identifying unknown TPs in water samples, the hybrid MS detector (3200 QTRAP, Sciex, Canada) was used first in quadrupole-

ion trap (Q-LIT) mode and then in triple quadrupole (QQQ) mode. To develop a more selective, sensitive, and fast SRM method in the QQQ, the Q-LIT mode has been used to generate the precursor/product ion transitions. Q-LIT mode enables non-target analysis and the identification of the species found in the studied samples. The data was acquired using IDA, in which the mass spectrometer operated in cycles with an Enhanced MS experiment (EMS) at 1000 Da/s as a survey scan and two dependent scans – an Enhanced Resolution (ER) scan at 250 Da/s and an Enhanced Product Ion (EPI) scan at 1000 Da/s. The EMS scanned between m/z 100 and m/z 700 on the most abundant ion, using dynamic background subtraction. The total cycle time of the analysis was 1.96 s. The following DDA conditions had to be met in order for the dependent scans to be triggered: the ion of the survey scan must be within the range m/z 100 and 700, and it had to exceed the 10,000 counts per second (cps) threshold. If an ion had >3 occurrences, it was excluded from the subsequent scans for 5 s. The overall DDA run time was 20 min, with a flow rate of 0.30 mL/min and the following gradient profile: 0.0-1.0 min 10% B, 17.0 min 100% B, 17.0-18.0 min 100% B, 18.1 min 10% until 20.0 min.

3.3.4 Identification of Aliskiren TPs using HRMS

Identification of the TPs formed from aliskiren photodegradation was achieved using an Ultimate 3000 HPLC system coupled with LTQ-Orbitrap mass spectrometer (Thermo Scientific, Bremen, Germany) in ESI positive mode. The analyses were performed by injecting 20 μ L sample into a Luna (2) C18 column (150 x 2 mm, 3 μ m; Phenomenex, Bologna, Italy) using a mixture of acetonitrile and 20 mM formic acid solution as the mobile phase with the following gradient: 0 min, 95:5 v/v; 18 min, 60:40 v/v; 23 min, 0:100 v/v; and then reconditioning the column. The mobile phase flow rate was 0.2 mL/min.

Nitrogen (N₂) gas was employed as a sheath and auxiliary gas in the ESI ion source. The following source settings were used: sheath gas was 30 arbitrary units (arb); auxiliary gas was 25 arbs; capillary voltage was 4.0 kV; and capillary temperature was 275 °C. Full MS data were collected in positive ion mode with a mass range of m/z 50–500 and a resolution of 30,000. Multi-stage mass spectra (MSⁿ) were collected in the region between the ion trap cut-off and the m/z of the precursor ion. The accuracy of the analyzed m/z (as compared to the estimated value) was 0.001 (without internal calibration).

3.3.5 Real water samples

The validated UHPLC-MS/MS methods were applied to various real water samples. Some water samples were taken nearby a wastewater treatment plant (WWTP) outlet in Turin,

while others were taken from the Po river (near the WWTP exit and near the Molinette Hospital), and from the hospital effluent. Groundwater and well water (pre- and post-chlorination) were collected in a rural region on the outskirts of Turin. All blank samples were taken from the protected area of Gran Paradiso National Park (Piedmont, Italy), around Noasca, Orco Valley, where we assumed there would be no irinotecan and aliskiren contamination. Prior to direct injection into the UHPLC-MS/MS system or SPE, all water samples were filtered using 0.2 μm polytetrafluoroethylene (PTFE) filters (VWR International, Darmstadt, Germany).

3.4 Results and Discussion

3.4.1 Development of UHPLC-MS/MS methods

Standard aqueous solutions of either irinotecan or aliskiren irradiated at different intervals were analyzed using the IDA strategy outlined in the experimental section to gather as much information as possible on the features of the new compounds (TPs) produced during photoirradiation. As a result of the method development and optimization procedures performed using the Q-LIT and QQQ modes of the MS, an SRM method was built using the precursor/product ion transitions assigned to each chromatographic peak. However, the collision energy values were re-optimized, as the values obtained by EPI experiments were slightly different from those that can be obtained from a typical MS/MS experiment performed by a QQQ instrument. As a result, the degraded samples were infused into the MS, and all compound-dependent parameters were re-optimized for each photodegradation product (PDP), including the Declustering Potential (DP), Entrance Potential (EP), Collision Energy (CE), and Collision eXit Potential (CXP). The final MRM transitions and corresponding mass spectrometric parameters are summarized in Table 3.2a for irinotecan and Table 3.2b for aliskiren.

Table 3.2a. Mass spectrometry parameters and MRM transitions for irinotecan and its PDPs. In all cases, the dwell time was 20 ms. The transitions in Q3 are listed in descending order, beginning with the most intense (quantifier ion) and ending with the least.

Compound	Q1	Q3	DP	EP	CE	CXP
Irinotecan	587.3	167.3/124.2/195.3	95.9	9.6	57.89/51.93/42.98	2.40/2.15/2.77
PDP1	437.3	167.2/124.3/229.3	71.2	10.5	42.52/38.91/36.00	2.32/2.25/2.84
PDP2	439.4	124.1/167.3/195.2	63.3	10.8	41.66/54.36/2.74	2.26/2.74/2.42
PDP3	423.2	167.2/124.2/195.3	69.6	12.0	56.1/40.77/35.68	2.45/2.21/2.49
PDP4	619.4	167.2/124.4/195.4	88.8	11.1	75.87/65.63/48.63	2.38/2.03/2.37
PDP5	603.4	124.3/167.2/195.3	79.4	11.1	58.68/61.1/39.91	2.22/2.39/2.97
PDP6	557.3	167.3/124.2/195.3	81.9	10.5	54.74/48.77/41.41	2.40/2.15/2.48
PDP7	529.4	124.4/167.0/195.3	75.1	11.1	42.88/55.35/36.17	2.23/2.47/2.77
PDP8	573.3	124.4/195.3/167.5	73.2	10.1	45.69/40.99/59.89	2.11/2.48/2.25

Table 3.2b. Mass spectrometry parameters and MRM transitions for aliskiren and its PDPs.

Compound	Q1	Q3	DP	EP	CE	CXP
Aliskiren	552.4	534.4/436.3	46.7	8.0	47.38/28.74	2.47/3.35
TP1	340.3	323.2/306.2	39.7	9.7	26.61/44.07	2.36/2.20
TP2	436.3	346.3/419.1	40.6	11.1	21.94/39.22	3.33/2.33
TP3	436.3	346.3/419.1	41.7	11.1	21.94/39.22	3.33/2.33
TP4	548.4	530.4/432.3	43.8	9.4	27.38/43.01	3.12/2.35
TP5	566.4	548.4/450.3	50.1	10.1	20.82/26.98	3.22/2.81
TP6	568.3	550.2/434.1	49.8	10.4	22.20/43.73	3.50/2.19

3.4.2 Validation of the UHPLC-MS/MS methods

External calibration plots for irinotecan (IRI) and aliskiren (ALK) were created independently using eleven different standard solutions (LOQ, 0.100, 0.500, 1.00, 5.00, 10.0, 50.0, 100, 250, 500, and 1.00×10^3 ng/mL) and injected in randomized sequence to avoid memory effects. For each analyte, the chromatographic peak area of the quantifier transition (y) was correlated against the standard concentration (x) with a weighting factor of $1/x$, resulting in a linear regression fit with R^2 values of 0.9992 for irinotecan and 0.9988 for aliskiren. The variances explained by the models were significant, as confirmed by the F-test ($p=0.01$).

The limits of detection (LOD) and the limits of quantitation (LOQ) were calculated in accordance with guidelines provided by the International Council for Harmonization of Technical Requirements for Pharmaceuticals for Human Use (ICH) regulation as follows: $LOD = 3.3 \cdot (s_B/b)$ and $LOQ = 10 \cdot (s_B/b)$, where s_B represents the blank standard deviation, equal to the residual standard deviation ($s_{y/x}$), and b is the slope of the calibration curve. The LODs were 0.019 ng/mL and 0.051 ng/mL, and LOQs were 0.048 ng/mL and 0.22 ng/mL, respectively for IRI and ALK, demonstrating the high sensitivity of both methods.

The method detection limit (MDL) was also determined using seven replicates of each investigated blank real water sample (river water, groundwater, well water, and wastewater) spiked with a solution of the target compound at a concentration giving a S/N ratio between 2.5 and 5. MDL was calculated as $MDL = t_{(n-1, 1-\alpha=0.99)} \cdot S_d$, where $t = 3.14$ corresponds to a t -Student's value for 99% confidence level and 6 degrees of freedom, and S_d represents the standard deviation of the replicate analyses. The method quantification limit (MQL) was defined as 3 times the MDL value. The MDLs and MQLs obtained for four different water matrices are summarized in Table 3.3.

The intraday precision was determined by analyzing five replicates of each real sample spiked with the target analyte at the corresponding MQL values, while the inter-day precision was determined by replicating the intraday analyses for 7 days. As shown in Table 3.3, the intraday relative standard deviations (RSD) were all below 5%, and the inter-day RSDs were all less than 9%.

Table 3.3. Precision (intraday and inter-day RSD), MDL, and MQL values for IRI and ALK calculated in four different real water samples.

Sample	Intraday RSD (%)		Inter-day RSD (%)		MDL (ng/mL)		MQL (ng/mL)	
	IRI	ALK	IRI	ALK	IRI	ALK	IRI	ALK
River water	2.0	3.2	5.6	6.3	0.028	0.069	0.10	0.23
Groundwater	1.9	1.7	5.6	6.1	0.020	0.094	0.058	0.23
Well water	2.1	2.4	5.7	7.3	0.033	0.096	0.087	0.26
Wastewater	3.4	4.6	5.9	8.6	0.054	0.12	0.20	0.28

Each method's selectivity was evaluated using the blank real samples and no interfering species were detected at the target analyte's retention time in any of the real blank samples. Furthermore, matrix effect (ME) was evaluated by calculating the ME percentage (ME, %) using Eq. (3.1):

$$ME (\%) = \frac{Slope_{add}}{Slope_{ext}} * 100 - 100 \quad \text{Eq. (3.1)}$$

where $slope_{ext}$ is the slope of the external calibration plot and $slope_{add}$ is that of the standard addition curve built by spiking the real water sample with a standard solution of the target analyte at 50.0, 100 and 1.00×10^3 ng/mL. The spiked samples were prepared in triplicate and passed through the SPE procedure before being analyzed by the proper LC-MS/MS method. The comparison of the slopes can provide the following results: ME (%) = 0 (no matrix effects), ME (%) < 0 (signal suppression), or ME (%) > 0 (signal enhancement). ME was not significant for irinotecan and aliskiren in river, groundwater, or well water samples, but a signal suppression of 7% (IRI) and 12.3 % (ALK) was observed in wastewater samples.

The reproducibility of the SPE procedures was also evaluated for both irinotecan and aliskiren by calculating the percentage recovery (R, %) as follows:

$$Recovery (R, \%) = \frac{C_{obs}}{C_{ref}} * 100 \quad \text{Eq. (3.2)}$$

where C_{obs} was the concentration of the analyte determined following the LC-MS/MS analysis, and C_{ref} was that of a spiked solution. The analyte solutions were prepared at concentrations of 0.100, 10.0 and 100.0 ng/mL to cover as much of the linearity range as possible and were used to spike the blank real samples. The analysis was replicated three times for each concentration level. The %R values calculated for each spiked concentration level are reported in Table 3.4. The recovery values were highly reproducible and were independent of the

analyte concentration within the investigated range: in fact, a *t*-test (95% confidence level) showed that there was no difference among the R (%) values of the three concentration levels for all the investigated real water samples. As a result, an average recovery percentage was calculated for each investigated real sample, with the values ranging from 94.8 to 105.9% (irinotecan) and 91.9 to 103.7% (aliskiren), implying the satisfactory reproducibility of the SPE methods.

Table 3.4. Recovery values at three different concentration levels and average percentage recovery (R, %) of IRI and ALK in real water samples.

Sample	Spiked (ng/mL)	R (%)		Average R (%)	
		IRI	ALK	IRI	ALK
River water	0.100	104.1 ± 5.8	102.4 ± 4.1		
	10.0	112.5 ± 6.0	107.1 ± 6.7	105.0 ± 7.1	103.7 ± 5.8
	100	98.4 ± 8.0	101.6 ± 5.2		
Groundwater	0.100	100.3 ± 5.8	98.3 ± 4.9		
	10.0	102.1 ± 7.1	105.1 ± 6.3	101.9 ± 1.6	102.4 ± 2.3
	100	103.5 ± 4.6	103.7 ± 5.2		
Well water	0.100	102.9 ± 4.2	104.3 ± 5.2		
	10.0	107.6 ± 5.0	109.1 ± 5.6	105.9 ± 2.6	108.2 ± 3.1
	100	107.2 ± 4.6	111.3 ± 7.4		
Wastewater	0.100	95.0 ± 5.5	89.7 ± 8.1		
	10.0	94.7 ± 2.4	93.7 ± 5.0	94.8 ± 0.2	91.9 ± 2.2
	100	94.6 ± 4.5	94.2 ± 3.9		

3.4.3 Identification of TPs of irinotecan and aliskiren

3.4.3.1 Irinotecan

UV-Vis spectral analyses (Appendix I, Fig. S3.1) revealed that after 7.5 days, the original peak intensity (absorbance) of irinotecan at λ_{max} value of 220 nm was decreased by almost 90%. It is important to note that no substantial decline in absorbance values was detected between 296 h (12.3 days) and 312 h (13 days) of irradiation which could be attributed to the very low amount (<5% of the original) of the undegraded irinotecan.

First, a CID MS/MS characterization analysis of the target analyte was performed to provide information about the analyte fragmentation pathway, which was valuable for identifying unknown PDPs. Because the positive ESI mode was more sensitive and suitable for both the

parent compounds and the PDPs, all MS/MS investigations were performed in positive ionization mode. Regarding irinotecan, the precursor ion $[M+H]^+$ was identified at m/z 587.3 with good signal intensity, and consequently MS/MS data was acquired for this ion. Fig. 3.2 depicts the proposed IRI fragmentation pathway.

The reaction order of the irinotecan photodegradation was determined by plotting $\ln A$ (where A represents the chromatographic peak area) against the irradiation time (h) (Appendix I, Fig. S3.2), and the data fitted a pseudo-first order kinetic model. The determination coefficient (R^2) was 0.95, with a half-life time ($t_{1/2}$) of 8.24 h and a rate constant of 0.0841 h^{-1} . However, because the starting concentration of the irinotecan affects the kinetics of photodegradation, these results do not accurately represent the true decay rate of the drug in natural waters. On the contrary, we had to start with an initial concentration of 10.0 mg/L of the compound in order to acquire adequate chromatographic peak intensities which were necessary to unambiguously follow the formation of PDPs and develop the LC-MS method for their identification. Additional kinetic experiments were performed to provide with a more realistic photodegradation half-life time of the drug with initial concentrations of 1.0, 0.1, and 0.05 mg/L, which resulted in kinetics half-times of 38.5, 57.7, and 77.0 h, respectively.

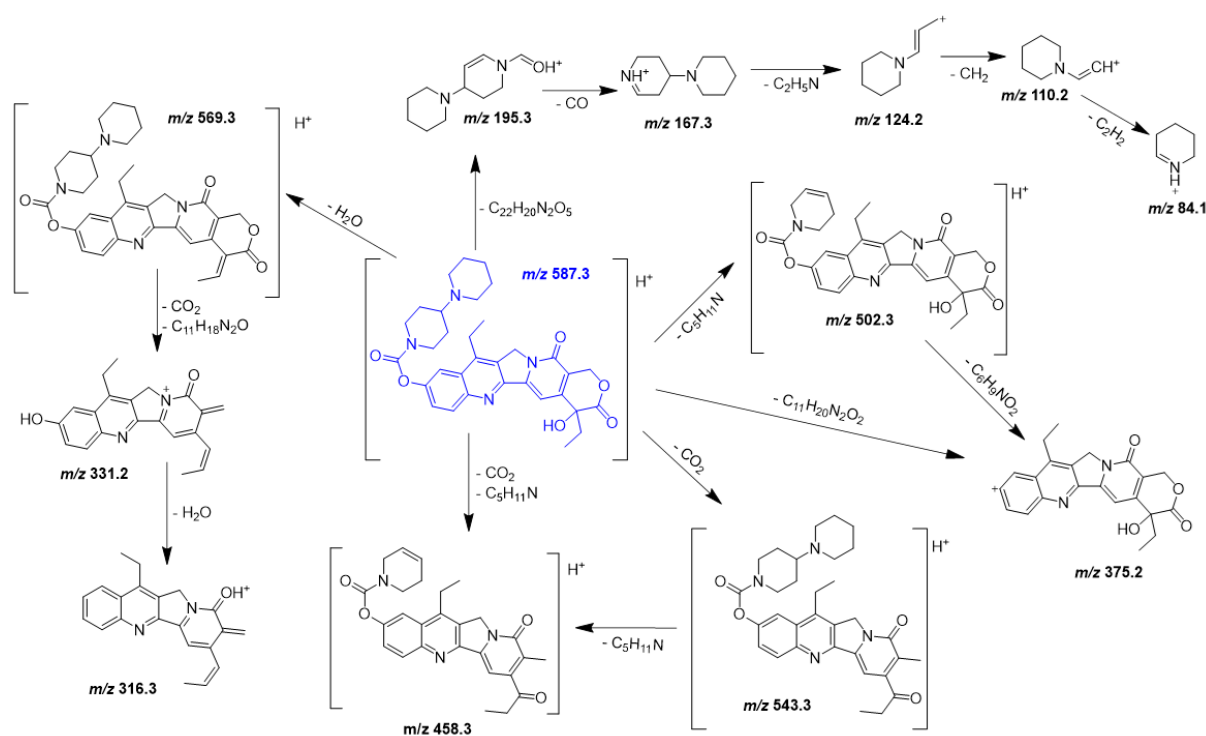


Figure 3.2. Proposed fragmentation pathways of the protonated irinotecan molecule.

Control experiments conducted in the dark for 13 days revealed no appreciable decay of IRI or the formation of degradation products, whereas eight PDPs were identified from the photo-

irradiated samples. The total ion chromatogram (TIC) in Fig. 3.3 shows the irinotecan peak gradually disappearing at retention time 5.96 min and the PDP peaks increasing to the left and right of the IRI peak.

A total of eight PDPs of IRI were identified at m/z 437.3 (PDP1), m/z 439.3 (PDP2), m/z 423.3 (PDP3), m/z 619.4 (PDP4), m/z 603.4 (PDP5), m/z 557.3 (PDP6), m/z 529.3 (PDP7), and m/z 573.3 (PDP8). PDP5 had two isomers, the first of which was twice as intense as the latter and eluted at 5.76 min, and the second of which co-eluted with the IRI peak. Fig. 3.4 depicts the evolutionary profile of the four most abundant PDPs. In general, the trend for the PDPs was described by a rapid spike in the first 4 hours, followed by a roughly sharp drop. The PDPs were then on the verge of disappearing within 24 hours. The lone exception was PDP2, which was produced at a rapid rate in the first two hours and steadily increased for approximately 24 h and then began to decline. This feature of PDP2 could be linked to the contributions of the other PDPs to its production [50].

In a similar way to irinotecan, a CID MS/MS characterization study was conducted on each of the PDPs to elucidate their chemical structures. According to the MS/MS data acquired in this study, all the PDPs appeared to have undergone modifications in the lactone ring (i.e., the 7-ethyl-camptothecin nucleus). The fragmentation spectra of IRI and all PDPs showed a similar loss of the distal piperidine (m/z 85.1). Additionally, the presence of fragments at m/z 110.3, 124.3, 167.3, and 195.3 due to the bipiperidine moiety (previously identified during IRI characterization, see Fig. 3.2), combined with the absence of decarboxylation of the lactone moiety, indicates that this latter moiety was the site of modification leading to the formation of the PDPs. PDP4 and PDP5 were hydroxylation byproducts, which were rapidly dehydrated upon initial H₂O loss. Moreover, two isomers of PDP5 were identified (PDP5a at RT = 5.76 min and PDP5b at RT = 6.03 min), with PDP5a being twice as intense as PDP5b.

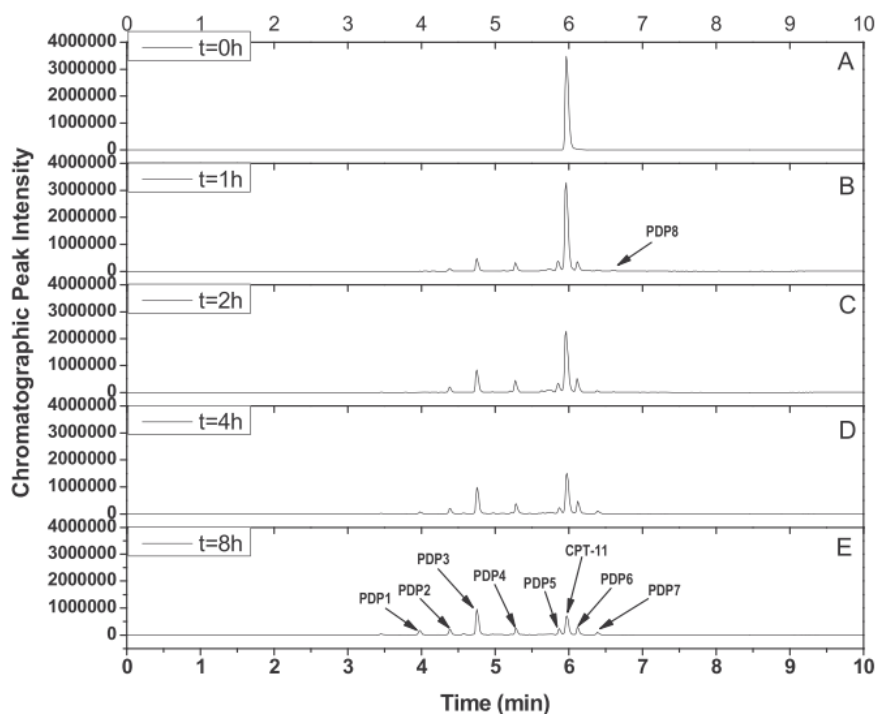


Figure 3.3. The TIC of irinotecan and its PDPs for non-irradiated (A), and after irradiation for 1-8 h (B-E). PDP8 (B) and PDP1-PDP7 (E) are indicated by arrows.

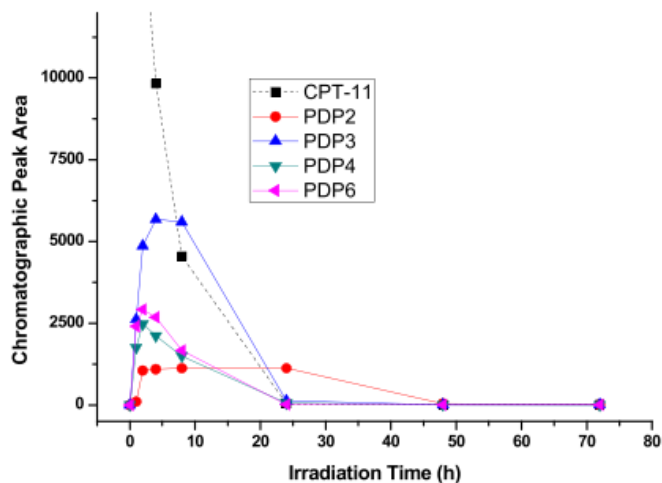
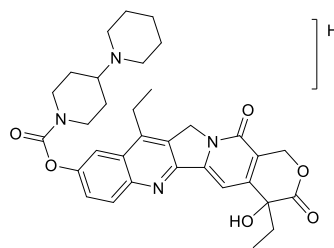
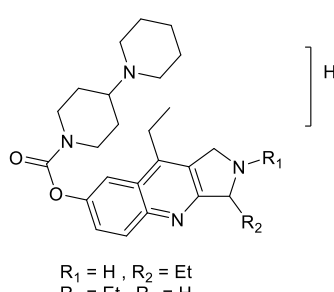
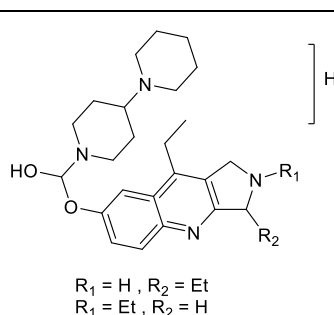
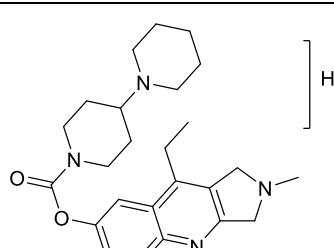


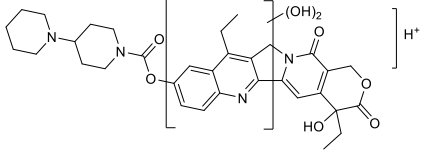
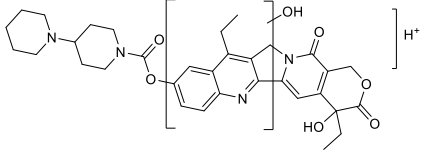
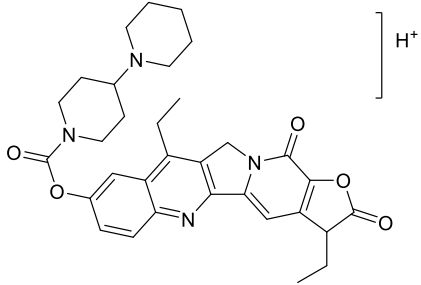
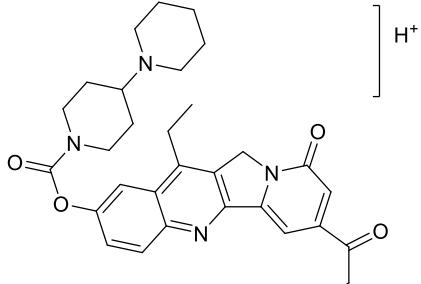
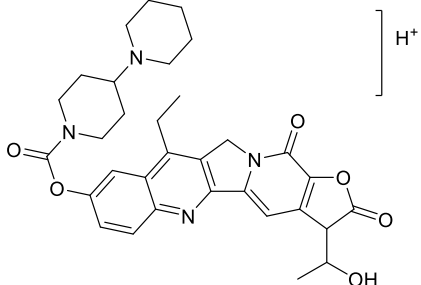
Figure 3.4. The evolution profile of the four most abundant PDPs of irinotecan.

In order to propose the chemical structures of the unknown species formed during the photoirradiation process, we used the following experimental data: (a) the precursor ion from the MS experiment used to determine the molecular mass, (b) the ER spectrum used to determine the isotopic pattern, (c) the number of nitrogen atoms (even or odd) used to determine the even or odd molecular mass, and (d) the EPI MS/MS spectrum used to determine the main fragment ions of the considered species. In this way, the compounds PDP1, PDP2, PDP3, PDP4 and PDP8 were identified for the first time. The MS/MS spectra of the

PDPs with assigned structures are reported in Appendix, Fig. S3.3a-h. The structure of PDP5 was analogous to a molecule previously identified from bile and urine samples of a patient receiving irinotecan treatment [51]. The chemicals PDP6 and PDP7 had also been detected during pharmacological degradation experiments on aqueous solutions exposed to laboratory light [50]. Table 3.5 summarizes the LC-MS/MS data and proposed structures of the irinotecan photodegradation products.

Table 3.5. Proposed chemical structures of irinotecan photodegradation products.

Compound	RT	[M+H] ⁺ m/z	Chemical formula	Proposed structure	Main MS/MS fragment ions
Irinotecan	5.96	587.4	C ₃₃ H ₃₉ N ₄ O ₆ ⁺		543, 502, 331
PDP1 (TP-437)	3.98	437.3	C ₂₆ H ₃₇ N ₄ O ₂ ⁺	 R ₁ = H, R ₂ = Et R ₁ = Et, R ₂ = H	352, 229, 225
PDP2 (TP-439)	4.39	439.3	C ₂₆ H ₃₉ N ₄ O ₂ ⁺	 R ₁ = H, R ₂ = Et R ₁ = Et, R ₂ = H	354, 227, 154
PDP3 (TP-423)	4.75	423.3	C ₂₅ H ₃₅ N ₄ O ₂ ⁺		338, 229, 211

PDP4 (TP-619)	5.28	619.4	$C_{33}H_{39}N_4O_8^+$		601, 575, 557
PDP5 (TP-603)	5.84	603.4	$C_{33}H_{39}N_4O_7^+$		585, 518, 347
PDP6 (TP-557)	6.12	557.3	$C_{32}H_{37}N_4O_5^+$		472, 345, 327
PDP7 (TP-529)	6.41	529.3	$C_{31}H_{37}N_4O_4^+$		444, 317, 261
PDP8 (TP-573)	6.66	573.3	$C_{32}H_{37}N_4O_6^+$		529, 343, 287

3.4.3.2 Aliskiren

Similar to irinotecan, we studied the photodegradation of aliskiren by subjecting ultrapure or river water spiked solutions (10 mg/L) to simulated sunlight in order to establish the presence of direct and indirect photolysis. Preliminary UV-Vis spectral measurements (see Fig. S3.4 in Appendix I) revealed the decrease by 50% of the peak at λ_{max} (220 nm) in ultrapure water samples, and there was at least one new peak appearing along the 245-255 nm wavelength. However, no significant drop or rise in absorbance values was observed from 240 h up to the

maximum irradiation time of 312 h, which may be due to the very low amount of the undegraded aliskiren remaining in the solution. Fig. 3.5 demonstrates that the drug was removed more rapidly in ultrapure water than in river water, indicating the more significant role of direct photolysis played a significant role in the degradation. On the other hand, the molecule's degradation under dark conditions was negligible. The degradation half-life was 5 h in ultrapure water, five times faster than that of river water ($t_{1/2} = 24$ h). The slower degradation observed in river water may be attributed to a scavenging action exerted by one or more components of river water, which obstructs light absorption or quenches reactive species [52].

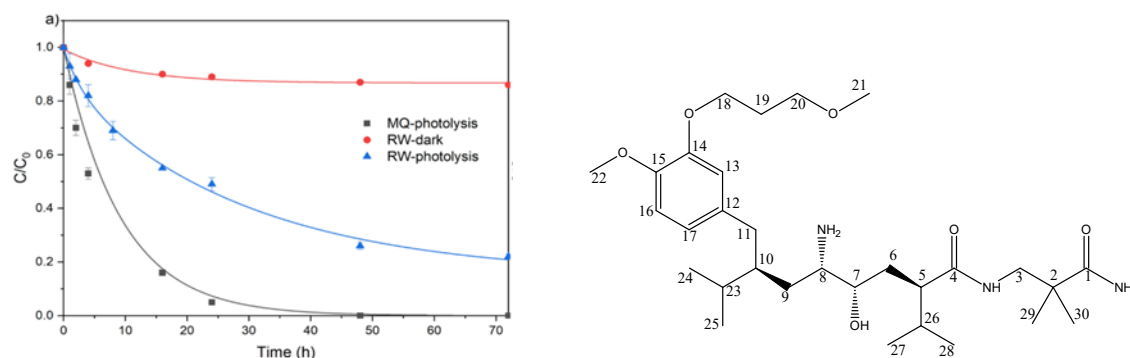


Figure 3.5. Degradation of aliskiren in ultrapure water (MQ-black line) and river water (RW-blue line) under irradiation and in the absence of light (red line).

Collision-induced dissociation (CID) experiments were performed to study the mechanism of aliskiren fragmentation, allowing the most likely losses from the protonated molecule to be determined. The proposed fragmentation pathway is shown in Fig. 3.6 and the list of MS² and MS³ fragment ions is given in Table 3.6. The protonated aliskiren precursor ion (m/z 552.4015) was fragmented into the product ions at m/z 534 and 436 through the loss of water and C₅H₁₂N₂O, respectively. MS³ spectrum from the precursor ion at m/z 534 produces four ions: the ions with m/z 517 and 500 through the loss of one (or two) NH₃ molecules, and the product ion at m/z 418 and 401 from the loss of C₅H₁₂N₂O and the joint loss of C₅H₁₂N₂O and NH₃, respectively. MS³ performed on the ion at m/z 436 fragmented into m/z 418 and 419 ions by involving the loss of H₂O and NH₃, respectively. The observed fragmentation pathways agreed with literature data [54].

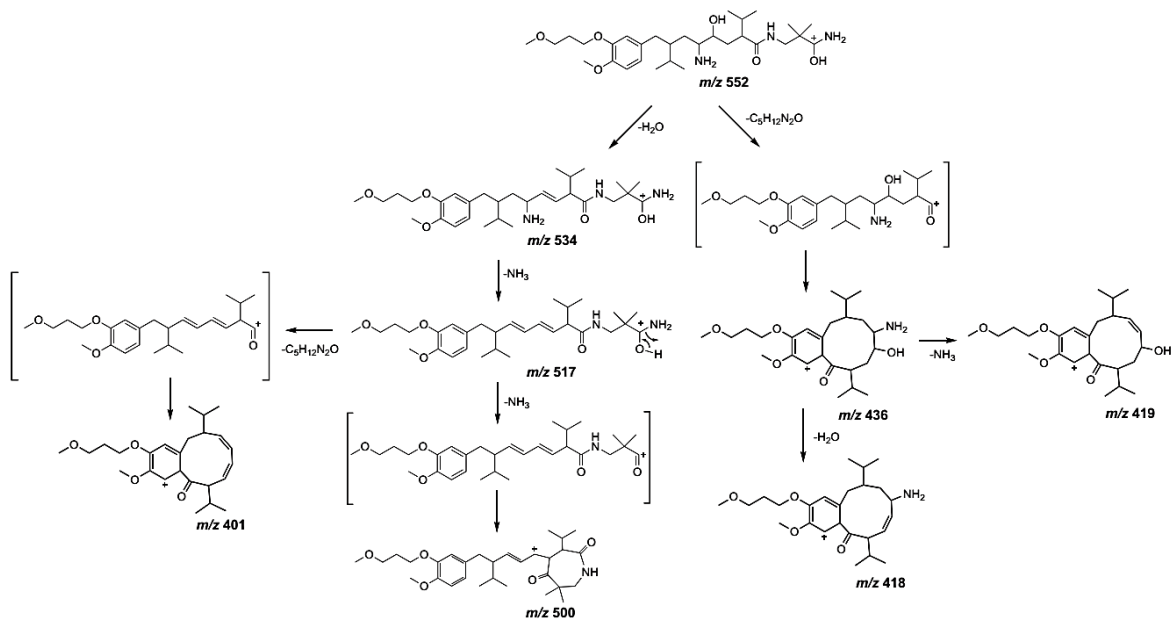


Figure 3.6. Fragmentation pathway proposed for the protonated aliskiren molecule.

Aliskiren transformation products (TPs) were identified by analyzing the irradiated samples using LC-HRMS in ESI positive mode. A total of six TPs were identified, and their m/z ratios, elemental compositions, retention periods, and product ions are listed in Table 3.6. The probable elemental composition of the TPs was deduced using Thermo Xcalibur software [2.1.0], based on mass accuracy (<5 ppm) and RDB (ring double bond) index. We explored for potential TPs based on possible modifications reported in the literature [53] giving known m/z differences. The non-target methodology described by Schymanski et al. [55] was used to identify all observed TPs at level 2. The parent aliskiren molecule was mono hydroxylated, resulting in the formation of TP6, a chemical with m/z 568.3962 and the protonated molecular formula $\text{C}_{30}\text{H}_{54}\text{O}_7\text{N}_3^+$ (see Appendix I, Fig. S3.5). This precursor ion was fragmented into m/z 550, 452, and 434 by H_2O loss, $\text{C}_5\text{H}_{12}\text{N}_2\text{O}$ loss (identical to the parent compound fragmentation), and further H_2O loss, in that order. MS³ fragmentation of the m/z 434 resulted in the formation of the structural diagnostic ion at m/z 238, which allowed the hydroxylation to be restricted to C_{11} or the aromatic ring. However, information was insufficient to attribute a unique structure.

The oxidation of an alcoholic group in TP6 to a carbonyl group resulted in TP5 with m/z 566.3805 and the protonated chemical formula $\text{C}_{30}\text{H}_{52}\text{O}_7\text{N}_3^+$. Indeed, TP5 exhibited the same fragmentation patterns as TP6. However, the product ion at m/z 236 allowed us to suggest the oxygen addition in the C_{11} and rule out the involvement of the aromatic ring, as shown in Appendix Fig. S3.6. As a result, it is possible to conclude that the OH group in TP6 is located on the same carbon.

Table 3.6. Summary of $[M+H]^+$ ions and main product ions from CID experiments.

Compound	$[M+H]^+$	Empirical Formula	RDB	Δ (ppm)	RT (min)	MS ²				MS ³			
						<i>m/z</i>	Empirical formula	loss	Δ (ppm)	<i>m/z</i>	Empirical formula	loss	Δ (ppm)
Aliskiren	552.4015	C ₃₀ H ₅₄ O ₆ N ₃	5.5	0.45	15.3	534.3898	C ₃₀ H ₅₂ O ₅ N ₃	H ₂ O	-1.53	517.3642	C ₃₀ H ₄₉ O ₅ N ₂ (15)	NH ₃	1.18
										500.3369	C ₃₀ H ₄₆ O ₅ N (25)	(NH ₃) ₂	-0.4
										418.2941	C ₂₅ H ₄₀ O ₄ N (100)	C ₅ H ₁₂ ON ₂	-2.49
										401.2696	C ₂₅ H ₃₇ O ₄ (8)	C ₅ H ₁₅ ON ₃	2.42
						436.3033	C ₂₅ H ₄₂ O ₅ N	C ₅ H ₁₂ ON ₂	-2.10	419.2811	C ₂₅ H ₃₉ O ₅ (100)	NH ₃	-1.88
										418.2970	C ₂₅ H ₄₀ O ₄ N (45)	H ₂ O	-2.07
TP1	340.2601	C ₁₈ H ₃₄ O ₃ N ₃	3.5	0.30	9.3	323.2336	C ₁₈ H ₃₁ O ₃ N ₂ (65)	NH ₃	1.95				
						306.2070	C ₁₈ H ₂₈ O ₃ N (100)	(NH ₃) ₂	2.22				
TP2	436.3061	C ₂₅ H ₄₂ O ₅ N	5.5	0.18	16.2	419.2795	C ₂₅ H ₃₉ O ₅ (100)	NH ₃	-0.50	401.2692	C ₂₅ H ₃₇ O ₄ (100)	H ₂ O	1.41
										387.2534	C ₂₄ H ₃₅ O ₄ (5)	CH ₃ OH	-0.30
										369.2432	C ₂₄ H ₃₃ O ₃ (9)	CH ₆ O ₂	1.92
										346.2383	C ₂₁ H ₃₂ O ₃ N (60)	C ₄ H ₁₀ O ₂	0.09
TP3	436.3061	C ₂₅ H ₄₂ O ₅ N	5.5	0.18	16.7	419.2795	C ₂₅ H ₃₉ O ₅ (100)	NH ₃	-0.50	401.2692	C ₂₅ H ₃₇ O ₄ (100)	H ₂ O	1.41
										387.2534	C ₂₄ H ₃₅ O ₄ (5)	CH ₃ OH	-0.30
										369.2432	C ₂₄ H ₃₃ O ₃ (9)	CH ₆ O ₂	1.92
										346.2383	C ₂₁ H ₃₂ O ₃ N (58)	C ₄ H ₁₀ O ₂	0.09
TP4	548.3701	C ₃₀ H ₅₀ O ₆ N ₃	7.5	0.18	13.5	530.3591	C ₃₀ H ₄₈ O ₅ N ₃ (28)	H ₂ O	-0.61	513.33234	C ₃₀ H ₄₅ O ₅ N ₂ (70)	NH ₃	0.080
										496.30585	C ₃₀ H ₄₄ O ₅ N (100)	H ₃ N ₂	0.20
										414.2644	C ₂₅ H ₃₆ O ₄ N (25)	C ₅ H ₁₂ ON ₂	-0.15
						432.2748	C ₂₅ H ₃₈ O ₅ N (100)	C ₅ H ₁₂ ON ₂	-0.57	414.2644	C ₂₅ H ₃₆ O ₄ N (100)	H ₂ O	-0.15
										400.2486	C ₂₄ H ₃₄ O ₄ N (93)	CH ₄ O	0.96
										360.2176	C ₂₁ H ₃₀ O ₄ N (27)	C ₄ H ₈ O	0.29

						414.2644	C ₂₅ H ₃₆ O ₄ N (18)	C ₅ H ₁₄ O ₂ N ₂	-0.15	382.2382	C ₂₄ H ₃₂ O ₃ N (100)	CH ₄ O	1.44
										342.2070	C ₂₁ H ₂₈ O ₃ N (11)	C ₄ H ₈ O	1.93
										218.1544	C ₁₄ H ₂₀ ON (4)	C ₁₁ H ₁₆ O ₃	2.11
TP5	566.3805	C ₃₀ H ₅₂ O ₇ N ₃	6.5	0.59	13.7	548.3697	C ₃₀ H ₅₀ O ₆ N ₃ (85)	H ₂ O	-0.62	531.3427	C ₃₀ H ₄₇ O ₆ N ₂ (81)	NH ₃	0.29
										514.3162	C ₃₀ H ₄₄ O ₆ N (46)	(NH ₃) ₂	0.3
										432.2746	C ₂₅ H ₃₈ O ₅ N (100)	C ₅ H ₁₂ ON ₂	0.42
										400.2487	C ₂₄ H ₃₄ O ₄ N (3)	C ₆ H ₁₆ O ₂ N ₂	-0.23
										360.2173	C ₂₁ H ₃₀ O ₄ (10)	C ₉ H ₂₀ O ₂ N ₂	-0.04
						236.1650	C ₁₄ H ₂₂ O ₂ N (32)	C ₁₆ H ₂₈ O ₄ N ₂	-0.31				
						450.2853	C ₂₅ H ₄₀ O ₆ N (100)	C ₅ H ₁₂ ON ₂	-0.69				
432.2745	C ₂₅ H ₃₈ O ₅ N (15)	C ₅ H ₁₄ O ₂ N ₂	0.42										
TP6	568.3962	C ₃₀ H ₅₄ O ₇ N ₃	5.5	0.76	14.3	550.3864	C ₃₀ H ₅₂ O ₆ N ₃ (100)	H ₂ O	-1.05	532.3746	C ₃₀ H ₅₀ O ₅ N (100)	H ₂ O	1.27
										516.3323	C ₃₀ H ₄₆ O ₆ N (21)	(NH ₃) ₂	-0.90
										434.2906	C ₂₅ H ₄₀ O ₅ N (72)	C ₅ H ₁₂ ON ₂	-0.20
						452.3009	C ₂₅ H ₄₂ O ₆ N (60)	C ₅ H ₁₂ ON ₂	0.45	434.2906	C ₂₅ H ₄₀ O ₅ N (100)	H ₂ O	-0.20
						434.2906	C ₂₅ H ₄₀ O ₅ N (33)	C ₅ H ₁₄ O ₂ N ₂	-0.20	417.2640	C ₂₅ H ₃₇ O ₅ (26)	NH ₃	-0.29
										399.2534	C ₂₅ H ₃₅ O ₄ (13)	H ₇ O ₂ N	-0.27
										402.2644	C ₂₄ H ₃₆ O ₄ N (17)	CH ₃ OH	1.21
										362.2331	C ₂₁ H ₃₂ O ₄ N (12)	C ₄ H ₈ O	-0.04
										238.1808	C ₁₄ H ₂₄ O ₂ N (17)	C ₉ H ₁₆ O ₃	-0.44

Through the elimination of a water molecule from TP5, TP4 was formed with m/z 548.3701 and empirical formula $C_{30}H_{50}O_6N_3^+$. Dehydrogenation could result in a C₈-C₉ or C₁₀-C₁₁ double bond formation, yielding in both cases to stable species. However, the presence of the identical fragmentation routes postulated for TP5 (and TP6) supports the formation of a double bond between C₁₀ and C₁₁ which was supported once again by the formation of the structural diagnostic ion at m/z 218 (see Appendix I, Fig. S3.7).

The degradation product TP1 had a protonated mass of m/z 340.2601, and its production involved molecular breakdown with the loss of the aromatic ring, cleavage of carbon atoms 10 and 11, and subsequent cyclization. As seen in Fig. S3.8 (Appendix I), the precursor ion fragmented into m/z 323 and 306, with the loss of one or two NH₃ molecules. TP1 might potentially be formed by adding a hydroxyl group to the C₁₀ position of TP6.

Furthermore, two isomers of the ions at m/z 436.3061 with the formula $C_{25}H_{42}O_5N^+$ were found. This is because the amide bond was broken, then water was lost, and then the ions cyclized into lactones for TP2 and lactams for TP3 (see Appendix I, Fig. S3.9). One of the main product ions, m/z 419, emerged from the loss of NH₃, while the other, m/z 346, from the loss of H₂O. Due to the loss of methanol and then water, the m/z 419 fragmented into m/z 387 and m/z 369. Regardless of structural differences, TP3 produced similar product ions, as illustrated in Fig. S3.10 (Appendix I). These two isomers were previously found and identified during the drug's stress degradation [54] and were discriminated in this study based on the compound's polarity. Additionally, TP2 has been identified as an aliskiren human metabolite that is excreted in the urine and feces [29].

Based on the TPs described above, we can propose that the degradation pathways depicted in Fig. 3.7 represent a possible photo-induced transformation of aliskiren in river water.

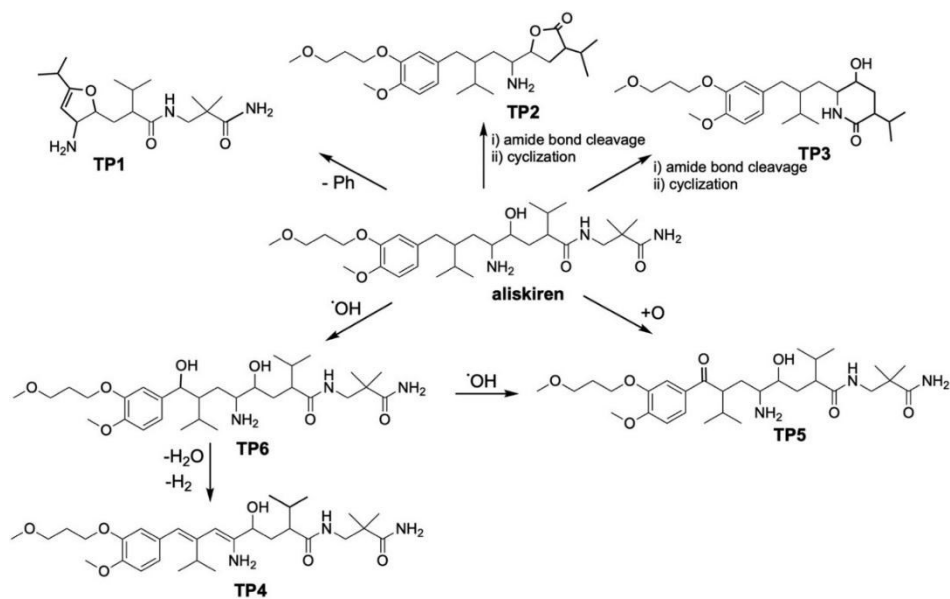


Figure 3.7. Proposed photodegradation pathways for aliskiren

Fig. 3.8 shows the time curve of the produced TPs under the various experimental conditions. Two TPs (TP3 and TP5) were detected in a dark-stored river water sample, both exhibiting a delayed formation commensurate with the significantly slower elimination observed in the dark (see Fig. 3.8). Six TPs were found in ultrapure water following irradiation, whereas only five of them were identified in river water, all of which disappeared at a slower rate than in MilliQ water; in fact, some TPs were still detectable at the conclusion of the time window studied (72 h). Notably, only one isomer of the photoproduct at m/z 436 (TP3) was identified in river water, whereas two isomers were formed in Milli-Q water.

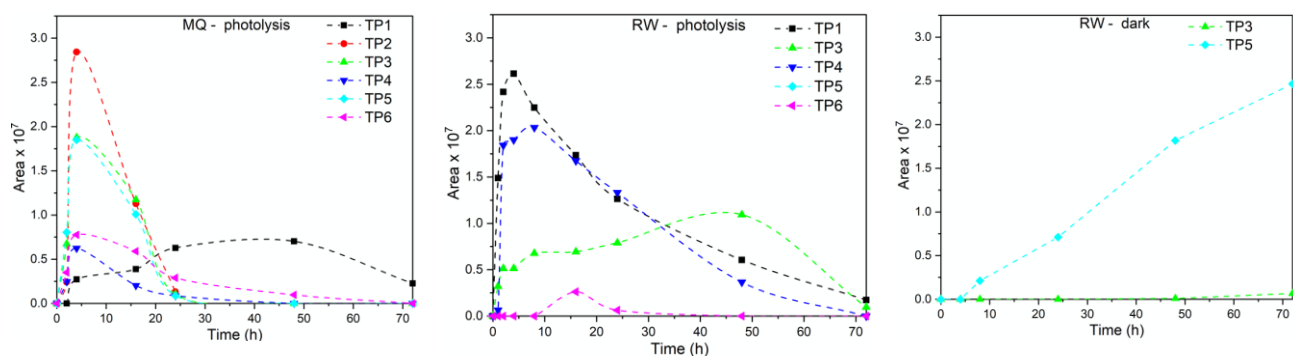


Figure 3.8. Profile over time of aliskiren TPs observed in ultrapure water (MQ) and river water (RW) in the dark and under irradiation.

3.4.4 Analysis of real samples

The irinotecan and aliskiren validated UHPLC-MS/MS methods were used to analyse several water samples. The collected samples were: Two river waters, one groundwater, two well waters (before and after chlorination), three samples taken near a depurator outlet, and one hospital effluent. Each sample was analyzed three times.

Irinotecan (0.43 ± 0.19 ng/mL) and one of its transformation products (i.e., PDP3) were detected only in hospital effluents. Additionally, water samples collected from the Po river were irradiated after being spiked with 10.0 mg/L irinotecan. The samples were photo-irradiated for 8 hours (the time during which most degradation products were formed), then pretreated with the SPE procedure and subsequently analyzed by UHPLC-MS/MS. Experiments were performed in triplicates. The results confirmed the formation of IRI's eight PDPs in both river and ultrapure water (Appendix I, Fig. S3.11).

3.4.5 Retrospective analysis of aliskiren and its TPs

For retrospective analysis, the Digital Sample Freezing Platform (DSFP) developed by NORMAN to store environmental samples [56] was used. The retrospective investigation included digitally stored environmental samples from the National and Kapodistrian University of Athens (Greece) and the Environmental Institute (Slovakia). Analytical methods and instrumental parameters are described elsewhere [38, 44], as well as the DSFP retrospective suspect screening methodology [56]. A total of 754 environmental samples were screened retrospectively for the presence of the parent drug aliskiren and the five TPs. A complete list of all examined samples can be found in our published article [38]. Most of the samples were collected in national and international monitoring campaigns such as joint Danube survey 4 (JDS4) [57, 58], river monitoring campaigns, e.g., Donets/ Dniester/ Dnieper [59], monitoring of the Black Sea (EMBLAS-II) [60], and monitoring of top predators and their prey from specimen banks in context of LIFE APEX (<https://lifeapex.eu/>) among others. The component list generated following the retrospective screening was searched for a 'yes/no' response of virtually any compound compatible with LC-MS analysis using a combination of information on its (i) exact mass (< 2 mDa), (ii) predicted retention time window in the chromatogram (20% retention time range), (iii) isotopic fit ($> 90\%$ using MOLGEN [61] if available) (iv) qualifier fragment ions (at least two qualifier fragment ions). TPs that fulfilled the identification criteria were confirmed present in the samples. Based on prior wide-scope target screening investigations, the screening detection limits (SDL) were found to be 1.00 ng/L for ground water, 1.25 ng/L for surface water, 2.0 ng/L for wastewater, 5 $\mu\text{g}/\text{kg}$ dry weight

for sediment, and 1.00 µg/kg wet weight for biota [44, 59]. The retrospective screening results in terms of frequency of appearance (FoA) are summarized in Table 3.7.

Table 3.7. Frequency of appearance (FoA) of aliskiren and its TPs in various environmental samples. Substances that were not detected are marked as “N.D.”

Environmental matrix	N° of samples	Aliskiren	TP1	TP2	TP3	TP4	TP5
Influent wastewater	120	0.22	0.32	N.D.	0.32	N.D.	N.D.
Effluent wastewater	126	0.43	0.06	N.D.	0.22	N.D.	N.D.
River	78	N.D.	0.23	N.D.	0.01	N.D.	N.D.
Seawater	105	N.D.	0.21	N.D.	0.02	N.D.	N.D.
Groundwater	7	N.D.	N.D.	N.D.	N.D.	N.D.	N.D.
Biota coastal	101	N.D.	0.09	N.D.	0.02	N.D.	N.D.
Biota river	71	N.D.	N.D.	N.D.	0.03	N.D.	N.D.
Biota terrestrial	52	N.D.	N.D.	N.D.	N.D.	N.D.	N.D.
Biota marine	62	N.D.	0.02	N.D.	0.07	N.D.	N.D.
Sediment river and marine	32	N.D.	0.19	N.D.	0.09	N.D.	N.D.

Two out of the five screened TPs were detected in the samples. Aliskiren had the highest FoA (43%) in effluent wastewater, whereas the highest FoAs for TP1 and TP3 (both 32%) in influent wastewater. Aliskiren was detected only in wastewater (influent and effluent), whereas TP1 and TP3 were found in a variety of other matrices, implying that the drug was degraded through the production of more persistent TPs. Both TPs were detected in freshwater sediments, surface waters (river and seawater), and biota. However, TP3 was detected rarely in samples other than wastewater, with a FoA less than 6% for all screened matrices. Overall, the TP1 was found to be the most prevalent, which corresponded to its increased abundance in comparison to other TPs seen during degradation experiments in river water (see Fig. 3.8). None of the compounds were detected in groundwater samples. The detection of TP1 and TP3 in a variety of matrices, even at low FoAs, demonstrates the importance of environmental transformation mechanisms of the drug. These findings suggest that the aliskiren degradation mechanism may generate TPs with unknown behavior and toxicity, which should be investigated using bioassays on both target and non-targeted organisms.

3.5 Conclusions

We developed and validated two highly sensitive UHPLC-MS/MS methods for the evaluation of irinotecan and aliskiren in aqueous samples, as well as their respective transformation products. The validated LC-MS/MS workflows allowed us to identify and propose the chemical structures of eight irinotecan TPs, five of which were identified for the first time (PDP1, PDP2, PDP3, PDP4, and PDP8). Only two TPs (PDP6 and PDP7) were previously reported in aqueous laboratory samples. Analysis of various real water samples revealed the presence of irinotecan and PDP3 in hospital effluents. Given that the chemical structures of the TPs contain the mappicine core, it is reasonable to conclude that the irinotecan TPs may exhibit cytotoxic properties as evidenced in previous reports [50].

Similarly, by combining the advantages of HPLC separation with low-resolution MS (QTRAP) and high-resolution MS (Orbitrap) detectors, six aliskiren TPs were identified and their structures have been suggested. Retrospective suspect screening of various environmental samples demonstrated the presence of two aliskiren TPs (TP1 and TP3). Notably, TP3 was shown to be more toxic to Fathead minnows and fish than aliskiren [38], raising concerns about its potential hazardous effects. The findings of the present study suggest that the aliskiren degradation mechanism may generate TPs with unknown behavior and toxicity and requires further investigations using bioassays on both target and non-targeted organisms.

PART II – Ten Pharmaceuticals

Development and Validation of a Fully Automated On-line SPE LC-MS/MS Method

In this second part of chapter 3, we describe the development and validation of an on-line solid phase extraction (SPE) LC-MS/MS method for determining ten pharmaceutical compounds in wastewater. The target compounds belong to three pharmacological groups: anticancer, antihypertensive, and antidepressant drugs. The compounds were aliskiren (ALK), cabazitaxel (CTX), docetaxel (DTX), doxorubicin (DOX), etoposide (ETP), irinotecan (IRI), maprotiline (MAP), methotrexate (MTX), topotecan (TOP), and paclitaxel (PTX). The selection of these target compounds, as well as the knowledge gap we intended to address, have been discussed in the INTRODUCTION section. Additional information on these target analytes can also be found in Table S3.1 (Appendix I). Thus, only the experimental procedure, results, and discussion will be covered in this section.

3.6 Optimization of LC-MS/MS conditions

To achieve the best online SPE-LC-MS performance for individual analytes, a series of experiments were performed aimed at: optimizing compound-dependent MS parameters and establishing the MRM method; selecting the best online SPE column from 4 different variants tested; determining the appropriate online SPE loading solution; selecting the best analytical column among the 3 columns tested; and determining the appropriate HPLC mobile phase and optimize the gradient conditions. The workflows and results obtained at each stage are discussed in the following sections.

3.6.1 Optimization of the MRM method

To evaluate the chromatographic nature of the target compounds, a scouting reversed-phase LC-MS analysis was first performed on the standards of each compound (1.0 µg/mL) using a generic C18 column with a mobile phase mixture of water and acetonitrile, both containing 0.1 % (*v/v*) formic acid. This preliminary assessment was carried out using a multiple reaction monitoring (MRM) method created based on precursor ion/product ion transitions of each compound reported in the literature. At this stage, the detection of all ten target analytes was confirmed; however, several of them had extremely low sensitivities. As a result, the actual step-by-step method development and optimization was carried out.

Following the scouting analysis, automated optimization of the compound-dependent parameters for the MRM method development was performed using the Agilent MassHunter Optimizer software (*version* B.09.00). The Optimizer automatically executed four acquisitions for each target ion: (i) MS² SIM Scan acquired data to optimize the fragmentor voltage for each precursor ion, (ii) Product Ion Scan identified product ions for each precursor ion, (iii) MRM

Scan optimized the collision energy (CE) by defining an MRM mode on the product ions found in step (ii), and (iv) Product Ion Scan validated the optimal CE and masses using a smaller scan range for product ions.

In detail, the MRM method was optimized by injecting via the column 1.0 µg/mL of individual standard solutions of the target compounds prepared in methanol/water (90:10, v/v) and fine-tuning the fragmentor voltage in the range 100-200 V with a step of 5 and collision energy in the range 5-50 V with a step of 2, while the Cell Accelerator Voltage was held constant at 7 V. Mass spectral data was acquired in both positive and negative polarity electrospray ionization (ESI) modes. Setting up a minimum abundance of 1000 counts, the most abundant precursor ion among $[M+H]^+$, $[M+NH_4]^+$, and $[M+Na]^+$ ions for positive ESI and $[M-H]^-$ for negative ESI were selected, with a charge state of ± 1 . Product ion selection was performed with a low mass cut-off value of m/z 40 and excluding masses due to neutral losses of H₂O that had an abundance of at least 1000 counts. Even though both positive and negative ESI scans were performed, all target analytes were suitably ionized in positive ESI mode producing more intense precursor and product ions compared to their counterparts in the negative ESI. This automatic optimization enabled the selection of the best precursor ion, the optimization of the fragmentor voltage for each precursor ion, the selection of four best product ions, and the optimization of the collision energy values for each transition for a list of the specified compounds.

It is worth mentioning that the MRM optimization results automatically generated for doxorubicin and etoposide were not adequate (i.e., only one product ion fulfilling the 1000 counts abundance limit was detected). Hence, manual optimization was performed on both compounds, which resulted in improved results (Fig. 3.9). Thus, the optimal CE values for DOX and ETP were 10 V and 15 V, respectively, as obtained through the manual procedure.

The goal of this optimization procedure was to maximize precursor ion transmission by reducing collision-induced dissociation (CID) with fragmentor voltage, which was crucial for achieving the highest possible sensitivity for each target analyte. Moreover, product ion signals were maximized with CE optimization, resulting in enhanced detection and quantification of the compounds. For each analyte, two of the most intense precursor-product ion transitions were identified and the one with the greater response was chosen to be the quantifier ion, while the other was the qualifier ion.

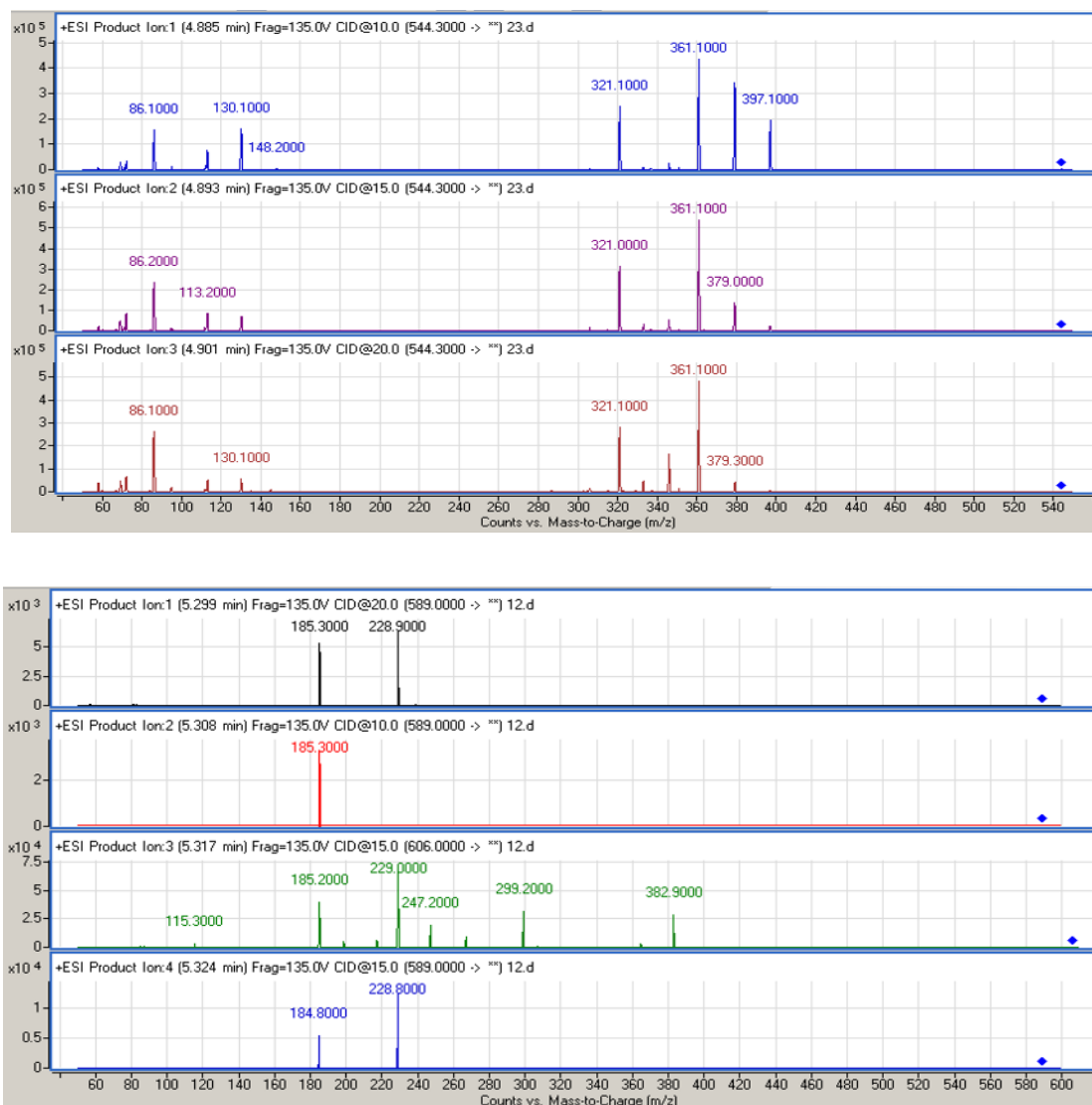


Figure 3.9. CID product ions of doxorubicin (top) and etoposide (bottom).

3.6.2 Selection of on-line SPE cartridges

To ensure an effective and reproducible sample pre-treatment procedure, on-line SPE optimization experiments focusing on the type of SPE sorbent were performed. The online SPE cartridges tested were the polymeric PLRP-s cartridge (2.1 x 12.5 mm, 15-20 μm ; Agilent Technologies, Santa Clara, CA, USA), the HyperSep™ Hypercarb (2.1 x 20 mm, 7.0 μm ; Thermo Fisher, Waltham, MA, USA), the Hypersil GOLD™ aQ online SPE columns (2.1 x 20 mm, 12 μm ; Thermo Fisher, Waltham, MA, USA), and the Oasis HLB cartridge (2.1 x 20 mm, 5.0 μm ; Waters, Milford, MA, USA). The loading solution was composed of 0.1% (*v/v*) formic acid solution and methanol.

The automated SPE-LC-MS/MS procedure began with loading 0.5 mL water sample onto the SPE cartridge for 1.1 min at a flow rate of 1.0 mL/min, followed by activating the divert valve

of the column switching array, back-flushing the SPE and transferring the trapped analytes to the chromatographic column where they were separated and subsequently detected by the MS/MS. At 10.0 min, the valve was returned to the load position to re-equilibrate both the SPE and the chromatographic column for 5.0 min.

3.6.3 Optimization of LC-dependent conditions

To optimize LC-dependent conditions, we tested different mobile phase compositions focusing on the type of organic phases and the modifiers. Methanol and acetonitrile were tested as the organic phases with or without formic acid (0.1%, *v/v*) as additive. In addition, the aqueous phase modifiers formic acid (0.1%, *v/v*) and ammonium formate (5 mM, pH 3) were evaluated. Furthermore, the chromatographic separation of the analytes was evaluated using three different analytical columns: Eclipse Plus C18 column (150 mm x 2.1 mm, 3.5 μm ; Agilent Technologies, Santa Clara, CA, USA), Kinetex C18 column (2.1 x 150 mm, 2.6 μm ; Phenomenex, Aschaffenburg, Germany), and Luna Omega Polar C18 (150 x 2.1 mm, 3.0 μm ; Phenomenex, Aschaffenburg, Germany). After selecting the optimal column and mobile phases, the elution gradient, flow rate, and column temperature were modified.

3.6.4 Sample collection and preparation

The method was optimized using ultrapure water and WWTP influent obtained from Vejen (Denmark). The optimized method was subsequently applied to analyze six hospital effluents collected from Aalborg in Denmark (coded as A1 and A2) and Valencia in Spain (coded as V1, V2, V3, and V4). Sample bottles were 500 mL capacity amber glass bottles with Teflon-lined caps which were thoroughly cleaned as follows: rinsing three times with tap water, three times with organic-free water, twice with washing acetone, once with special UV-grade acetone, twice with pesticide grade hexane and dry (uncapped) in a hot air oven at 360 °C for 24 h.

All samples were collected using the pre-cleaned amber glass bottles. During sampling, the bottles were first rinsed twice with roughly 100 mL of the sample before filling them up. All collected samples were immediately transferred into an ice-cooled container and delivered to the lab in chilled conditions. Upon arrival in the lab, water samples were acidified with HCl to pH 2 before being filtered first using Whatman 1.6 μm fiberglass filters and then 0.45 μm filters. To minimize microbial degradation, the original pH was restored using NaOH solution and samples were always extracted within 24 hours of collection. When this was not practicable, samples were kept frozen at -20 °C until analysis.

3.7 Results and Discussion

3.7.1 Optimization of the HPLC-MS/MS

A sensitive and reproducible on-line SPE LC-MS/MS method for the analysis of ten pharmaceuticals of emerging concern was developed to meet the ever-increasing demand for the large-scale determination of target drugs in environmental water samples. The method was optimized by fine-tuning several critical parameters that are directly related to the extraction, chromatographic and mass spectrometric behaviors of the target drugs. Table 3.8 presents the empirical formula of the 10 pharmaceuticals and the IS (atrazine-d₅), the retention times, and the optimized MS parameters.

Table 3.8. Formula, retention time, and the optimized LC-MS/MS parameters for analyzing the target pharmaceutical compounds.

Compound (Abbreviation)	Chemical Formula	RT (min)	Q1 (m/z)	Q3 (m/z)	Frag (V)	CE (V)
Aliskiren (ALK)	C ₃₀ H ₅₃ N ₃ O ₆	5.0	552.4	346.3; 534.5	135	27; 40
Cabazitaxel (CTX)	C ₄₅ H ₅₇ NO ₁₄	7.5	836.3	555.3; 433.1	135	20; 20
Docetaxel (DTX)	C ₄₃ H ₅₃ NO ₁₄	6.5	808.3	527.1; 509.0	135	20; 15
Doxorubicin (DOX)	C ₂₇ H ₂₉ NO ₁₁	6.1	544.0	361.2; 397.2	135	10; 10
Etoposide (ETP)	C ₂₉ H ₃₂ O ₁₃	4.3	589.2	229.1; 185.2	135	15; 15
Irinotecan (IRI)	C ₃₃ H ₃₈ N ₄ O ₆	1.6	587.3	124.1; 167.1	120	45; 21
Maprotiline (MAP)	C ₂₀ H ₂₃ N	5.3	278.1	250.0; 191.1	135	15; 15
Methotrexate (MTX)	C ₂₀ H ₂₂ N ₈ O ₅	1.4	455.2	308.1; 175.1	120	10; 25
Paclitaxel (PTX)	C ₄₇ H ₅₁ NO ₁₄	7.1	854.0	105.1; 286.0	100	19; 10
Topotecan (TOP)	C ₂₃ H ₂₃ N ₃ O ₅	3.8	422.2	377.1; 320.0	120	10; 21
Atrazine-d ₅ (ATZ)	C ₈ H ₅ H ₉ ClN ₅	5.6	221.1	179.2; 101.2	135	20; 20

The pharmaceutical compounds targeted in this study consisted of eight anticancer drugs, one antidepressant and one antihypertensive. According to recent studies, C18-based analytical columns are the most suitable and often employed for the analysis of a similar group of compounds in water [12, 25, 28]. In this work, we tested three reversed-phase C18 analytical columns of which one column had additional polar functionality. A 15-min chromatographic run was established for each column. The results indicated that the performance of Luna Omega Polar C18 towards the nonpolar high-molecular-weight compounds was extremely poor. The Kinetex C18 and Eclipse Plus C18 columns, on the other hand, enabled the separation of all 10 compounds with better sensitivity and improved peak shapes. In general, the Kinetex

C18 achieved higher sensitivity for most compounds, which also provided peaks with improved efficiency and symmetry (asymmetry factor ranged from 0.95 to 1.61, see Table S3.2 in Appendix I). As an example, Figure 3.10 depicts the performance of the three columns, with PTX indicating a condition in which the columns had comparable performance and ALK demonstrating a clear difference of its retention and abundance of the product ions. The enhanced peak profiles of the target compounds obtained using the Kinetex C18 phase could be partly explained by the higher peak capacities and greater sensitivities of the core-shell technology compared to the fully porous columns since this 2.6 μm particle size column performs like a fully porous sub-2 μm columns [62, 63]. Therefore, the Kinetex C18 column was selected for chromatographic separation of the target pharmaceutical compounds in the final optimized method.

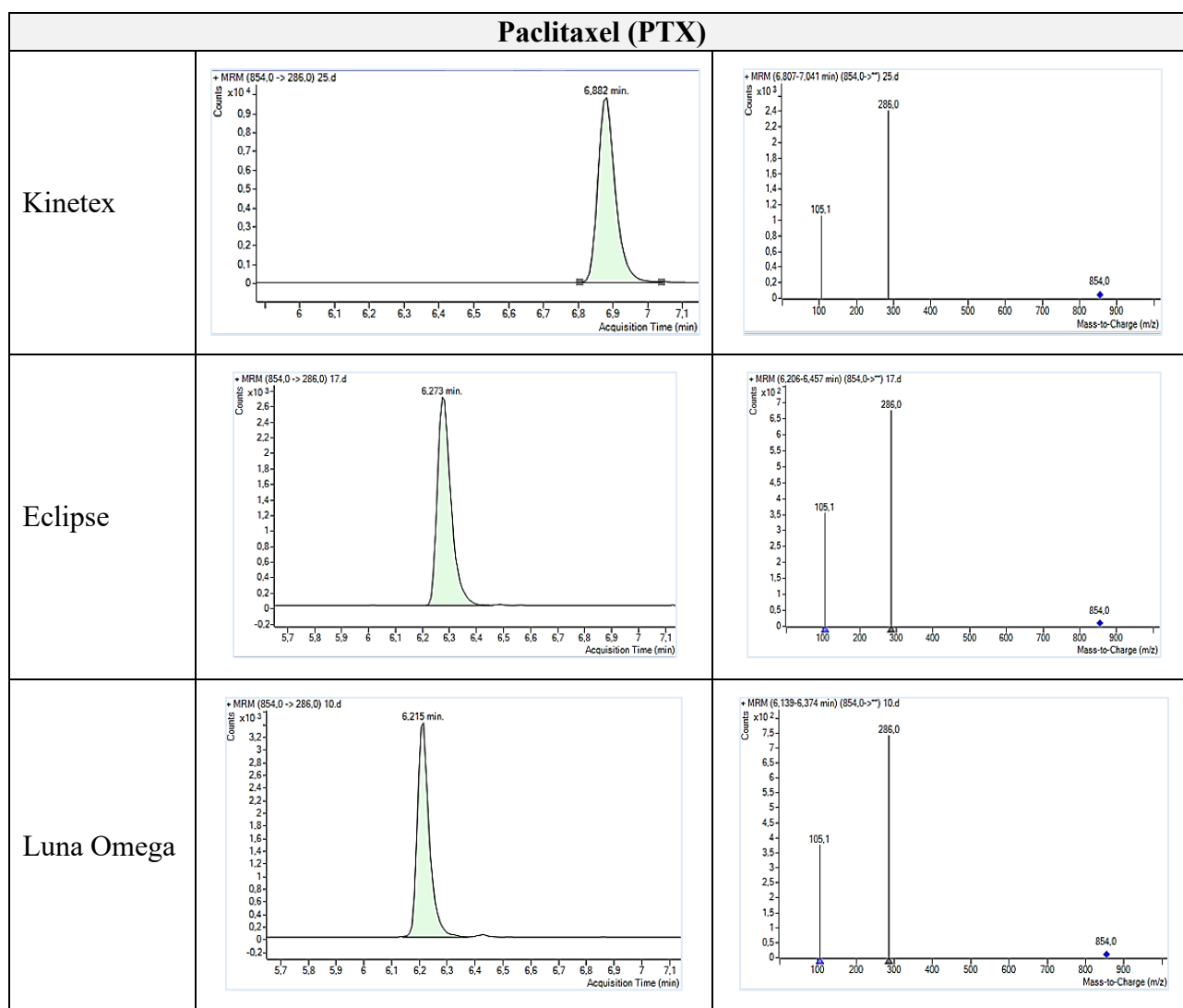


Figure 3.10a. Performance of the three columns towards paclitaxel.

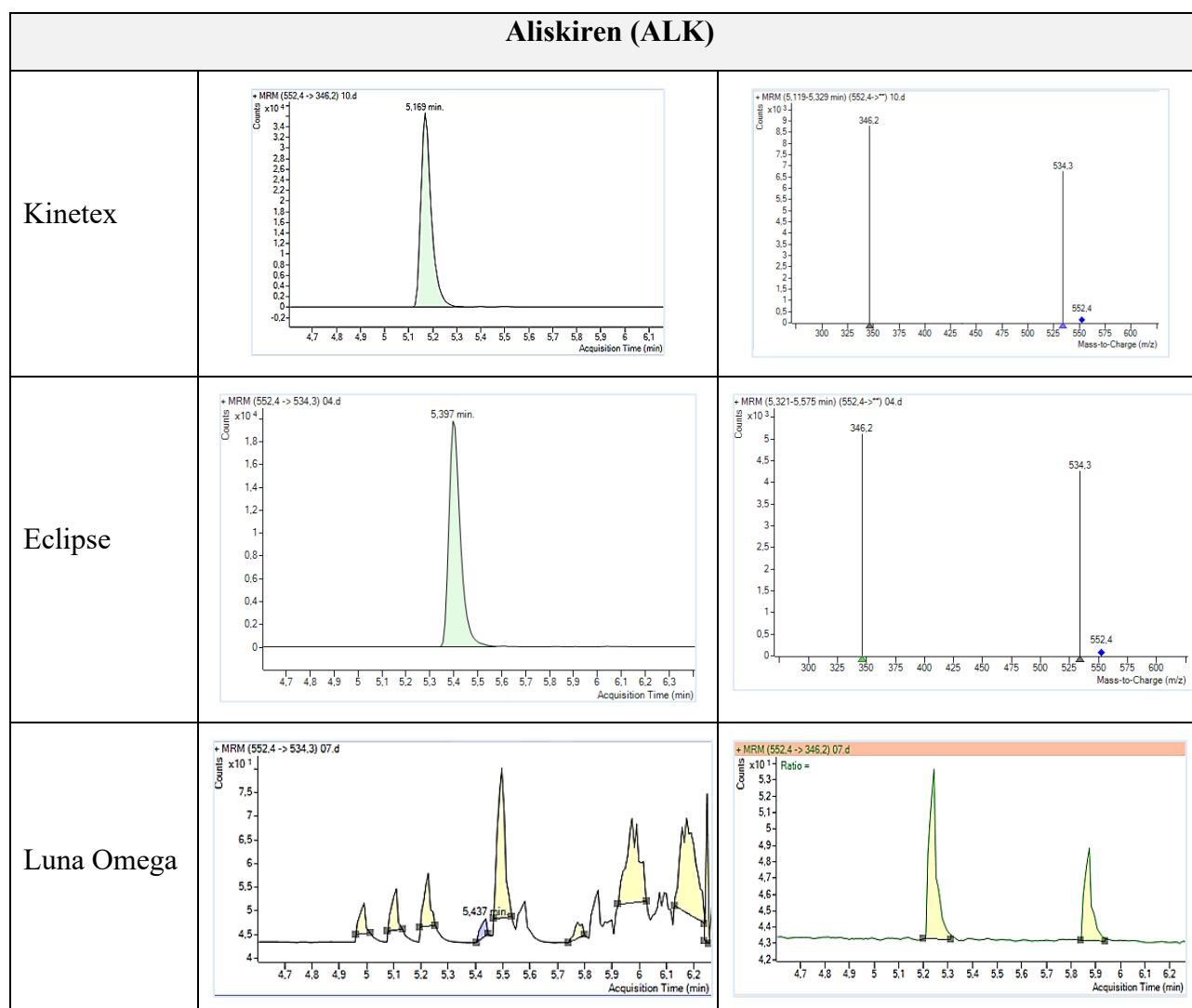


Figure 3.10b. Performance of the three columns towards aliskiren.

The mobile phase composition and chemical changes in the solute can have an impact on the processes occurring within the column. Changes in organic solvent and additive concentrations, pH, and other variables such as ionic strength can all affect peak profiles. We investigated a series of mobile phase compositions and the results showed that adding low concentrations (0.1%, *v/v*) of formic acid both to the aqueous and organic phases greatly improved peak shape, detector signal intensity and S/N ratio of the precursor ion detected under SIM mode. When ammonium formate was used as an additive, distorted peaks were obtained in addition to poor ionization and co-elution of the target compounds. Considering all these results, a mobile phase system composed of water and acetonitrile, both containing 0.1% (*v/v*) formic acid, provided better peak profiles (peak shape, sensitivity, and resolution) for the majority of the analytes. The addition of formic acid was necessary to boost ionization in positive ESI mode and improve peak shapes.

3.7.2 Optimization of the on-line SPE

Following the LC-MS optimization, experiments were performed, focused on the selection of the best online SPE cartridge for the extraction of the target analytes. Sample preparation using an online SPE method not only improves analytical results but also saves time and reduces solvent consumption. Thus, choosing an online SPE cartridge capable of providing high recoveries for all target analytes is a crucial step in developing a reproducible method. To this effect, four online SPE cartridges were evaluated: Hypersil GOLD aQ, Hypersil Hypercarb, PLRP-s, and Oasis HLB. Samples were prepared in three replicates by spiking ultrapure water with a mix of the target compounds at 1.0 µg/L levels. For each analyte, the extraction efficiency of each online SPE cartridge was calculated as percentages of the peak areas obtained for the online SPE analysis and that of the direct chromatographic injection of an equivalent amount of the standard mixtures.

The relative response of peak areas obtained with all four cartridges is shown in Fig. 3.11. The selection of the SPE sorbent depends essentially on the physico-chemical characteristics of the target analytes and the nature of the matrix. For most analytes, the Hypersil GOLD aQ (C₁₈, Octadecyl) and PLRP-s (a crosslinked styrene-divinylbenzene polymer) exhibited good recoveries with acceptable repeatability. The Oasis HLB (a macroporous copolymer of divinylbenzene and n-vinylpyrrolidone) on the other hand, produced lower recoveries and repeatability for some compounds. The results obtained using PLRP-s and Oasis HLB partly agreed with a previous report [25], in which the PLRP-s had better efficiencies for irinotecan and the Oasis HLB for methotrexate, etoposide, doxorubicin and paclitaxel.

In the present study, the performance of the Hypercarb online SPE cartridge was characterized by low recoveries and repeatability. This cartridge contained porous graphitic carbon (PGC) suitable for the retention of highly polar compounds, and the poor recoveries obtained in this study could be due to the low polarities of the target compounds. In the final optimized method, the Hypersil GOLD aQ online column was selected for extraction of all target analytes since it showed better retention and less peak broadening (narrower and symmetrical peaks, Table S3.2) for most of the analytes. In the literature, the Hypersil GOLD aQ on-line column was found to have good recoveries for the extraction of synthetic and natural estrogens from river water and wastewater [64]. Moreover, the results found in our study were reproducible, as evidenced by the very modest error bars of triplicate analyses reported in Fig. 3.11. The greater peak broadening seen in the other SPE columns might be attributed to the incompatibility of their stationary phases with that of the analytical column [14, 65].

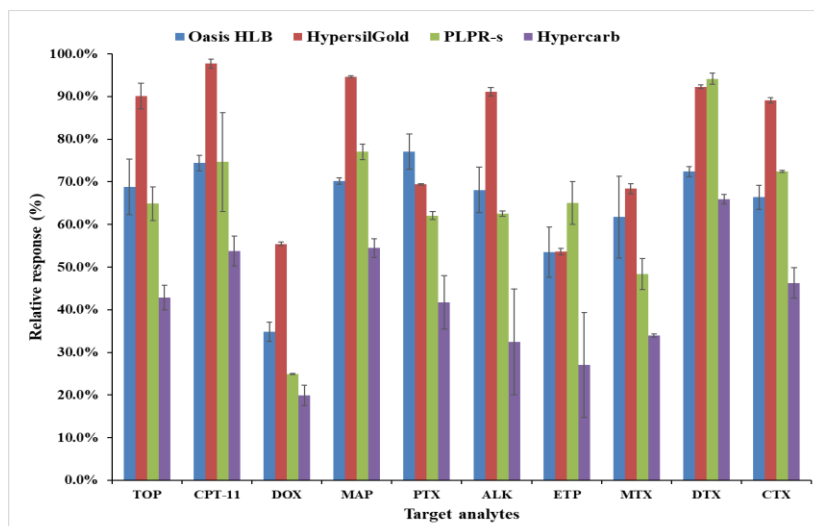


Figure 3.11. Comparison of recoveries (the relative peak area responses) obtained with four online SPE cartridges (analyte concentration 1.0 µg/L, sample volume 500 µL).

3.7.3 The optimized on-line SPE-LC-MS/MS method

The on-line SPE and HPLC conditions for the optimized method are shown in Table 3.9. As a result of better analyte recoveries and good peak shapes achieved for most compounds, the Hypersil GOLD aQ SPE cartridge combined with the Kinetex C18 analytical column were selected respectively for preconcentration and separation of all the target analytes.

Table 3.9. Program for the loading and analytical pumps (A = 0.1% formic acid in water, B = methanol, C = 0.1% formic acid in water, and D = 0.1% formic acid in acetonitrile).

Time (min)	Loading pump (SPE)			Valve position	Analytical pump (HPLC)	
	A (%)	B (%)	Flow rate (mL/min)		C (%)	D (%)
0.00	95.0	5.0	1.0	Loading	95.0	5.0
1.10	95.0	5.0	1.0	Loading	95.0	5.0
1.15	95.0	5.0	1.0	Injection	95.0	5.0
5.00	0.0	100	0.1	Injection	0.0	100
7.00	0.0	100	0.1	Injection	0.0	100
8.00	0.0	100	0.1	Injection	0.0	100
10.0	95.0	5.0	1.0	Loading	95.0	5.0
15.0	95.0	5.0	1.0	Loading	95.0	5.0

The chromatographic separation was accomplished using a binary mobile phase system consisting of water (**C** in Table 3.9) and acetonitrile (**D** in Table 3.9) both containing 0.1% (v/v) formic acid. The column and autosampler temperatures were set at 40 and 4 °C, respectively. The mobile phase flow rate was 0.4 mL/min and the injection volume was 20 µL. The elution began at 5% D, held for 1.15 min before increasing to 100% D in 5.0 min and held for another 3.0 min, and returned to initial conditions in 2.0 min. Then, the column was equilibrated for 5.0 min at the initial elution conditions before the next injection. The online SPE procedure was fully automated, and the total chromatographic run was 15 min. In order to eliminate/minimize carryover effects, a washing step for the syringe and the injection valve was programmed before each injection, first with 0.1% formic acid in acetonitrile and then with 0.1% formic acid in ultrapure water. Furthermore, after every 8 samples, a blank control water sample was run through all steps in processing to check for target analyte carryover.

The mass spectral data were acquired using the ESI source conditions presented in Table 3.10. Dynamic multiple reaction monitoring (dMRM) was used to monitor two specific transitions for each analyte over a delta retention period of 1-min with a dwell time of 150 ms. To confirm the presence of an analyte in a sample, the criteria of the SRM ratio between the qualifier and quantifier transition as suggested by European Commission Decision 2002/657/CE [66] and comparison of the retention time with that of the authentic standard were adopted. Quantification was achieved with calibration curves established using the analyte peak area of quantifier ions and the standard concentrations.

Table 3.10. ESI source parameters.

Parameter	Value
Ionization mode	ESI Agilent JetStream
Polarity	Positive
Drying gas temperature	250 °C
Drying gas flow	8 L/min
Nebulizer pressure	45 psi
Sheath gas heater	350 °C
Sheath gas flow	11 L/min
Capillary voltage	2500 V
Delta electron multiplier voltage (EMV)	500

3.7.4 Method validation

The optimized on-line SPE-LC-MS/MS method was validated in accordance with the ISO/IEC 17025 guideline. The parameters evaluated in the validation process were selectivity, linearity, LOD and LOQ, precision, and recovery. Table 3.11 summarizes the results of the validation procedure. Moreover, Fig. 3.12 depicts a representative chromatogram obtained for a 500 ng/L mix of all target compounds which also contained a 250 ng/L IS and 0.1% formic acid.

The method's selectivity was determined by comparing the MRM chromatograms of blank water samples with those obtained from the spiked ones. Given the retention times of the analytes and the IS, there were no overlapping peaks within the 1-min delta retention time window operated in dMRM mode, indicating that no interfering species were found and that all analytes separated satisfactorily.

The linearity of the method was investigated by analyzing a calibration mix of standards at eleven concentration levels (LOQ, 1.00, 2.50, 5.00, 10.0, 25.0, 50.0, 100, 250, 500, 1.00×10^3 ng/L) prepared in methanol/water (10:90, v/v) in three independent replicates. A 250 ng/L IS and 0.1% formic acid were added to all calibration standards. Due to the lack of isotope-labelled standards that could fit the set of pharmaceuticals targeted in this study, atrazine- d_5 was used as the IS since good results were reported for multi-residue methods [14, 67] containing four of the drugs targeted in this study. As can be seen in Table 4.11, all the calibration curves had good linearity with coefficients of determination (R^2) greater than 0.99 for all compounds. The variances explained by the models were significant as confirmed by the F-test ($p=0.05$) and no lack-of-fit was detected in any of them.

The limits of detection (**LOD**) and quantification (**LOQ**) were determined from the standard calibration curves using the Hubaux-Vos method [68]. LODs were all below 10 ng/L except for aliskiren which was only slightly higher. In general, the LODs were in the ranges 1.30-10.6 ng/L, while LOQs were in the range 4.30-35.5 ng/L, indicating that the present method was highly sensitive allowing ultratrace quantification. LODs slightly lower than those obtained in this study were reported for MTX, IRI, ETP and DOX [25], which could partly be explained by the larger volume of sample (5 mL) loaded onto the online SPE against the 0.9 mL used in our study.

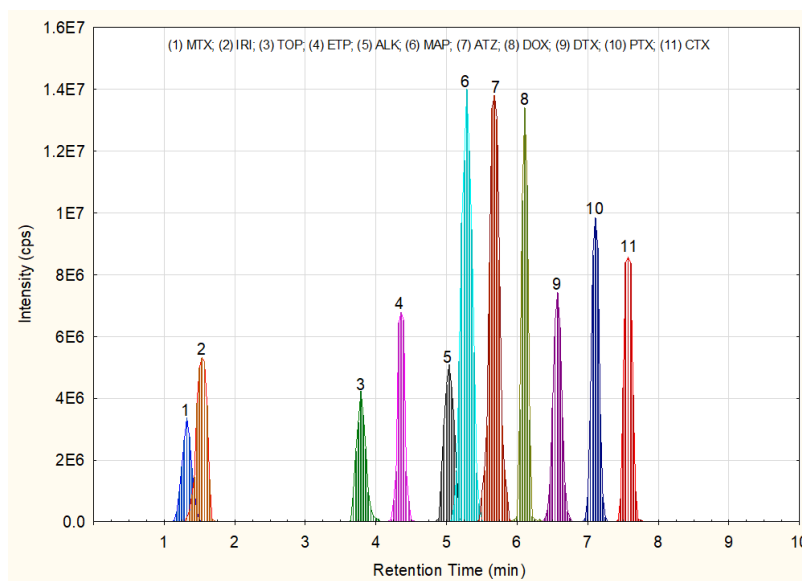


Figure 3.12. Representative chromatogram of the target pharmaceuticals in a mixture of standards (peaks are for the quantifier ion transition of each target compounds)

One of the requirements for a well-established analytical method is the achievement of consistent and satisfactory results for precision and recovery analysis at varied concentration levels. **Precision** was evaluated by determining intra-day and inter-day precisions, expressed as RSD (%). In all cases, the intra-day precisions (n=5) were below 10% and the inter-day RSD values (n=15) fell below 15% (Table 3.11). In fact, intraday RSD (%) values were in the ranges 1.6-7.8 for QC_L, 3.2-7.4 for QC_M, and 2.1-6.7 for QC_H. On the other hand, inter-day RSDs (%) were in the ranges 7.00-13.2 for QC_L, 4.3-9.4 for QC_M, and 3.30-12.7 for QC_H.

Complex matrices can have a significant impact on target compound stability and extraction efficiency. **Matrix effect (ME)** was evaluated using wastewater influent samples at the three QC levels by comparing the analyte mean peak areas of standards prepared in solvent (A_{solvent}) with those of spiked wastewater influent samples (A_{spike}) after correcting for the peak areas of the target compound in the unspiked wastewater influent (A_{blank}). Three independent replicates were analyzed at each QC level and were reported as percentages (ME %) calculated using Eq. (3.3):

$$ME (\%) = \frac{A_{\text{spike}} - A_{\text{blank}}}{A_{\text{solvent}}} * 100 \quad \text{Eq. (3.3)}$$

The average matrix effects obtained in this study ranged from 69.0% to 113.0% (Fig. 3.13). Signal suppression was observed for TOP (31%), DOX (31%), IRI (20%), ALK (16%), MTX (8%), ETP (6%), while signal enhancement was observed for CTX (6%), DTX (8%), MAP (8%), and PTX (13%). Some of these results agreed with previous studies which had reported ion

suppression for IRI, ETP and DOX [14, 25] in wastewater effluents and influents. Thus, in order to acquire accurate results when quantifying these compounds in complex matrices, isotopically labeled compounds must be used.

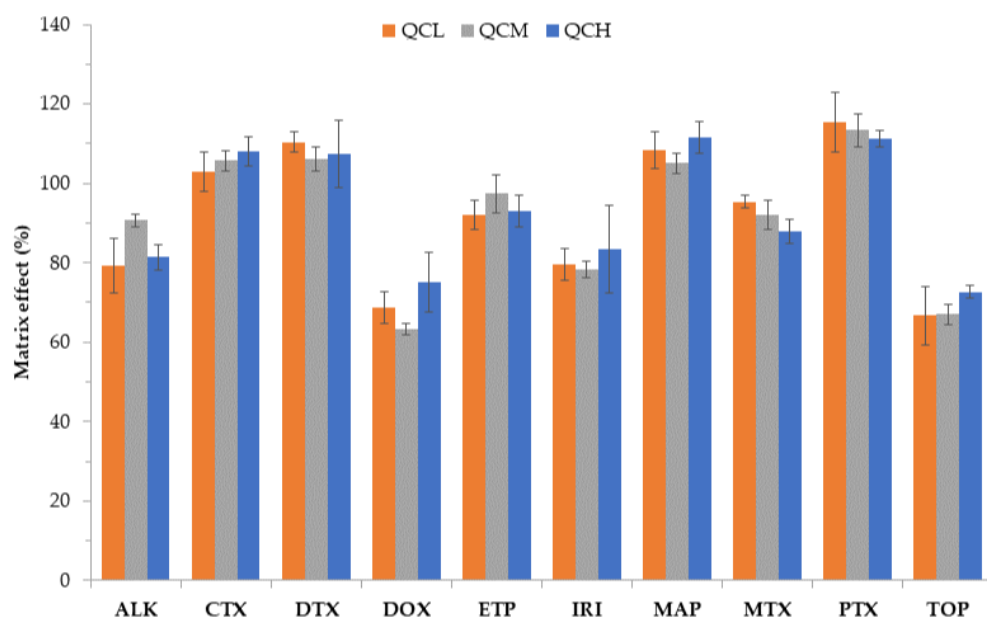


Figure 3.13. Matrix effects in wastewater influent samples.

Recoveries of analytes from real water matrices were also determined at three QC levels, following the same procedure as matrix effects. Recoveries (%) were calculated using Eq. (4.4):

$$Recovery (\%) = \frac{C_{spike} - C_{blank}}{C_{actual}} * 100 \quad \text{Eq. (4.3)}$$

where C_{spike} was the measured concentration of the analyte in the spiked wastewater matrix, C_{blank} was the original concentration of the analyte in the wastewater matrix, and C_{actual} was the known concentration spiked in the wastewater matrix. Recoveries (%) obtained from spiked wastewater influent samples analyzed using the optimized method resulted in satisfactory values, ranging from 84.0 to 105.6% at QC_L , 78.4 to 103.4% at QC_M , and 79.9 to 111.4% at QC_H .

Table 3.11. Method validation parameters. The lowest level of the calibration curve was always the LOQ value. Spiked QC levels for the evaluation of precision and recovery were QC_L (LOQ), QC_M (100 ng/L) and QC_H (800 ng/L) for each target compound. RSDs for recoveries shown in parentheses.

Compound	Linearity (R ²)	LOD (ng/L)	LOQ (ng/L)	Spiked QC	Precision (RSD %)		Recovery (%)
					Intraday	Inter-day	
ALK	0.9978	10.7	35.5	QC _L	5.6	13	101.6 (5.4)
				QC _M	3.3	9.2	95.7 (10)
				QC _H	3.7	7.9	94.6 (2.0)
CTX	0.9937	7.98	26.6	QC _L	5.5	7.0	101.3 (2.2)
				QC _M	6.0	4.3	94.7 (7.5)
				QC _H	2.9	3.5	96.3 (7.1)
DTX	0.9987	2.67	8.89	QC _L	7.8	11	84.0 (11)
				QC _M	6.7	7.9	95.3 (8.9)
				QC _H	8.4	6.4	96.9 (7.8)
DOX	0.9978	2.27	7.57	QC _L	6.1	7.5	79.9 (13)
				QC _M	4.1	9.1	85.8 (2.9)
				QC _H	5.5	13	87.6 (9.1)
ETP	0.9947	3.25	10.9	QC _L	3.7	9.6	104.5 (6.9)
				QC _M	3.2	6.8	96.9 (3.8)
				QC _H	6.2	12	93.3 (6.8)
IRI	0.9975	7.96	26.5	QC _L	4.8	9.3	78.4 (7.6)
				QC _M	5.1	8.0	89.2 (5.4)
				QC _H	3.9	11	86.5 (4.4)
MAP	0.9997	1.30	4.34	QC _L	2.6	8.5	103 (14)
				QC _M	3.3	5.4	103.2 (6.4)
				QC _H	2.1	5.5	98.6 (8.2)
MTX	0.9991	4.43	14.8	QC _L	2.1	10	85.4 (9.0)
				QC _M	4.4	7.7	94.4 (5.6)
				QC _H	3.0	5.2	111.0 (6.4)
PTX	0.9969	6.99	23.3	QC _L	6.6	7.8	96 (12)
				QC _M	5.1	5.2	88.8 (9.2)
				QC _H	6.7	3.3	94.6 (7.4)
TOP	0.9982	4.22	14.1	QC _L	7.5	12	92 (11)
				QC _M	7.4	9.4	93.7 (9.1)
				QC _H	6.1	9.8	96.6 (7.4)

3.7.5 Analysis of real water samples

The developed method was applied to the analysis of six hospital wastewater effluents collected from Aalborg (Denmark) and Valencia (Spain), both of which use primary advanced treatment. During the analysis, both low- and high-level QCs spiked with the analytes at 100 ng L⁻¹ and 800 ng L⁻¹, respectively, were run in between samples. Potential carryover problems were evaluated with procedural blanks of plain HPLC water. Results are summarized in Table 3.12. Out of the ten target analytes, only MAP and MTX were detected respectively in 3 WWTP samples obtained from Denmark and 2 WWTP samples from Spain. The concentrations ranged from 11.2 to 23.1 ng L⁻¹ for maprotiline and 4.7 to 9.3 ng L⁻¹ for methotrexate. MTX consumption in Spain has been estimated at 144-196 g/day during the period 2010-2015 [26] with predicted environmental concentration (PEC) values of 1.5 and 0.056 ng L⁻¹ respectively in effluent and river waters. Previous studies have also reported methotrexate with concentrations of 12.6 ng L⁻¹ in STP effluent [69], 1.6–18.1 ng L⁻¹ in STP influents and up to 200 ng L⁻¹ in hospital effluents [28], and 3.5-18.1 ng L⁻¹ in WWTP influents [22]. Furthermore, maprotiline was previously reported at 0.4 ng L⁻¹ in WWTP effluents [70] and up to 16.5 ng L⁻¹ in EU WWTP effluents [71]. The other compounds were not detected in hospital effluent samples, which may be explained by the fact that hospitals contribute a small proportion of pharmaceutical load, as reported in [72, 73], with over 85% of 28 pharmaceutical loads not originating in hospitals. Similarly, another study [74] reported that only 7.5% of antineoplastics included in their study were detected in hospital effluent, implying that the remaining was consumed by patients and probably excreted in household sewage.

Table 3.12. Analysis results of hospital effluent samples. N.D. = below LOD.

Sample Code	Collection date	Concentration (ng/L)									
		ALK	CTX	DTX	DOX	ETP	IRI	MAP	MTX	PTX	TOP
A1	12/02/2020	N.D.	N.D.	N.D.	N.D.	N.D.	N.D.	N.D.	4.7	N.D.	N.D.
A2	20/02/2020	N.D.	N.D.	N.D.	N.D.	N.D.	N.D.	N.D.	9.3	N.D.	N.D.
V1	19/02/2020	N.D.	N.D.	N.D.	N.D.	N.D.	N.D.	23.1	N.D.	N.D.	N.D.
V2	19/02/2020	N.D.	N.D.	N.D.	N.D.	N.D.	N.D.	11.2	N.D.	N.D.	N.D.
V3	19/02/2020	N.D.	N.D.	N.D.	N.D.	N.D.	N.D.	N.D.	N.D.	N.D.	N.D.
V4	19/02/2020	N.D.	N.D.	N.D.	N.D.	N.D.	N.D.	20.2	N.D.	N.D.	N.D.

3.8 Conclusions

A new rapid, sensitive, and fully automated online SPE–LC–MS/MS method has been developed, allowing for the simultaneous multi-analyte determination of 10 pharmaceutical

compounds in water samples at the ng/L levels. The automation of the SPE procedure in tandem with the LC–MS/MS run resulted in analysis times per sample of only 15 minutes. We observed that matrix ionization effects have a substantial impact on certain compounds. Thus, the use of isotopically labelled internal standards is necessary for accurate quantification. Only two of the studied compounds (methotrexate and maprotiline) were found in relatively low quantities (between 4.70 and 23.1 ng/L) in hospital effluents from Denmark and Spain. However, environmental effects of these compounds cannot be ignored. As a result, sensitivity of the method is of the highest significance. To the best of our knowledge, this is the first multi-residue LC-MS/MS method based on on-line SPE established for the determination of pharmaceuticals in the aquatic environment, including antineoplastics, an antihypertensive, and an antidepressant. Furthermore, previously optimized methods for environmental samples did not include maprotiline, aliskiren, cabazitaxel, docetaxel, and topotecan. Therefore, this new analytical method can be of great value to the evaluation of the target drugs in various wastewaters and obtain data useful for their environmental monitoring.

3.9 Materials

3.9.1 Chemicals

All solvents were of LC-MS grade, and all chemicals were of analytical reagent grade. Doxorubicin hydrochloride (98-102%), etoposide (98-105%), topotecan hydrochloride hydrate ($\geq 98\%$), paclitaxel ($\geq 95\%$), docetaxel ($\geq 97\%$), methotrexate ($\geq 98\%$), and irinotecan hydrochloride ($\geq 97\%$), aliskiren ($\geq 98\%$) were purchased from Sigma-Aldrich (Milan, Italy). Cabazitaxel ($\geq 95\%$), maprotiline hydrochloride ($> 99\%$), formic acid (98-100%), acetonitrile ($\geq 99.9\%$, Chromasolv™), methanol (99.8%, LiChrosolv®), water (LiChrosolv®, LC-MS), and hydrochloric acid (Emsure®, ACS, 37%) were from Merck Life Science A/S (Søborg, Denmark). Ammonium formate (5 mol/L) was from Agilent Technologies Denmark ApS (Glostrup, Denmark). Atrazine- d_5 (100 mg/L) from Dr. Ehrenstorfer GmbH (Augsburg, Germany). Moreover, methanol (Chromasolv™, $> 99.9\%$), water (LC-MS grade), and formic acid for LC-MS were purchased from Sigma-Aldrich (Milan, Italy). Ultrapure water was generated using a Millipore Milli-Q® Gradient water purification system and had a resistance of 18.2 M Ω /cm (at 25 °C) and TOC value below 5 ppb.

Stock standard solutions (100 $\mu\text{g}/\text{mL}$) of each analyte were prepared in methanol and used for the development and validation of the LC-MS methods. Furthermore, a 25 $\mu\text{g}/\text{mL}$ standard mixture (mix) of all the ten analytes was prepared in methanol. All vials were stored in a dark standard-only freezer at -20 °C. For method optimization, working solutions (1 $\mu\text{g}/\text{mL}$) were

made by proper dilution of the stock solutions. Similarly, calibration standards were prepared by appropriate dilution of the individual or mix in methanol/water (10:90, v/v). On the other hand, the aqueous solutions of irinotecan and aliskiren used in the irradiation experiments were always freshly prepared.

3.9.2 Instrumentation

Part I: The simulated sunlight irradiation was provided by a Solarbox 3000e (CoFoMeGra, Milan, Italy), equipped with a xenon lamp and a soda-lime glass UV filter used to better simulate the outdoor exposure. UV-Vis analyses were performed by V-550 spectrophotometer (Jasco International Co., Tokyo, Japan). The LC/MS analyses were performed by Nexera Liquid Chromatography Shimadzu (Kyoto, Japan) system equipped with a DGU-20A3R Degasser, two LC-30AD Pumps, a SIL-30AC Autosampler, a CTO-20AC column compartment and a CMB-20A Lite system controller. The system was interfaced with a 3200 QTrap™ LC-MS/MS system (Sciex, Concord, Canada) by a Turbo V™ interface equipped with an electrospray (ESI) source. The 3200 QTrap™ data were processed by Analyst 1.5.2 software (Toronto, Canada). Moreover, identification of aliskiren TPs was performed using an Ultimate 3000 HPLC with an LTQ-Orbitrap mass spectrometer (Thermo Scientific, Bremen, Germany) operated in ESI mode.

Part II: All analyses were performed using an Agilent 1260 Infinity High-Performance Liquid Chromatography (HPLC) system (Agilent Technologies, Santa Clara, CA, USA) equipped with a quaternary pump (G1311C) used for sample loading into the SPE and a binary pump (G1312B) for sample elution of the analytes from the SPE cartridge and subsequent separation in the analytical column. The system consisted of an Agilent 1260 Infinity Standard Autosampler with a 900- μ L loop (G1329B ASL), Agilent 1260 Infinity Thermostated Column Compartment (G1316A TCC), and Agilent Valve Drive (G1170A) with Agilent 1200 series 2-position/6-port valve (G1158A). The HPLC system was interfaced with an Agilent 6460 Triple Quadrupole Mass Spectrometer (G6460C TQ), which was equipped with an Agilent jet stream technology ion source (AJS). The final optimized method utilized the Hypersil GOLD™ aQ on-line SPE column (2.1 x 20 mm, 12 μ m; Thermo Fisher, Waltham, MA, USA) and the Kinetex C18 column (2.1 x 150 mm, 2.6 μ m; Phenomenex, Aschaffenburg, Germany). All qualitative and quantitative data were evaluated employing the Agilent MassHunter Workstation software.

References

1. Ferrando-Climent, L., Rodriguez-Mozaz, S., & Barceló, D. (2013). Development of a UPLC-MS/MS method for the determination of ten anticancer drugs in hospital and urban wastewaters, and its application for the screening of human metabolites assisted by information-dependent acquisition tool (IDA) in sewage samples. *Analytical and bioanalytical chemistry*, 405(18), 5937-5952.
2. Boix, C., Ibáñez, M., Sancho, J. V., Rambla, J., Aranda, J. L., Ballester, S., & Hernández, F. (2015). Fast determination of 40 drugs in water using large volume direct injection liquid chromatography–tandem mass spectrometry. *Talanta*, 131, 719-727.
3. de Jongh, C. M., Kooij, P. J., de Voogt, P., & ter Laak, T. L. (2012). Screening and human health risk assessment of pharmaceuticals and their transformation products in Dutch surface waters and drinking water. *Science of the Total Environment*, 427, 70-77.
4. Grabicova, K., Lindberg, R. H., Östman, M., Grabic, R., Randak, T., Larsson, D. J., & Fick, J. (2014). Tissue-specific bioconcentration of antidepressants in fish exposed to effluent from a municipal sewage treatment plant. *Science of the Total Environment*, 488, 46-50.
5. Jureczko, M., & Kalka, J. (2020). Cytostatic pharmaceuticals as water contaminants. *European Journal of Pharmacology*, 866, 172816.
6. Deo, R. P., & Halden, R. U. (2013). Pharmaceuticals in the built and natural water environment of the United States. *Water*, 5(3), 1346-1365.
7. Petrie, B., Barden, R., & Kasprzyk-Hordern, B. (2015). A review on emerging contaminants in wastewaters and the environment: current knowledge, understudied areas and recommendations for future monitoring. *Water research*, 72, 3-27.
8. Papageorgiou, M., Kosma, C., & Lambropoulou, D. (2016). Seasonal occurrence, removal, mass loading and environmental risk assessment of 55 pharmaceuticals and personal care products in a municipal wastewater treatment plant in Central Greece. *Science of the Total Environment*, 543, 547-569.
9. Patrolecco, L., Capri, S., & Ademollo, N. (2015). Occurrence of selected pharmaceuticals in the principal sewage treatment plants in Rome (Italy) and in the receiving surface waters. *Environmental Science and Pollution Research*, 22(8), 5864-5876.
10. Vymazal, J., Březinová, T. D., Koželuh, M., & Kule, L. (2017). Occurrence and removal of pharmaceuticals in four full-scale constructed wetlands in the Czech Republic—the first year of monitoring. *Ecological Engineering*, 98, 354-364.
11. Chander, V., Sharma, B., Negi, V., Aswal, R., Singh, P., Singh, R., & Dobhal, R. (2016). Pharmaceutical compounds in drinking water. *Journal of xenobiotics*, 6(1), 1-7.
12. Heath, E., Česen, M., Negreira, N., de Alda, M. L., Ferrando-Climent, L., Blahova, L., ... & Kosjek, T. (2016). First inter-laboratory comparison exercise for the determination of anticancer drugs in aqueous samples. *Environmental Science and Pollution Research*, 23(15), 14692-14704.
13. Carioli, G., Bertuccio, P., Boffetta, P., Levi, F., La Vecchia, C., Negri, E., & Malvezzi, M. (2020). European cancer mortality predictions for the year 2020 with a focus on prostate cancer. *Annals of Oncology*, 31(5), 650-658.
14. Rabii, F. W., Segura, P. A., Fayad, P. B., & Sauvé, S. (2014). Determination of six chemotherapeutic agents in municipal wastewater using online solid-phase extraction coupled to liquid chromatography-tandem mass spectrometry. *Science of the total environment*, 487, 792-800.
15. Santos, L. H., Araújo, A. N., Fachini, A., Pena, A., Delerue-Matos, C., & Montenegro, M. C. B. S. M. (2010). Ecotoxicological aspects related to the presence of pharmaceuticals in the aquatic environment. *Journal of hazardous materials*, 175(1-3), 45-95.
16. Besse, J. P., Latour, J. F., & Garric, J. (2012). Anticancer drugs in surface waters: what can we say about the occurrence and environmental significance of cytotoxic, cytostatic, and endocrine therapy drugs? *Environment international*, 39(1), 73-86.

17. Lutterbeck, C. A., Baginska, E., Machado, Ê. L., & Kümmerer, K. (2015). Removal of the anti-cancer drug methotrexate from water by advanced oxidation processes: aerobic biodegradation and toxicity studies after treatment. *Chemosphere*, 141, 290-296.
18. Kümmerer, K., Al-Ahmad, A., & Mersch-Sundermann, V. (2000). Biodegradability of some antibiotics, elimination of the genotoxicity and affection of wastewater bacteria in a simple test. *Chemosphere*, 40(7), 701-710.
19. Kovalova, L., McArdell, C. S., & Hollender, J. (2009). Challenge of high polarity and low concentrations in analysis of cytostatics and metabolites in wastewater by hydrophilic interaction chromatography/tandem mass spectrometry. *Journal of Chromatography A*, 1216(7), 1100-1108.
20. Yin, J., Shao, B., Zhang, J., & Li, K. (2010). A preliminary study on the occurrence of cytostatic drugs in hospital effluents in Beijing, China. *Bulletin of environmental contamination and toxicology*, 84(1), 39-45.
21. Martín, J., Camacho-Muñoz, D., Santos, J. L., Aparicio, I., & Alonso, E. (2011). Simultaneous determination of a selected group of cytostatic drugs in water using high-performance liquid chromatography–triple-quadrupole mass spectrometry. *Journal of separation science*, 34(22), 3166-3177.
22. Negreira, N., de Alda, M. L., & Barceló, D. (2014). Cytostatic drugs and metabolites in municipal and hospital wastewaters in Spain: filtration, occurrence, and environmental risk. *Science of the total environment*, 497, 68-77.
23. Buerge, I. J., Buser, H. R., Poiger, T., & Müller, M. D. (2006). Occurrence and fate of the cytostatic drugs cyclophosphamide and ifosfamide in wastewater and surface waters. *Environmental science & technology*, 40(23), 7242-7250.
24. Valcárcel, Y., Alonso, S. G., Rodríguez-Gil, J. L., Gil, A., & Catalá, M. (2011). Detection of pharmaceutically active compounds in the rivers and tap water of the Madrid Region (Spain) and potential ecotoxicological risk. *Chemosphere*, 84(10), 1336-1348.
25. Negreira, N., de Alda, M. L., & Barceló, D. (2013). On-line solid phase extraction–liquid chromatography–tandem mass spectrometry for the determination of 17 cytostatics and metabolites in waste, surface and ground water samples. *Journal of Chromatography A*, 1280, 64-74.
26. Franquet-Griell, H., Gómez-Canela, C., Ventura, F., & Lacorte, S. (2017). Anticancer drugs: consumption trends in Spain, prediction of environmental concentrations and potential risks. *Environmental Pollution*, 229, 505-515.
27. Booker, V., Halsall, C., Llewellyn, N., Johnson, A., & Williams, R. (2014). Prioritising anticancer drugs for environmental monitoring and risk assessment purposes. *Science of the Total Environment*, 473, 159-170.
28. Yin, J., Yang, Y., Li, K., Zhang, J., & Shao, B. (2010). Analysis of anticancer drugs in sewage water by selective SPE and UPLC-ESI-MS-MS. *Journal of chromatographic science*, 48(10), 781-789.
29. Waldmeier, F., Glaenzel, U., Wirz, B., Oberer, L., Schmid, D., Seiberling, M., ... & Vaidyanathan, S. (2007). Absorption, distribution, metabolism, and elimination of the direct renin inhibitor aliskiren in healthy volunteers. *Drug metabolism and disposition*, 35(8), 1418-1428.
30. Isidori, M., Lavorgna, M., Russo, C., Kundi, M., Žegura, B., Novak, M., ... & Heath, E. (2016). Chemical and toxicological characterisation of anticancer drugs in hospital and municipal wastewaters from Slovenia and Spain. *Environmental Pollution*, 219, 275-287.
31. Nassour, C., Barton, S. J., Nabhani-Gebara, S., Saab, Y., & Barker, J. (2020). Occurrence of anticancer drugs in the aquatic environment: a systematic review. *Environmental Science and Pollution Research*, 27(2), 1339-1347.
32. Vieno, N., Hallgren, P., Wallberg, P., Pyhälä, M., Zandaryaa, S., & Baltic Marine Environment Protection Commission. (2017). *Pharmaceuticals in the aquatic environment of the Baltic Sea region: a status report* (Vol. 1). UNESCO Publishing.
33. Fáberová, M., Bodík, I., Ivanová, L., Grabic, R., & Mackuľak, T. (2017). Frequency and use of pharmaceuticals in selected Slovakian town via wastewater analysis. *Monatshefte für Chemie-Chemical Monthly*, 148(3), 441-448.

34. Singer, H. P., Wössner, A. E., McArdeell, C. S., & Fenner, K. (2016). Rapid screening for exposure to “non-target” pharmaceuticals from wastewater effluents by combining HRMS-based suspect screening and exposure modeling. *Environmental science & technology*, 50(13), 6698-6707.
35. Gosetti, F., Belay, M. H., Marengo, E., & Robotti, E. (2020). Development and validation of a UHPLC-MS/MS method for the identification of irinotecan photodegradation products in water samples. *Environmental Pollution*, 256, 113370.
36. Gonçalves, N. P., Varga, Z., Bouchonnet, S., Dulio, V., Alygizakis, N., Dal Bello, F., ... & Calza, P. (2021). Study of the photoinduced transformations of maprotiline in river water using liquid chromatography high-resolution mass spectrometry. *Science of the Total Environment*, 755, 143556.
37. Calza, P., Medana, C., Padovano, E., Giancotti, V., & Minero, C. (2013). Fate of selected pharmaceuticals in river waters. *Environmental Science and Pollution Research*, 20(4), 2262-2270.
38. Gonçalves, N. P., Iezzi, L., Belay, M. H., Dulio, V., Alygizakis, N., Dal Bello, F., ... & Calza, P. (2021). Elucidation of the photoinduced transformations of Aliskiren in river water using liquid chromatography high-resolution mass spectrometry. *Science of The Total Environment*, 800, 149547.
39. Slatter, J. G., Schaaf, L. J., Sams, J. P., Feenstra, K. L., Johnson, M. G., Bombardt, P. A., ... & Lord, R. S. (2000). Pharmacokinetics, metabolism, and excretion of irinotecan (CPT-11) following iv infusion of [14C] CPT-11 in cancer patients. *Drug Metabolism and Disposition*, 28(4), 423-433.
40. Gómez-Canela, C., Ventura, F., Caixach, J., & Lacorte, S. (2014). Occurrence of cytostatic compounds in hospital effluents and wastewaters, determined by liquid chromatography coupled to high-resolution mass spectrometry. *Analytical and bioanalytical chemistry*, 406(16), 3801-3814.
41. Ferre-Aracil, J., Valcárcel, Y., Negreira, N., de Alda, M. L., Barceló, D., Cardona, S. C., & Navarro-Laboulais, J. (2016). Ozonation of hospital raw wastewaters for cytostatic compounds removal. Kinetic modelling and economic assessment of the process. *Science of the Total Environment*, 556, 70-79.
42. Sousa, J. C., Ribeiro, A. R., Barbosa, M. O., Pereira, M. F. R., & Silva, A. M. (2018). A review on environmental monitoring of water organic pollutants identified by EU guidelines. *Journal of hazardous materials*, 344, 146-162.
43. Olalla, A., Negreira, N., de Alda, M. L., Barceló, D., & Valcárcel, Y. (2018). A case study to identify priority cytostatic contaminants in hospital effluents. *Chemosphere*, 190, 417-430.
44. Gago-Ferrero, P., Bletsou, A. A., Damalas, D. E., Aalizadeh, R., Alygizakis, N. A., Singer, H. P., ... & Thomaidis, N. S. (2020). Wide-scope target screening of > 2000 emerging contaminants in wastewater samples with UPLC-Q-ToF-HRMS/MS and smart evaluation of its performance through the validation of 195 selected representative analytes. *Journal of Hazardous Materials*, 387, 121712.
45. Boulard, L., Dierkes, G., Schlüsener, M. P., Wick, A., Koschorreck, J., & Ternes, T. A. (2020). Spatial distribution and temporal trends of pharmaceuticals sorbed to suspended particulate matter of German rivers. *Water research*, 171, 115366.
46. Bottaro, M., Frascarolo, P., Gosetti, F., Mazzucco, E., Gianotti, V., Polati, S., ... & Gennaro, M. C. (2008). Hydrolytic and photoinduced degradation of tribenuron methyl studied by HPLC-DAD-MS/MS. *Journal of the American Society for Mass Spectrometry*, 19(8), 1221-1229.
47. Gosetti, F., Chiuminatto, U., Mazzucco, E., Mastroianni, R., & Marengo, E. (2015). Ultra-high-performance liquid chromatography/tandem high-resolution mass spectrometry analysis of sixteen red beverages containing carminic acid: Identification of degradation products by using principal component analysis/discriminant analysis. *Food chemistry*, 167, 454-462.
48. Gosetti, F., Bolfi, B., Chiuminatto, U., Manfredi, M., Robotti, E., & Marengo, E. (2018). Photodegradation of the pure and formulated alpha-cypermethrin insecticide gives different products. *Environmental Chemistry Letters*, 16(2), 581-590.

49. Gosetti, F., Robotti, E., Bolfi, B., Mazzucco, E., Quasso, F., Manfredi, M., ... & Marengo, E. (2019). Monitoring of water quality inflow and outflow of a farm in Italian Padana plain for rice cultivation: a case study of two years. *Environmental Science and Pollution Research*, 26(21), 21274-21294.
50. Dodds, H. M., Craik, D. J., & Rivory, L. P. (1997). Photodegradation of irinotecan (CPT-11) in aqueous solutions: identification of fluorescent products and influence of solution composition. *Journal of pharmaceutical sciences*, 86(12), 1410-1416.
51. Lokiec, F., du Sorbier, B. M., & Sanderink, G. J. (1996). Irinotecan (CPT-11) metabolites in human bile and urine. *Clinical Cancer Research*, 2(12), 1943-1949.
52. Bodhipaksha, L. C., Sharpless, C. M., Chin, Y. P., & MacKay, A. A. (2017). Role of effluent organic matter in the photochemical degradation of compounds of wastewater origin. *Water research*, 110, 170-179.
53. Kotthoff, L., O'Callaghan, S. L., Lisec, J., Schwerdtle, T., & Koch, M. (2020). Structural annotation of electro-and photochemically generated transformation products of moxidectin using high-resolution mass spectrometry. *Analytical and Bioanalytical Chemistry*, 412(13), 3141-3152.
54. Kushwah, B. S., Gupta, J., Singh, D. K., Kurmi, M., Sahu, A., & Singh, S. (2018). Characterization of solution stress degradation products of aliskiren and prediction of their physicochemical and ADMET properties. *European Journal of Pharmaceutical Sciences*, 121, 139-154.
55. Schymanski, E. L., Jeon, J., Gulde, R., Fenner, K., Ruff, M., Singer, H. P., & Hollender, J. (2014). Identifying small molecules via high resolution mass spectrometry: communicating confidence.
56. Alygizakis, N. A., Oswald, P., Thomaidis, N. S., Schymanski, E. L., Aalizadeh, R., Schulze, T., ... & Slobodnik, J. (2019). NORMAN digital sample freezing platform: A European virtual platform to exchange liquid chromatography high resolution-mass spectrometry data and screen suspects in "digitally frozen" environmental samples. *TrAC Trends in Analytical Chemistry*, 115, 129-137.
57. Alygizakis, N. A., Besselink, H., Paulus, G. K., Oswald, P., Hornstra, L. M., Oswaldova, M., ... & Slobodnik, J. (2019). Characterization of wastewater effluents in the Danube River Basin with chemical screening, in vitro bioassays and antibiotic resistant genes analysis. *Environment international*, 127, 420-429.
58. Liška, I., Wagner, F., Sengl, M., Deutsch, K., Slobodnik, J., & Paunović, M. (2021). Joint Danube Survey 4-A Shared Analysis of the Danube River, Scientific Report. *ICPDR-International Commission for the Protection of The Danube River, Vienna, Austria*.
59. Diamanti, K. S., Alygizakis, N. A., Nika, M. C., Oswaldova, M., Oswald, P., Thomaidis, N. S., & Slobodnik, J. (2020). Assessment of the chemical pollution status of the Dniester River Basin by wide-scope target and suspect screening using mass spectrometric techniques. *Analytical and Bioanalytical Chemistry*, 412(20), 4893-4907.
60. Slobodnik, J., Alexandrov, B., Komorin, V., Mikaelyan, A. S., Guchmanidze, A., Arabidze, A., & Korshenko, A. (2016). National Pilot Monitoring Studies and Joint Open Sea Surveys in Georgia. *Russian Federation and Ukraine (Report ENPI/2013/313-169), Scientific Report-Joint Black Sea Surveys*, 2016, 573.
61. Meringer, M., & Schymanski, E. L. (2013). Small molecule identification with MOLGEN and mass spectrometry. *Metabolites*, 3(2), 440-462.
62. Fekete, S., Ganzler, K., & Fekete, J. (2011). Efficiency of the new sub-2 µm core-shell (Kinetex™) column in practice, applied for small and large molecule separation. *Journal of pharmaceutical and biomedical analysis*, 54(3), 482-490.
63. Preti, R. (2016). Core-shell columns in high-performance liquid chromatography: Food analysis applications. *International journal of analytical chemistry*, 2016.
64. Čelić, M., Insa, S., Škrbić, B., & Petrović, M. (2017). Development of a sensitive and robust online dual column liquid chromatography-tandem mass spectrometry method for the analysis of natural and synthetic estrogens and their conjugates in river water and wastewater. *Analytical and Bioanalytical Chemistry*, 409(23), 5427-5440.
65. Oliferova, L., Statkus, M., Tsysin, G., Shpigun, O., & Zolotov, Y. (2005). On-line solid-phase extraction and HPLC determination of polycyclic aromatic hydrocarbons in water using fluorocarbon polymer sorbents. *Analytica Chimica Acta*, 538(1-2), 35-40.

66. European Commission. *Commission Decision 2002/657/EC of 12 August 2002 implementing Council Directive 96/23/EC concerning the performance of analytical methods and the interpretation of results*. Official Journal of the European Communities, 2002. 50: p. 8-36.
67. Garcia-Ac, A., Segura, P. A., Viglino, L., Fürtös, A., Gagnon, C., Prévost, M., & Sauvé, S. (2009). On-line solid-phase extraction of large-volume injections coupled to liquid chromatography-tandem mass spectrometry for the quantitation and confirmation of 14 selected trace organic contaminants in drinking and surface water. *Journal of chromatography A*, 1216(48), 8518-8527.
68. Caruso, R., Scordino, M., Traulo, P., & Gagliano, G. (2012). Determination of volatile compounds in wine by gas chromatography-flame ionization detection: comparison between the US Environmental Protection Agency 3 σ approach and Hubaux-Vos calculation of detection limits using ordinary and bivariate least squares. *Journal of AOAC International*, 95(2), 459-471.
69. Castiglioni, S., Bagnati, R., Calamari, D., Fanelli, R., & Zuccato, E. (2005). A multiresidue analytical method using solid-phase extraction and high-pressure liquid chromatography tandem mass spectrometry to measure pharmaceuticals of different therapeutic classes in urban wastewaters. *Journal of Chromatography A*, 1092(2), 206-215.
70. Das, S., Ray, N. M., Wan, J., Khan, A., Chakraborty, T., & Ray, M. B. (2017). Micropollutants in wastewater: fate and removal processes. *Physico-chemical wastewater treatment and resource recovery*, 3, 75-117.
71. Loos, R., Carvalho, R., António, D. C., Comero, S., Locoro, G., Tavazzi, S., ... & Gawlik, B. M. (2013). EU-wide monitoring survey on emerging polar organic contaminants in wastewater treatment plant effluents. *Water research*, 47(17), 6475-6487.
72. Ort, C., Lawrence, M. G., Reungoat, J., Eaglesham, G., Carter, S., & Keller, J. (2010). Determining the fraction of pharmaceutical residues in wastewater originating from a hospital. *Water research*, 44(2), 605-615.
73. Feldmann, D. F., Zuehlke, S., & Heberer, T. (2008). Occurrence, fate and assessment of polar metamizole (dipyrone) residues in hospital and municipal wastewater. *Chemosphere*, 71(9), 1754-1764.
74. Weissbrodt, D., Kovalova, L., Ort, C., Pazhepurackel, V., Moser, R., Hollender, J., ... & McArdell, C. S. (2009). Mass flows of X-ray contrast media and cytostatics in hospital wastewater. *Environmental science & technology*, 43(13), 4810-4817.

CHAPTER 4

Non-target Screening By LC/MS-based Technique

4. NON-TARGET SCREENING BY LC/MS-BASED TECHNIQUES

4.1 Introduction

This chapter explores the importance of non-target screening in identifying unknown environmental contaminants, with an emphasis on the aquatic environment. Due to the complexity of the majority of sample matrices, environmental samples are exceptionally difficult to analyze. Traditionally, trace and ultra-trace analysis of water samples has been accomplished using targeted analytical methods that focus on a specific sample type and a set of known chemicals. For several decades, targeted analytical methods have been effectively used to identify and quantify target chemicals and they have proven to be highly sensitive and reliable. However, targeted methodologies overlook those substances that were not included in the initial analysis workflow - a fundamental drawback. Indeed, it is likely that all unknowns or untargeted compounds with potentially higher concentrations and/or more severe adverse effects than the targeted analytes will be disregarded.

There are ample reasons to infer that the concentration of unknown substances typically exceeds the concentration of known ones. Furthermore, various effect studies have indicated that concentrations of known contaminants are insufficient to account for the toxic effects found in certain samples. Thus, approaches based on non-target screening can play a vital role in bridging this knowledge gap in environmental analysis. Recent years have seen remarkable improvements in analytical techniques and software tools that considerably increase the practicality and affordability of non-target screening today.

In line with this, the AQUALITY project, with which my PhD was affiliated, decided to conduct untargeted analysis with the goal of identifying potential contaminants of emerging concern (CECs), and the data would eventually be used to improve the databases of the European network of laboratories monitoring emerging pollutants (NORMAN). For this purpose, two sampling campaigns took place in 2019 and 2020. Sample locations were systematically selected in three countries (France, Greece, and Italy). I was involved in the overall organization of the non-target screening task, from establishing the sampling and sample pre-treatment methods to LC-HRMS analysis, data processing, and reporting. The discussion in this thesis, however, will be limited to the samples collected in the first sampling campaign in 2019, during which I was more directly involved in the sampling, extraction, LC-HRMS analysis, and data processing stages.

4.2 Background of the study

When the aim is to analyze a water sample possibly containing many unknown substances, the question of how to identify contaminants that may be of environmental importance (in terms of potential toxic effects) emerges. To address this, various analytical approaches and strategies based on biological or chemical analyses have been developed over the last decades. Depending on the purpose and scope of analysis required, three analytical approaches are possible as described elsewhere, e.g., [1]. These are: targeted analysis, semi-targeted (suspect) screening, and untargeted (non-target) screening.

A **targeted screening** typically involves a quantitative determination of a relatively small number of known compounds. Reference standards are used for comparative purposes and to maximize the degree of certainty associated with identification. The analysis involves a highly specific (targeted) signal acquisition mode, which is accomplished by utilizing well-established standards for the compounds being analyzed. In **suspect screening**, an evaluation of HRMS data is typically assisted by information on potentially occurring compounds or suspect lists (e.g., MS/MS libraries). This approach is also aimed at identifying a limited number of compounds. A genuine **non-target screening** begins with no *a priori* information and aims to identify as many compounds as possible. This approach involves prediction of molecular formulas for substances that were not identified by target or suspect screening, followed by exploring databases for probable structures. After that, the structures are compared to the unknown compounds using methods such as retention-time prediction or MS/MS prediction tools, e.g., MetFrag [2]. Moreover, mass spectra can be used to predict structures using tools such as MOLGEN-MS [3]. Obviously, not all chemicals have records in existing databases, and identifying truly unknown substances is a difficult task that requires a great deal of expertise and time. A systematic workflow for the three analytical approaches is shown in Fig. 4.1. However, it is important to highlight that, in most cases, suspect and non-target screening approaches cannot be strictly distinguished.

In recent years, the use of high-resolution mass spectrometry coupled with either liquid chromatography (LC-HRMS) or gas chromatography (GC-HRMS) has evolved into a powerful tool for the screening of environmental contaminants from different complex matrices [4-8]. In the field of water analysis, linear ion trap instruments with orbitrap technology (Orbitrap) and quadrupole time-of-flight (Q-TOF) mass spectrometers coupled with HPLC are commonly used. The advantages associated with the new generation of HRMS instruments are high mass resolving power, good mass accuracy, good isotopic abundance accuracy, and extremely high sensitivity [1].

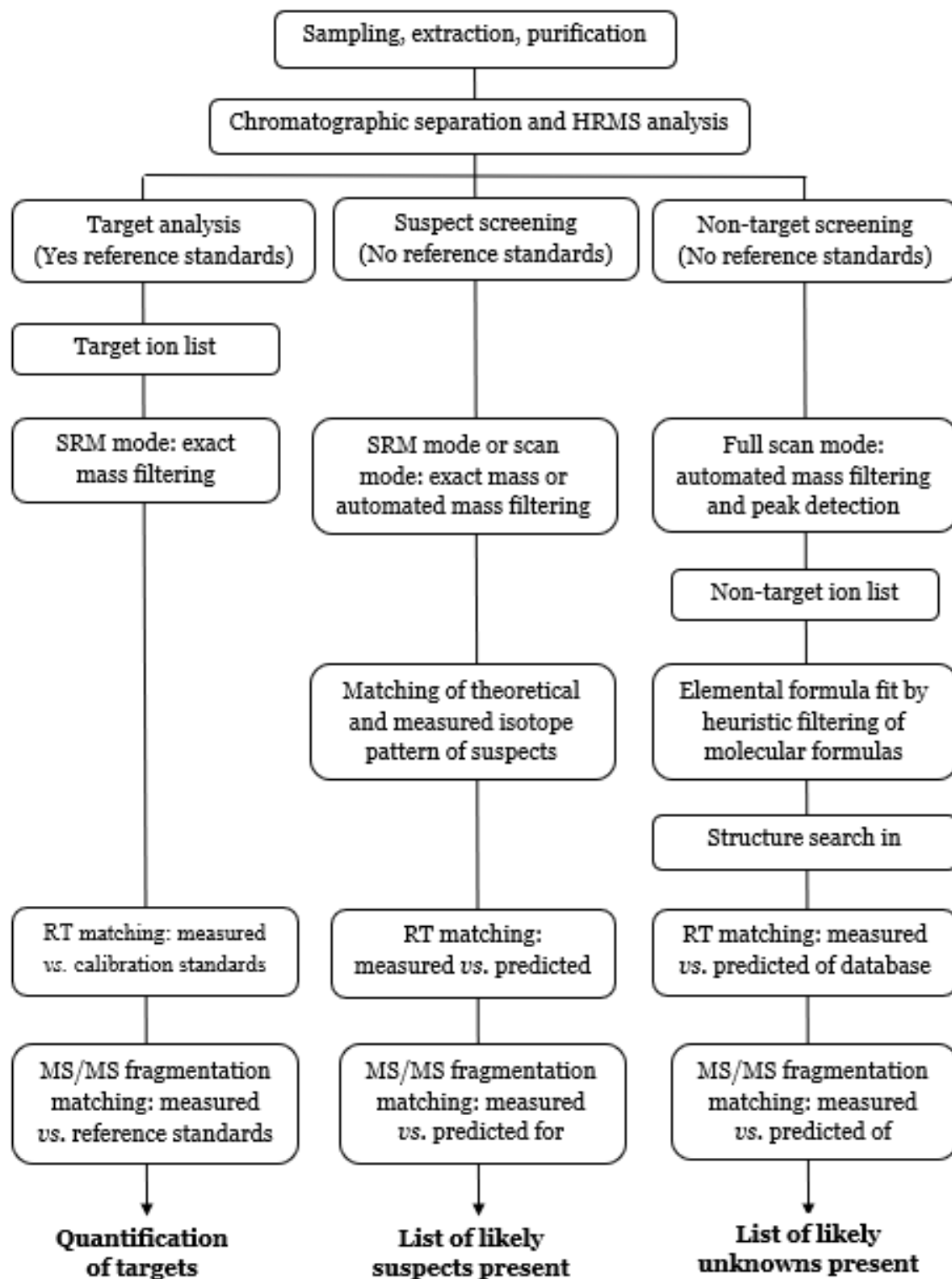


Figure 4.1. Workflow for the three analytical approaches, adapted from [9].

Generally, water analysis involves a chromatographic separation prior to identifying the constituents in a sample. Additionally, sample extraction is typically required due to the complexity of certain samples (e.g., wastewater). However, sample preparation for suspect and non-target screening should be kept to a minimum to preserve as much information as possible [10]. Liquid chromatography (LC) is more frequently utilized for separation purposes than gas chromatography (GC), as it permits for a greater coverage of compounds without requiring sophisticated sample treatment [11]. Moreover, LC-MS equipment (specifically LC-HRMS) are more adaptable and widely available in laboratories than GC-MS devices. GC is best suited to volatile and thermally stable substances, whereas LC tend to be suitable with a large variety of molecules possessing a variety of chemical properties. Additionally, GC frequently involves a chemical derivatization step, which may complicate the non-target identification of unknowns. However, GC-based systems are valuable and complementary techniques for analyzing non-polar and volatile substances [12], for which the sensitivity of LC-based techniques is frequently lower [13].

The first thing that affects how well a chromatographic separation works is the nature and properties of the stationary phase that is being used. In general, reversed phase (RP) systems (e.g., C18 stationary phases), which have been around for a long time, remain the most common way to screen for suspect or untargeted substances. Hydrophilic Interaction Liquid Chromatography (HILIC) [14] could be used to separate polar compounds where reversed phase LC does not work well. Another way to separate only ionic compounds is capillary electrophoresis. This method is not used as often as RPLC or HILIC, and it is more difficult to use with MS because of the small amount of sample that can be used [15]. Two further factors that can influence the outcome of a chromatographic separation are the type of the mobile phase and the settings of the elution gradient. Suspect and untargeted screening approaches typically use less selective and more broad chromatographic settings to cover the widest range of potential markers possible, rather than focusing on a small number of known substances.

Choosing suitable ionization and signal acquisition methods is critical to the success of mass spectrometry analysis following the separation of chromatographic components. Because of its ease of use and extensive applicability [16], electrospray ionization (ESI) in both positive and negative modes is commonly used in LC-HRMS non-target screening. To be able to detect a greater variety of compounds with the desired sensitivity and selectivity, a full scan non-selective acquisition mode must be performed in HRMS for both suspect and non-target screening [10]. The most commonly used mass analyzers in this regard are time-of-flight (ToF or Q-ToF) and Orbitrap (IT-Orbitrap or Q-Orbitrap). Another feasible option is Fourier transform ion cyclotron resonance (FT-ICR); however, it is rarely employed due to its expensive cost and slow acquisition rate [1].

Given their availability within the AQUALity consortium, the LC-HRMS instrumentation (Q-ToF and Orbitrap) was used in the context of untargeted screening under the WP2 workplan. The aim of this study was to maximize the LC-HRMS information collected from the considered water samples and identify potential CECs. Finally, the large amount of HRMS data, as well as the list of identified compounds, was used to enrich the NORMAN databases through Suspect List Exchange (SLE) and Digital Sample Freezing Platform (DSFP).

4.3 Experimental approach

4.3.1 Apparatus and materials

The sample containers were amber glass bottles with stoppers or Teflon-lined screw caps. All bottles were cleaned by rinsing them three times with tap water, three times with organic-free water, twice with cleaning acetone, once with special UV-grade acetone, and twice with pesticide grade hexane before being dried (uncapped) in a hot air oven at 360 °C. Clear glass autosampler vials (1.5 mL) were used for sample injection into the HPLC. Multiple injections from the same vial are not recommended due to unknown potential evaporation effects. Glass micro syringes with capacities of 5, 50, 100, 500, and 1000 L were used to prepare samples and stock solutions, while pipettes were used to prepare solvents. Weighing was performed using an analytical balance capable of weighing to the closest 0.1 mg.

The SPE cartridges were Oasis HLB (6 cc/200 mg; Waters, Milan, Italy) and Supelclean ENVI-Carb Plus reversible tubes (0.4 g/mL; Sigma-Aldrich, Milan, Italy). ENVI-Carb Plus cartridges were used in conjunction with empty 6-mL SPE tubes (without frits), and male and female luer couplers. LC-MS analyses of the samples were carried out using an Ultra-High Performance Liquid Chromatography (UHPLC) Vanquish Flex system (Thermo Scientific, Rodano, Italy) coupled with an Orbitrap Q-Exactive Plus (Thermo Scientific, Rodano, Italy).

4.3.2 Chemicals and Reagents

Ultrapure water was obtained from a Millipore Milli-Q water purification system (MA, USA) and had a resistance of 18.2 M Ω /cm (at 25°C) and TOC value below 5 ppb. Methanol and water, both of which were of the highest quality for use in LC-MS analysis, were purchased from VWR (Milan, Italy), while acetone, formic acid for LC-MS, and pesticide-grade hexane were purchased from Sigma-Aldrich (Milan, Italy). As internal standards flunixin-d₃, diuron-d₆ and simazine-d₁₀ were used, and were purchased from Sigma-Aldrich (Milan, Italy).

4.3.3 Sample collection

Surface water and wastewater samples were collected in 2019 from three European countries (Italy, France, and Greece) through the involvement of several beneficiaries and partners of the AQUALity project. A sampling and sample pre-treatment protocol prepared by our group (UPO, Alessandria, Italy) was revised and approved by members of the WP2, which was then adopted as the standard protocol by all participating units.

Several considerations were made when collecting the samples, as described in several guidelines such as [17]. For rivers, the primary sampling point should be in the surface water layer (0-5 cm below the surface) at the center of the main flow. However, the top 1-2 cm of this surface layer should be avoided so as not to collect floating dust, oil, etc. For lakes, the sampling point should be chosen after taking into consideration such factors as geography, freshwater (rivers or streams) or wastewater inflows, depth, tides, currents and so on.

Before collecting the water samples, the pre-cleaned amber glass bottles were rinsed twice with about 100 mL of the sample. Then, the bottles were filled with 1 L of the water samples and immediately transferred into an ice-cooled container and delivered to the lab in chilled conditions. The information for the 17 samples collected during the first sampling campaign in 2019 is shown in Table 4.1. The samples comprised 13 surface waters (SW) and 4 wastewater effluents (WWEF). All samples were clearly labelled, with the name and code of the sample, the sampling date, the sample site name, and other relevant data.

Once the samples arrived in the laboratory, they were filtered with 0.7 μm GF-F fiberglass filters (Whatman) and stored in dark at ~ 4 °C until extraction. To minimize microbial degradation, the samples were always extracted within 24 hours of collection. When this was not practicable, samples were kept frozen at -20 °C until extraction.

Table 4.1. Details of the water samples collected for this study.

No.	Code	Country	Sample Type	Sampling date	Site Location
1	FR_S28	France	SW	04/09/2019	49.248417, 2.452667
2	FR_S30	France	WWEF	04/09/2019	49.245194, 2.451722
3	FR_S38	France	SW	04/25/2019	49.25525, 2.433944
4	FR_S40	France	SW	04/25/2019	49.2965, 2.451167
5	FR_S42	France	SW	04/25/2019	49.197, 2.418083
6	IT_SS1A	Italy	SW	06/19/2019	45.044222, 7.683028
7	IT_SS2A	Italy	SW	06/19/2019	44.953333, 7.705278

8	IT_SS3A	Italy	SW	06/19/2019	44.96643, 7.692994
9	IT_SS4A	Italy	SW	06/19/2019	45.01596, 7.677505
10	IT_SS5A	Italy	WWEF	06/19/2019	45.0925, 7.609947
11	IT_SU1A	Italy	SW	06/24/2019	45.044222, 7.683028
12	IT_SU2A	Italy	SW	06/22/2019	45.137306, 7.68025
13	IT_SU3A	Italy	SW	06/22/2019	45.171833, 7.624694
14	IT_SU4A	Italy	SW	06/21/2019	45.099972, 7.718611
15	GR_SHE	Greece	WWEF	06/03/2019	39.623, 20.842194
16	GR_SUE	Greece	WWEF	05/28/2019	39.709917, 20.827778
17	GR_SLW	Greece	SW	05/28/2019	39.655451, 20.865918

4.3.4 LC-HRMS analysis

LC-HRMS analysis of the samples was performed using an Ultra-High Performance Liquid Chromatography (UHPLC) Vanquish Flex system coupled to an Orbitrap Q-Exactive Plus. The Orbitrap was equipped with a heated electrospray ionization (HESI) source. The chromatographic separation was accomplished using a reversed phase column Accucore™ RP-MS (100 x 2.1 mm, 2.6 μm). For both positive and negative ionization modes, a binary mobile phase composed of water acidified with 0.01% (*v/v*) formic acid (A) and methanol acidified with 0.01% (*v/v*) formic acid (B) was used with a gradient of: 10% B at 0–1 min, 90% B at 15 min, 90% B at 17 min, 10% B at 17.6 min, and 10% B at 20 min allowing the column to re-equilibrate at the initial conditions for 2.4 min, with a flow rate of 0.300 mL/min. The total run time was 20 min. The column and autosampler were kept at 40 °C and 8 °C, respectively. The injection volume was 5 μL.

Mass spectrometry analysis was performed in both positive and negative ESI modes. The HESI source voltage was 3.5 kV for ESI+ and -3.3 kV for ESI-. The sheath gas and auxiliary gas flows were 40 and 8 arb, respectively. The capillary temperature was 300 °C for ESI+ and 275 °C for ESI-, and the S-lens RF level was maintained at 50%. The auxiliary gas heater temperature was 300 °C. For each sample, two different acquisition modes have been used: Full Scan (FS) and Full Scan data dependent MS/MS (FSddMS²). The FS performed a full scan in the mass range *m/z* 60-900 without fragmentation of the ions, while the FSddMS² was a top 5 experiment, where the 5 most abundant ions were fragmented in the defined mass range. In both positive and negative ion modes, survey FS analysis was performed at a mass resolution of 70,000 (at *m/z* 200), automatic gain control (AGC) target of 3x10⁶, and maximum ion injection time (IT) of 200 ms. Full scan data dependent was performed using high-energy c-trap dissociation

(HCD) at 17,500 mass resolution, isolation window of 2.0, AGC target of 2×10^5 , and maximum IT of 60 ms. The stepped normalized collision energy (SNCE) was set to 20, 40, and 80. For mixtures of small molecules with diverse structures, each of which are expected to have a different optimum collision energy level for fragmentation, SNCE makes it easier to perform automated MS/MS scans by eliminating the need to optimize collision energies on an individual basis. To ensure accurate mass-based analysis, lock mass and regular inter-run mass calibrations had been performed using the Pierce LTQ Velos Positive and Negative ion calibration solutions. Furthermore, an exclusion list for background ions was established using a procedural blank sample.

4.4 Results and Discussion

When performing untargeted screening using LC-MS/MS, one of the most difficult challenges is analyzing the massive amounts of data produced in the form of m/z and retention time features. There are several data processing methods available with powerful algorithms for peak detection, deconvolution, and alignment. Among the most popular are XCMS [18], and MS-DIAL [19], and MZmine 2 [20]. However, when applied to complex samples, none of these algorithms can produce error-free findings, necessitating the engagement of an experimenter on a more hands-on basis. Thus, manual curation to remove duplicate peaks, isotope features, chemical noise, and integrate numerous ion-adducts formed from the same molecule is often required, a process that is both time-consuming and error-prone.

4.4.1 Non-target identification workflow using MS-DIAL

Non-target screening of the generated LC-HRMS data was performed using the MS-DIAL software (*ver.* 4.70). Fig. 4.2 illustrates the data processing workflow, while the parameters employed at each level of the data processing workflow are summarized in Table 4.2. The workflow starts by importing the vendor's raw mass spectral data and applying a set of parameters to collect information about the precursor ions (MS₁) and product ions (MS/MS). The peak detection algorithm is based on two basic thresholds: minimum peak width and height values. Peaks that were less than the tolerances set for these parameters were disregarded. To accurately locate the peak's left and right edges, a linear-weighted moving average smoothing by three scans was applied. MS-DIAL uses the public mass spectral libraries to identify compounds based on four criteria: retention time, accurate mass, isotope ratio, and the MS/MS spectrum of the molecule under consideration.

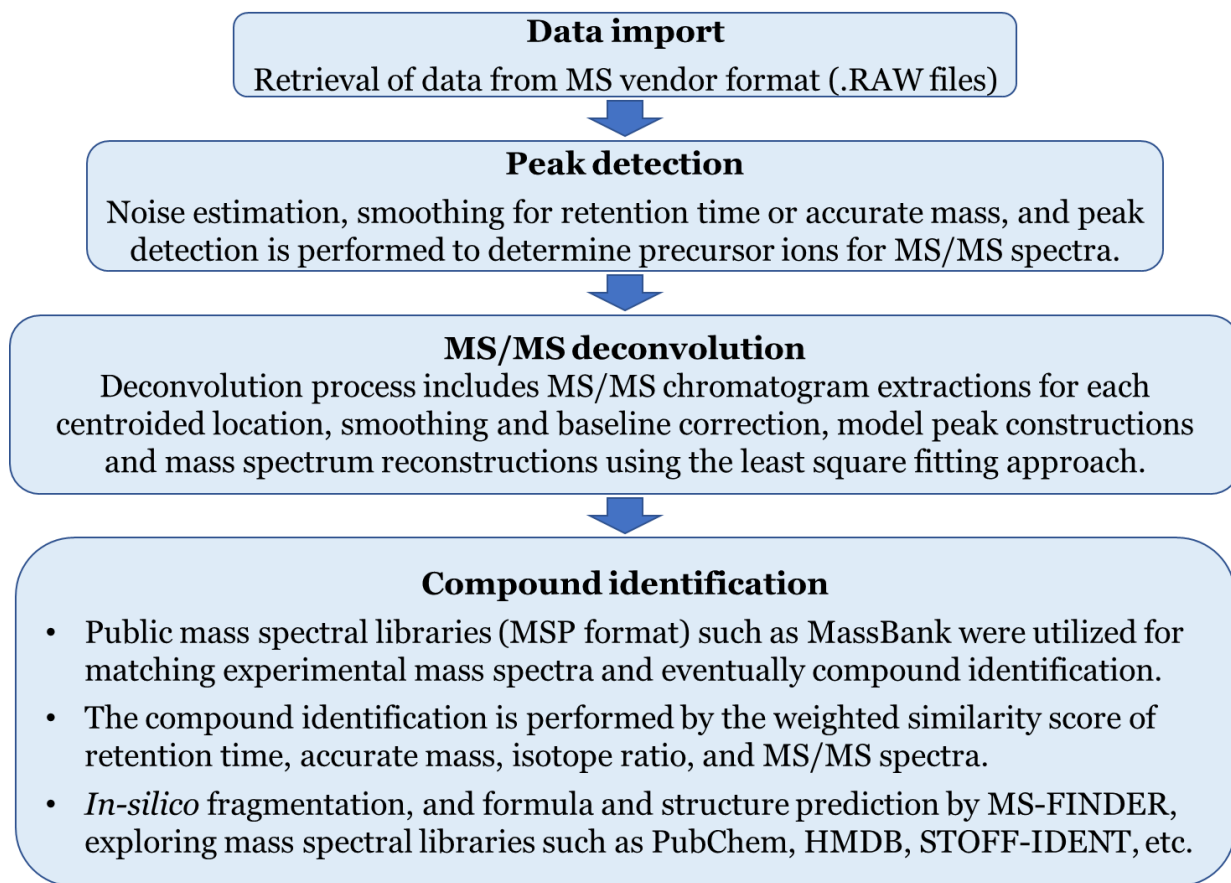


Figure 4.2. Overview of the workflow for LC-HRMS data processing using MS-DIAL

The version of MS-DIAL software used in this study had a total of 327,763 HRMS data for both ESI+ and ESI- gathered from public libraries such as MassBank, ReSpect, GNPS, Feihn HILIC, MetaboBase, and RIKEN. The records included pesticides, pharmaceuticals, personal care products, hormones, per- and polyfluoroalkyl compounds, and various metabolites and transformation products of environmental contaminants. The MS-FINDER program (*ver.* 3.52) was used to facilitate the identification of peak lists obtained by MS-DIAL, using online libraries such as HMDB, PubChem, and STOFF-IDENT. In addition, the Seven Golden Rules [21] was implemented for prediction and heuristic filtering of molecular formulas. Each score in the compound identification result ranged from “zero” (no match) to 1 (perfect match). MS-DIAL examines the dot-product, reverse dot-product, and matching fragments ratio (1:1:1) to the reference product ions for MS/MS spectral similarity. Finally, manual curation of the identified peaks was necessary to remove duplicates and false positives.

The MS-DIAL analysis resulted in a large number of features, providing a total of 29,581 peaks in ESI+ and 20,304 in ESI- (Fig. 4.3 and Table 4.3). Molecular formulas and/or structures were predicted (“suggested”) for 61.5% and 46.3% of the peaks respectively in ESI+ and ESI-.

Table 4.2. MS-DIAL parameters used for LC-HRMS data processing

Step	Parameters	Values/Setting
Data collection	RT range (min)	0 – 20
	MS1 mass range (m/z)	60 – 1000
	MS2 mass range (m/z)	50 – 1000
Centroiding and isotope recognition	MS1 tolerance (Da)	0.01
	MS2 tolerance (Da)	0.025
	Max charge number	2
Peak detection and spotting	Smoothing method	Linear weighted moving average
	Smoothing level (scan)	3
	Minimum peak width (scan)	5
	Min. peak height (amp.)	5x10 ⁴
	Mass slice width (Da)	0.05
MS2	Sigma window value	0.5
Deconvolution	MS2 abundance cut-off (amp.)	5
Identification	Database (MSP file) for ESI+	MSMS-Public-Pos-VS15
	Database (MSP file) for ESI-	MSMS-Public-Neg-VS15
	Retention time tolerance (min)	1.0
	MS1 accurate mass tolerance (Da)	0.01
	MS2 Accurate mass tolerance (Da)	0.025
	Identification score cut-off (%)	80
Adducts	Positive ESI	[M+H] ⁺ , [M+NH ₄] ⁺ , [M+Na] ⁺
	Negative ESI	[M-H] ⁻
Alignment	Retention time tolerance (min)	0.05
	MS1 tolerance (Da)	0.015
	Retention time factor	0.5
	MS1 factor	0.5
	Blank filter average fold change	5

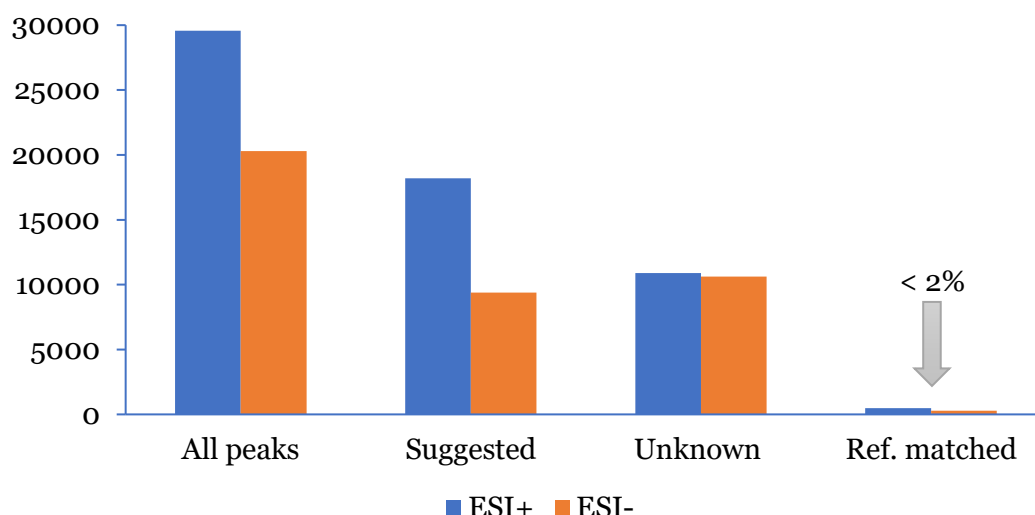


Figure 4.3. Results of the non-target screening using *MS-DIAL* and *MS-FINDER*.

The peaks were filtered with data from blanks, MS/MS, and feature matching using the public spectral databases. This significantly reduced the number of features, leaving only 490 and 284 compounds with database hits respectively in ESI+ and ESI-. This was followed by manual curation of the database hits to eliminate false positives. The peak list tables were exported to Excel and examined for duplicates. As reported in Table 4.3, a total of 264 compounds were identified at Level 2 confidence as described in Schymanski et al. [1].

Table 4.3. Sequential filtering and processing of the features obtained in *MS-DIAL*.

	ESI+	ESI-
Primary processing	29581	20304
(+) Blank filter	25774	17246
(+) MS2 acquired	4367	5388
(+) Reference matched	490	284
(+) Manual curation	177	87

To demonstrate how the 264 compounds were finally identified at Level 2, Fig. 4.4 illustrates the sample and spectral information within *MS-DIAL* for the lipid-lowering drug rosuvastatin that belongs to the statin class. This drug was detected in wastewater effluent samples from Greece with an average signal intensity of 5.9×10^6 . In this case, the compound annotation was confirmed using *LTQ-Orbitrap* database information, which revealed similarities in collision energy (CE) and MS/MS fragmentation, among other attributes.

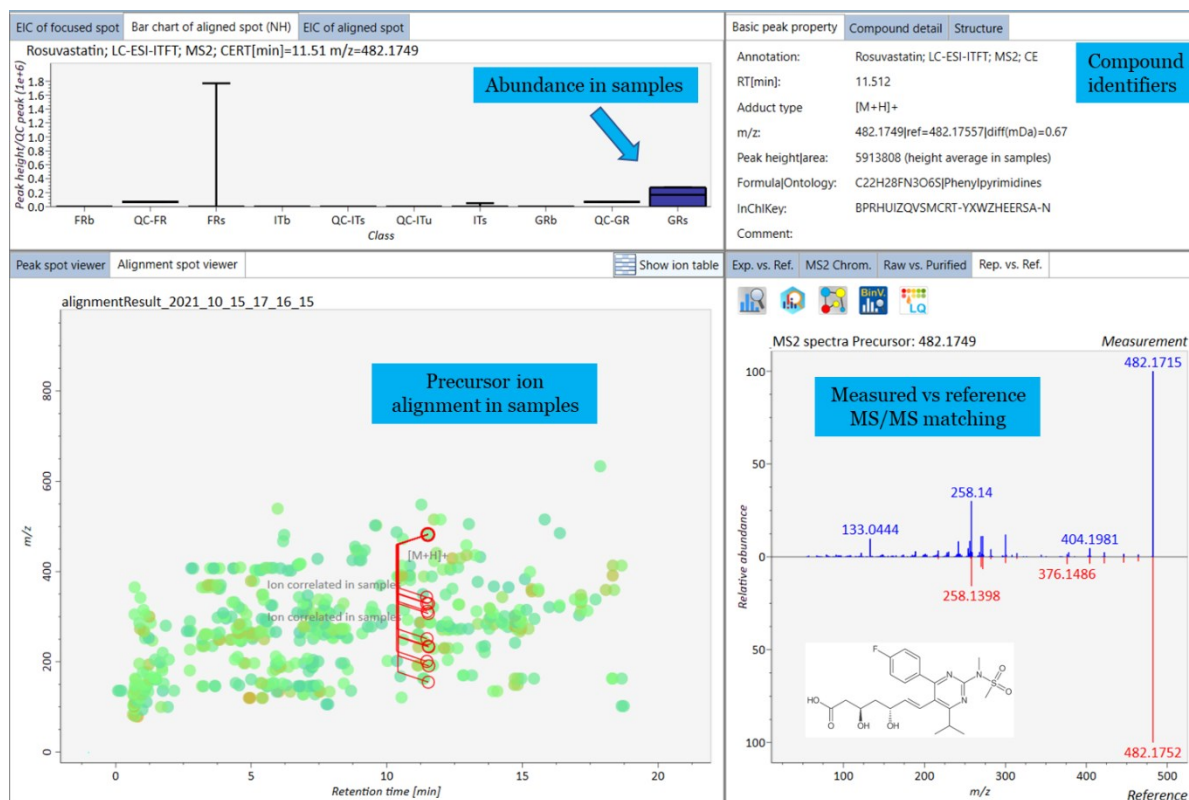


Figure 4.4. Detection and identification of the drug rosuvastatin

The results were also explored using Principal Component Analysis (PCA). PCA [22] is a multivariate method used for lowering multiple dimensionalities in large datasets while retaining as much information as possible, making them easier to read and interpret. It achieves this by generating new uncorrelated variables that maximize the variance in a stepwise manner.

The 2D PCA scores plot (**Fig. 4.5a**) illustrates correlations among the different samples considered in this study. For instance, Italy's samples are grouped together, showing that they were correlated. Notably, the samples from Greece were dispersed throughout the other groups. Interestingly, the GR_S(LW)-2 sample from Lake Pamvotis was correlated with the blanks. Although earlier studies on Lake Pamvotis have identified a range of environmental contaminants, including pharmaceuticals [23] and pesticides [24], the samples analyzed in this study were found to be less polluted. However, the GR S(HE)-2 sample from a Greek hospital effluent was more closely correlated with the French samples. A deeper examination of the loading plot (**Fig. 4.5b**) reveals that azoles, angiotensin receptor blockers (ARBs), and beta blockers were the variables most responsible for the variance between the samples.

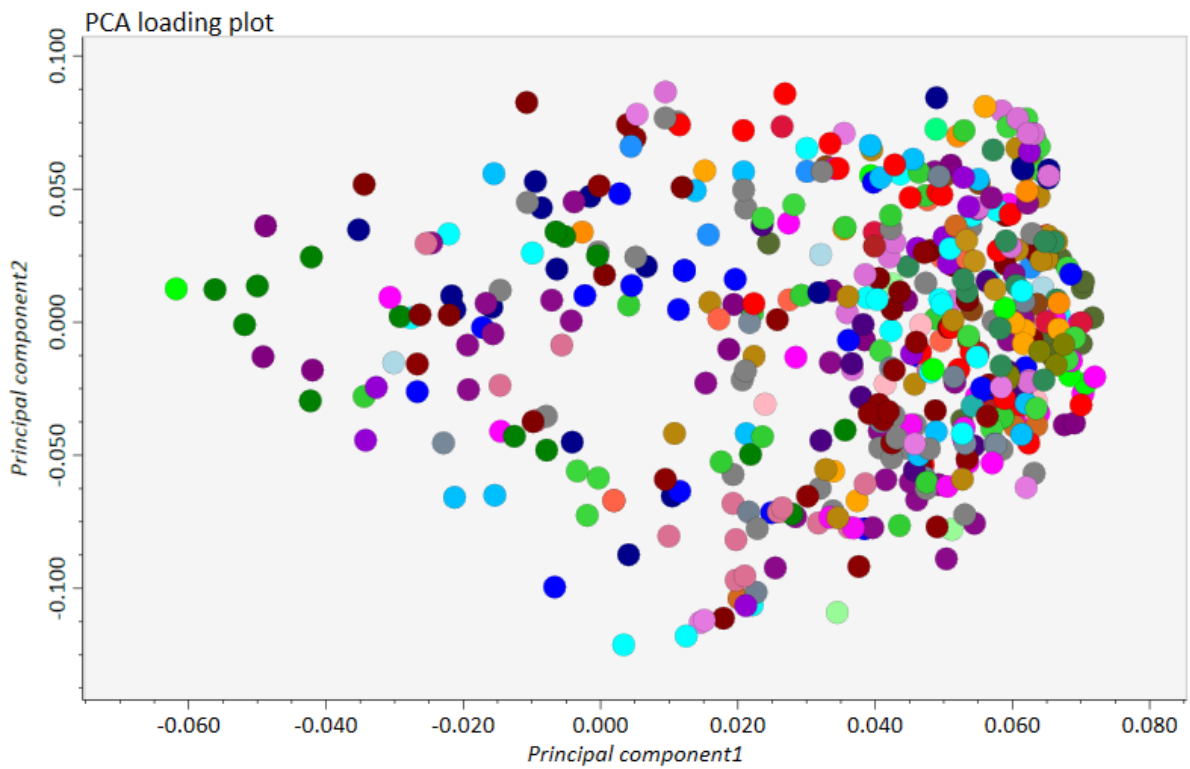
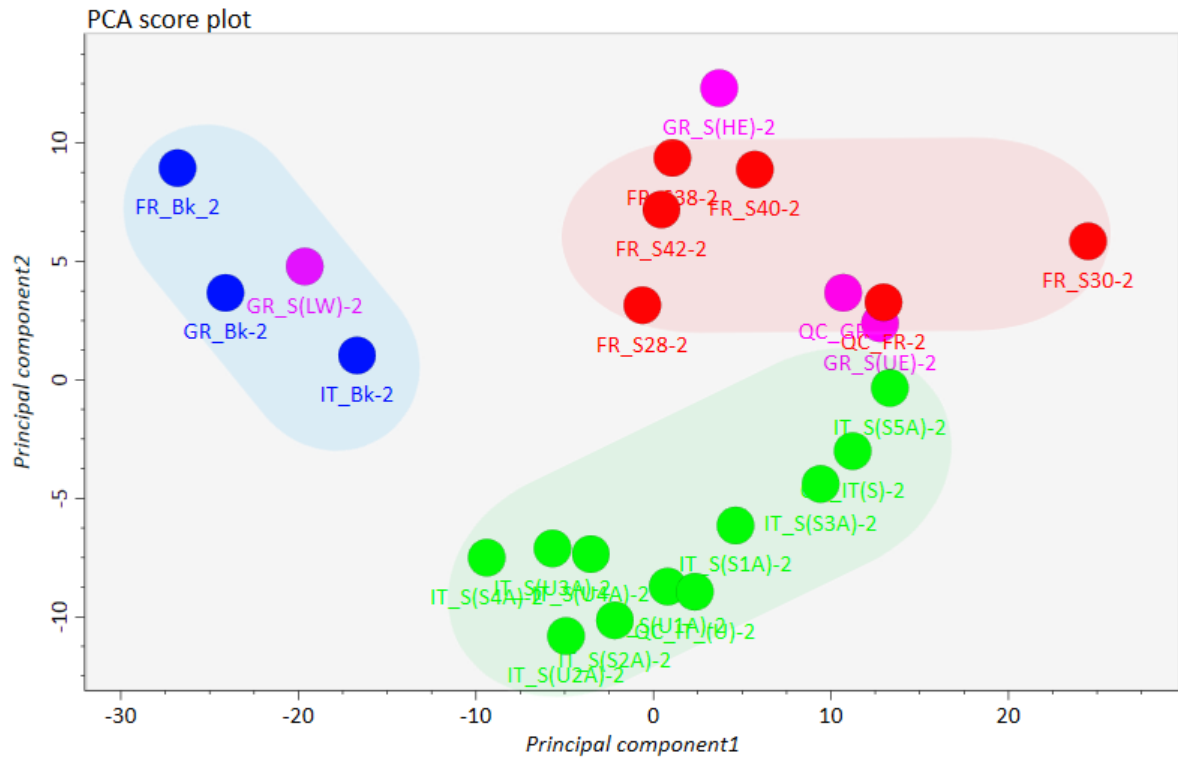


Figure 4.5. PCA scores (a) and loadings (b) plots

4.4.2 List of substances and their categorization

The list of 264 compounds identified at Level 2 is given in Table 4.4, out of which 20 compounds were identified in both ESI+ and ESI- (indicated with light red filled cells). From the total number of compounds identified in this study, 28 of them were also detected in samples collected in a second campaign and analyzed by other members of the AQUALity project (Table 4.5). Moreover, seven compounds were confirmed with the highest degree of confidence (i.e., Level 1) using suspect screening with standards for suspected analytes (indicated by green filled cells in Table 4.5).

Within the identified compounds there were pharmaceuticals, pesticides, personal care products (PCPs), food additives, industrial/research chemicals, metabolites, and transformation products. Interestingly, specific contaminants and some of their transformation products found in studies of other AQUALity members (including works from WP2 and WP3) were detected and identified in this study as well (e.g., Citalopram and by-products). Finally, some parent compounds were identified in one of the two campaigns, while their transformation products were identified in the other one, and vice versa (e.g., metolachlor and by-products, terbuthylazine and by-products, atrazine and by-products).

4.5 Improvement of the NORMAN database

4.5.1 Suspect List Exchange (SLE)

A list of contaminants containing the following information: Name, Monoisotopic Mass, Formula, CAS number, PubChem/ChemSpider number, RT, Peak Area, Ionization Mode, Confirmation Criteria, and SMILES for every identified compound, in both sampling campaigns, was prepared and uploaded into the Suspect List Exchange (SLE) database (<https://www.norman-network.com/nds/SLE/>).

4.5.2 Digital Sample Freezing Platform (DSFP)

The aim of archiving all HRMS data in the NORMAN's DSFP was to perform a wide-scope retrospective screening of the data obtained in this study, using information for exact mass, predicted retention time window in the chromatogram, isotopic fit and qualifying fragment ions [25] for a huge variety of contaminants and their transformation products.

First, in order to calculate the Retention Time Index (RTI), a sample of known compounds (2 sets of substances, one set for ESI- and another for ESI+) supplied by NORMAN was analyzed

with the same LC-HRMS method used for real water samples. The goal of this analysis was to predict retention times of different chemicals under different LC conditions and to uncover more usable retention time information for non-target screening [26]. Following that, an Excel file containing information about the organization where the analyses were performed, a sample description, details about the analytical methods and instrumentation, RTI data, and metadata was prepared and submitted to the NORMAN DSFP, along with all of the HRMS spectra converted to mzML format using ProteoWizard's msConvert [27], thus producing data files independent from the vendor software.

This work is still in progress. Once the storage of the HRMS data obtained from this study in online repositories is completed, it will be possible to use them for screening thousands of environmentally relevant suspect contaminants – using the NORMAN Suspect List Exchange database (SusDat) (<https://www.norman-network.com/nds/susdat/>). Finally, uploading the data in the DSFP will provide information that will help improve the spatial coverage of different environmental bodies across Europe for wide screening of contaminants presence and evaluation of their quality status.

4.6 Conclusions and forward

In this chapter, we demonstrated the potential of LC-HRMS for non-target screening by applying rigorous sample pre-treatment, analysis, and data processing methodologies to identify unknown environmental contaminants. Several environmental contaminants, including pharmaceuticals, pesticides, personal care products, food additives, industrial/research chemicals, metabolites, and transformation products, were identified in different water samples.

To ensure the highest level of confidence in the tentatively identified compounds, comparison and verification using reference/isolated standards is required. We believe that obtaining reference standards for the large number of compounds identified in this study will be challenging. We suggest that these substances be prioritized based on current knowledge about their usage, environmental occurrence, and toxic effects. Then, more advanced research is required on selected substances to determine their persistence, mobility, bioaccumulation, and potential for toxicity.

We also recommend that non-target data generated with HRMS instrumentation be uploaded into the NORMAN databases in order to fully exploit the collected data and knowledge, particularly for retrospective analysis, and to promote future research efforts in this field.

Table 4.4. List of compounds identified using public libraries, light-red filled cells are compounds identified both in ESI+ and ESI-.

No.	RT (min)	m/z	Ionization	Type	Compound name	Category/Class
1	0.81	79.0213	ESI+	[M+H] ⁺	Dimethyl sulfoxide	Industry; Research
2	0.71	81.0532	ESI+	[M+H] ⁺	Pyrimidine	Industry, Research
3	0.67	102.1276	ESI+	[M+H] ⁺	1-Hexylamine	Research; Surfactants
4	0.65	104.0704	ESI+	[M+H] ⁺	4-Aminobutanoate	Amino acids
5	7.78	106.0863	ESI+	[M+H] ⁺	Diethanolamine	Industry
6	0.70	109.0760	ESI+	[M+H] ⁺	2,5-Dimethylpyrazine	Food additive
7	0.73	110.0600	ESI+	[M+H] ⁺	4-Aminophenol	PCPs; Textiles, hair, furs
8	5.43	120.0555	ESI+	[M+H] ⁺	Benzotriazole	Industry; Corrosion inhibitor
9	10.54	121.0651	ESI+	[M+H] ⁺	Phenylacetaldehyde	Industry; PCPs
10	0.65	127.0726	ESI+	[M+H] ⁺	Melamine	Industry; Plastic dishware
11	6.94	128.1071	ESI+	[M+H] ⁺	Cyclohexylformamide	Industry; Drug R&D
12	0.89	130.0500	ESI+	[M+H] ⁺	L-5-Oxoproline	Amino acids
13	0.65	130.1087	ESI+	[M+H] ⁺	Metformin	Pharmaceutical; Diabetes medicine
14	1.01	132.1018	ESI+	[M+H] ⁺	DL-Norleucine	Research
15	6.44	134.0598	ESI+	[M+H] ⁺	Indoxyl sulfate	Metabolite; Human
16	1.20	134.0710	ESI+	[M+H] ⁺	2-Aminobenzimidazole	Research; Pharmaceuticals
17	7.49	134.0712	ESI+	[M+H] ⁺	5-Methyl-1H-benzotriazole	Industry; Environmental contaminant
18	8.68	136.0219	ESI+	[M+H] ⁺	Benzothiazole	Industry; Research
19	2.16	136.0504	ESI+	[M+H] ⁺	4-Hydroxybenzotriazole	Research; Industry
20	0.70	139.0501	ESI+	[M+H] ⁺	Urocanic acid	Carboxylic acids; Human origin
21	6.87	146.0599	ESI+	[M+H] ⁺	Indole-3-carboxyaldehyde	Metabolite (of Tryptophan)
22	3.19	146.0597	ESI+	[M+H] ⁺	4-Hydroxyquinoline	Research
23	7.34	147.0441	ESI+	[M+H] ⁺	Coumarin	Phytochemical; Anticoagulant
24	3.65	147.0915	ESI+	[M+H] ⁺	5,6-Dimethylbenzimidazole	Metabolite; TP of B12
25	4.55	148.0393	ESI+	[M+H] ⁺	Isatin	Industry; Corrosion inhibitor
26	0.71	148.0604	ESI+	[M+H] ⁺	L-Glutamic acid	Amino acids

No.	RT (min)	m/z	Ionization	Type	Compound name	Category/Class
27	7.47	148.0757	ESI+	[M+H] ⁺	Indole-3-carbinol	Pharmaceutical; Antitumor
28	6.30	148.0759	ESI+	[M+H] ⁺	3-Methoxyindole	Metabolite (of Tryptophan)
29	14.83	149.0232	ESI+	[M+H] ⁺	Phthalic anhydride	Industry; Plastics
30	1.01	150.1124	ESI+	[M+H] ⁺	Triethanolamine	Industry; PCPs; Surfactants
31	8.41	152.0169	ESI+	[M+H] ⁺	Benzisothiazolone (BIT)	Disinfectants; Toxicant
32	1.77	152.0706	ESI+	[M+H] ⁺	Paracetamol	Pharmaceutical; Analgesics and antipyretics
33	5.80	153.0550	ESI+	[M+H] ⁺	Vanillin	PCPs; Food additives
34	5.85	153.1020	ESI+	[M+H] ⁺	Pyrimidinol	PCPs
35	14.84	163.0386	ESI+	[M+H] ⁺	Umbelliferone	PCPs; UV protection
36	1.50	164.0930	ESI+	[M+H] ⁺	N,N-dimethyl-7H-purin-6-amine	Research
37	1.40	166.0861	ESI+	[M+H] ⁺	Phenylalanine	Amino acids
38	10.50	167.9933	ESI+	[M+H] ⁺	2-Mercaptobenzothiazole	Industry; Pesticides, rubber
39	12.81	170.0966	ESI+	[M+H] ⁺	Diphenylamine	Industry; Antioxidants; Pesticides
40	1.15	177.1020	ESI+	[M+H] ⁺	Cotinine	Metabolite; Stimulants
41	7.12	179.0703	ESI+	[M+H] ⁺	Coniferyl aldehyde	Industry; Drug R&D; Wine stoppers
42	1.72	181.0719	ESI+	[M+H] ⁺	Theobromine	Pharmaceutical; Stimulants
43	2.73	181.0719	ESI+	[M+H] ⁺	Theophylline	Pharmaceutical; Xanthines
44	5.90	183.0659	ESI+	[M+H] ⁺	Syringaldehyde	R&D; PPCPs, textiles, pulp and paper
45	8.56	183.0780	ESI+	[M+H] ⁺	Triethylphosphate	Industry
46	7.26	188.0697	ESI+	[M+H] ⁺	Desethylatrazine	TP (of Atrazin); Herbicides
47	6.10	188.0818	ESI+	[M+H] ⁺	Metamitron-desamino	TPs; Herbicides
48	6.05	189.1019	ESI+	[M+H] ⁺	Antipyrine	Pharmaceutical; Analgesics
49	11.13	192.1381	ESI+	[M+H] ⁺	DEET	Pesticides; Insect repellents
50	4.77	197.0810	ESI+	[M+H] ⁺	2-hydroxy-4-(4-hydroxyphenyl)butanoic acid	Research; Industry
51	7.47	201.1016	ESI+	[M+H] ⁺	Harmalol	Phytochemicals
52	10.03	202.0857	ESI+	[M+H] ⁺	Simazine	Herbicides
53	6.06	203.0929	ESI+	[M+H] ⁺	Metamitron	Herbicides
54	12.25	204.1384	ESI+	[M+H] ⁺	Crotamiton	Pharmaceutical; Scabicides; Antipruritics

No.	RT (min)	m/z	Ionization	Type	Compound name	Category/Class
55	1.45	205.0795	ESI+	[M+H] ⁺	Levamisole	Pharmaceutical; Antitumor; Veterinary
56	1.96	205.0979	ESI+	[M+H] ⁺	Tryptophan	Amino acids
57	4.40	205.1332	ESI+	[M+H] ⁺	N-Methylcytisine	Drug R&D; Phytochemicals
58	7.07	207.0653	ESI+	[M+H] ⁺	Citropen	Pharmaceutical; Antidepressants
59	5.91	212.1512	ESI+	[M+H] ⁺	Terbutylazine-2-hydroxy	Metabolite; Herbicides
60	1.74	220.1333	ESI+	[M+H] ⁺	Ritalinic acid	Metabolite; Psychostimulants
61	11.73	229.1236	ESI+	[M+H] ⁺	Bisphenol A	Industry; Plastics
62	12.28	230.1171	ESI+	[M+H] ⁺	Sebuthylazine	Herbicides
63	12.61	230.1172	ESI+	[M+H] ⁺	Terbuthylazine	Herbicides
64	12.11	230.2478	ESI+	[M+H] ⁺	N,N-Dimethyldodecylamine N-oxide	Industry; Surfactant
65	11.20	233.0238	ESI+	[M+H] ⁺	Diuron	Herbicides
66	3.17	235.1803	ESI+	[M+H] ⁺	Lidocaine	Pharmaceutical; Antibiotics
67	14.73	242.1170	ESI+	[M+H] ⁺	Mefenamic acid	Pharmaceutical; NSAID
68	11.38	245.0789	ESI+	[M+H] ⁺	Uridine	Pharmaceutical; Pyrimidine nucleosides
69	4.59	246.1234	ESI+	[M+H] ⁺	4-Acetamidoantipyrine	Pharmaceutical; Metabolite
70	6.79	247.1799	ESI+	[M+H] ⁺	Milnacipran	Pharmaceutical; SNRIs
71	3.19	250.0646	ESI+	[M+H] ⁺	Sulfapyridine	Pharmaceutical; Metabolite; Antibiotics
72	4.51	250.1807	ESI+	[M+H] ⁺	N,O-Didesmethylvenlafaxine	Pharmaceutical; Metabolite (of venlafaxine)
73	7.28	251.0371	ESI+	[M+H] ⁺	Bisphenol S	Industry; Plastics
74	5.05	251.1754	ESI+	[M+H] ⁺	Lidocaine hydrochloride monohydrate	Pharmaceutical; Anesthetic
75	1.09	252.1114	ESI+	[M+H] ⁺	Cordycepin	Drug R&D; Antitumor
76	8.50	253.0970	ESI+	[M+H] ⁺	Carbamazepine-10,11-epoxide	Metabolite (of Carbamazepine); Anticonvulsants
77	8.00	253.0977	ESI+	[M+H] ⁺	2-Hydroxycarbamazepine	Metabolite (of Carbamazepine); Anticonvulsants
78	5.05	256.0152	ESI+	[M+H] ⁺	Lamotrigine	Pharmaceutical; Phenyltriazines
79	4.96	258.1853	ESI+	[M+H] ⁺	Dextrorphan	Pharmaceutical; Antitussives
80	7.68	260.1646	ESI+	[M+H] ⁺	Propranolol	Pharmaceutical; Beta blockers
81	8.29	263.0813	ESI+	[M+H] ⁺	Indarubicin	Pharmaceutical; Antitumor
82	4.79	264.1954	ESI+	[M+H] ⁺	O-desmethylvenlafaxine	Pharmaceutical; Metabolite (of venlafaxine)

No.	RT (min)	m/z	Ionization	Type	Compound name	Category/Class
83	5.27	264.1959	ESI+	[M+H] ⁺	Tramadol	Pharmaceutical; Analgesics
84	6.98	264.1961	ESI+	[M+H] ⁺	N-Desmethylvenlafaxine	Pharmaceutical; Metabolite (of venlafaxine)
85	8.24	265.1402	ESI+	[M+H] ⁺	9-hydroxyparthenolide	Phytochemicals; Drug R&D
86	7.90	265.1696	ESI+	[M+H] ⁺	Mianserin hydrochloride	Pharmaceutical; Antidepressants
87	5.68	266.1653	ESI+	[M+H] ⁺	Mirtazapine	Pharmaceutical; Antidepressants
88	1.03	267.1704	ESI+	[M+H] ⁺	Atenolol	Pharmaceutical; Beta blockers
89	14.90	267.1722	ESI+	[M+H] ⁺	Tri-N-butyl phosphate (TBP)	Industry; Plastics
90	1.06	268.1042	ESI+	[M+H] ⁺	Adenosine	Pharmaceutical; Antiarrhythmic agent
91	2.63	268.1544	ESI+	[M+H] ⁺	Atenolol acid	TPs; Pharmaceuticals
92	5.33	268.1909	ESI+	[M+H] ⁺	Metoprolol	Pharmaceutical; Beta blockers
93	7.99	271.1075	ESI+	[M+H] ⁺	10,11-Dihydro-10,11-dihydroxycarbamazepine	Metabolite (of Carbamazepine); Anticonvulsants
94	0.90	273.1261	ESI+	[M+H] ⁺	Sotalol	Pharmaceutical; Beta blockers
95	15.23	273.1843	ESI+	[M+H] ⁺	Galaxolidone	PCPs; Cosmetics
96	4.46	275.0484	ESI+	[M+H] ⁺	Phenylbenzimidazole sulfonic acid	PCPs; UV protection
97	9.30	278.1900	ESI+	[M+H] ⁺	Maprotiline hydrochloride	Pharmaceutical; Antidepressants
98	7.78	278.1901	ESI+	[M+H] ⁺	2-Ethylidene-1,5-dimethyl-3,3-diphenylpyrrolidine	Metabolite (of Methadone); Opioid analgesics
99	9.44	278.1906	ESI+	[M+H] ⁺	Amitriptyline	Pharmaceutical; Antidepressants
100	6.92	278.2113	ESI+	[M+H] ⁺	Venlafaxine	Pharmaceutical; Antidepressants
101	12.00	279.0940	ESI+	[M+H] ⁺	Triphenylphosphine oxide (TPPO)	Industry; Solvent
102	14.72	279.1585	ESI+	[M+H] ⁺	Dibutyl phthalate	Industry; Plastics
103	13.94	283.0685	ESI+	[M+H] ⁺	Niflumic acid	Pharmaceutical; Anti-inflammatory
104	4.56	283.1752	ESI+	[M+H] ⁺	Hexaethylene glycol	Industry
105	13.67	284.1414	ESI+	[M+H] ⁺	Metolachlor	Herbicides
106	9.81	284.9612	ESI+	[M+H] ⁺	Tris(2-chloroethyl)phosphate	Flame retardants
107	1.29	286.1437	ESI+	[M+H] ⁺	Morphine	Pharmaceutical; Opioid analgesics
108	11.25	287.0582	ESI+	[M+H] ⁺	Oxazepam	Pharmaceutical; Benzodiazepines
109	14.22	287.1984	ESI+	[M+H] ⁺	Androstenedione	Steroid hormone
110	14.72	288.2531	ESI+	[M+H] ⁺	Lauryl diethanolamide	PCPs; Emulsifiers

No.	RT (min)	m/z	Ionization	Type	Compound name	Category/Class
111	5.61	290.1378	ESI+	[M+H] ⁺	Benzoylcegonine	Metabolites; Benzoic acid esters
112	7.44	291.2060	ESI+	[M+H] ⁺	D617	Metabolite (of Verapamil)
113	10.77	293.1052	ESI+	[M+H] ⁺	Climbazole	PCPs; Antifungals
114	5.52	294.1597	ESI+	[M+H] ⁺	Ondansetron	Pharmaceutical; Antiemetics
115	5.39	295.1156	ESI+	[M+H] ⁺	Buntansin C	Phytochemicals
116	14.09	296.0233	ESI+	[M+H] ⁺	Diclofenac	Pharmaceutical; NSAIDs
117	3.76	298.0963	ESI+	[M+H] ⁺	5'-Methylthioadenosine	Pharmaceutical R&D; Metabolite
118	4.27	300.1477	ESI+	[M+H] ⁺	Metoclopramide	Pharmaceutical; Prokinetic agents
119	1.24	300.1592	ESI+	[M+H] ⁺	Hydrocodone	Pharmaceutical; Opiate (narcotic) analgesics
120	1.24	300.159	ESI+	[M+H] ⁺	Codeine	Pharmaceutical; Opioid analgesics
121	14.34	301.1771	ESI+	[M+H] ⁺	Adrenosterone	Steroid hormone
122	14.73	303.2313	ESI+	[M+H] ⁺	Methyltestosterone	Pharmaceutical; Androgens
123	17.10	303.2313	ESI+	[M+H] ⁺	Abietic acid	Phytochemicals; Wood varnishes
124	1.11	304.2016	ESI+	[M+H] ⁺	Vildagliptin (LAF-237)	Pharmaceutical; Antidiabetic
125	7.03	307.1111	ESI+	[M+H] ⁺	Fluconazole	Pharmaceutical; Antifungal triazoles
126	7.55	308.0501	ESI+	[M+H] ⁺	Clopidogrel carboxylic acid	Metabolite (of Clopidogrel)
127	13.92	308.1517	ESI+	[M+H] ⁺	Tebuconazole	Pesticides
128	9.40	310.2156	ESI+	[M+H] ⁺	Methadone	Pharmaceutical; Opioid analgesic
129	13.30	312.0662	ESI+	[M+H] ⁺	Prothioconazole-desthio	Pesticides
130	1.03	315.1485	ESI+	[M+H] ⁺	Ranitidine	Pharmaceutical; H ₂ blockers
131	13.81	317.0951	ESI+	[M+H] ⁺	Febuxostat (Uloric)	Pharmaceutical; Xanthine oxidase inhibitors
132	13.79	319.0724	ESI+	[M+H] ⁺	Fenofibric acid	Pharmaceutical; Fibrates
133	11.70	321.1325	ESI+	[M+H] ⁺	Mycophenolic acid	Pharmaceutical; immunosuppressant
134	7.67	325.1693	ESI+	[M+H] ⁺	Citalopram	Pharmaceutical; Antidepressants
135	5.78	325.1908	ESI+	[M+H] ⁺	Quinidine	Pharmaceutical; Antimalarial agents
136	5.73	325.1916	ESI+	[M+H] ⁺	Quinine	Pharmaceutical; Antimalarial agents
137	7.11	326.2319	ESI+	[M+H] ⁺	Bisoprolol	Pharmaceutical; Beta blockers
138	12.64	327.0079	ESI+	[M+H] ⁺	Tris(1-chloro-2-propyl)phosphate	Flame retardants

No.	RT (min)	m/z	Ionization	Type	Compound name	Category/Class
139	7.71	327.1371	ESI+	[M+H] ⁺	Clozapine	Pharmaceutical; Atypical antipsychotics
140	6.92	329.1860	ESI+	[M+H] ⁺	Labetalol	Pharmaceutical; Beta blockers
141	4.30	332.1411	ESI+	[M+H] ⁺	Ciprofloxacin	Pharmaceutical; Antibiotics
142	5.46	337.2113	ESI+	[M+H] ⁺	Acebutolol HCl	Pharmaceutical; Beta blockers
143	7.49	338.1507	ESI+	[M+H] ⁺	Linezolid	Pharmaceutical; Antibiotics
144	17.20	338.3419	ESI+	[M+H] ⁺	Erucamide	Industry; Water-proofing
145	0.91	342.1487	ESI+	[M+H] ⁺	Levosulpiride	Pharmaceutical; Antipsychotic
146	14.25	343.2951	ESI+	[M+H] ⁺	Cocamidoprylbetaine	PCPs
147	12.17	349.1995	ESI+	[M+H] ⁺	Ingenol	Pharmaceutical; Cytotoxic agents
148	11.33	350.1216	ESI+	[M+H] ⁺	Voriconazole	Pharmaceutical; Antifungal triazoles
149	18.08	359.3146	ESI+	[M+H] ⁺	1-Monostearin	Metabolite; Human
150	12.42	362.1145	ESI+	[M+H] ⁺	Bezafibrate	Pharmaceutical; Fibrates
151	3.77	362.1503	ESI+	[M+H] ⁺	Levofloxacin (Levaquin)	Pharmaceutical; Antibiotics
152	9.76	369.2376	ESI+	[M+H] ⁺	Perindopril	Pharmaceutical; ACE inhibitors
153	3.41	370.1795	ESI+	[M+H] ⁺	Amisulpride	Pharmaceutical; Benzamides
154	15.09	383.2028	ESI+	[M+H] ⁺	Corynoxene	Drug R&D
155	11.37	389.1621	ESI+	[M+H] ⁺	Cetirizine	Pharmaceutical; Antihistamines
156	10.52	391.2307	ESI+	[M+H] ⁺	Hexa(methoxymethyl)melamine	Industry; Plastics and resins
157	18.33	391.2846	ESI+	[M+H] ⁺	Di(2-ethylhexyl)phthalate (DEHP)	Phthalates; Plasticizer
158	15.28	399.2515	ESI+	[M+H] ⁺	Tri(butoxyethyl)phosphate	Industry; Plasticizer; Flame retardant
159	6.47	402.1783	ESI+	[M+H] ⁺	Moxifloxacin hydrochloride	Pharmaceutical; Antibiotics
160	12.35	404.1296	ESI+	[M+H] ⁺	Azoxystrobin	Pesticides
161	2.79	407.2217	ESI+	[M+H] ⁺	Lincomycin A	Pharmaceutical; Antibiotics
162	5.75	408.1245	ESI+	[M+H] ⁺	Sitagliptin	Pharmaceutical; DPP-4 inhibitors
163	6.71	414.1542	ESI+	[M+H] ⁺	Noscapine	Pharmaceutical; Antitussive agent
164	11.75	423.1684	ESI+	[M+H] ⁺	Losartan	Pharmaceutical; Angiotensin II receptor antagonists
165	8.99	425.1516	ESI+	[M+H] ⁺	Eprosartan	Pharmaceutical; Angiotensin II receptor antagonists
166	7.45	428.2539	ESI+	[M+H] ⁺	Ranolazine	Pharmaceutical; anti-anginals

No.	RT (min)	m/z	Ionization	Type	Compound name	Category/Class
167	12.41	429.2399	ESI+	[M+H] ⁺	Irbesartan	Pharmaceutical; Angiotensin II receptor antagonists
168	12.94	436.2348	ESI+	[M+H] ⁺	Valsartan	Pharmaceutical; Angiotensin II receptor antagonists
169	11.83	441.1675	ESI+	[M+H] ⁺	Candesartan	Pharmaceutical; Angiotensin II receptor antagonists
170	8.87	447.2131	ESI+	[M+H] ⁺	Olmesartan	Pharmaceutical; Angiotensin II receptor antagonists
171	8.83	455.2901	ESI+	[M+H] ⁺	Verapamil	Pharmaceutical; Calcium channel blocker
172	10.59	472.3174	ESI+	[M+H] ⁺	Terfenadine	Pharmaceutical; Antihistamines
173	6.22	481.2249	ESI+	[M+H] ⁺	Anthothecol	Drug R&D; Antimalarial
174	11.51	482.1749	ESI+	[M+H] ⁺	Rosuvastatin	Pharmaceutical; Statins
175	9.61	502.2936	ESI+	[M+H] ⁺	Fexofenadine HCl	Pharmaceutical; Antihistamines
176	15.82	515.2399	ESI+	[M+H] ⁺	Telmisartan	Pharmaceutical; Antidiabetic
177	11.28	548.2437	ESI+	[M+H] ⁺	Darunavir Ethanolate (Prezista)	Pharmaceutical; Protease inhibitors
178	1.53	85.0296	ESI-	[M-H] ⁻	1,4-Butynediol	Industry; Plastics
179	0.91	89.0246	ESI-	[M-H] ⁻	Glyceraldehyde	Industry; PPCPs
180	0.84	94.9812	ESI-	[M-H] ⁻	Methanesulfonate	Toxicant; Carcinogen
181	1.09	115.0040	ESI-	[M-H] ⁻	Fumarate	Metabolite
182	4.90	118.0415	ESI-	[M-H] ⁻	1H-Benzotriazole	Industry; Corrosion inhibitor
183	4.33	121.0299	ESI-	[M-H] ⁻	2-Hydroxybenzaldehyde	Industry; Research
184	1.19	123.0126	ESI-	[M-H] ⁻	Propane sulfate	Toxicant; Carcinogen
185	0.89	128.0357	ESI-	[M-H] ⁻	Pyroglutamic acid	Amino acids
186	1.83	131.0354	ESI-	[M-H] ⁻	Glutaric acid	Industry
187	7.52	132.0571	ESI-	[M-H] ⁻	5-Methyl-1H-benzotriazole	Toxicant
188	1.27	136.0408	ESI-	[M-H] ⁻	Salicylamide	Pharmaceutical; Analgesics
189	2.88	137.0248	ESI-	[M-H] ⁻	Salicylic acid	Industry; PCPs
190	6.65	138.0199	ESI-	[M-H] ⁻	4-Nitrophenol	Industry; Pharmaceuticals & Pesticides
191	2.29	151.0402	ESI-	[M-H] ⁻	P-Anisic acid	Industry; Antiseptics
192	5.32	151.0403	ESI-	[M-H] ⁻	Vanillin	PCPs
193	10.56	151.0407	ESI-	[M-H] ⁻	2-Hydroxyphenylacetic acid	Research
194	1.84	153.0198	ESI-	[M-H] ⁻	Protocatechuic acid	Metabolite

No.	RT (min)	m/z	Ionization	Type	Compound name	Category/Class
195	5.10	159.0669	ESI-	[M-H]-	Pimelic acid	Industry; Plastics
196	6.94	160.0409	ESI-	[M-H]-	Indole-3-carboxylic acid	Research
197	6.05	161.0246	ESI-	[M-H]-	Umbelliferone	Industry; PCPs
198	6.74	163.0404	ESI-	[M-H]-	3-Hydroxycinnamic acid	Research; Industry
199	5.99	163.0405	ESI-	[M-H]-	trans-4-Coumaric acid	Research; Industry
200	4.39	167.0355	ESI-	[M-H]-	Vanillic acid	Industry; Food flavour
201	4.74	171.0125	ESI-	[M-H]-	P-Toluenesulfonic acid	Industry; Pharmaceuticals & Pesticides
202	7.71	175.0404	ESI-	[M-H]-	4-Methylumbelliferone	Pharmaceutical; Choleric and antispasmodics
203	7.10	177.0564	ESI-	[M-H]-	Coniferyl aldehyde	Metabolite; Antifungals
204	2.95	179.0580	ESI-	[M-H]-	Theophylline	Pharmaceutical; Xanthines
205	2.99	180.0341	ESI-	[M-H]-	Acamprosate	Pharmaceutical; Psychiatry agents
206	5.88	181.0510	ESI-	[M-H]-	Syringaldehyde	Phytochemicals
207	7.34	183.0049	ESI-	[M-H]-	2,4-Dinitrophenol	Industry; Dyes, Preservatives, Pesticides
208	6.98	184.0982	ESI-	[M-H]-	Ecgonine	Metabolite; Industry
209	6.06	186.0674	ESI-	[M-H]-	Metamitron-desamino	Pesticides; TPs
210	9.63	187.0405	ESI-	[M-H]-	1-Hydroxy-2-naphthoic acid	Industry
211	10.23	187.1340	ESI-	[M-H]-	10-Hydroxydecanoic acid	Research; Cytotoxics
212	9.20	191.0355	ESI-	[M-H]-	6,8-dihydroxy-3-methyl-1H-2-benzopyran-1-one	Research
213	7.09	193.0508	ESI-	[M-H]-	trans-4-Hydroxy-3-methoxycinnamate	Metabolite
214	7.64	193.0509	ESI-	[M-H]-	trans-Ferulic acid	Industry
215	6.24	197.0455	ESI-	[M-H]-	2-Hydroxy-3,4-Dimethoxybenzoic Acid	Unknown
216	5.02	197.0461	ESI-	[M-H]-	Syringic acid	Phytochemicals; Drug R&D
217	11.75	199.0172	ESI-	[M-H]-	MCPA	Unknown
218	1.94	203.0833	ESI-	[M-H]-	Tryptophan	Amino acids
219	11.24	205.0873	ESI-	[M-H]-	4-hydroxy-3-(3-methylbut-2-enyl)benzoic acid	Food additives; Parabanes
220	8.26	207.0123	ESI-	[M-H]-	2-Naphthalenesulfonic acid	Industry; Dyes
221	3.56	209.0685	ESI-	[M-H]-	1,3,7-Trimethyluric acid	Metabolite; Human
222	5.89	210.1367	ESI-	[M-H]-	Terbutylazine-2-hydroxy	TPs; Pesticides

No.	RT (min)	m/z	Ionization	Type	Compound name	Category/Class
223	7.15	212.0028	ESI-	[M-H]-	Indoxyl sulfate	Metabolite; Toxins
224	6.46	213.9639	ESI-	[M-H]-	2-Benzothiazolesulfonic acid	Research
225	6.46	220.0287	ESI-	[M-H]-	Chloridazon	Pesticides
226	7.13	221.0460	ESI-	[M-H]-	Isofraxidin	Phytochemicals
227	11.23	221.0825	ESI-	[M-H]-	Monoisobutyl phthalate	Metabolite
228	16.87	227.2021	ESI-	[M-H]-	Myristic acid	Fatty acids
229	11.10	231.0097	ESI-	[M-H]-	Diuron	Herbicides
230	12.68	232.9778	ESI-	[M-H]-	Dichlorprop	Pesticides
231	9.61	239.0495	ESI-	[M-H]-	Bentazone	Industry; Pesticides
232	8.42	241.0739	ESI-	[M-H]-	7,8-dimethylalloxazine (lumichrome)	TPs; riboflavin
233	9.11	251.0829	ESI-	[M-H]-	2-Hydroxycarbamazepine	Metabolite; Anticonvulsant drugs
234	7.48	267.0695	ESI-	[M-H]-	6-Methoxyflavonol	Phytochemicals
235	0.89	271.1125	ESI-	[M-H]-	Sotalol	Pharmaceutical; Beta blockers
236	4.44	273.0343	ESI-	[M-H]-	Phenylbenzimidazolesulfonic acid	PCPs; UV protection
237	12.57	278.1397	ESI-	[M-H]-	Metolachlor OA	TPs; Pesticides
238	17.42	279.2326	ESI-	[M-H]-	Linoleic acid	Fatty acids
239	18.06	281.2493	ESI-	[M-H]-	Oleic acid	Fatty acids
240	13.07	287.1660	ESI-	[M-H]-	Estriol	Steroid; Hormone
241	1.63	295.9577	ESI-	[M-H]-	Hydrochlorothiazide	Pharmaceutical; Diuretics
242	9.93	297.1139	ESI-	[M-H]-	Enterolactone	Metabolite; Plant lignans
243	9.69	300.0910	ESI-	[M-H]-	Dimethachlor ESA	TPs; Pesticides
244	7.35	305.0965	ESI-	[M-H]-	Fluconazole	Pharmaceutical; Antifungal triazoles
245	10.16	307.0288	ESI-	[M-H]-	Benzophenone-4	PCPs; UV protection
246	11.68	319.1190	ESI-	[M-H]-	Mycophenolic acid	Pharmaceutical; Immunosuppressant
247	11.78	319.1552	ESI-	[M-H]-	Zearalenol	Metabolite
248	14.39	319.1916	ESI-	[M-H]-	3-hydroxy-4- (succin-2-yl)-caryolane delta-lactone	Phytochemicals
249	8.85	322.0863	ESI-	[M-H]-	Metazachlor ESA	TPs; Pesticides
250	0.86	323.0286	ESI-	[M-H]-	Uridine 5'-monophosphate	Drug R&D; Foods

No.	RT (min)	m/z	Ionization	Type	Compound name	Category/Class
251	17.36	325.1853	ESI-	[M-H]-	Dodecylbenzenesulfonic acid	Industry; PCPs; Sufactants
252	12.61	328.1231	ESI-	[M-H]-	Metolachlor ESA	TPs; Pesticides
253	9.06	329.0005	ESI-	[M-H]-	Furosemide	Pharmaceutical; Diuretics
254	8.37	338.0919	ESI-	[M-H]-	Topiramate	Pharmaceutical; Anticonvulsants
255	15.49	391.2853	ESI-	[M-H]-	Deoxycholic acid	Metabolite; Human
256	16.90	412.9672	ESI-	[M-H]-	Perfluorooctanoic acid	PFAS
257	12.42	427.2252	ESI-	[M-H]-	Irbesartan	Pharmaceutical; Angiotensin II receptor antagonists
258	6.80	428.0783	ESI-	[M-H]-	SMZ-PtO	TPs; Antibiotics
259	11.76	429.0544	ESI-	[M-H]-	Bicalutamide	Pharmaceutical; Antitumor
260	12.95	434.2193	ESI-	[M-H]-	Valsartan	Pharmaceutical; Angiotensin II receptor antagonists
261	11.83	439.1526	ESI-	[M-H]-	Candesartan	Pharmaceutical; Angiotensin II receptor antagonists
262	8.89	445.1996	ESI-	[M-H]-	Olmesartan	Pharmaceutical; Angiotensin II receptor antagonists
263	8.45	477.1035	ESI-	[M-H]-	Isorhamnetin-3-O-glucoside	Metabolite
264	11.74	513.2291	ESI-	[M-H]-	Telmisartan	Pharmaceutical; Angiotensin II receptor antagonists

Table 4.5. List of identified compounds detected in both sampling campaigns. Compounds confirmed at Level 1 confidence by analyzing a mix of standards of suspected analytes are indicated with green filled cells.

No.	Compound name	Category/Class
1	Amisulpride	Pharmaceutical
2	Atenolol	Pharmaceutical
3	Ciprofloxacin	Pharmaceutical
4	Cotinine	Drug/Alkaloid
5	DEET	Insecticide
6	Diclofenac	Pharmaceutical
7	Eprosartan	Pharmaceutical
8	Furosemide	Pharmaceutical
9	Irbesartan	Pharmaceutical
10	Levamisole	Pharmaceutical
11	Lidocaine	Drug/Anesthetic
12	Mefenamic acid	Pharmaceutical
13	Metformin	Pharmaceutical
14	Methyltestosterone	Hormone
15	Metolachlor	Pesticide/Insecticide
16	Mycophenolic acid	Pharmaceutical
17	Niflumic acid	Pharmaceutical
18	Noscapine	Drug/pharmaceutical
19	Palitantin	Metabolite
20	Perfluorooctanoic acid (PFOA)	PFAS
21	Simazine	Pesticide/Insecticide
22	Telmisartan	Pharmaceutical
23	Terbuthylazine	Pesticide/Insecticide
24	Terbutylazine-2-hydroxy	Pesticide/Insecticide, TP
25	Theobromine	Alkaloid
26	Theophylline	Pharmaceutical
27	Tramadol	Drug/Pharmaceutical
28	Verapamil	Pharmaceutical

References

1. Schymanski, E. L., Singer, H. P., Slobodnik, J., Ipolyi, I. M., Oswald, P., Krauss, M., ... & Hollender, J. (2015). Non-target screening with high-resolution mass spectrometry: critical review using a collaborative trial on water analysis. *Analytical and Bioanalytical Chemistry*, 407(21), 6237-6255.
2. Ruttkies, C., Schymanski, E. L., Wolf, S., Hollender, J., & Neumann, S. (2016). MetFrag relaunched: incorporating strategies beyond in silico fragmentation. *Journal of cheminformatics*, 8(1), 1-16.
3. Schymanski, E. L., Meringer, M., & Brack, W. (2011). Automated strategies to identify compounds on the basis of GC/EI-MS and calculated properties. *Analytical Chemistry*, 83(3), 903-912.
4. Moschet, C., Lew, B. M., Hasenbein, S., Anumol, T., & Young, T. M. (2017). LC-and GC-QTOF-MS as complementary tools for a comprehensive micropollutant analysis in aquatic systems. *Environmental science & technology*, 51(3), 1553-1561.
5. Kind, T., Tsugawa, H., Cajka, T., Ma, Y., Lai, Z., Mehta, S. S., ... & Fiehn, O. (2018). Identification of small molecules using accurate mass MS/MS search. *Mass spectrometry reviews*, 37(4), 513-532.
6. Rostkowski, P., Haglund, P., Aalizadeh, R., Alygizakis, N., Thomaidis, N., Arandes, J. B., ... & Yang, C. (2019). The strength in numbers: comprehensive characterization of house dust using complementary mass spectrometric techniques. *Analytical and bioanalytical chemistry*, 411(10), 1957-1977.
7. Young, T. M., Black, G. P., Wong, L., Bloszies, C. S., Fiehn, O., He, G., ... & Durbin-Johnson, B. (2021). Identifying toxicologically significant compounds in urban wildfire ash using in vitro bioassays and high-resolution mass spectrometry. *Environmental science & technology*, 55(6), 3657-3667.
8. Hug, C., Ulrich, N., Schulze, T., Brack, W., & Krauss, M. (2014). Identification of novel micropollutants in wastewater by a combination of suspect and nontarget screening. *Environmental pollution*, 184, 25-32.
9. Krauss, M., Singer, H., & Hollender, J. (2010). LC-high resolution MS in environmental analysis: from target screening to the identification of unknowns. *Analytical and bioanalytical chemistry*, 397(3), 943-951.
10. Bader, T., et al., *General strategies to increase the repeatability in non-target screening by liquid chromatography-high resolution mass spectrometry*. *Analytica chimica acta*, 2016. 935: p. 173-186.
11. He, P., & Aga, D. S. (2019). Comparison of GC-MS/MS and LC-MS/MS for the analysis of hormones and pesticides in surface waters: advantages and pitfalls. *Analytical Methods*, 11(11), 1436-1448.
12. Oberacher, H., Schubert, B., Libiseller, K., & Schweissgut, A. (2013). Detection and identification of drugs and toxicants in human body fluids by liquid chromatography-tandem mass spectrometry under data-dependent acquisition control and automated database search. *Analytica Chimica Acta*, 770, 121-131.
13. Bichon, E., Guiffard, I., Vénisseau, A., Marchand, P., Antignac, J. P., & Le Bizec, B. (2015). Ultra-trace quantification method for chlordecone in human fluids and tissues. *Journal of Chromatography A*, 1408, 169-177.
14. Kovalova, L., McArdell, C. S., & Hollender, J. (2009). Challenge of high polarity and low concentrations in analysis of cytostatics and metabolites in wastewater by hydrophilic interaction chromatography/tandem mass spectrometry. *Journal of Chromatography A*, 1216(7), 1100-1108.
15. Boudah, S., Olivier, M. F., Aros-Calt, S., Oliveira, L., Fenaille, F., Tabet, J. C., & Junot, C. (2014). Annotation of the human serum metabolome by coupling three liquid chromatography methods to high-resolution mass spectrometry. *Journal of Chromatography B*, 966, 34-47.
16. Beccaria, M., & Cabooter, D. (2020). Current developments in LC-MS for pharmaceutical analysis. *Analyst*, 145(4), 1129-1157.
17. Madrid, Y., & Zayas, Z. P. (2007). Water sampling: Traditional methods and new approaches in water sampling strategy. *TrAC Trends in Analytical Chemistry*, 26(4), 293-299.

18. Smith, C. A., Want, E. J., O'Maille, G., Abagyan, R., & Siuzdak, G. (2006). XCMS: processing mass spectrometry data for metabolite profiling using nonlinear peak alignment, matching, and identification. *Analytical chemistry*, 78(3), 779-787.
19. Tsugawa, H., Cajka, T., Kind, T., Ma, Y., Higgins, B., Ikeda, K., ... & Arita, M. (2015). MS-DIAL: data-independent MS/MS deconvolution for comprehensive metabolome analysis. *Nature methods*, 12(6), 523-526.
20. Olivon, F., Grelier, G., Roussi, F., Litaudon, M., & Touboul, D. (2017). MZmine 2 data-preprocessing to enhance molecular networking reliability. *Analytical chemistry*, 89(15), 7836-7840.
21. Kind, T., & Fiehn, O. (2007). Seven Golden Rules for heuristic filtering of molecular formulas obtained by accurate mass spectrometry. *BMC bioinformatics*, 8(1), 1-20.
22. Jolliffe, I. T., & Cadima, J. (2016). Principal component analysis: a review and recent developments. *Philosophical Transactions of the Royal Society A: Mathematical, Physical and Engineering Sciences*, 374(2065), 20150202.
23. Nannou, C. I., Kosma, C. I., & Albanis, T. A. (2015). Occurrence of pharmaceuticals in surface waters: analytical method development and environmental risk assessment. *International Journal of Environmental Analytical Chemistry*, 95(13), 1242-1262.
24. Hela, D. G., Lambropoulou, D. A., Konstantinou, I. K., & Albanis, T. A. (2005). Environmental monitoring and ecological risk assessment for pesticide contamination and effects in Lake Pamvotis, northwestern Greece. *Environmental Toxicology and Chemistry: An International Journal*, 24(6), 1548-1556.
25. Alygizakis, N. A., Oswald, P., Thomaidis, N. S., Schymanski, E. L., Aalizadeh, R., Schulze, T., ... & Slobodnik, J. (2019). NORMAN digital sample freezing platform: A European virtual platform to exchange liquid chromatography high resolution-mass spectrometry data and screen suspects in "digitally frozen" environmental samples. *TrAC Trends in Analytical Chemistry*, 115, 129-137.
26. Aalizadeh, R., Alygizakis, N. A., Schymanski, E. L., Krauss, M., Schulze, T., Ibanez, M., ... & Thomaidis, N. S. (2021). Development and application of liquid chromatographic retention time indices in HRMS-based suspect and nontarget screening. *Analytical Chemistry*, 93(33), 11601-11611.
27. Adusumilli, R., & Mallick, P. (2017). Data conversion with ProteoWizard msConvert. In *Proteomics* (pp. 339-368). Humana Press, New York, NY.

CHAPTER 5

Robustness Studies By Experimental Design

5. ROBUSTNESS STUDIES BY EXPERIMENTAL DESIGN

5.1 Introduction

In this chapter, the application of experimental design (DOE) techniques for the optimization and robustness study of photolytic and photocatalytic removal of contaminants of emerging concern (CECs) will be described. Three applications will be covered in detail: i) irinotecan photodegradation in the presence of simulated solar irradiation, ii) photocatalytic degradation of maprotiline using Ce doped ZnO, and iii) photocatalytic degradation of maprotiline using Ce and Cu co-doped ZnO. The majority of the work described in this chapter is based on experimental data collected during my secondment research at the University of Ioannina (Ioannina, Greece) and the University of Turin (Turin, Italy).

As reported in Part I of Chapter 3, we investigated the photodegradation of irinotecan in ultrapure and river water during the first year of the PhD program and identified eight transformation products. In fact, irinotecan and one of its TPs were detected in hospital effluents. The robustness of this same photodegradation removal procedure was further investigated by exploiting DOE, as presented in the first part of this chapter.

The processes indicated in (ii) and (iii) above, were principally developed by collaborators at the University of Turin (UniTO) in Italy, as part of the AQUALity project. As a result, the photocatalytic degradation mechanism of maprotiline and the identification of its transformation products will not be explored in this work; however, related material may be found in other publications [1, 2]. Thus, the second part of this chapter will be dedicated to the DOE approaches we used to optimize and investigate the robustness of the processes previously developed by our UniTO collaborators.

5.2 Background of the study

There has been notable research and development in alternative wastewater treatment technologies over the last few decades to address new water treatment challenges such as inefficient CEC abatement in municipal wastewater treatment plants, rising demand for sustainable processes and technologies, and the circular economy [3]. The presence of refractory and persistent CECs, such as pharmaceuticals and personal care products (PPCPs), is likely the most critical challenge, as these substances are harmful to aquatic organisms and human health. As previously stated, the AQUALity project was dedicated to the development of

several techniques of CECs abatement, including advanced oxidation processes (AOPs), membrane filtration systems, and a combination of both. However, full-scale deployment of AOPs in wastewater treatment systems is still challenging due to the complexity of the wastewater matrix and process and technological constraints [3]. In the case of the AQUALITY project, the ultimate goal was to create effective CECs abatement strategies that can potentially be used in actual wastewater treatment plants (WWTPs). To that end, it is critical to establish operating guidelines for a WWTP in terms of the parameters that can influence the efficiency of the abatement of the CECs under consideration. This can be achieved by performing robustness experiments to examine the effect of various parameters on the removal of CECs using the processes under consideration.

Robustness investigations involve the use of design of experiments (DOE) [4-6] to determine the effect of each experimental parameter (e.g., CEC concentration, plant operating conditions, temperature, etc.) on the selected experimental response (e.g., residual CEC concentration, rate of degradation, etc.). Various studies in this field have demonstrated that the efficiency of AOPs in removing organic microcontaminants is dependent on a variety of factors, including the pollutant's properties (e.g., concentration, nature, etc.), the photocatalyst's properties (e.g., amount, size, structure, surface area, doping, etc.), the aqueous solution's properties (e.g., pH, matrix components, etc.), and the reaction conditions (e.g., light intensity, temperature, time, etc.) [7-11]. In this case, the aim of the robustness study was to provide guidelines for operating the WWTP in order to maximize abatement as much as possible and to provide information on which parameters have no influence on the abatement efficiency or, on the contrary, which ones must be closely monitored.

Plackett-Burman designs [12, 13] are the most widely used approach in robustness studies. However, the applications described in this Thesis make use of full or fractional factorial designs, with the addition of star designs [14]. This approach was chosen to allow for parallel optimization and robustness investigation while keeping the number of experiments to a minimum. Indeed, the employment of such experimental designs enables the evaluation of factor interactions and quadratic effects (when the star design is included), both of which were ostensibly relevant in the present applications. The degradation studies must then be expressed in terms of abatement effectiveness: either by measuring the remaining concentration of CEC or by calculating the rate of abatement as C/C_o (where C represents the concentration measured at a given time, and C_o is the initial concentration). To ensure the presence of a significant number of TPs, all experiments in the present applications were characterized for the concentration of the remaining CEC and, in some cases, for the chromatographic signals of certain TPs, at a time greater than the half-time calculated at the center of the experimental domain. Thus, the experimental response was modelled using the

surface response method in the studied experimental domain in order to build a model capable of explaining the effects of the factors involved, their interactions, and, ultimately, their quadratic effects. The generated model can provide the optimal operating conditions for the WWTP and information on the changes that should be made to the various parameters in the event of WWTP-related constraints (e.g., a fixed concentration of CEC, a constraint acting on the power of irradiation or the pH, etc.). The same model can be used to establish the robustness region of a certain WWTP, which provides guidance for process operation.

Here, the procedure was applied mainly to photolysis and photo-catalysis processes on two CECs, maprotiline (an antidepressant) and irinotecan (an anticancer agent). Following a thorough review of the literature, both irinotecan and maprotiline were identified as emerging contaminants worthy of further investigation. Like many other pharmaceuticals, irinotecan [15] and maprotiline [16, 17] have been detected in influent and effluent of WWTPs and surface waters, due to improper disposal and excretion in their unmetabolized forms. Despite their presence and persistence in the environment, significant knowledge gaps exist, such as a lack of information on exposure levels, associated adverse effects, environmental fate, or the lack of sensitive analytical methods for their accurate detection and quantification at ultra-trace levels. As a result, irinotecan has been included to the list of CECs (specifically, the extended list of CECs) that were considered for inclusion in the AQUALity project, along with other anticancer agents. Additionally, maprotiline was selected in accordance with the NORMAN prioritizing scheme outlined in [1].

As detailed in Chapter 3, we identified eight TPs during irinotecan photodegradation using simulated sunlight [18], with the main irinotecan molecule and one of its TPs being detected in a hospital wastewater effluent. Similarly, researchers working on the AQUALity project identified 32 maprotiline TPs using photocatalysis with TiO_2 and Ce-ZnO [1, 2], and 16 of these were detected retrospectively in wastewater effluents. Based on these findings, we concluded that it would be scientifically reasonable to explore the effects of several major factors on the photolytic and photocatalytic abatement of these CECs, as the information provided by this study can potentially be useful in real-world applications of the procedures considered for water and wastewater treatment.

For the robustness studies, we performed three independent applications: (i) the photocatalytic degradation of maprotiline using cerium doped zinc oxide (Ce-ZnO), (ii) the photocatalytic degradation of maprotiline using cerium and copper co-doped zinc oxide (Ce/Cu-ZnO), and (iii) the photolysis of irinotecan using simulated solar irradiation. Due to the similarities in the underlying workflows of these three studies, we present the experimental procedures and results for all three applications combined.

5.3 The irradiation procedures

5.3.1 Photodegradation of irinotecan

Photodegradation experiments were carried out using simulated solar irradiation provided in a Solarbox (Fig. 5.1, a) equipped with a xenon lamp (2500 W) and a UV outdoor filter to better simulate the outdoor sunlight exposure by allowing 290-800 nm wavelength to pass through. The test settings were programmed using microprocessor controllers. During the experiments, the Solarbox monitored and regulated irradiance and black standard temperature (BST). Furthermore, a control system with a UV radiation sensor positioned near the samples compensated for lamp and UV filter ageing.

The steps involved in the photolytic degradation procedure for irinotecan were: i) preparation of irinotecan solution in Milli-Q water at the desired concentration, ii) adjusting the pH to the desired value, iii) taking an aliquot (sample t_0), iv) irradiation under constant magnetic stirring using the programmed intensities v) monitoring the completion of the process with a timer; vi) after irradiation, aliquots were withdrawn at prefixed irradiation periods and immediately preserved in dark vials at $-20\text{ }^{\circ}\text{C}$ until LC-HRMS analysis.

Degradation experiments were performed using 14-mL quartz glass cylindrical cuvettes (Fig. 5.1, b). The pH was fixed using freshly prepared solutions of 0.1 N HCl or 0.1 N NaOH, under pH-meter control. Each experiment was examined for irinotecan concentration and the formation of TPs following 60 minutes of irradiation, a time close to the half-time ($t_{1/2} = 29.38$ min, see Results and Discussion) calculated at the center of the experimental domain.

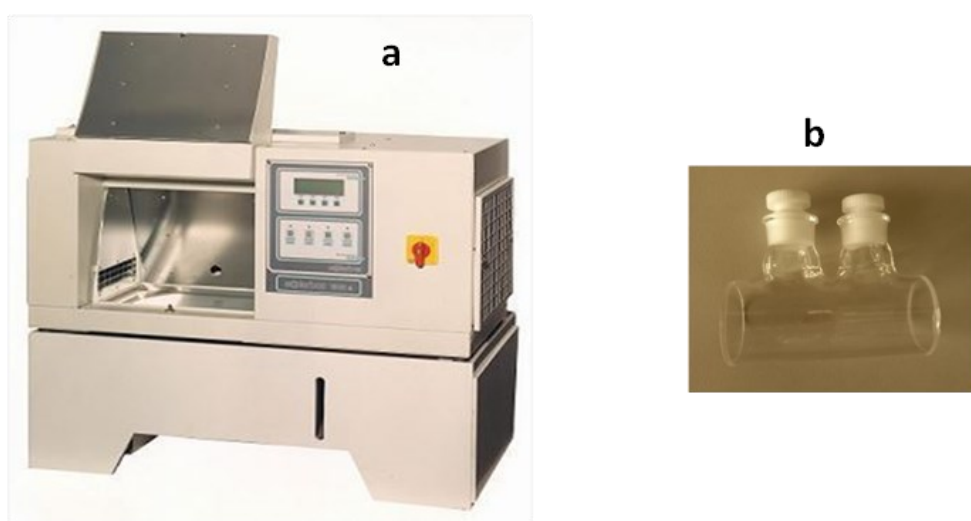


Figure 5.1. Solarbox 3000e (a) and a quartz cuvette (b)

5.3.2 Photocatalytic degradation of maprotiline

Photocatalytic degradation experiments were carried out using a home-made ultraviolet irradiation system (UV-A, Fig. 5.2), which allows for adjustment of parameters, including the distance between the solution and the UV-A lamps and the intensity of the UV irradiation. Six identical UV-A lamps (PHILIPS TL-D 15W, ACTINIC BL) were installed in the system and can be switched on/off independently.

Temperature change within the irradiation system was investigated near the maximum irradiation period considered, with the lowest (30 W) and highest (90 W) UV-A power and the corresponding distances. The maximum temperature recorded after 10 min of irradiation with all the six lamps turned on (i.e., irradiance 90 W/m^2) was $28.5 \pm 0.2 \text{ }^\circ\text{C}$. Thus, the temperature monitor was set to maintain the system below $30 \text{ }^\circ\text{C}$.

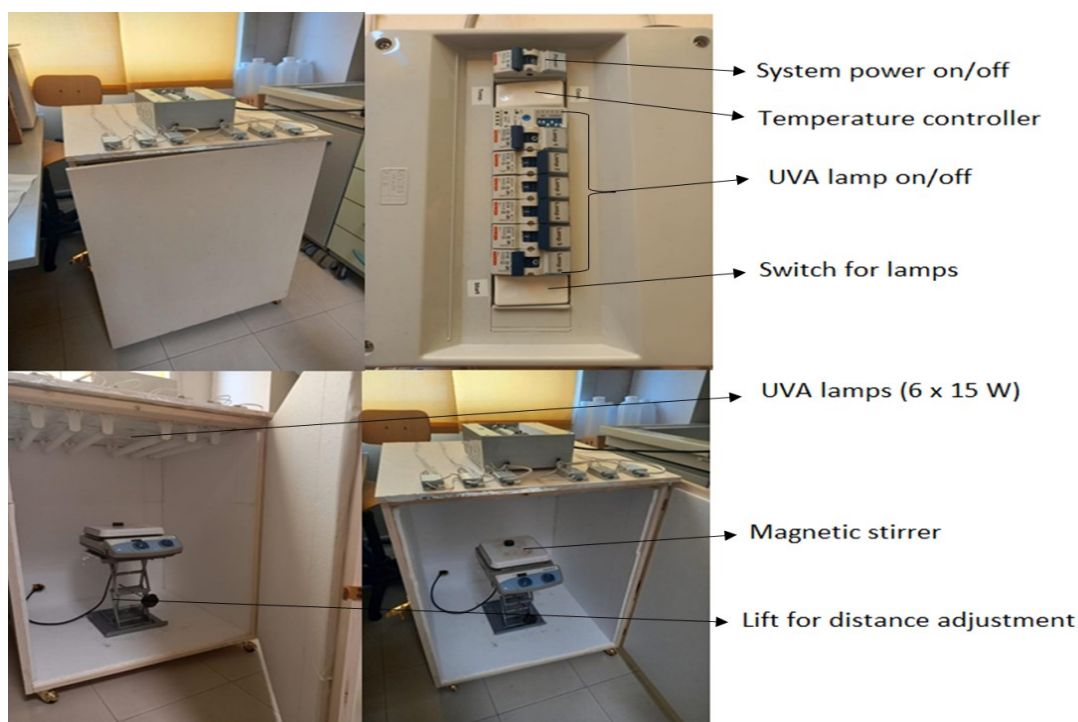


Figure 5.2. The home-made UV-A irradiation system

The steps involved in the photocatalytic degradation procedure for maprotiline were: i) preparation of maprotiline solution in Milli-Q water at the desired concentration; ii) adjusting the pH to the desired value; iii) taking an aliquot (sample t_0), adding the desired amount of catalyst and formation of a suspension via sonication for 15 min; iv) fixing the distance through the adjustable lift; v) UV irradiation under constant magnetic stirring using the desired number of lamps and vi) controlling the completion of the process with a timer; vii) after irradiation, the catalyst was removed using a Whatman $0.45 \mu\text{m}$ PTFE membrane filter.

Aliquots were withdrawn at prefixed irradiation periods and immediately preserved in dark vials at -20 °C until LC-HRMS analysis.

Degradation experiments were performed using 14-mL quartz glass cylindrical cuvettes. The pH was fixed using freshly prepared solutions of 0.1 N HCl or 0.1 N NaOH, under pH-meter control. Each experiment was examined for maprotiline concentration and the formation of TPs following 7.0 minutes (Ce-ZnO) or 4.0 minutes (Ce/Cu-ZnO) of irradiation, a time close to the half-times calculated at the center of the experimental domain.

5.4 LC-HRMS analyses

5.4.1 Irinotecan

The determination of irinotecan and identification of its transformation products was performed using an Ultimate Dionex 3000 UHPLC hyphenated with Orbitrap Fusion Mass Spectrometer (Thermo Fisher, Massachusetts, USA), equipped with an electrospray ionization (ESI) source. The ESI source parameters are given in Table 5.1.

Table 5.1. ESI source parameters for irinotecan analysis.

Parameter	Value
Polarity	Positive
Spray Voltage (V)	4000, static
Sheath Gas (arb)	35
Aux gas (arb)	21
Ion Transfer Tube Temp (°C)	300
Vaporizer Temp (°C)	275

The chromatographic separation was achieved with a reversed-phase Luna C18(2) column (150 mm × 2.0 mm, 3 μm; Phenomenex, Milan, Italy) using a mobile phase mixture of a 0.1% formic acid in water (A) and acetonitrile (B), set at a flow of 0.20 mL/min. The total run time was 48 min, and the gradient program was as follows: 0.0 min 5% B, 30.0 min 50% B, 34.0 min 100% B, 35.0 min 5% B, and 48.0 min 5% B. The column temperature was set at 40 °C.

For each sample, two different acquisition modes have been performed: Full Scan (FS) and Collision-Induced Dissociation (CID MS/MS) scan. The first performed a full scan in the range 100-800 m/z without fragmentation of the precursor ions, and the second one was a top 5 experiment where the 5 most abundant ions were fragmented in the range 100-800 m/z . Full scan analysis was performed at 60,000 mass resolution in positive ion mode with AGC target

of 4.0×10^5 , RF lens of 60% and maximum injection time of 50 ms. Injection volume was 20 μL . The CID MS² experiments were performed at 30,000 mass resolution, isolation window 3.0, AGC target 5.0×10^4 , maximum injection time 54 ms, and collision energy of 20.

Irinotecan was detected at retention time (RT) of 17.6 min with the protonated exact mass value of m/z 587.2868, which was further confirmed by the well-defined isotopic pattern and fragmentation pathways as described in Chapter 3. Fig. 5.3 depicts the extracted ion chromatogram (EIC) of the precursor ion and the embedded graph for the ions in the isotopic pattern.

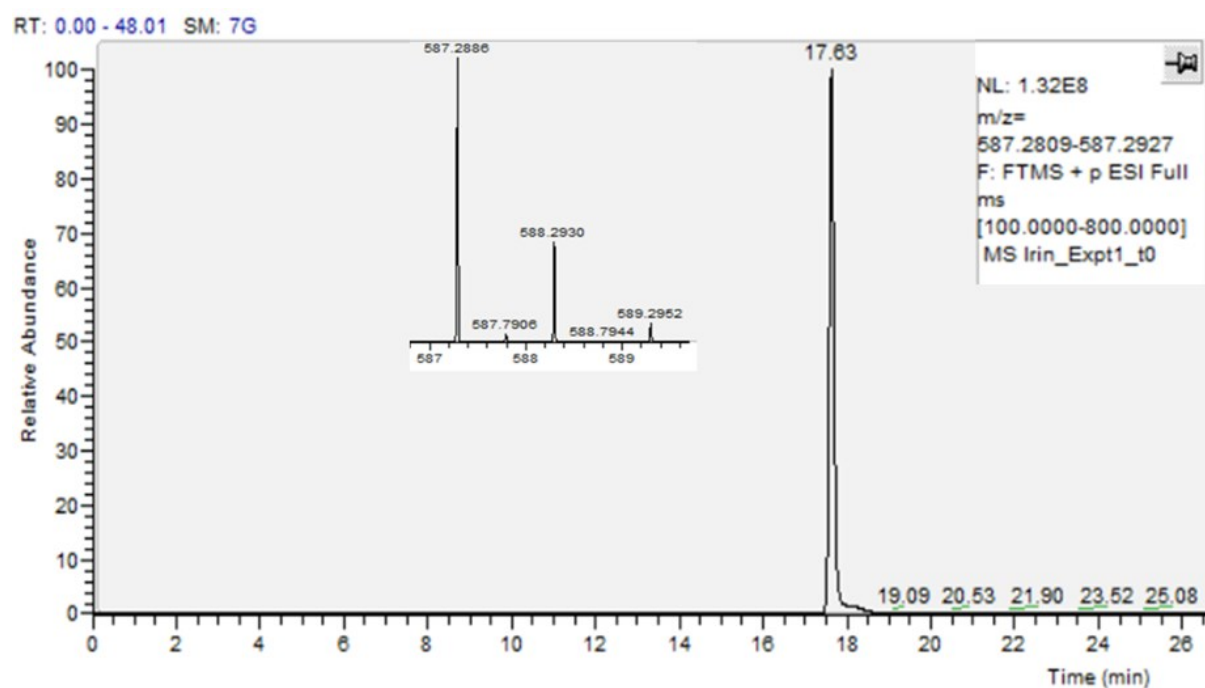


Figure 5.3. EIC of the irinotecan precursor ion (m/z 587.2886) and the isotopic pattern.

5.4.2 Maprotiline

The identification of maprotiline and the transformation products in ultrapure water samples was performed according to the method described in [1] with some modifications, using a Vanquish UHPLC hyphenated with Orbitrap Q-Exactive Plus mass spectrometer (Thermo Fisher, Massachusetts, USA) equipped with an electrospray ionization (ESI) source. The ESI source parameters are presented in Table 5.2.

Table 5.2. ESI source parameters for maprotiline analysis.

Parameter	Value
Polarity	Positive
Sheath gas flow rate (L/min)	35
Auxiliary gas flow rate (L/min)	5
Spray voltage (kV)	3.5
Capillary temperature (°C)	275
S-Lens RF level	50
Auxiliary gas heater temperature (°C)	300

The chromatographic separation was achieved with a reversed phase Aquity UPLC BEH C18 column (150 × 2.1 mm, 1.7 μm; Waters, Milan, Italy) using a simple gradient program of the mobile phase, which consisted of a 0.1% formic acid in water (A) and 0.1% formic acid in acetonitrile (B), set at a flow of 0.26 mL/min. The total run time was 40 min with the gradient program: 0.0 min 5% B, 30.0 min 100% B, 31.0 min 100% B, 31.1 min 5% B, 40.0 min 5% B. The column temperature was fixed at 30 °C.

For each sample, two different acquisition modes have been carried out: Full Scan (FS) and Full Scan data dependent (FSddMS²). The first performed a full scan in the range 50-700 *m/z* without fragmentation of the ions, and the second one was a top 5 experiment where the 5 most abundant ions were fragmented in the range *m/z* 50-700. Full scan analysis was performed at 70,000 mass resolution in positive ion mode with AGC target of 3.0×10⁶ and maximum injection time of 200 ms. Injection volume was 5 μL. Full scan data dependent was performed at 17,500 mass resolution, isolation window 2.0, AGC target 2.0×10⁵, maximum injection time 60 ms, and stepped normalized collision energy (SNCE) of 20, 40, and 80.

Maprotiline was detected at retention time (RT) of 11.3 min with the protonated exact mass value of *m/z* 278.1907, which was further confirmed by the well-defined isotopic pattern and fragmentation pathway as described in [1]. The extracted ion chromatogram (EIC) and mass spectrum are shown in Fig. 6.4 a and b respectively.

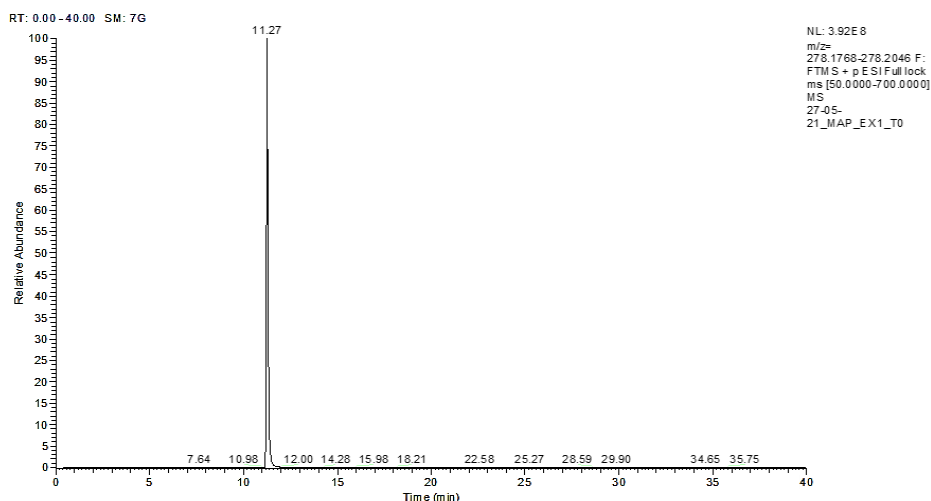


Figure 5.4a: Maprotiline (m/z 278.1907) EIC

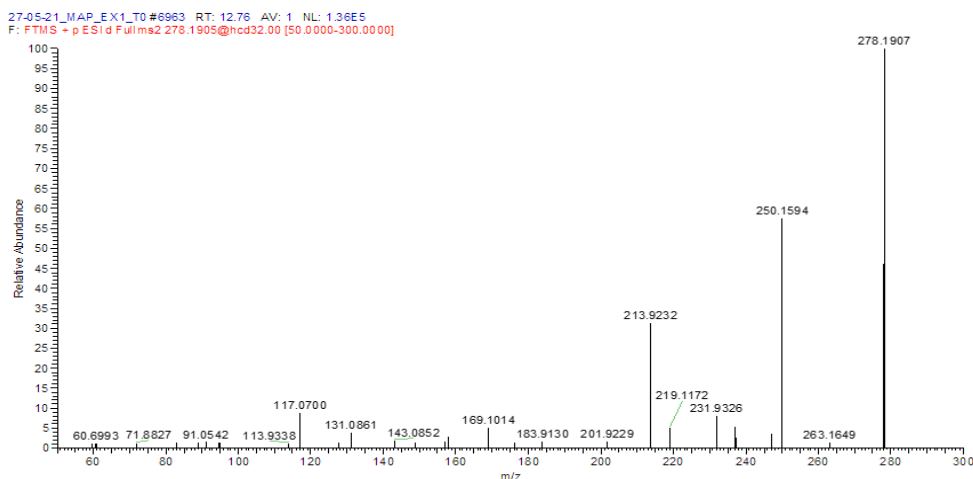


Figure 5.4b: Maprotiline (m/z 278.1907) mass spectrum

5.5 The experimental plans adopted

5.5.1 Photodegradation of irinotecan

The robustness study involved three parameters: the intensity of radiation (W), concentration of irinotecan (IRI), and initial pH of the solution (pH). The levels adopted for each parameter are given in Table 5.3. The values for the center of the domain were chosen partly to provide measurable concentrations in HPLC-MS (e.g., IRI concentration) and partly as common values adopted in water treatment plants (e.g., the pH value is usually quite close to neutrality). Also, the irradiance levels were selected based on values relevant to environmental applications and the average irradiance in sunny days for low, medium, and high latitudes [19-22].

Table 5.3. Levels of each parameter adopted in the robustness study of irinotecan photolysis.

Level	W (W/m ²)	IRI (mg/L)	pH
-1	450	1.0	5.0
0	600	5.0	7.0
1	750	9.0	9.0

The three factors considered were studied by a 2-level full factorial design. A total of 19 experiments were performed (Table 5.4), which included eight experiments of the full factorial design, five replications at the center of the domain and six experiments of the star design. From the LC-MS analysis, the C/C₀ of irinotecan was computed for each experiment.

Table 5.4. DOE experiments performed for irinotecan photolysis.

Nº	W	IRI	pH	C/C ₀	
1	-1	-1	-1	0.65	Full Factorial Design (2 ³)
2	1	-1	-1	0.77	
3	-1	1	-1	0.59	
4	1	1	-1	0.74	
5	-1	-1	1	0.031	
6	1	-1	1	0.026	
7	-1	1	1	0.019	
8	1	1	1	0.033	
9	0	0	0	0.35	Center points
10	0	0	0	0.33	
11	0	0	0	0.29	
12	0	0	0	0.31	
13	-1	0	0	0.23	Star Design
14	1	0	0	0.29	
15	0	-1	0	0.48	
16	0	1	0	0.25	
17	0	0	-1	0.68	
18	0	0	1	0.030	
19	0	0	0	0.30	

5.5.2 Photocatalytic degradation of maprotiline

The robustness experiments involved the study of five parameters: distance of the lamp from the solution (*d*), intensity of the UV radiation (*W*), concentration of the catalyst (*K*), concentration of maprotiline (MAP), and initial pH of the solution (pH), with the levels indicated in Table 5.5a (Ce-ZnO) and Table 5.5b (Ce/Cu-ZnO). It is worth noting that preliminary studies with Ce-ZnO and Ce/Cu-ZnO revealed that the latter was more efficient at degrading maprotiline. In fact, the kinetics of maprotiline elimination was more than twice as fast with the Ce/Cu-ZnO ($t_{1/2} = 2.36$ min). As a result, the catalyst concentrations adopted in the DOEs for Ce-ZnO and Ce/Cu-ZnO were different, as indicated by the column *K*.

Table 5.5a. Levels of each parameter adopted in the robustness study of maprotiline photocatalytic degradation using Ce-ZnO.

Level	<i>d</i> (cm)	<i>W</i> (W)	<i>K</i> (mg/L)	MAP (mg/L)	pH
-1	10	30	100	1.0	5.0
0	30	60	300	5.0	7.0
1	50	90	500	9.0	9.0

Table 5.5b. Levels of each parameter adopted in the robustness study of maprotiline photocatalytic degradation using Ce/Cu-ZnO.

Level	<i>d</i> (cm)	<i>W</i> (W)	<i>K</i> (mg/L)	MAP (mg/L)	pH
-1	10	30	50	1.0	5.0
0	30	60	100	5.0	7.0
1	50	90	150	9.0	9.0

The five factors were studied by a 2-level fractional factorial design. Each DOE had a total of 23 experiments (Table 5.7), which included 8 fractional factorial experiments, 5 center runs, and 10 experiments of the star design. Four replications were initially performed at the center of the domain and the star designs were added ($2p+1 = 11$ experiments, including one more replication of the center; to also investigate the quadratic effects). Finally, some replications of some of the experiments were also performed.

The fourth parameter (MAP) was confounded with the interaction between factors 2 and 3 (i.e., $X_4 = X_2 * X_3$), and the fifth factor (pH) was confused with the interaction between factors 1 and 2 (i.e., $X_5 = X_1 * X_2$). It is clear that we cannot get an independent estimate of the interaction effect

for $X_1 * X_2$ from an estimate of the main effect for X_5 . The same is true for the interaction effect $X_2 * X_3$ and the main effect X_4 . This is one of the costs of using the $X_1 * X_2$ in fractional factorial designs to get the column X_5 . The confusion structure is even more complex since the two generated confusions gave birth to a confusion structure that will be represented hereafter. The two confusions generated for the maprotiline DOE can be indicated as: $X_5 = X_1 X_2$ (or 5=12), and $X_4 = X_2 X_3$ (or 4=23). It is worth noting that in the short representations, '12' refers to the type of column multiplication we are using to build the factorial design, and any column multiplied by itself yields the identity column of all 1's. The design generators are: $I=125$ (primary generator), $I=234$ (primary generator), and $I=125 \times 234 = 1345$ (secondary generator). As a result, the confounding structure is shown in Table 5.6a (blue cells indicate the potentially relevant confounded effects), while the more important confusions are shown in Table 5.6b.

Table 5.6a. The complete confounding structure.

	1	2	3	12	23	13	123
125	25	15	1235	5	135	235	35
234	1234	34	24	134	4	124	14
1345	345	12345	145	2345	1245	45	245

Table 5.6b. The confounding structure for principal factors and two-way interactions. Factors in red are main factors, whereas those in green are potentially nonsignificant.

Factors of the factorial design	Factors confused
d	W*pH
W	d*pH + K*MAP
K	W*MAP
d*W	pH
d*K	MAP*pH
W*K	MAP
d*W*K	K*pH + d*MAP

From the confusion structure it is possible to highlight that some principal factors are confused with two-way interactions. However, these confusions can be considered as solved since the overall design also included a star design, from which it is possible to evaluate independently the role played by principal factors and their quadratic effects: in this way, the effect played by the principal factors is known and can be subtracted from the confusion.

Table 5.7. DOE experiments performed for maprotiline photocatalysis.

DOE 1: Maprotiline with Ce-ZnO								DOE 2: Maprotiline with Ce/Cu-ZnO						
N°	d	W	K	MAP	pH	C/C ₀		N°	D	W	K	MAP	pH	C/C ₀
1	-1	-1	-1	1	1	0.92	Fractional factorial design	1	-1	-1	-1	1	1	0.60
2	1	-1	-1	1	-1	0.82		2	1	-1	-1	1	-1	0.50
3	-1	1	-1	-1	-1	0.28		3	-1	1	-1	-1	-1	0.43
4	1	1	-1	-1	1	0.24		4	1	1	-1	-1	1	0.036
5	-1	-1	1	-1	1	0.45		5	-1	-1	1	-1	1	0.12
6	1	-1	1	-1	-1	0.51		6	1	-1	1	-1	-1	0.095
7	1	-1	1	-1	-1	0.45		7	-1	1	1	1	-1	0.25
8	-1	1	1	1	-1	0.56		8	1	1	1	1	1	0.50
9	1	1	1	1	1	0.68		9	0	0	0	0	0	0.40
10	1	1	1	1	1	0.70		10	0	0	0	0	0	0.32
11	0	0	0	0	0	0.67	Center runs	11	0	0	0	0	0	0.39
12	0	0	0	0	0	0.63		12	0	0	0	0	0	0.36
13	0	0	0	0	0	0.57		13	0	0	0	0	0	0.35
14	0	0	0	0	0	0.70		14	-1	0	0	0	0	0.29
15	0	0	0	0	0	0.65	Star design	15	1	0	0	0	0	0.34
16	-1	0	0	0	0	0.52		16	0	-1	0	0	0	0.37
17	1	0	0	0	0	0.60		17	0	1	0	0	0	0.32
18	0	-1	0	0	0	0.85		18	0	0	-1	0	0	0.42
19	0	1	0	0	0	0.67		19	0	0	1	0	0	0.32
20	0	0	-1	0	0	0.56		20	0	0	0	-1	0	0.14
21	0	0	1	0	0	0.59		21	0	0	0	1	0	0.55
22	0	0	1	0	0	0.50		22	0	0	0	0	-1	0.44
23	0	0	0	-1	0	0.23		23	0	0	0	0	1	0.28

5.6 Results and Discussion

5.6.1 Irinotecan

5.6.1.1 Kinetic study

To understand the behavior of irinotecan photodegradation, a preliminary kinetic study was conducted at the center of the experimental domain. This allowed the determination of the half-time disappearance of irinotecan in standard conditions. The irradiation periods considered were 0, 2, 4, 6, 8, 10, 15, 30, 60, 120 min. Fig. 5.5 depicts the photodegradation of irinotecan with an embedded graph showing the degradation rate. The degradation kinetics followed a pseudo-first order decay fitting the line given by Eq. (5.1), where C_0 represents the maprotiline initial concentration, C is the concentration at reaction time t , and k is the pseudo-first-order kinetic constant.

$$\ln(C) = -kt + \ln(C_0) \quad \text{Eq. (5.1)}$$

The R^2 was equal to 0.9817 and the calculated half-time ($t_{1/2}$) was 29.28 min with a kinetic rate constant of 0.02411 min^{-1} . Furthermore, most TPs had maximal abundance in the region between 30 and 60 min of irradiation. As a result, the irradiation time for all DOE studies was set to 60 minutes to ensure both a time higher than the half-life under standard conditions and the presence of considerable amounts of the TPs. This allows for the investigation of the degradation process not only in terms of irinotecan disappearance rate, but also the production of certain TPs.

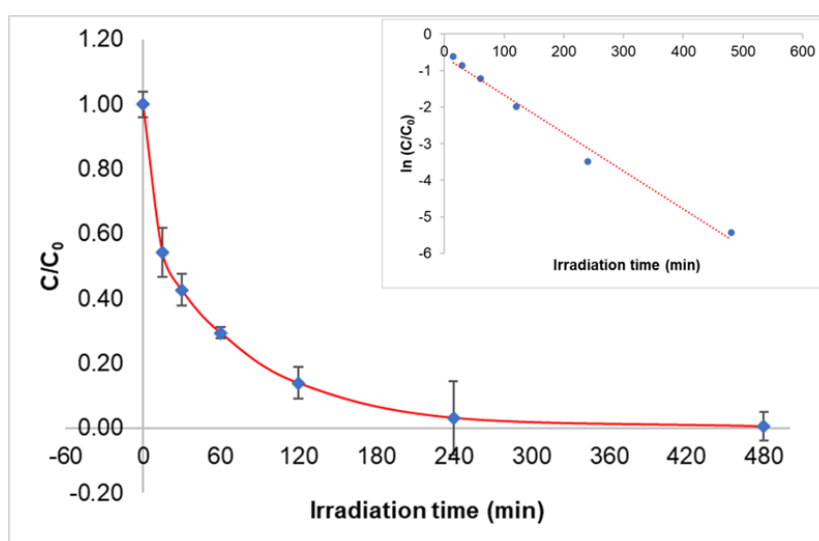


Figure 5.5. Photodegradation of irinotecan and the kinetics

5.6.1.2 Modelling the response C/C_0

Each experiment of the DOE was carried out and aliquots of the sample were taken both at time $t_0 = 0$ min and $t_1 = 60$ min, which were then analysed by LC-HRMS. For each experiment, the experimental response C/C_0 value was calculated from the concentration of irinotecan at t_0 and t_1 . After that, C/C_0 was modelled with respect to the three factors considered in this study. The initial model, shown by the Pareto chart in Fig. 5.6, contained all the principal factors, their interactions, and the quadratic effects. However, the main effect from pH was the most dominant and the only statistically significant ($\alpha = 0.05$).

The response was further modelled by sequentially eliminating the least significant effects (particularly, the interaction effects) and the final model contained only the three main effects (Fig. 5.7). In fact, the main effects from irinotecan concentration and irradiation intensity were a little less than the 5% significance level. The parameters considered significant and included in the final model are summarized in Table 5.8, along with their coefficients and p-values. In the final model, pH showed a high level of significance, while the concentration of irinotecan and the solar radiation intensity were included with a significance level of about 10%. The calculated model resulted in a very good R^2 value of 0.9596. The relevant ANOVA results are shown in Table 5.9, and the corresponding Pareto chart is shown in Fig. 5.7.

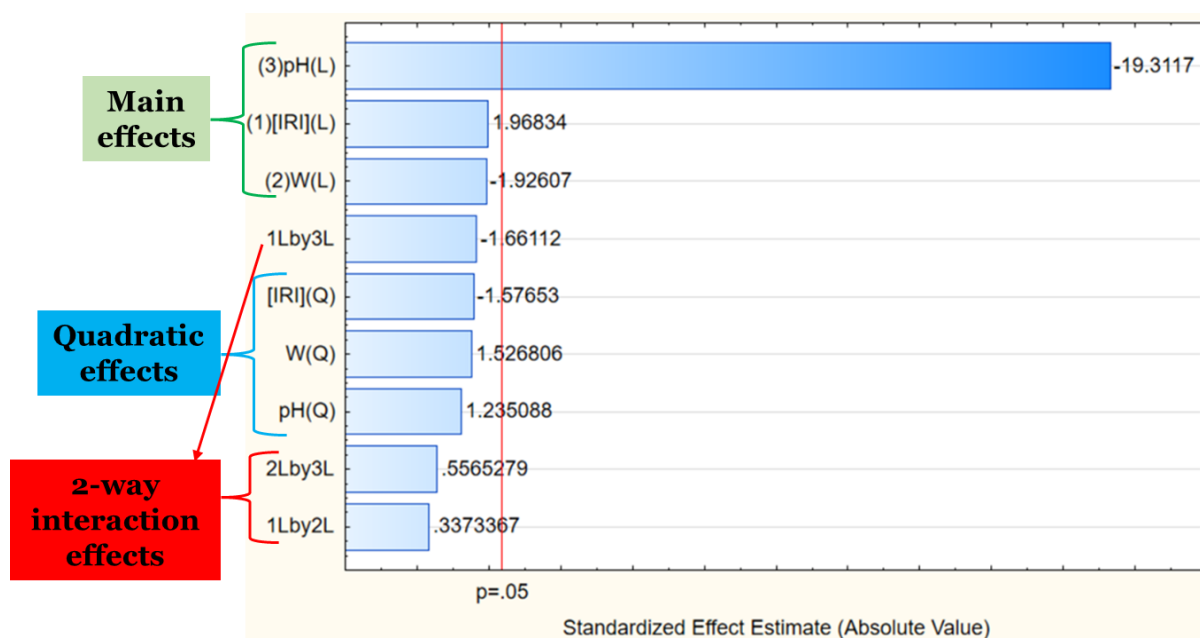


Figure 5.6. Pareto chart showing the parameters included in the initial model.

Table 5.8. Parameters included in the final model: *t*-Student calculated, *p*-level, coefficient, and the corresponding standard error of the coefficient.

	t-calc	p-level	Coeff.	Std. Err. Coeff.
Intercept	23.47	0.0000	0.341	0.015
IRI	1.77	0.0997	0.034	0.019
W	-1.73	0.1064	-0.033	0.019
pH	-17.39	0.0000	-0.330	0.019

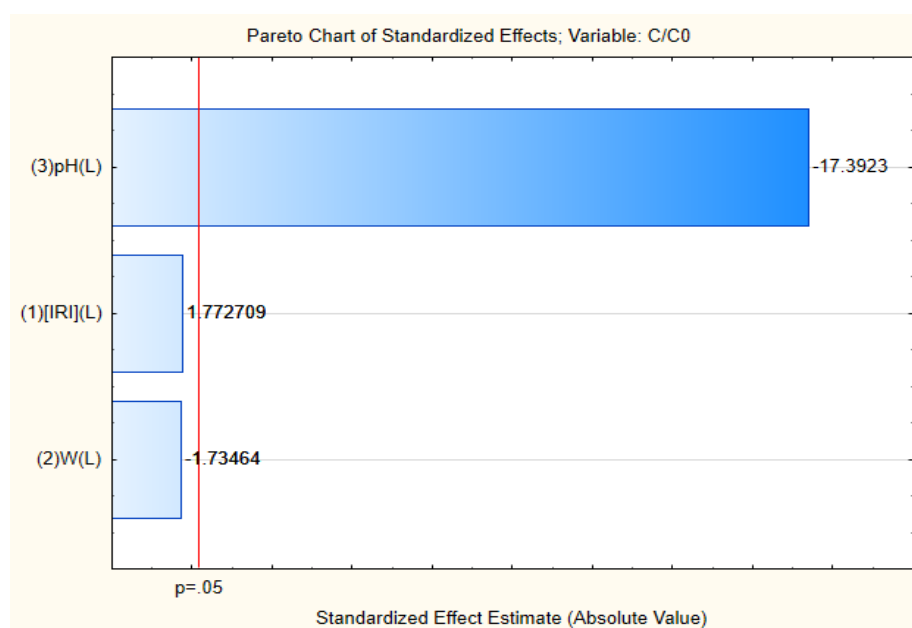


Figure 5.7. Pareto chart reporting the parameters included in the final model

Table 5.9. ANOVA results of the main parameters included in the final model.

	SS	df	MS	F	p
IRI	0.0113	1	0.0113	3.14	0.0997
W	0.0108	1	0.0108	3.01	0.1064
pH	1.0880	1	1.0880	302.49	0.0000
Error	0.0468	13	0.0036		
Total SS	1.1569	16			

As shown in Fig. 5.8, the model demonstrated a very good consistency between experimental and predicted responses, and the representation of the residuals indicates no notable pattern.

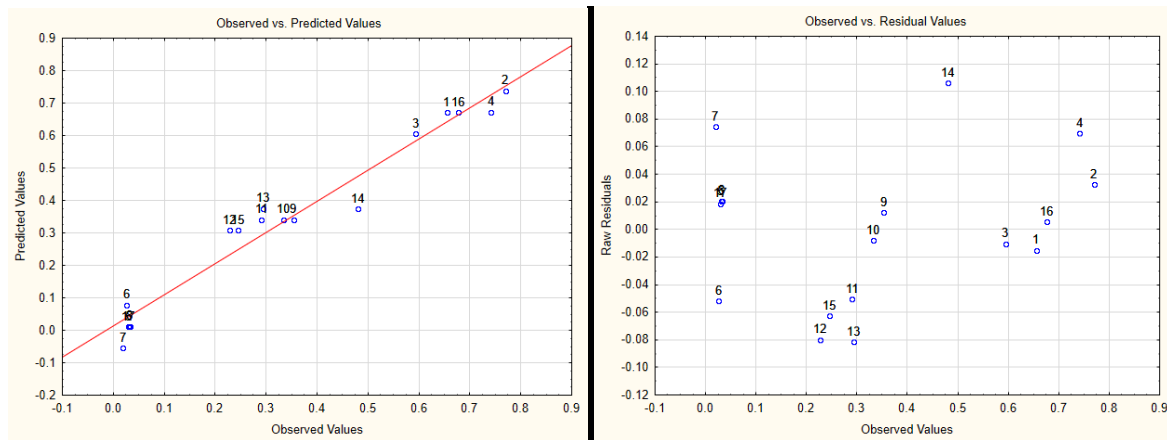


Figure 5.8. Predicted vs experimental (left); residuals vs experimental response (right).

The final regression model is given by Eq. (5.2) as follows:

$$C/C_0 = 0.341 + 0.034*[IRI] - 0.033*W - 0.33*pH \quad \text{Eq. (5.2)}$$

The model contains only the principal parameters, therefore response surfaces are not needed to identify the best conditions, however, for a clearer discussion, they are presented in Fig. 5.9 for the interaction between irinotecan and pH, separately for three different levels of W.

The surfaces show a huge effect of pH. Increasing the pH leads to better results regardless of irinotecan concentration or irradiation intensity values, even if slightly better results are achieved when [IRI] is low and W is high. The effectiveness of degradation appears quite robust with respect to radiation intensity and the concentration of irinotecan since variations of these two parameters in the experimental domain investigated are hardly significant. For what regards pH, instead, the process appears not very robust. In most situations, wastewaters have a pH value between 6.5 to 8.0 [23], which is also the optimal range for the majority of aquatic organisms, and many public and industrial treatment plants tend to operate as near to pH values around 7 (the center of the experimental domain) as possible. In these conditions C/C_0 reaches values between 0.30 and 0.35 if the pH is maintained between 7.2 and 7.5. When pH increases, best degradation rates are obtained (between 0 and 0.15); nevertheless, in these conditions, to have a good robustness of the final degradation, pH should be strictly controlled.

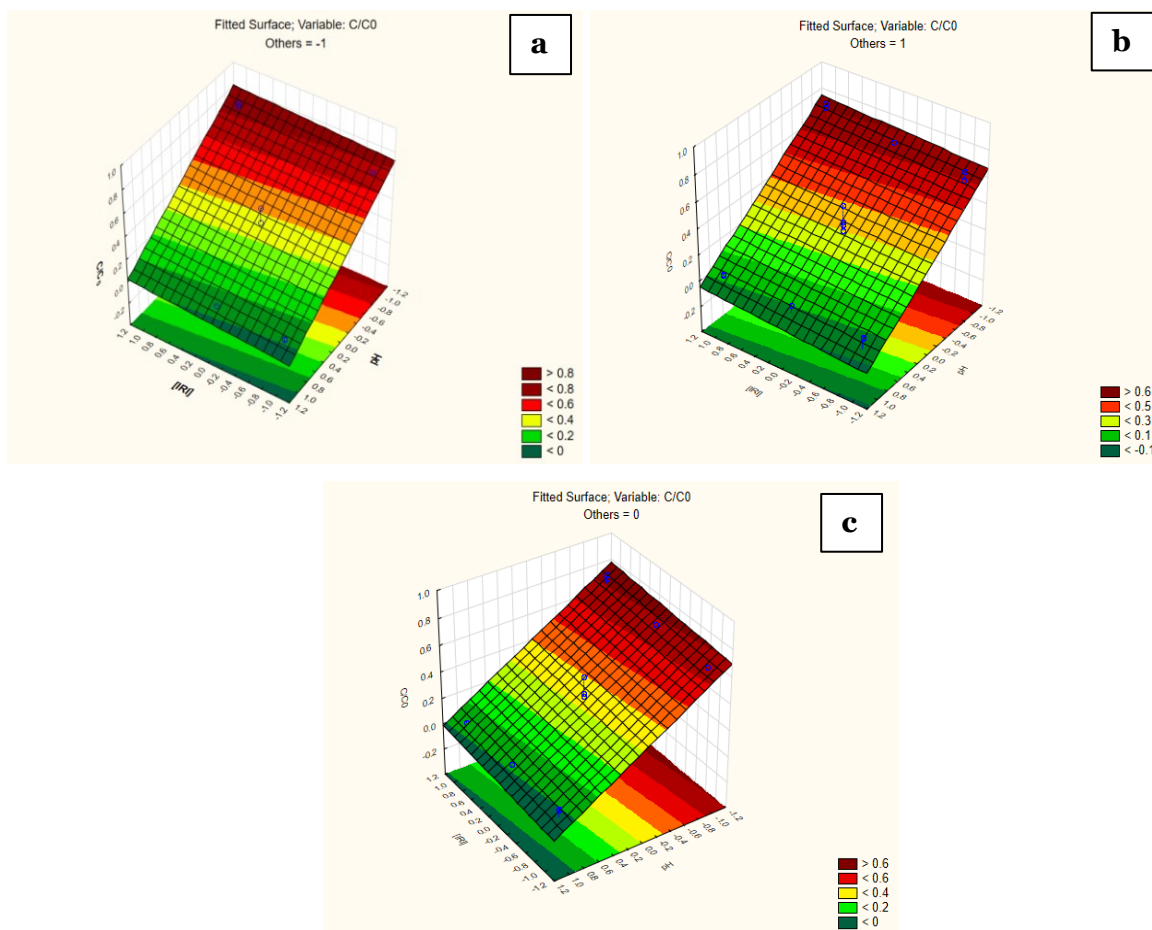


Figure 5.9. Response surfaces for the interaction between pH and IRI concentration when radiation intensity W is at (a) low (-1) level, (b) high (+1) level, and (c) center (0) level.

Changing the W value corresponds to carrying out solar degradation under different environmental conditions (i.e., sunny days for low, medium, or high latitudes): these conditions cannot be fixed but are experienced during the experimentation. Fortunately, the model shows that the W value does not play a very significant role and the photolysis can be considered quite robust with respect to both the concentration of Irinotecan and the W value. The same cannot be concluded for the pH value that should be controlled to guarantee a robust degradation procedure, above all if the pH values shift towards more acidic values. Finally, the best conditions for the overall process were obtained (Table 5.10) and experiments performed at these conditions resulted in the removal of greater than 98% of irinotecan in 60 minutes of solar irradiation.

Table 5.10. Best conditions obtained for the photodegradation of irinotecan.

Conditions	W	IRI	pH	Y pred	Y exp
Global optimum	1	-1	1	< 0	0.0194

5.6.2 Maprotiline

5.6.2.1 Kinetic studies

Preliminary kinetic studies were initially carried out at the center of the experimental domain (separately for Ce-ZnO and Ce/Cu-ZnO), to understand the nature of the degradation processes and identify the half-times of maprotiline disappearance in standard conditions. The irradiation periods considered were 0, 1, 2, 4, 6, 8, 10, 15, 30, and 60 min. In both cases, the degradation kinetics followed a pseudo-first order decay fitting the line given by Eq. (5.1). The kinetics of degradation are depicted in Fig. 5.10 and the estimated kinetic parameters are shown in Table 5.11.

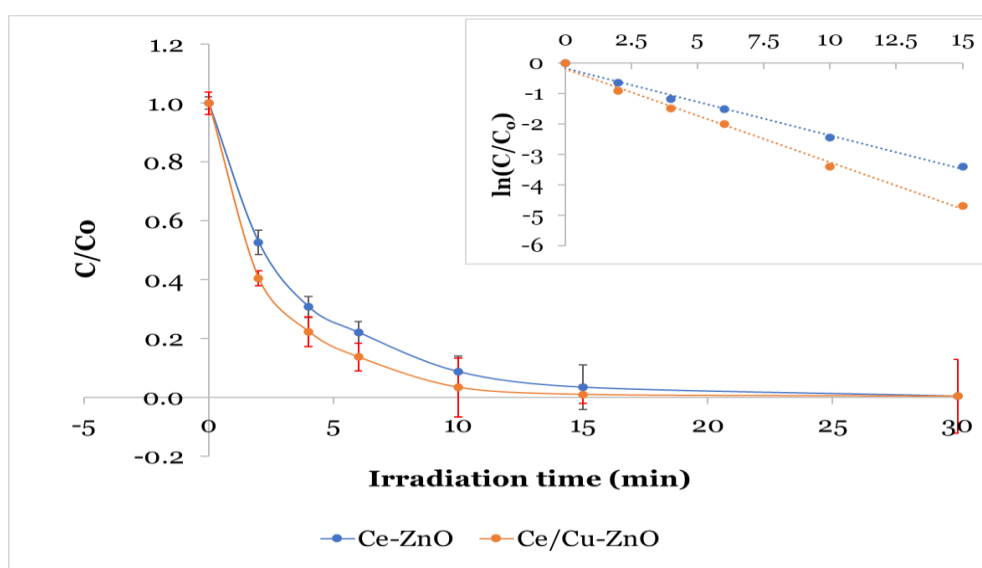


Figure 5.10. Photocatalytic degradation of maprotiline using Ce-ZnO and Ce/Cu-ZnO

The estimated maprotiline degradation half-times were 5.13 and 2.36 min respectively for Ce-ZnO and Ce/Cu-ZnO. For all the experiments of the DOEs, samples were taken after 7.0 minutes (for Ce-ZnO) and 4.0 minutes (for Ce/Cu-ZnO) of irradiation to ensure both a time higher than the half-time in standard conditions and the possible presence of significant amounts of the TPs.

Table 5.11. Kinetic parameters estimated for maprotiline degradation

Photocatalyst	R ²	Half-time (min)	k (min ⁻¹)
Ce-ZnO	0.9955	5.13	0.1348
Ce/Cu-ZnO	0.9869	2.36	0.2936

5.6.2.2 Modelling the response C/C₀

Each experiment of the maprotiline DOEs for Ce-ZnO and Ce/Cu-ZnO was carried out in the same manner as the irinotecan DOE, and an aliquot of the sample was taken both at time t₀ (0 min) and time t₁ (7.0 min for Ce-ZnO and 4.0 min for Ce/Cu-ZnO). The C/C₀ value was determined for each experiment and used as the experimental response.

Because the principal factors were evaluated through the star designs, it is possible to separate the contribution of the principal factors from that of the two-way interactions. The C/C₀ values were modelled in relation to the parameters considered in the study. The initial models included all of the principal factors, their interactions, and the quadratic effects (Fig. 5.11).

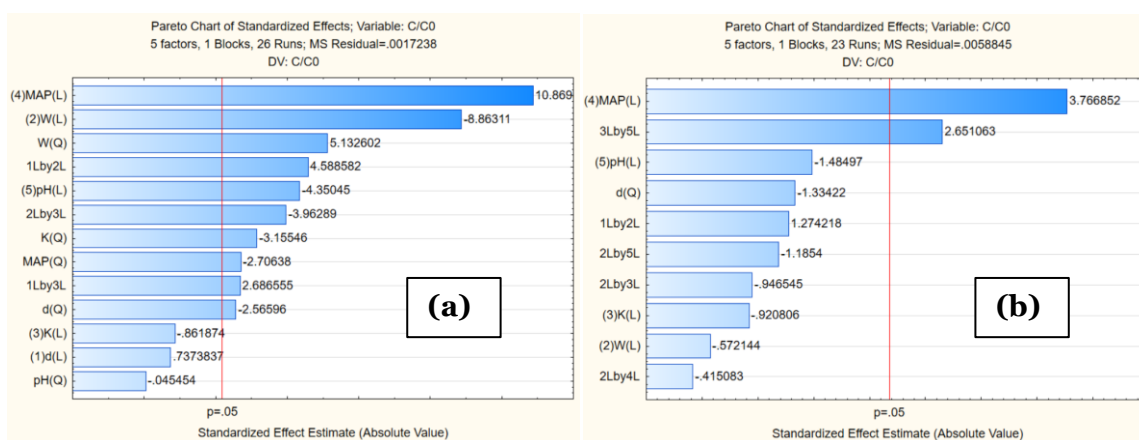


Figure 5.11. Pareto chart of the initial model for Ce-ZnO (a) and Ce/Cu-ZnO (b).

Then, the data were sequentially modelled by eliminating the non-significant terms and the parameters considered significant and included in the final model are displayed in the Pareto charts in Fig. 5.12 and the statistical values in Table 5.12 and Table 5.13, together with their coefficients and related p-values. All of the parameters included have a p-value below 0.05.

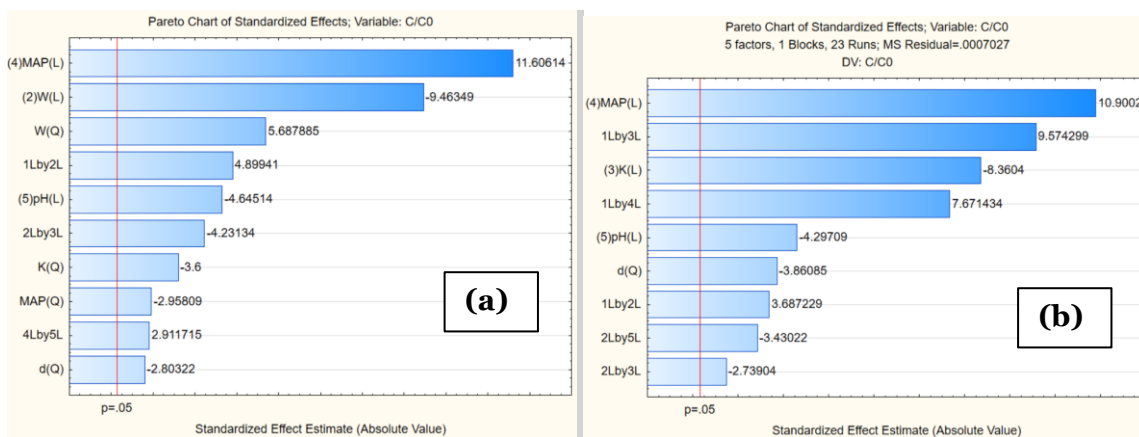


Figure 5.12. Pareto chart of the final model using Ce-ZnO (a) and Ce/Cu-ZnO (b).

Table 5.12. The parameters included in the models and the values for the t-Student calculated (t-calc), the p-level, the coefficients (Coeff.) and the standard error of coefficient (SEC).

Model 1: Maprotiline using Ce-ZnO					Model 2: Maprotiline using Ce/Cu-ZnO				
Param	t-calc	p	Coeff.	SEC	Param	t-calc	p	Coeff.	SEC
Intercept	55.35	0.0000	0.631	0.011	Intercept	48.79	0.0000	0.359	0.007
d²	-2.80	0.0134	-0.067	0.024	d²	-3.86	0.0020	-0.043	0.011
W	-9.46	0.0000	-0.109	0.012	K	-8.36	0.0000	-0.070	0.008
W²	5.69	0.0000	0.136	0.024	MAP	10.90	0.0000	0.204	0.019
K²	-3.60	0.0026	-0.076	0.021	pH	-4.30	0.0009	-0.081	0.019
MAP	11.61	0.0000	0.319	0.027	d*W	3.69	0.0027	0.077	0.021
MAP²	-2.96	0.0098	-0.070	0.024	d*K	9.57	0.0000	0.089	0.009
pH	-4.65	0.0003	-0.128	0.027	d*MAP	7.67	0.0000	0.072	0.009
d*W	4.90	0.0002	0.148	0.030	W*K	-2.74	0.0169	-0.057	0.021
W*K	-4.23	0.0007	-0.128	0.030	W*pH	-3.43	0.0045	-0.032	0.009
MAP*pH	2.91	0.0107	0.037	0.013					

Table 5.13. ANOVA table for maprotiline photocatalysis with Ce-ZnO and Ce/Cu-ZnO.

ANOVA 1: MAP with Ce-ZnO						ANOVA 2: MAP with Ce/Cu-ZnO					
Param	SS	df	MS	F	p	Param	SS	df	MS	F	p
d²	0.0119	1	0.0119	7.86	0.0134	d²	0.0105	1	0.0105	14.91	0.0020
W	0.1354	1	0.1354	89.56	0.0000	K	0.0491	1	0.0491	69.90	0.0000
W²	0.0489	1	0.0489	32.35	0.0000	MAP	0.0835	1	0.0835	118.81	0.0000
K²	0.0196	1	0.0196	12.96	0.0026	pH	0.0130	1	0.0130	18.46	0.0009
MAP	0.2037	1	0.2037	134.70	0.0000	d*W	0.0096	1	0.0096	13.60	0.0027
MAP²	0.0132	1	0.0132	8.75	0.0098	d*K	0.0644	1	0.0644	91.67	0.0000
pH	0.0326	1	0.0326	21.58	0.0003	d*MAP	0.0414	1	0.0414	58.85	0.0000
d*W	0.0363	1	0.0363	24.00	0.0002	W*K	0.0053	1	0.0053	7.50	0.0169
W*K	0.0271	1	0.0271	17.90	0.0007	W*pH	0.0083	1	0.0083	11.77	0.0045
MAP*pH	0.0128	1	0.0128	8.48	0.0107	Error	0.0091	13	0.0007		
Error	0.0227	15	0.0015			Total SS	0.4520	22			
Total SS	0.7964	25									

The calculated models resulted in very good R^2 values, equal to 0.9715 for Ce-ZnO and 0.9798 for Ce/Cu-ZnO. Additionally, the models demonstrated excellent consistency between experimental and predicted responses, and the residuals displayed no apparent trend (Fig. 5.13 and Fig. 5.14).

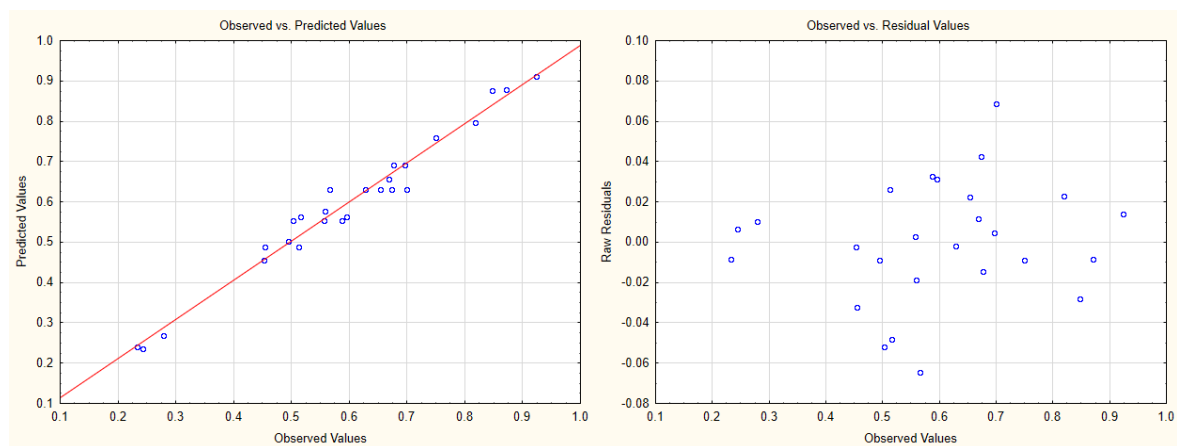


Figure 5.13. Model for MAP photocatalysis using Ce-ZnO: predicted vs experimental response (left) and residuals vs experimental response (right).

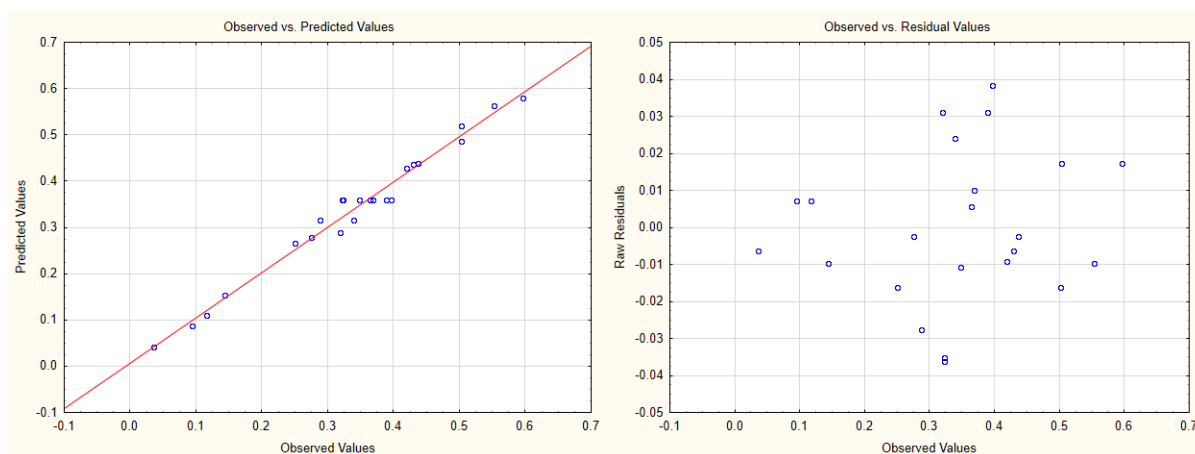


Figure 5.14. Model for MAP photocatalysis using Ce/Cu-ZnO: predicted vs experimental response (left) and residuals vs experimental response (right).

5.6.2.3 Response surface Methodology (RSM)

The response surface methodology (RSM) approach was applied to analyze the effect of the independent parameters, optimize process parameters, and determine optimal conditions for the maprotiline removal procedures.

RSM study of the MAP photocatalysis using Ce-ZnO

Fig. 5.15 depicts the response surface for the interaction of pH and MAP when the other parameters are set to -1, 0 or 1. The best results are obtained when the pH is high and the maprotiline concentration is low. When the pH is high or low, an increase in maprotiline concentration slows the degradation rate, and the effect is amplified when the pH is high. When maprotiline is low, all pH values provide a favorable degradation rate; however, when maprotiline is high, the degradation rate is always poor. When all the other factors are at their low, high, or central values, the surface is identical, but increasing the level of the other parameters in general affects the degradation rate, especially when maprotiline is low.

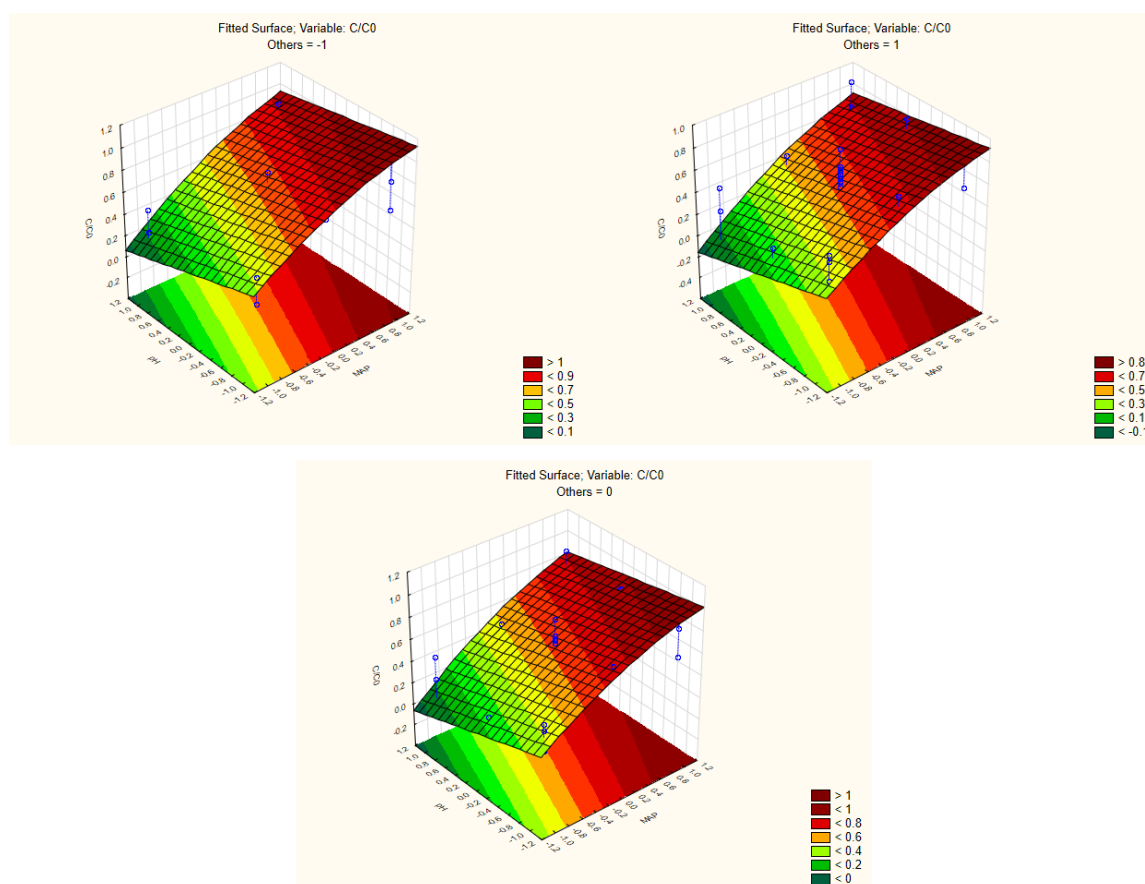


Figure 5.15. Response surfaces for the interaction between pH (x-axes) and MAP (z-axes) when all other parameters are at level -1 (top left), 1 (top right) and 0 (bottom).

In terms of the interaction between catalyst (K) and UV intensity (W), as shown in Fig. 5.16, the poorest results are produced when W is low and K is high, and all other parameters are low or medium. When all of the other parameters are set to their maximum levels, the worst results are produced when W is high and K is low, and when K is high and W is low. At low W values, maprotiline degradation is low for nearly all K values (degradation occurs a little more efficiently when K is low). When W is high, degradation is more efficient with almost all K values, but especially when K is high. This is particularly true when all the other parameters are set to a low or medium level. When all other parameters are low or medium, increasing W improves degradation at all K levels, although this impact is more pronounced when K is high. On the other hand, when all other parameters are set to high levels, increasing W improves degradation when K is high, but worsens degradation when K is low.

In general, the best results are obtained when W and K are both at the high level, and the other parameters are all low or medium. When all other parameters are high, the optimal conditions correspond to medium or low W values and low K values, although good results can also be obtained when W is medium to high, and the catalyst is high.

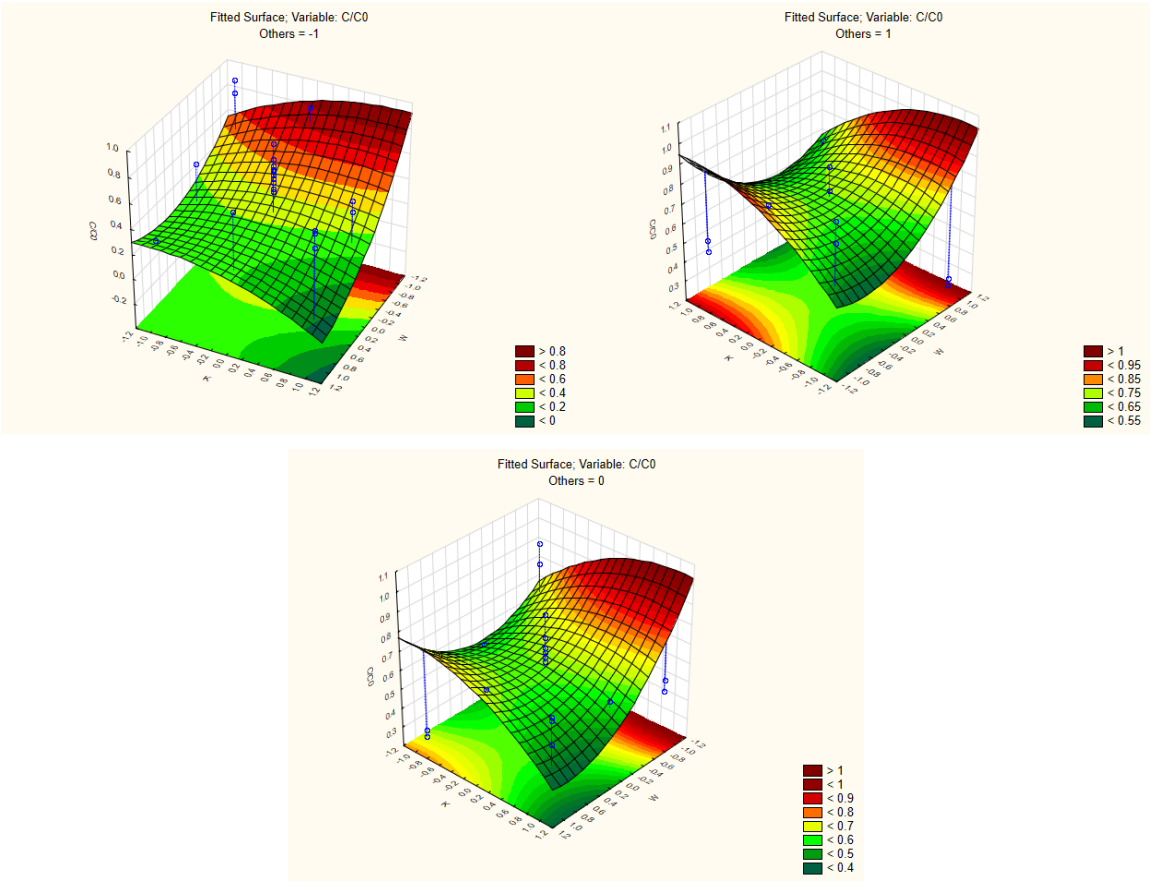


Figure 5.16. Response surfaces for the interaction between K (x-axes) and W (z-axes) when all other parameters are at level -1 (top left), 1 (top right) and 0 (bottom).

For what concerns the interaction between distance (d) and UV-A power (W), as illustrated in Fig. 5.17, the worst conditions are obtained when both d and W are small, regardless of the value of the other parameters. When the other parameters are set to a low value, however, high values of both d and W provide an undesirable effect. When d is high, increasing W worsens the degradation when the other factors are low, while it slightly improves when the other factors are high; and when the other factors are medium, the best results are obtained with intermediate W values. When d is low, regardless of the value of the other parameters, increasing W improves the degradation efficiency. At low W , increasing d improves degradation, even if degradation is generally ineffective. At high W , instead, an increase of d worsens the degradation, irrespective of the value of the other parameters. The best results are obtained when W is low and d is high, or when W is high and d is low when the others are low, or with high W and low d keeping the other parameters at medium or high levels.

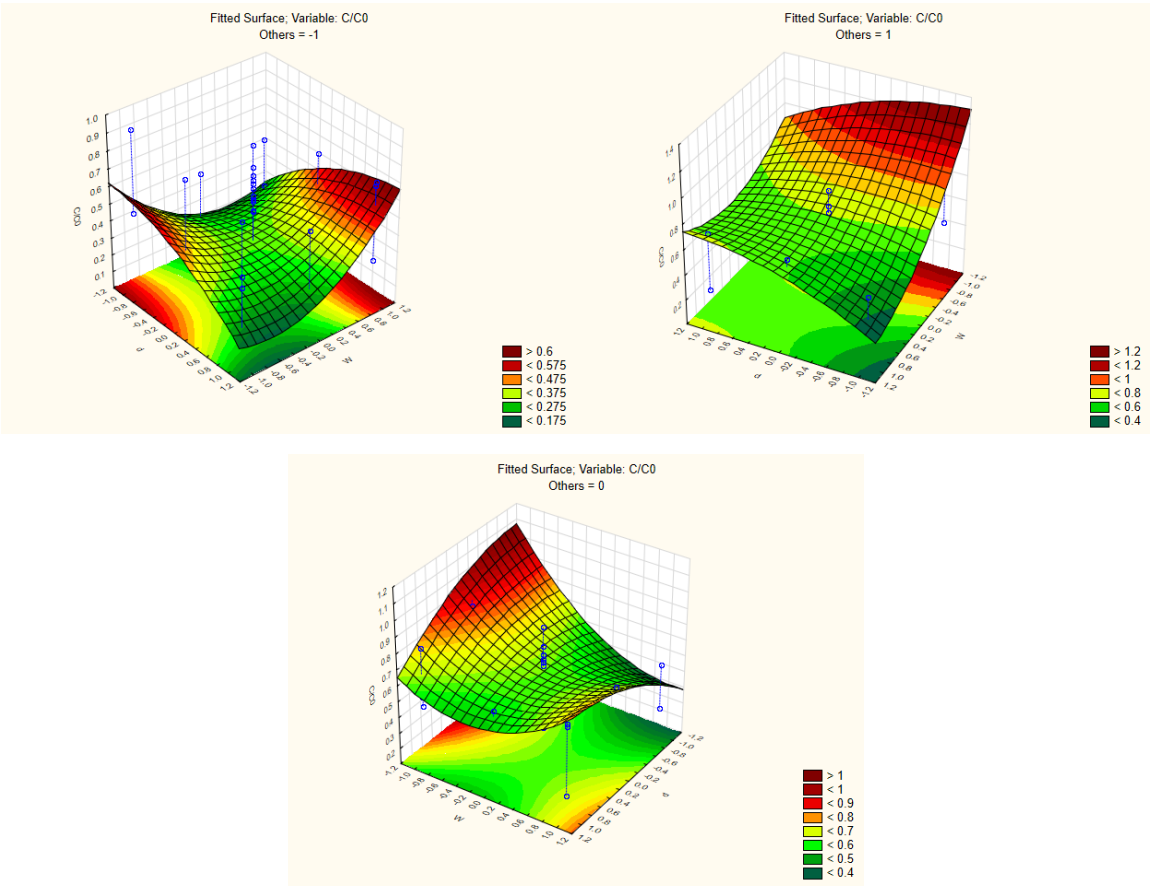


Figure 5.17. Response surfaces for the interaction between W (x-axes) and d (z-axes) when the other parameters are at level -1 (top left), 1 (top right) and 0 (bottom).

RSM study of the MAP photocatalysis using Ce/Cu-ZnO

Fig. 5.18 reports the response surface for the interaction between distance (d) and maprotiline concentration (MAP). When all parameters are at a **low (-1) level**, the best conditions are reached with a high distance and a low maprotiline concentration. When MAP is low, increasing the distance greatly improves the result. When the distance is low, an increase in maprotiline concentration worsens the already poor degradation efficiency. Additionally, increasing MAP has a negative effect on the degradation efficiency. When the other parameters are at the **central (o) value**, the best conditions are always at a high d and low MAP; nevertheless, the influence of d and MAP differs. At a low MAP, increasing d slightly improves the efficiency. At a high MAP, increasing distance worsens the degradation rate. In any case, the results were always poor when MAP was high. An increase in MAP worsens the result for both high and low d levels, with the effect being stronger for high d levels. The surfaces are considerably different when all other parameters are at the **high (1) level**, with the best conditions at low levels of both MAP and d. When MAP is low, increasing d slows the degradation rate, but the results are generally quite good. At high MAP levels, the same increase strongly affects the degradation efficiency. At both high and low d levels, increasing MAP worsens the degradation efficiency, although the effect is stronger at high MAP levels.

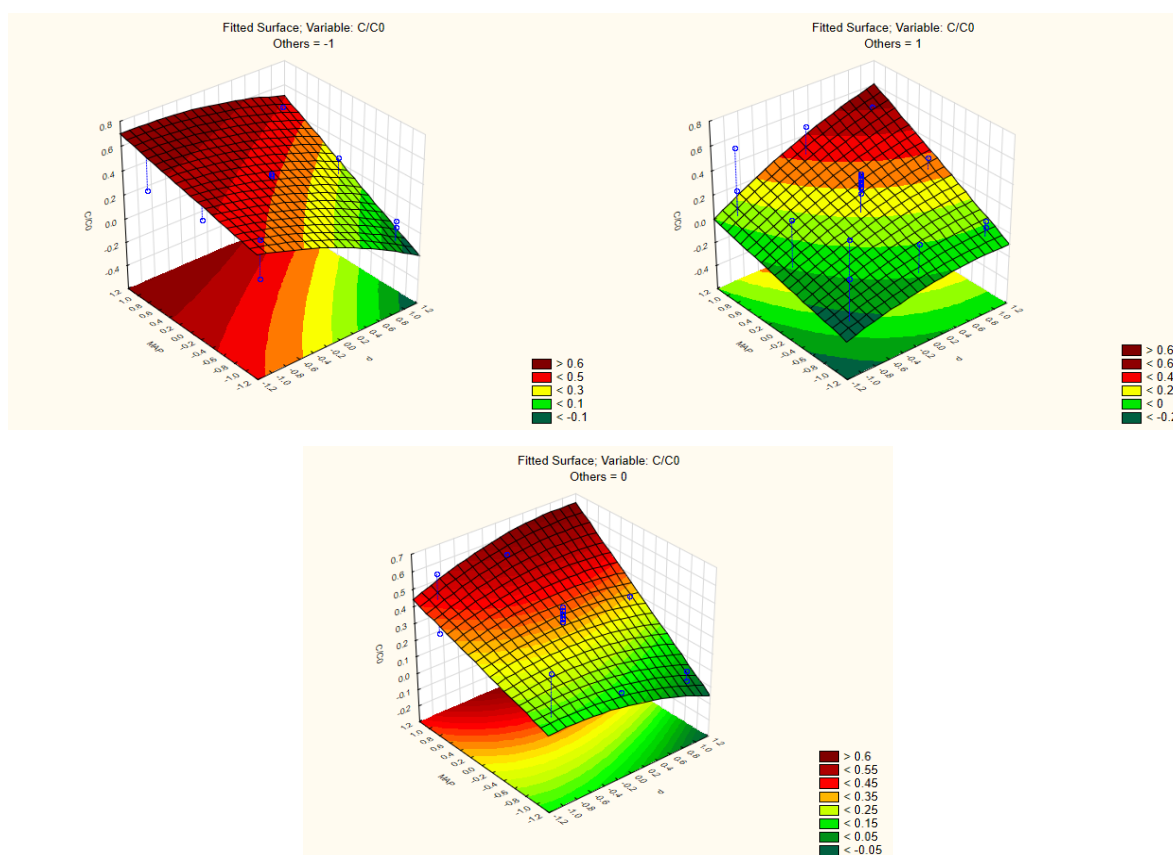


Figure 5.18. Response surfaces for the interaction between MAP (x-axes) and d (z-axes) when the other parameters are at level -1 (top left), 1 (top right) and 0 (bottom).

In terms of the interaction between distance (d) and UV intensity (W), the surfaces are shown in Fig. 5.19. When all other parameters are low or medium, the best results are obtained when W is low and d is high, and the optimal conditions are high W and low distance when all other parameters are high. When all other parameters are **low (-1)**, increasing d when W is low improves the result greatly, whereas increasing d when W is high causes a smaller improvement. At a low d , the effect of W is negligible, whereas at a high d , increasing W decreases the degradation efficiency. When the other parameters are at **intermediate (0)** levels, combining high W and low d or low W and high d yields the best results. When W is low, increasing d improves the results, whereas increasing d when W is high W worsens the results. When d is low, increasing W improves the degradation rate, but when the distance is high, the degradation efficiency decreases gradually. Finally, when the other parameters are **high (1)** and W is low or high, increasing distance worsens the degradation rate, and this effect is more significant at high W . When the distance is low, increasing W improves the results, however increasing W has no effect on the degradation rate when the distance is high.

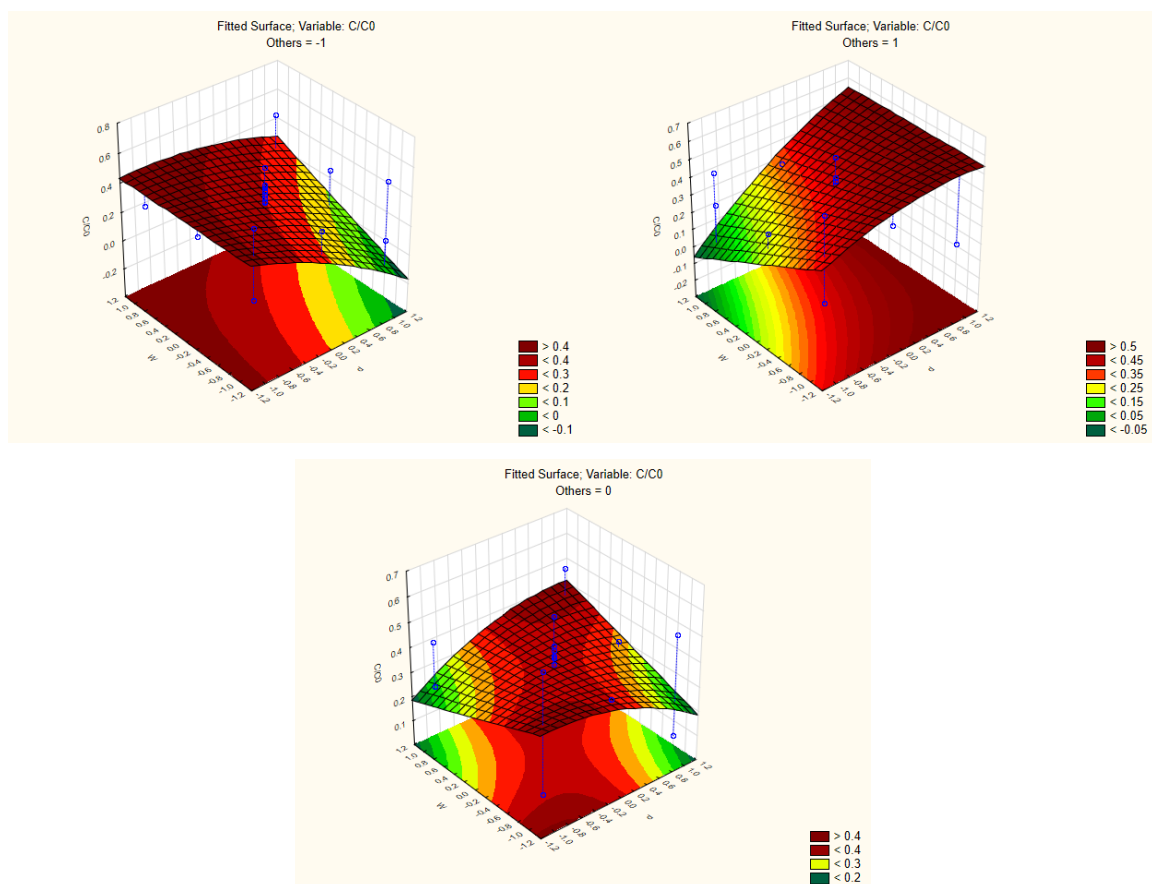


Figure 5.19. Response surfaces for the interaction between W (x-axes) and d (z-axes) when the other parameters are at level -1 (top left), 1 (top right) and 0 (bottom).

In terms of the relationship between pH (pH) and UV power (W), as shown in **Fig. 5.20**, the optimal conditions are obtained when both pH and W are high. The three surfaces reported when the other parameters are at low, medium, or high levels are roughly comparable, with a progressive shift of the surface from lower to higher C/C_0 values as the other parameters are increased from low to high levels. When the pH is low, an increase in W has no effect on the results, whereas when the pH is high, the same increase in W increases the degradation rate. At both high and low W values, an increase in pH improves the results, with the effect being stronger when W is high.

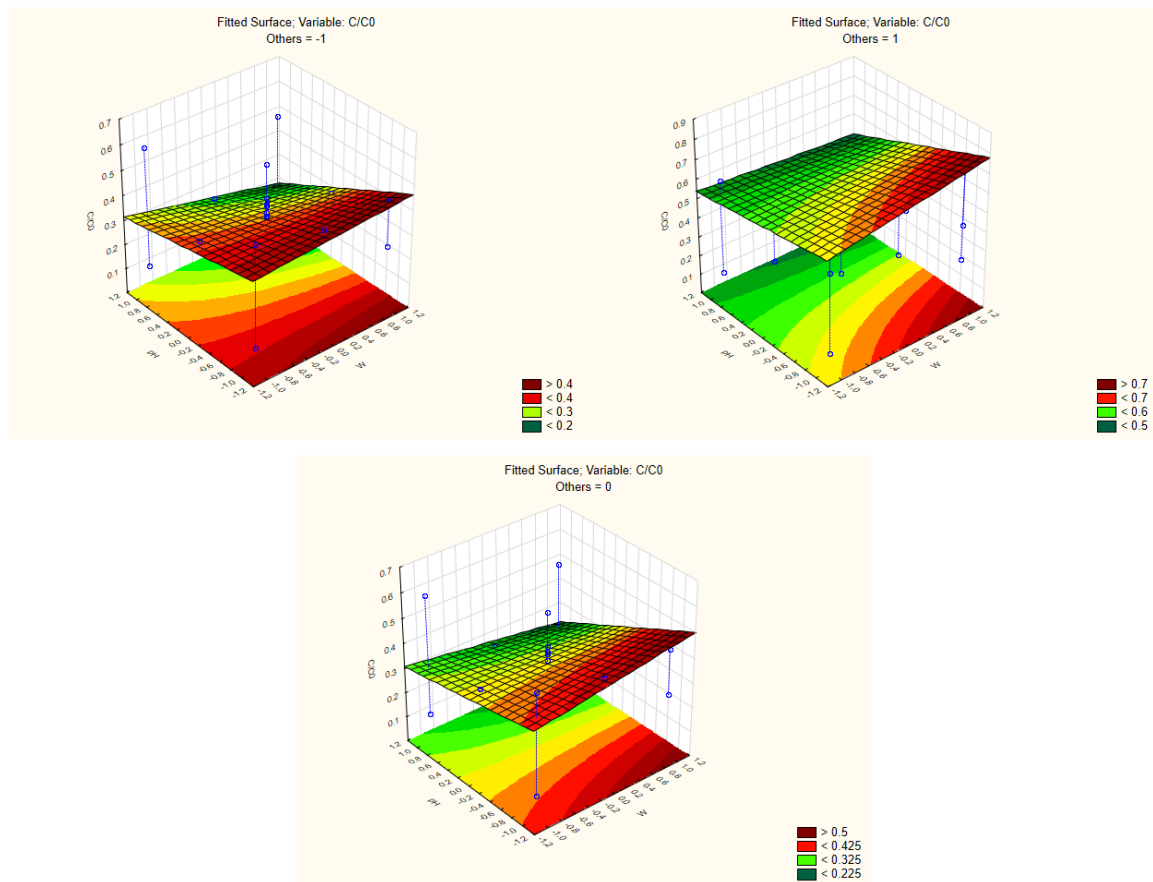


Figure 5.20. Response surfaces for the interaction between pH (x-axes) and W (z-axes) when the other parameters are at level -1 (top left), 1 (top right) and 0 (bottom).

The calculated models and investigation of robustness

The regression model for maprotiline photocatalysis using Ce-ZnO is given by:

$$C/C_0 = 0.63 - 0.067d^2 - 0.11W + 0.14W^2 - 0.076K^2 + 0.32MAP - 0.070MAP^2 - 0.13pH + 0.15(d * W) - 0.13(W * K) + 0.037(MAP * pH) \quad \text{Eq. (5.3)}$$

Similarly, the regression model for maprotiline photocatalysis using Ce/Cu-ZnO is given by:

$$C/C_0 = 0.036 - 0.043d^2 - 0.070K + 0.20MAP - 0.081pH + 0.077(d * W) + 0.090(d * K) + 0.072(d * MAP) - 0.057(W * K) - 0.032(W * pH) \quad \text{Eq. (5.4)}$$

A grid search algorithm was used to discover the optimal overall conditions and to verify the behavior of these two systems when some constraints are present. There were four distinct wastewater treatment plant (WWTP) scenarios identified:

- WWTP with a UV lamp very close to the wastewater to be treated and pH around 7, with low (WWTP-A) or high (WWTP-B) concentration of maprotiline.
- WWTP with a UV lamp far from the wastewater to be treated and pH around 7, with low (WWTP-C) or high (WWTP-D) concentration of maprotiline.

The optimal conditions obtained for the overall process and for each of the four plants are summarized in Table 5.14a and 5.14b; negative values of the Y variable show that maprotiline is completely degraded after 7.0 minutes with Ce-ZnO and 4.0 minutes with Ce/Cu-ZnO.

Table 5.14a. Best conditions obtained using Ce-ZnO by the grid search algorithm.

Conditions	D	W	K	MAP	pH	Y pred
Global optimum	-1	1	1	-1	1	< 0
Plant A	-1	1	1	-1	0	< 0
Plant B	-1	1	1	1	0	0.48
Plant C	1	-0.6	-1	-1	0	0.14
Plant D	1	-0.6	-1	1	0	0.68

Table 5.14b. Best conditions obtained for using Ce/Cu-ZnO by grid search algorithm.

Conditions	D	W	K	MAP	pH	Y pred
Global optimum	-1	1	1	-1	1	< 0
Plant A	-1	1	1	-1	0	< 0
Plant B	-1	1	1	1	0	0.15
Plant C	1	-1	-1	-1	0	< 0
Plant D	1	-1	-1	1	0	0.44

The response surface methodology was used to further differentiate the four WWTPs and to identify the robust region within each of them, ultimately providing guidance on which parameters may be disregarded within the examined boundaries and which factors require close monitoring.

For the **photocatalysis of maprotiline using Ce-ZnO**, Fig. 5.21 represents the response surfaces for the interaction between catalyst dose (K) and irradiation intensity (W) for the four WWTPs identified. For WWTP-A and WWTP-B, the best results are obtained with high values of K and W. When W is high, the degrading efficacy appears to be robust with respect to K, and satisfactory results are achieved in the region between 0.6 and 1 of W, as well as across the entire range for K. Even though the surface plots for Plant A and B are quite similar, Plant B is less efficient in general, and in this case, the region characterized by the best results is very close to high values of both W and K, and very slight deviations in these two parameters are tolerable. On the other hand, WWTP-C and WWTP-D offer the greatest outcomes in two situations: 1) when W is between -0.2 and 1 and K is high; and 2) when W is between 0 and 1 and K is low. WWTP-C performs well in the region where W is moderate and K might range between -1 and 1. Additionally, despite the same surface of WWTP-C and WWTP-D, the latter is less effective, and in this case, very slight differences in W and K are tolerable in the two best regions identified.

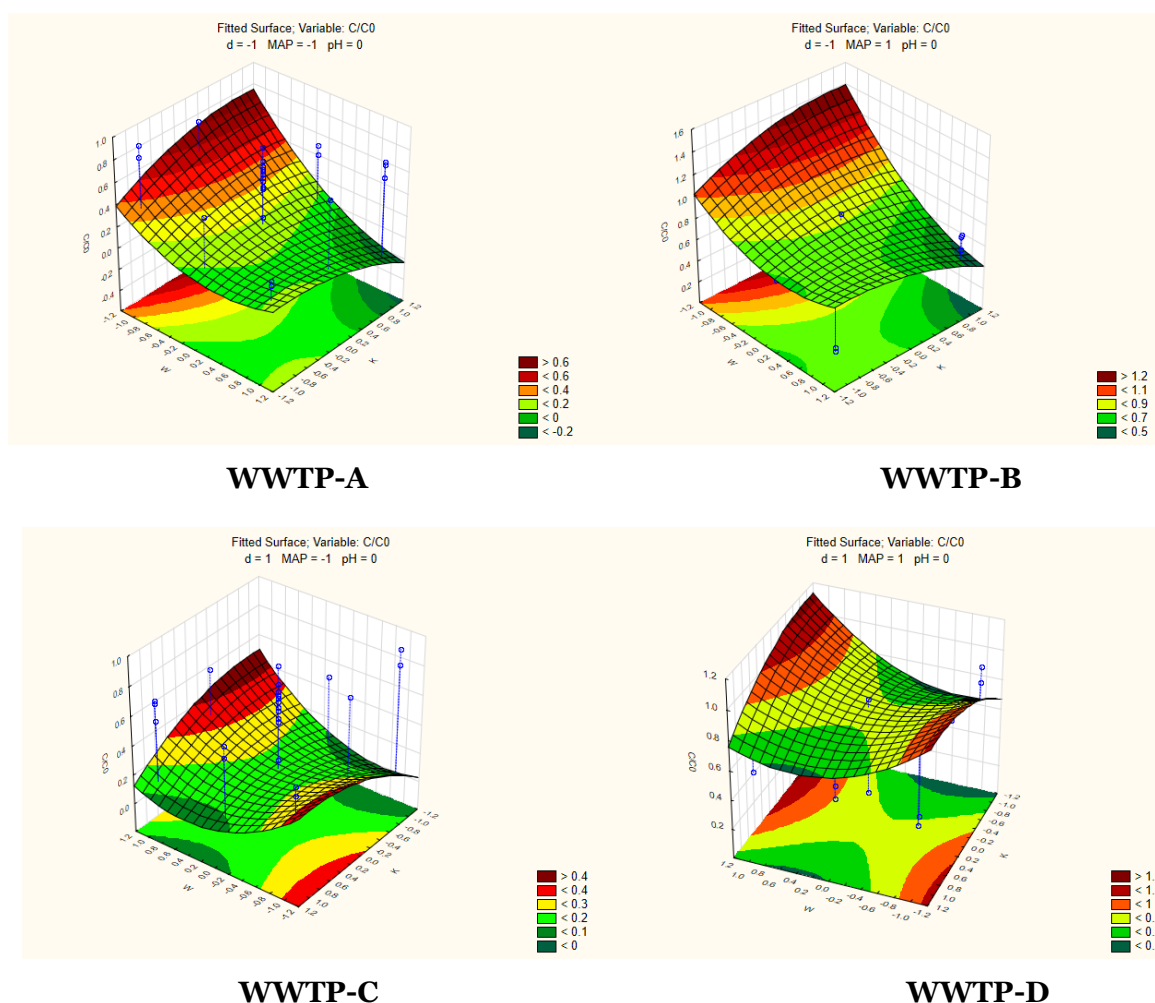


Figure 5.21. Response surfaces for the interaction between K and W for the four WWTPs identified: the case of maprotiline photocatalysis using Ce-ZnO.

The surfaces for the interaction of K and W for the four WWTPs proposed for **maprotiline photocatalytic degradation with Ce/Cu-ZnO** are shown in Fig. 5.22. The best results for WWTP-A and WWTP-B are obtained with high values of both K and W. When W is low, the degradation effectiveness is not very robust with respect to K, particularly for WWTP-B. For WWTP-A, satisfactory results are obtained when both values are between 0.7 and 1. While the surface of WWTP-A and WWTP-B appear to be similar, WWTP-B is less successful in general, and the region for best results in this case is very close to high values of both W and K, and very small deviations of these two parameters are tolerable.

At low levels of both K and W, WWTP-C and WWTP-D produce the best outcomes. Even though WWTP-C and WWTP-D have similar surface plots, WWTP-D is less effective. The robustness range for WWTP-C corresponds to values of both parameters between 0 and -1. The robustness range for WWTP-D, on the other hand, is extremely narrow, and only little fluctuations in W and K are tolerated.

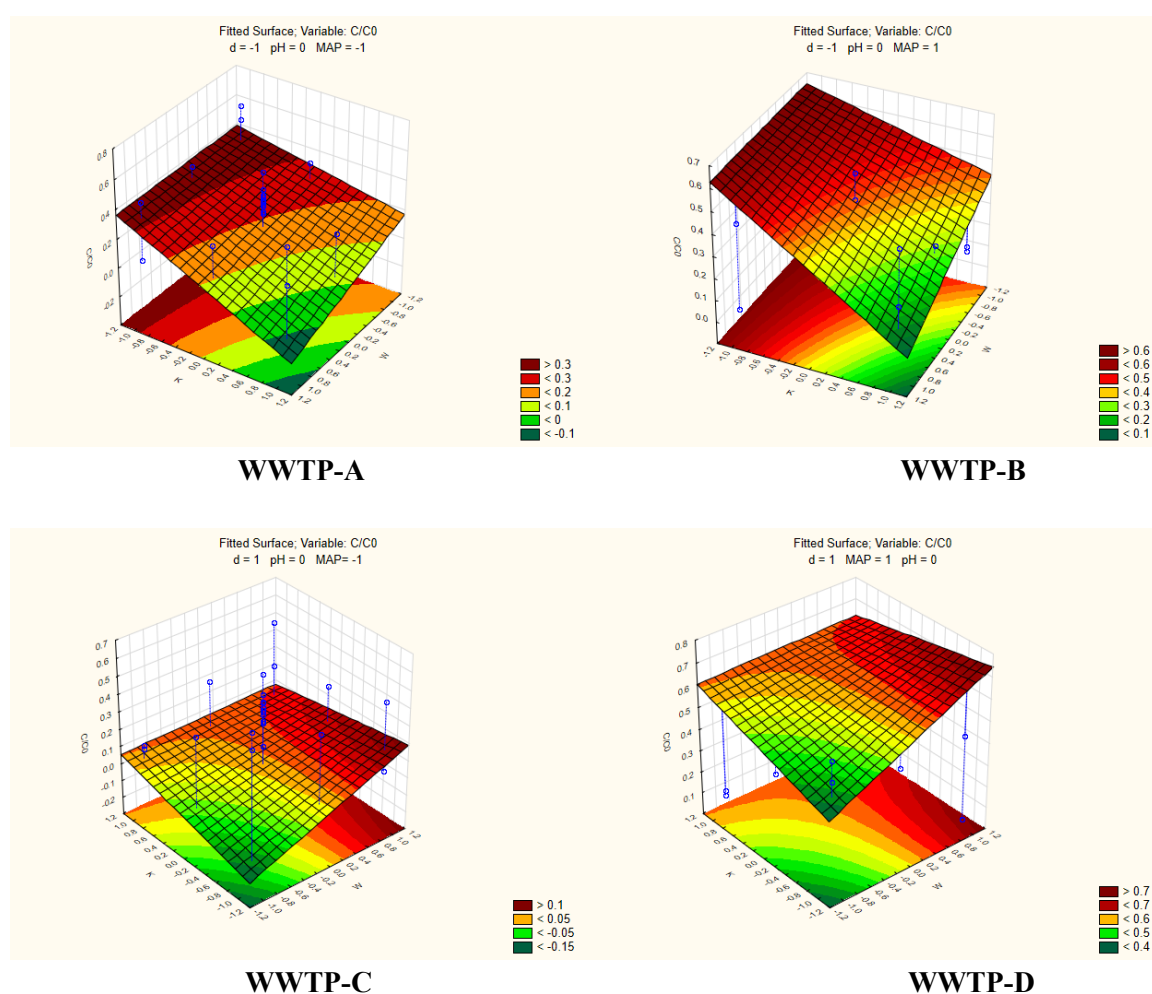


Figure 5.22. Response surfaces for the interaction between K and W for the four WWTPs identified: the case of maprotiline photocatalysis using Ce-ZnO.

5.7 Conclusions and forward

The techniques of experimental design (DOE) have been successfully used to optimize and investigate the robustness of CECs removal methods in water. We investigated the photolytic degradation of irinotecan and the photocatalytic degradation of maprotiline. Each procedure was evaluated for applicability to wastewater treatment plants (WWTPs) by examining the major parameters affecting the degradation of the CECs studied. The optimal settings for each procedure were established based on results obtained for the significance of effects as identified through sequential statistical models.

In the case of maprotiline photocatalysis, four WWTPs were postulated, and using response surface methodology (RSM) – a powerful tool for multivariate optimization via sequential experimentation – detailed guidelines for each WWTP were established, emphasizing on both the factors that have no effect on the degradation efficiency and those that must be closely monitored because their fluctuations may result in poor degradation efficiency. In the event of WWTP-related constraints, the constructed models can be used to find optimal WWTP operating conditions and information on parameter adjustments (e.g., a fixed concentration of CEC, a constraint acting on the power of irradiation or the pH, etc.) and the same model can be used to determine a WWTP's robustness region, which guides process operation.

The findings of this study are encouraging and may serve as valuable inputs for future efforts to integrate advanced oxidation processes (AOPs) into water and wastewater treatment processes. However, we recommend that additional research focusing on plant operational parameters be conducted and that the findings reported in this study be confirmed, for example, through pilot plant studies in real wastewaters.

5.8 Materials and safety

5.8.1 Chemicals

Methanol (Ultra CHROMASOLV, >99.9%), water (LC-MS grade), formic acid (98-100%), hydrochloric acid (HCl, 37%), sodium hydroxide ($\geq 97\%$, pellets), irinotecan ($\geq 97\%$), and maprotiline (>99%) were purchased from Sigma-Aldrich (Milan, Italy). Acetonitrile (LC-MS grade) was obtained from VWR (Milan, Italy). Individual stock standard solutions of irinotecan and maprotiline were prepared in methanol at 1000 mg/L and used after proper dilutions for the LC-MS method development and optimization. The stock solutions were preserved at $-20\text{ }^{\circ}\text{C}$ in dark glass vials in a dark standard-only freezer. For the degradation experiments, irinotecan and maprotiline aqueous solutions at the desired concentrations were always freshly

prepared in Milli-Q water. The Ce-ZnO and Ce/Cu-ZnO photocatalysts were synthesized and characterized at the University of Turin (Italy) and kindly provided to us by researchers working for AQUAlity.

5.8.2 Instrumentation

Simulated solar irradiation was generated in a Solarbox 3000e (CoFoMeGra, Milan, Italy), whereas ultraviolet (UV) irradiation was provided by a home-made system which had six Philips Actinic BL TL-D (15 W) UV-A lamps purchased from a local supplier. LC-HRMS analysis of maprotiline samples was performed using Vanquish UHPLC system hyphenated with Orbitrap Q-Exactive Plus mass spectrometer (Thermo Fisher, Massachusetts, USA). The analytical column was an Aquity UPLC BEH C18 (150 × 2.1 mm, 1.7 μm) obtained from Waters (Milan, Italy). On the other hand, the LC-HRMS instrumentation used for irinotecan analysis was an Ultimate Dionex 3000 UHPLC system hyphenated with Orbitrap Fusion Mass Spectrometer (Thermo Fisher, Massachusetts, USA) and the analytical column was a Luna C18(2) (150 mm × 2.0 mm, 3 μm) purchased from Phenomenex (Milan, Italy). All LC-MS data were processed using Thermo Xcalibur software (*version 3.0.63*) and DOE analyses were performed using Microsoft Excel and Statistica software (*version 12.5.192.5*).

5.8.3 Safety

To guarantee the best possible protection for personnel when working with irinotecan and maprotiline, all reagents must be handled with caution in accordance with the corresponding safety data sheet (SDS). In this study, all stock solutions were made in a biological safety hood with laminar airflow, and absorbent paper was used to protect the work surfaces. All disposable materials that came into touch with the substance under investigation were discarded as hazardous waste. Moreover, appropriate safety glasses, hand gloves, and lab coats were always worn to prevent chemical contamination and UV irradiation.

References

1. Gonçalves, N. P., Varga, Z., Bouchonnet, S., Dulio, V., Alygizakis, N., Dal Bello, F., ... & Calza, P. (2021). Study of the photoinduced transformations of maprotiline in river water using liquid chromatography high-resolution mass spectrometry. *Science of the Total Environment*, 755, 143556.
2. Gonçalves, N. P., Varga, Z., Nicol, E., Calza, P., & Bouchonnet, S. (2021). Comparison of advanced oxidation processes for the degradation of maprotiline in water—kinetics, degradation products and potential ecotoxicity. *Catalysts*, 11(2), 240.
3. Iervolino, G., Zammit, I., Vaiano, V., & Rizzo, L. (2020). Limitations and prospects for wastewater treatment by UV and visible-light-active heterogeneous photocatalysis: a critical review. *Heterogeneous Photocatalysis*, 225-264.
4. Ferreira, S. L., Caires, A. O., Borges, T. D. S., Lima, A. M., Silva, L. O., & dos Santos, W. N. (2017). Robustness evaluation in analytical methods optimized using experimental designs. *Microchemical Journal*, 131, 163-169.
5. Sakkas, V. A., Islam, M. A., Stalikas, C., & Albanis, T. A. (2010). Photocatalytic degradation using design of experiments: a review and example of the Congo red degradation. *Journal of Hazardous Materials*, 175(1-3), 33-44.
6. Barth, A. B., De Oliveira, G. B., Malesuik, M. D., Paim, C. S., & Volpato, N. M. (2011). Stability-indicating LC assay for butenafine hydrochloride in creams using an experimental design for robustness evaluation and photodegradation kinetics study. *Journal of chromatographic science*, 49(7), 512-518.
7. Gnanaprakasam, A., Sivakumar, V. M., & Thirumarimurugan, M. (2015). Influencing parameters in the photocatalytic degradation of organic effluent via nanometal oxide catalyst: a review. *Indian Journal of Materials Science*, 2015.
8. Gao, X., Guo, Q., Tang, G., Peng, W., Luo, Y., & He, D. (2019). Effects of inorganic ions on the photocatalytic degradation of carbamazepine. *Journal of Water Reuse and Desalination*, 9(3), 301-309.
9. Klavarioti, M., Mantzavinos, D., & Kassinos, D. (2009). Removal of residual pharmaceuticals from aqueous systems by advanced oxidation processes. *Environment international*, 35(2), 402-417.
10. Ayodele, B. V., Alsaffar, M. A., Mustapa, S. I., & Vo, D. V. N. (2020). Backpropagation neural networks modelling of photocatalytic degradation of organic pollutants using TiO₂-based photocatalysts. *Journal of Chemical Technology & Biotechnology*, 95(10), 2739-2749.
11. Tang, K., Casas, M. E., Ooi, G. T., Kaarsholm, K. M., Bester, K., & Andersen, H. R. (2017). Influence of humic acid addition on the degradation of pharmaceuticals by biofilms in effluent wastewater. *International Journal of Hygiene and Environmental Health*, 220(3), 604-610.
12. Mašković, M., Jančić-Stojanović, B., Malenović, A., Ivanović, D., & Medenica, M. (2010). Assessment of liquid chromatographic method robustness by use of Plackett-Burman design. *Acta Chromatographica*, 22(2), 281-296.
13. Dejaegher, B., Dumarey, M., Capron, X., Bloomfield, M. S., & Vander Heyden, Y. (2007). Comparison of Plackett–Burman and supersaturated designs in robustness testing. *Analytica Chimica Acta*, 595(1-2), 59-71.
14. Box, G. E., Hunter, W. H., & Hunter, S. (1978). *Statistics for experimenters* (Vol. 664). New York: John Wiley and sons.

15. Souza, D. M., Reichert, J. F., & Martins, A. F. (2018). A simultaneous determination of anti-cancer drugs in hospital effluent by DLLME HPLC-FLD, together with a risk assessment. *Chemosphere*, *201*, 178-188.
16. Loos, R., Carvalho, R., António, D. C., Comero, S., Locoro, G., Tavazzi, S., ... & Gawlik, B. M. (2013). EU-wide monitoring survey on emerging polar organic contaminants in wastewater treatment plant effluents. *Water research*, *47*(17), 6475-6487.
17. Das, S., Ray, N. M., Wan, J., Khan, A., Chakraborty, T., & Ray, M. B. (2017). Micropollutants in wastewater: fate and removal processes. *Physico-chemical Wastewater Treatment and Resource Recovery*, *3*, 75-117.
18. Gosetti, F., Belay, M. H., Marengo, E., & Robotti, E. (2020). Development and validation of a UHPLC-MS/MS method for the identification of irinotecan photodegradation products in water samples. *Environmental Pollution*, *256*, 113370.
19. Katsoni, A., Gomes, H. T., Pastrana-Martínez, L. M., Faria, J. L., Figueiredo, J. L., Mantzavinos, D., & Silva, A. M. (2011). Degradation of trinitrophenol by sequential catalytic wet air oxidation and solar TiO₂ photocatalysis. *Chemical Engineering Journal*, *172*(2-3), 634-640.
20. Kuo, W. S., & Wu, C. L. (2012). Treatment of color filter wastewater by fresnel lens enhanced solar photo-Fenton process. *Advances in Materials Science and Engineering*, *2012*.
21. Weber, J., Halsall, C. J., Wargent, J. J., & Paul, N. D. (2009). A comparative study on the aqueous photodegradation of two organophosphorus pesticides under simulated and natural sunlight. *Journal of Environmental Monitoring*, *11*(3), 654-659.
22. Fraser, T. R., Ross, K. E., Alexander, U., & Lenehan, C. E. (2021). Current knowledge of the degradation products of tattoo pigments by sunlight, laser irradiation and metabolism: a systematic review. *Journal of Exposure Science & Environmental Epidemiology*, 1-13.
23. Arabian, D. (2021). Optimization of electrocoagulation system for municipal wastewater treatment. *Desalination And Water Treatment*, *217*, 145-158.

CHAPTER 6

Conclusions

6. CONCLUSIONS

The main conclusions for each chapter are summarized as follows.

Chapter 3 – Development and validation of (U)HPLC-MS/MS methods for CECs determination

1. A new analytical method based on offline solid-phase extraction (SPE) has been developed and validated for the identification of the contaminant of emerging concern (CEC) irinotecan and its eight transformation products (TPs) using LC-MS/MS. For each of the eight TPs, proposed structures have been elucidated. The proposed LC-MS/MS method was applied to nine water samples (river water, ground water, well water, treated water, and hospital effluent) from Italy's Piemonte region, and irinotecan and one of its TPs were found in hospital wastewater effluents.
2. A new analytical method based on offline SPE has been developed and validated for the identification of the CEC aliskiren and its six TPs using LC-MS/MS. For each of the eight transformation products, proposed structures have been elucidated using LC-HRMS. The proposed LC-MS/MS method was applied to nine water samples (river water, ground water, well water, treated water, and hospital effluent) from Italy's Piemonte region. Furthermore, aliskiren and its two TPs were detected in a variety of aquatic compartments by retroactive analysis of digitally frozen samples.
3. A new multiresidue method based on on-line SPE has been successfully developed and validated for the determination of 10 pharmaceuticals in aqueous samples by LC-MS/MS. The proposed LC-MS/MS method was applied to six effluents of hospital wastewaters from Vejen (Denmark) and Valencia (Spain): maprotiline was quantified in 3 Spanish samples while methotrexate was detected in 2 Danish samples.

Chapter 4 – Non-targeted screening by LCMS-based techniques

1. A sample pre-treatment strategy based on offline SPE has been developed for the non-target screening of environmental contaminants by LC-HRMS. The proposed method was applied to 17 surface waters and wastewaters from France, Greece, and Italy. Using open-source LC-MS data processing tools, a total of 264 environmental contaminants (pharmaceuticals, hormones, personal care products, pesticides, etc.) were identified at a confidence level of 2.

2. 28 of the 264 compounds identified in this study were also identified in a separate but similar study conducted within the AQUALity project: hence, reinforcing confidence in their environmental occurrence. Moreover, seven compounds were confirmed with the highest degree of confidence (i.e., Level 1) using suspect screening with standards for suspected analytes.
3. The raw HRMS data generated in this work and the non-target screening results have been used to enrich the databases in the European network of reference laboratories, research centers and related organizations for monitoring of emerging environmental substances (NORMAN). Information regarding the identified 264 compounds have been compiled and shared with NORMAN through the suspect list exchange (SLE). Moreover, all raw HRMS was uploaded to NORMAN's digital sample freezing platform (DSFP) for use in current and future retrospective screening analyses.

Chapter 5 – Robustness studies by experimental design

1. Experimental design (DOE) techniques based on full factorial designs combined with star designs were successfully applied to optimize and evaluate the robustness of the photodegradation abatement of irinotecan in water using simulated solar irradiation. The effect of three parameters (irinotecan concentration, solar irradiation intensity, and initial pH of the solution) was studied, and the optimal conditions for effective irinotecan elimination were established.
2. The effect of five parameters (maprotiline concentration, UV irradiation intensity, distance between UV lamps and sample, dose of a Ce doped ZnO photocatalyst, and solution initial pH) on the photocatalytic degradation of maprotiline in water was investigated using DOE techniques based on fractional factorial designs and star designs. A statistical model was constructed, and the optimal conditions established. Moreover, the robust regions were identified using response surface methodology (RSM).
3. DOE techniques based on fractional factorial designs and star designs were also satisfactorily applied to investigate the effect of five parameters (maprotiline concentration, UV irradiation intensity, distance between UV lamps and sample, dose of a Ce and Cu co-doped ZnO photocatalyst, and initial pH of the solution) on the photocatalytic degradation of maprotiline in water. Again, a statistical model was built, the optimal conditions were identified, and the robust regions were established using response surfaces.

4. Four wastewater treatment plants (WWTPs) were proposed for the methods specified in (2) and (3) above, taking into account the practical application of the abatement techniques in real-world settings. By exploiting the potential of response surfaces, operational guidelines were established for each proposed WWTP by identifying the parameters that have no effect on the degradation process and those that require close monitoring.

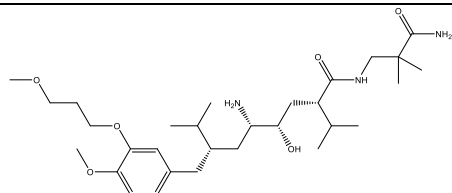
Appendix II – g-C₃N₄/ZnWO₄ composite photocatalyst

1. A new g-C₃N₄/ZnWO₄ composite photocatalyst was synthesized through a co-precipitation assisted hydrothermal process and its structural, morphological, and optical properties were characterized using XRD, TEM, XPS, Raman spectroscopy, and UV-Vis DRS.
2. The enhanced photocatalytic activity of the synthesized catalyst was evaluated using near visible light irradiation for the degradation of ibuprofen in ultrapure and resulted in a more than 5-fold increase in performance.

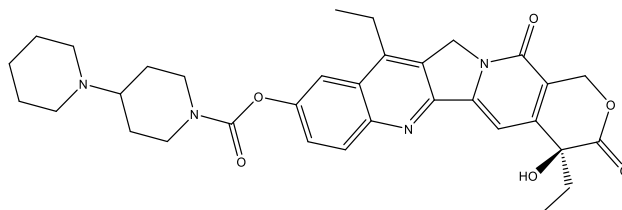
Appendices

Appendix I

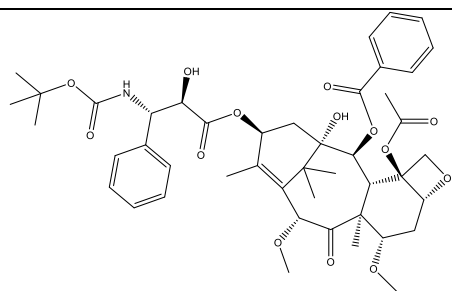
Table S3.1. Formula, structure and logP values of the ten pharmaceutical compounds



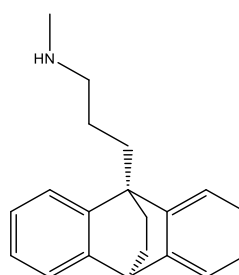
Aliskiren (C₃₀H₅₃N₃O₆); logP 3.51



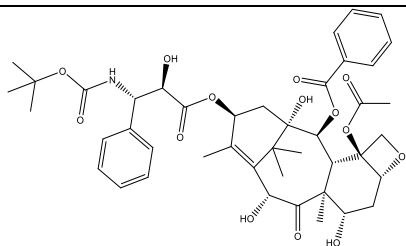
Irinotecan (C₃₃H₃₈N₄O₆); logP 2.43



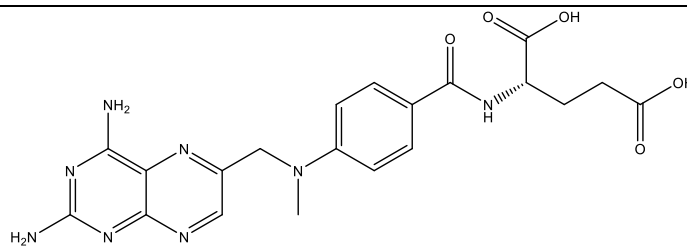
Cabazitaxel (C₄₅H₅₇NO₁₄); logP 5.44



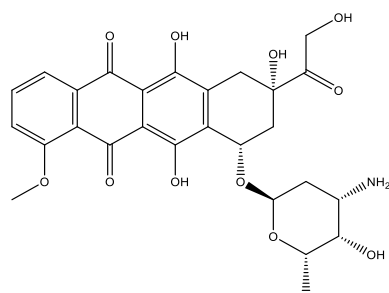
Maprotiline (C₂₀H₂₃N); logP 4.52



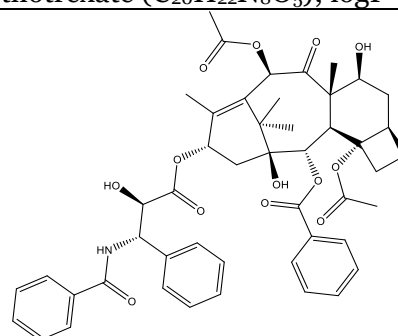
Docetaxel (C₄₃H₅₃NO₁₄); logP 4.08



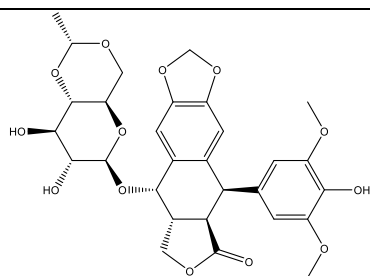
Methotrexate (C₂₀H₂₂N₈O₅); logP -0.53



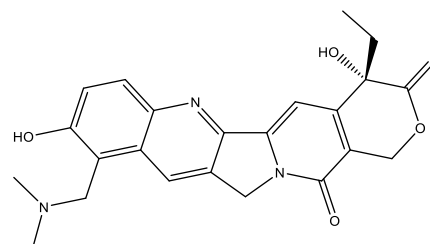
Doxorubicin (C₂₇H₂₉NO₁₁); logP 0.32



Paclitaxel (C₄₇H₅₁NO₁₄); logP 4.73



Etoposide (C₂₉H₃₂O₁₃); logP -0.11



Topotecan (C₂₃H₂₃N₃O₅); logP 0.43

Table S3.2: Efficiency and asymmetry factor obtained using three different analytical columns (mean values obtained from triplicate analysis of three independent samples containing 1.0 µg/L mix of the ten analytes and the IS). Efficiency results are reported as: mean values*10⁴ ± SD*10².

Compound	Efficiency (N)*			Asymmetry factor		
	Kinetex	Eclipse	Luna	Kinetex	Eclipse	Luna
Aliskiren (ALK)	8.4 ± 1.3	7.8 ± 2.2	6.7 ± 4.6	1.07 ± 0.05	1.07 ± 0.09	1.08 ± 0.15
Cabazitaxel (CTX)	6.1 ± 1.2	4.0 ± 6.9	4.0 ± 7.5	1.05 ± 0.16	1.16 ± 0.05	1.15 ± 0.06
Docetaxel (DTX)	4.9 ± 1.5	3.4 ± 3.6	9.1 ± 3.9	0.95 ± 0.07	1.22 ± 0.12	1.22 ± 0.13
Doxorubicin (DOX)	7.1 ± 1.2	6.4 ± 1.9	5.2 ± 5.0	1.57 ± 0.06	1.74 ± 0.04	1.74 ± 0.04
Etoposide (ETP)	7.4 ± 3.7	6.4 ± 5.8	5.3 ± 4.3	1.14 ± 0.19	1.66 ± 0.07	1.66 ± 0.07
Irinotecan (IRI)	6.2 ± 2.9	5.1 ± 4.9	5.1 ± 7.4	1.61 ± 0.08	1.88 ± 0.14	1.75 ± 0.14
Maprotiline (MAP)	6.5 ± 1.0	5.7 ± 4.8	4.8 ± 1.4	1.08 ± 0.04	1.11 ± 0.07	1.22 ± 0.15
Methotrexate (MTX)	5.1 ± 2.4	4.8 ± 5.0	4.0 ± 8.1	1.17 ± 0.04	1.28 ± 0.19	1.20 ± 0.10
Paclitaxel (PTX)	9.6 ± 2.0	8.0 ± 3.2	7.7 ± 2.9	1.35 ± 0.09	1.48 ± 0.17	1.75 ± 0.03
Topotecan (TOP)	5.8 ± 3.7	4.6 ± 2.6	4.4 ± 9.4	1.05 ± 0.09	1.17 ± 0.05	1.18 ± 0.19
Atrazine-d ₅ (ATZ)	7.1 ± 1.3	7.2 ± 1.2	6.7 ± 1.9	0.98 ± 0.06	0.92 ± 0.09	1.28 ± 0.03

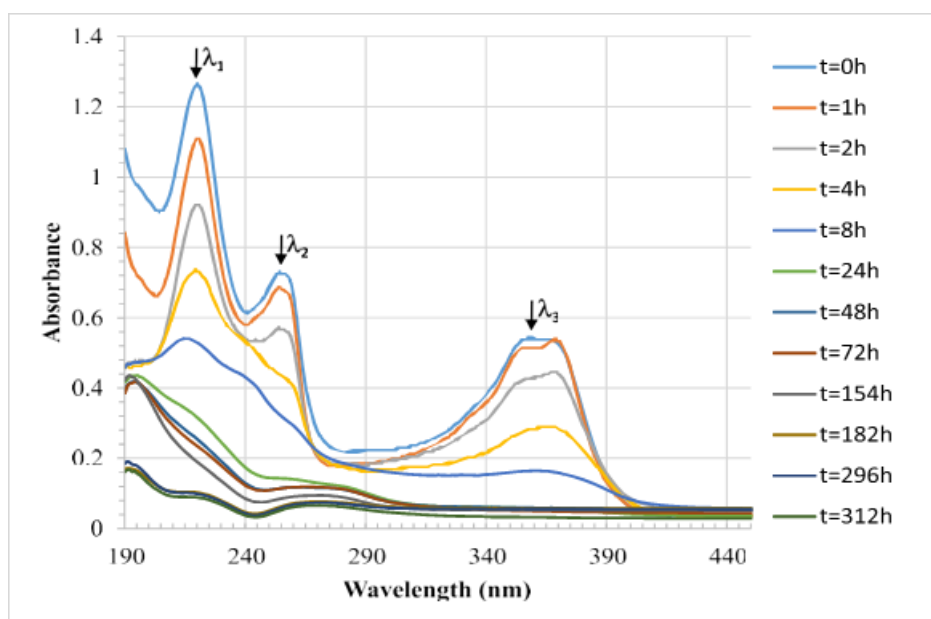


Fig. S3.1. The photodegradation of IRI: UV/Vis absorbance spectrum measured as a function of solar light irradiation time ($\lambda_1 = 221$ nm, $\lambda_2 = 255$ nm, $\lambda_3 = 359$ nm).

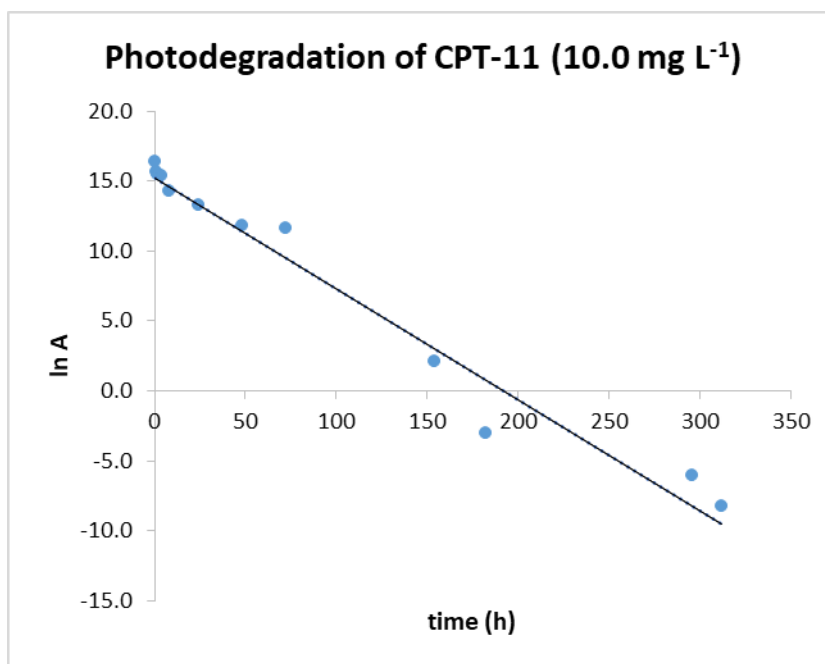


Fig. S3.2. First order kinetic plot of IRI aqueous solution at initial concentration of 10.0 mg/L (pH = 4.3±0.092). The plot shows the ln A (where A represents the chromatographic peak area of IRI) against the irradiation time (h).

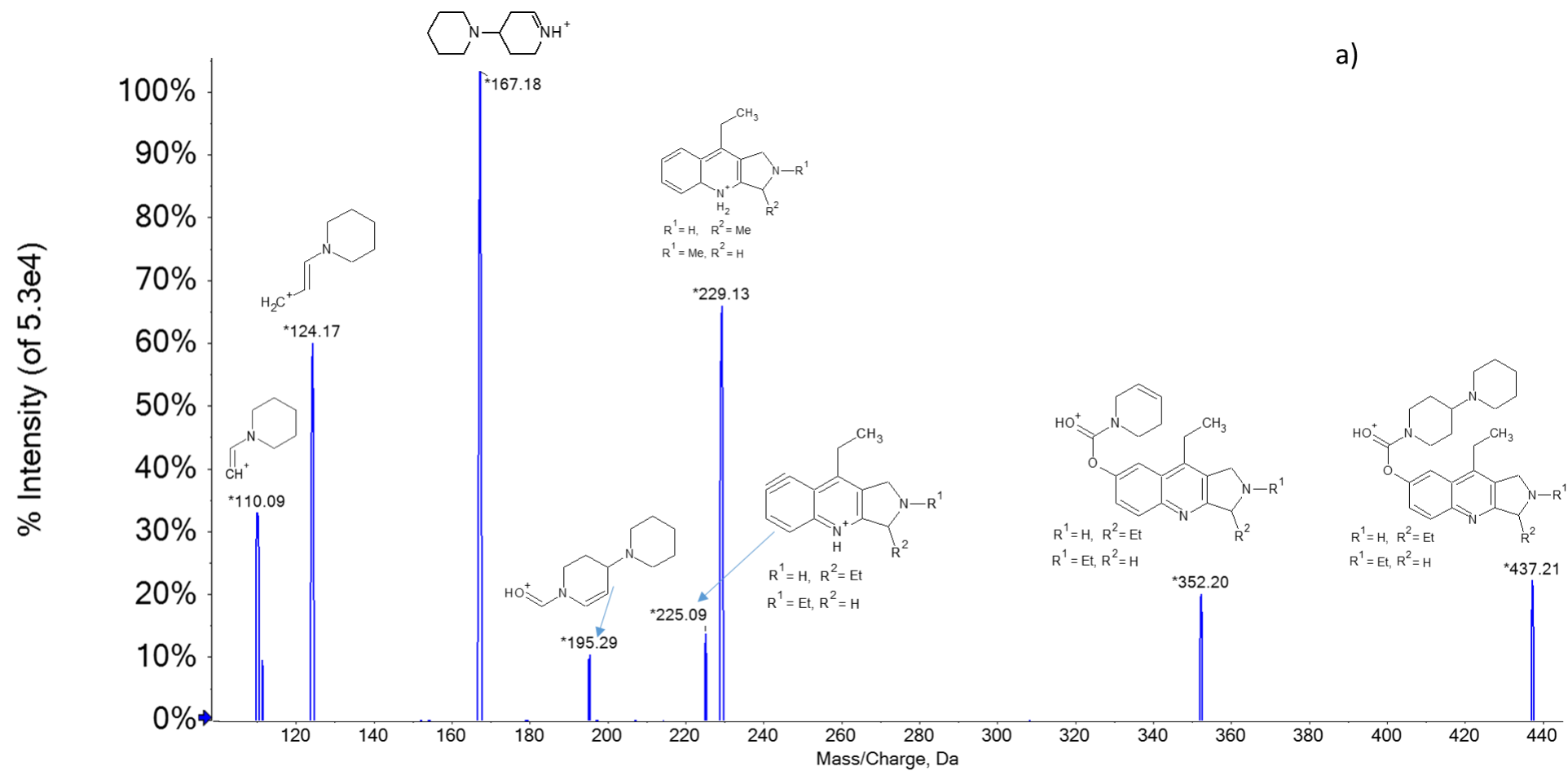


Figure S3.3a.

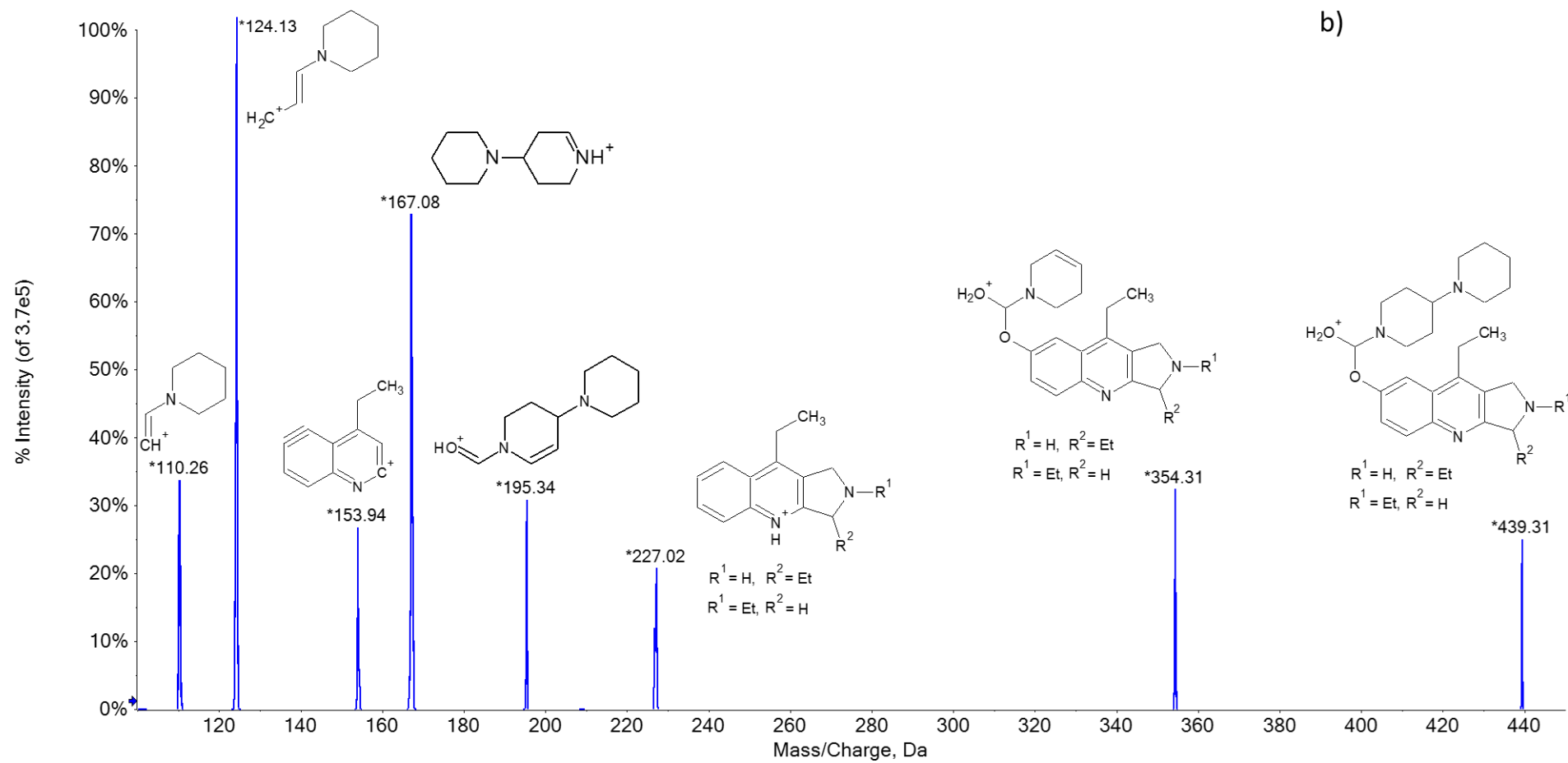


Figure S3.3b.

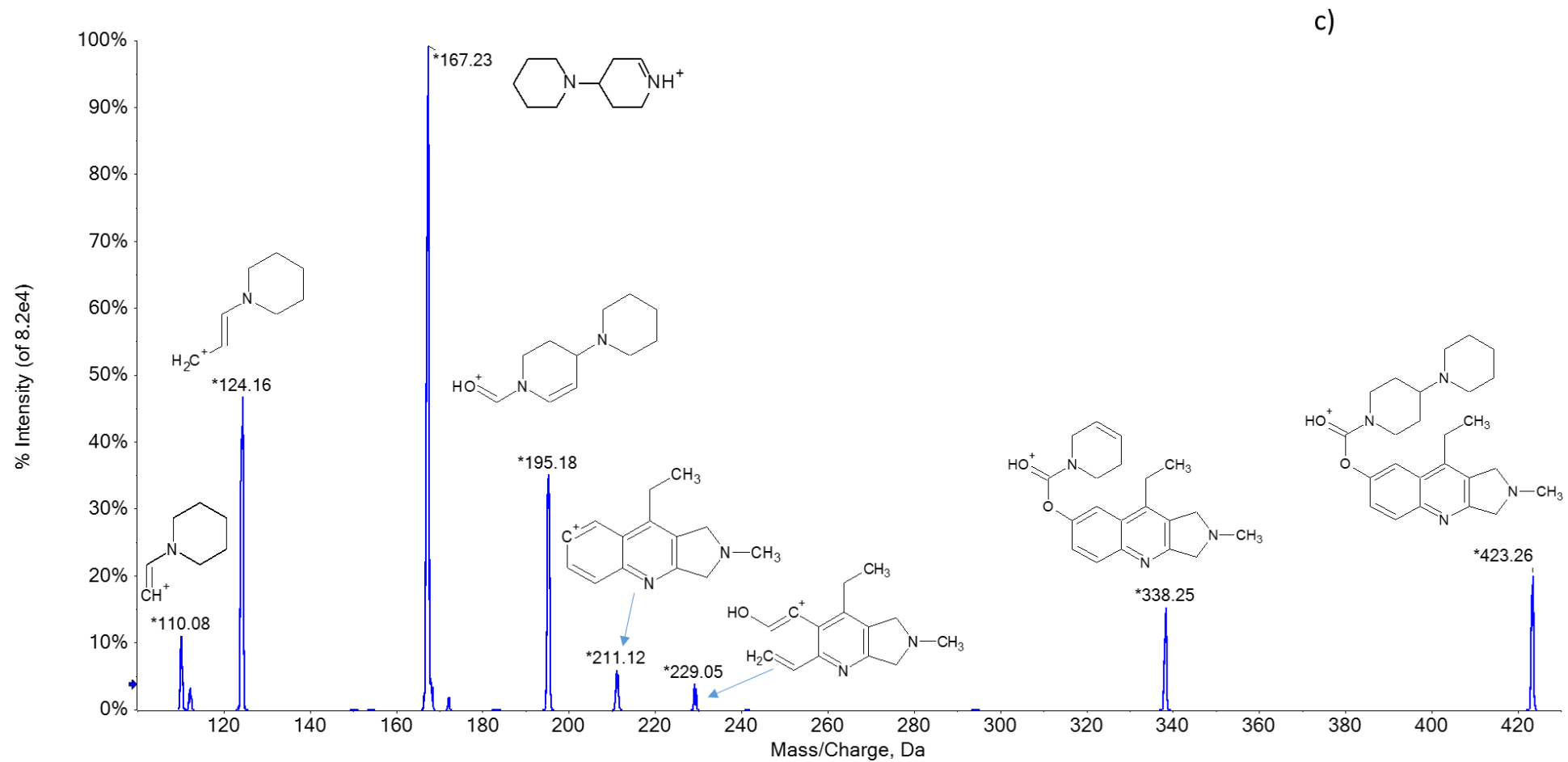


Figure S3.3c.

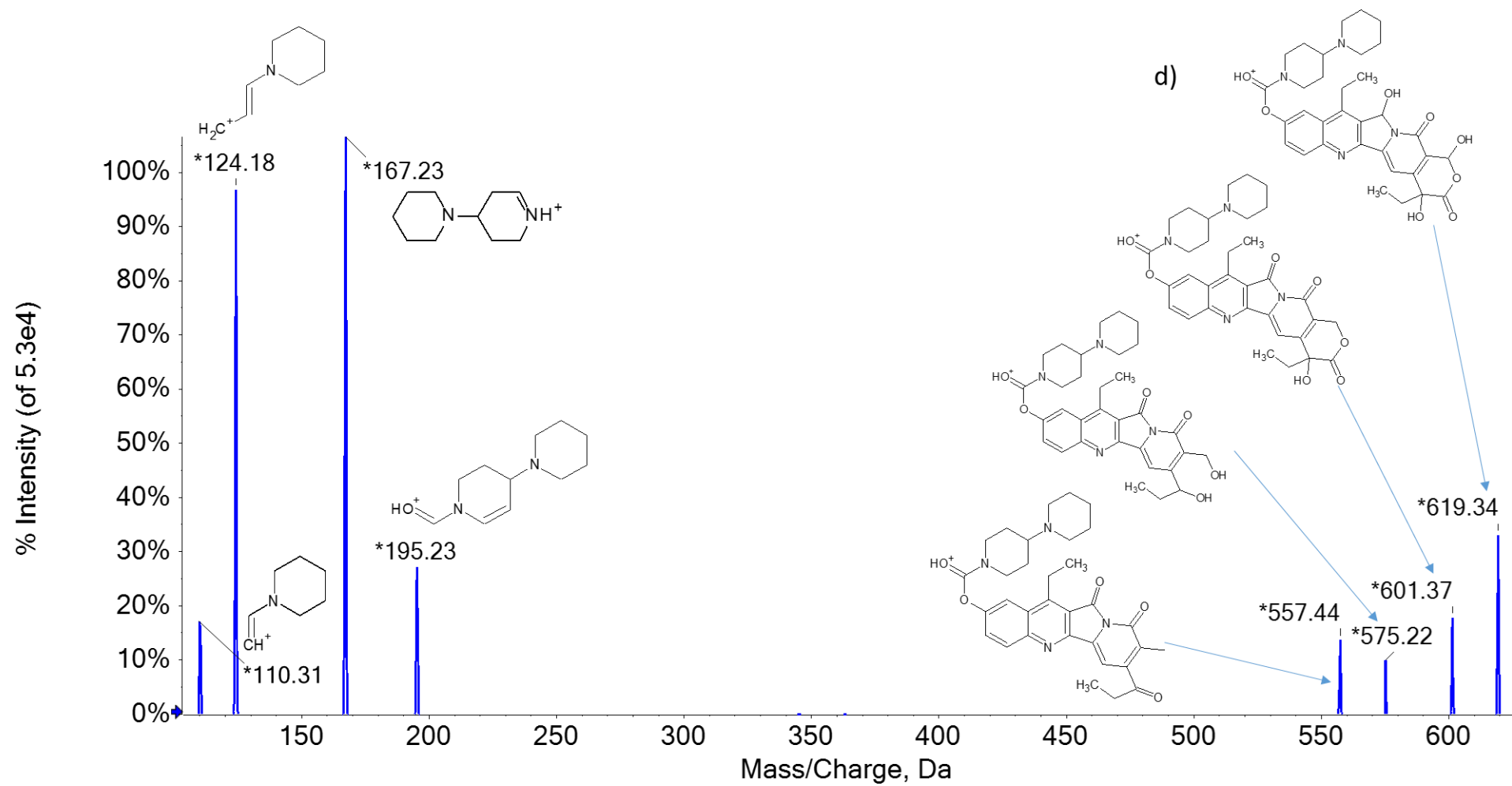


Figure S3.3d.

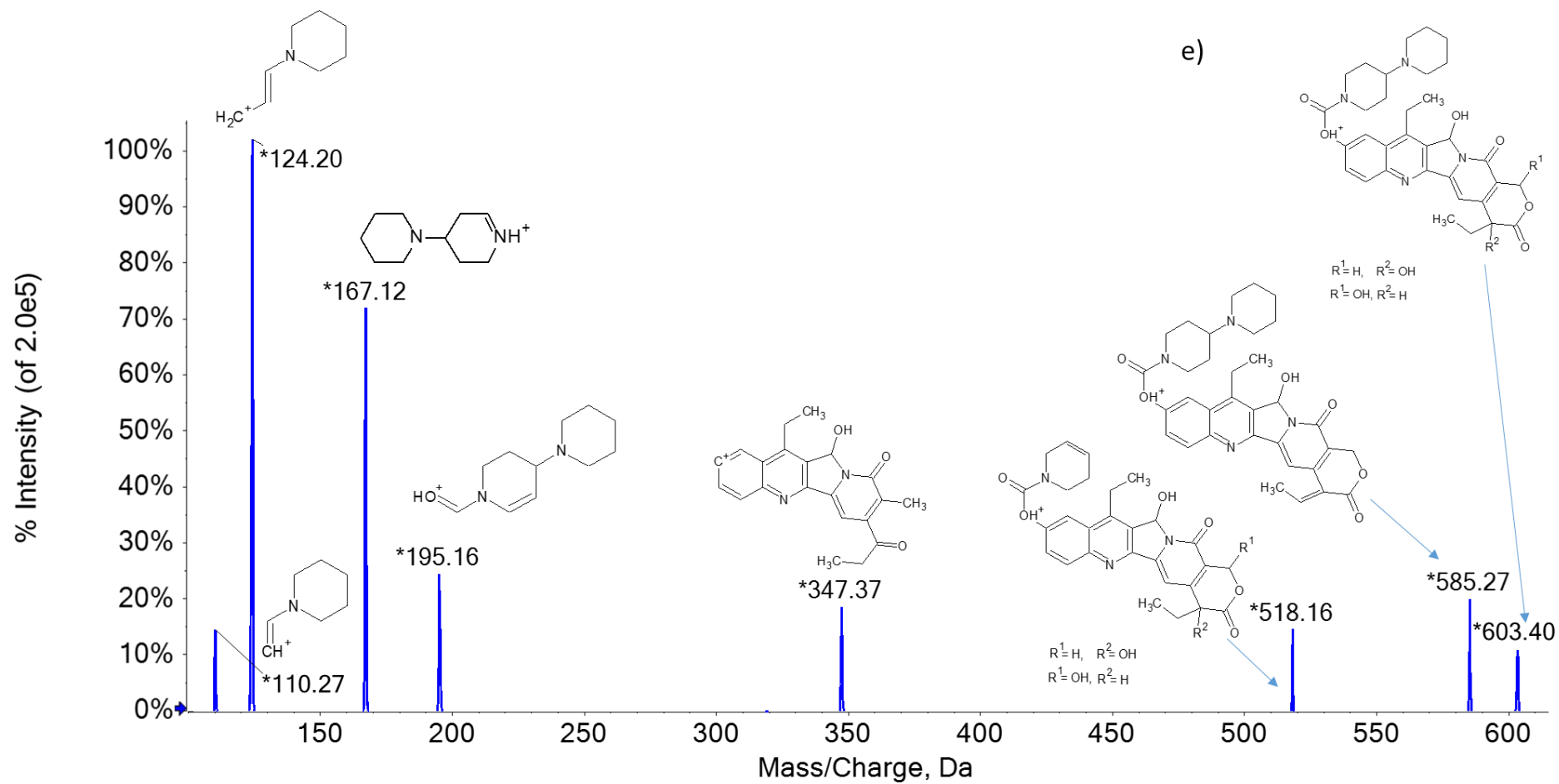


Figure S3.3e.

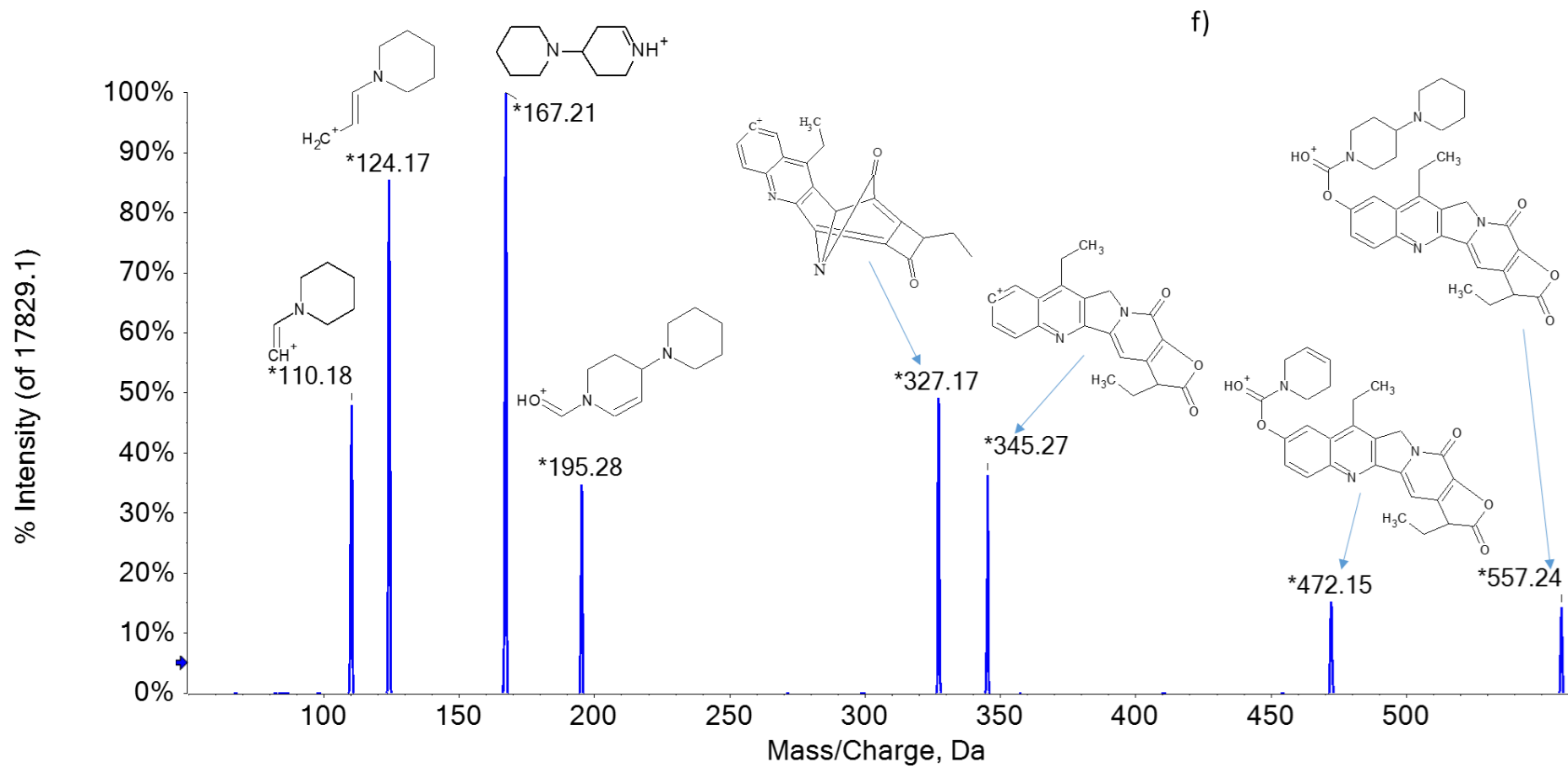


Figure S3.3f

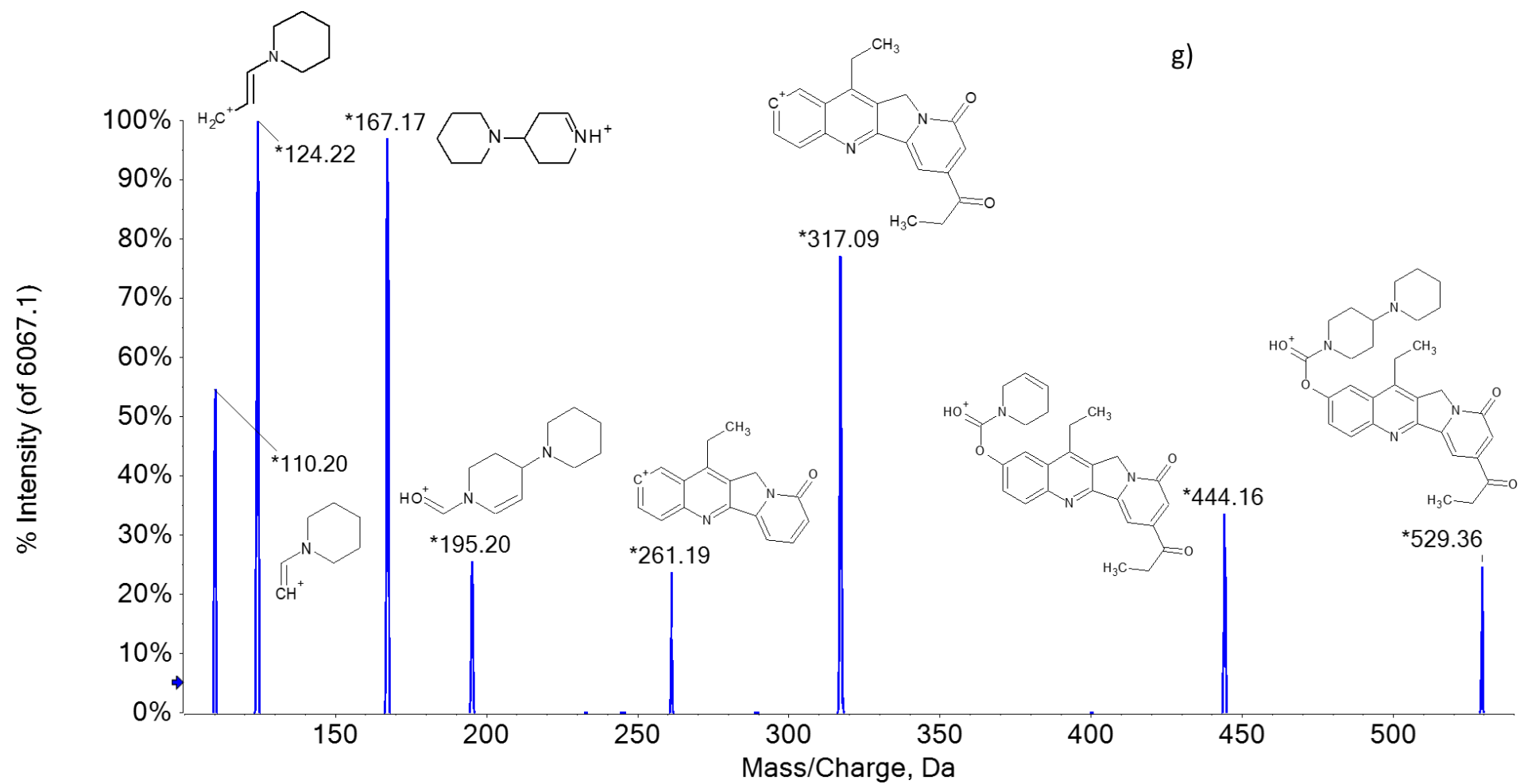


Figure S3.3g.

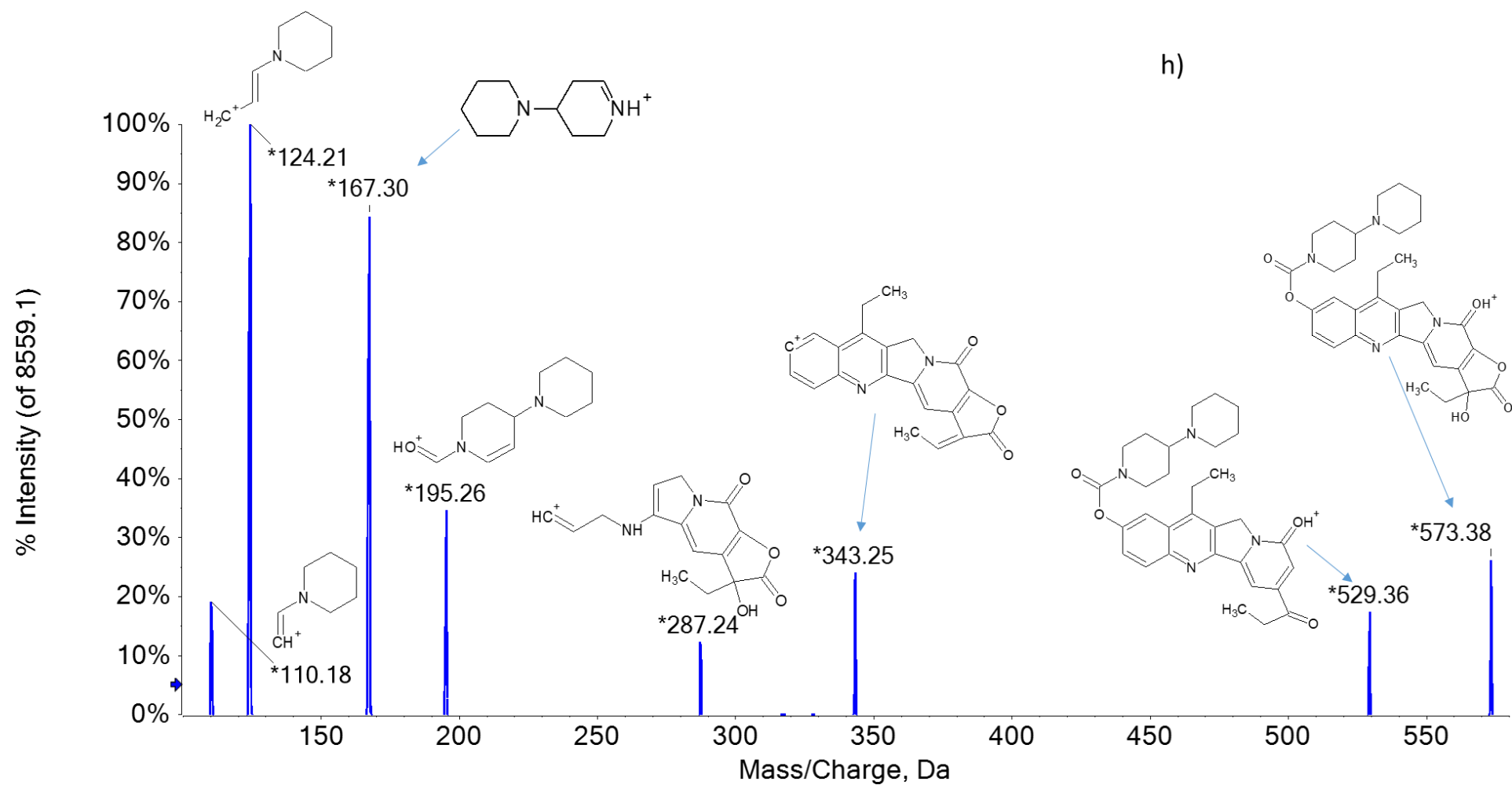


Figure S3.3h.

Figure S3.3. MS/MS spectra of PDPs with proposed chemical structures. a) PDP1; b) PDP2; c) PDP3; d) PDP4; e) PDP5; f) PDP6; g) PDP7; h) PDP8

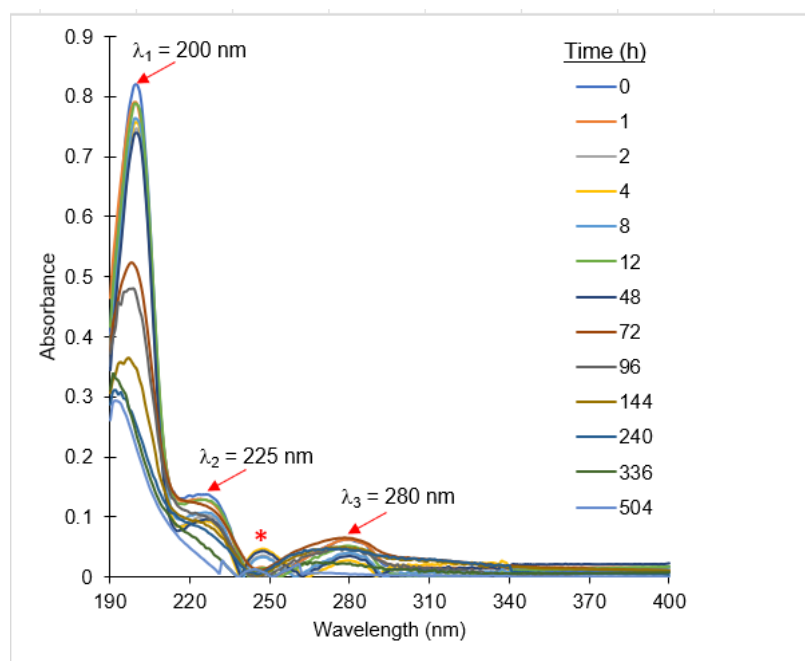


Figure S3.4. The photodegradation of aliskiren: UV/Vis absorbance spectrum measured as a function of solar light irradiation time ($\lambda_1 = 200$ nm, $\lambda_2 = 225$ nm, $\lambda_3 = 280$ nm).

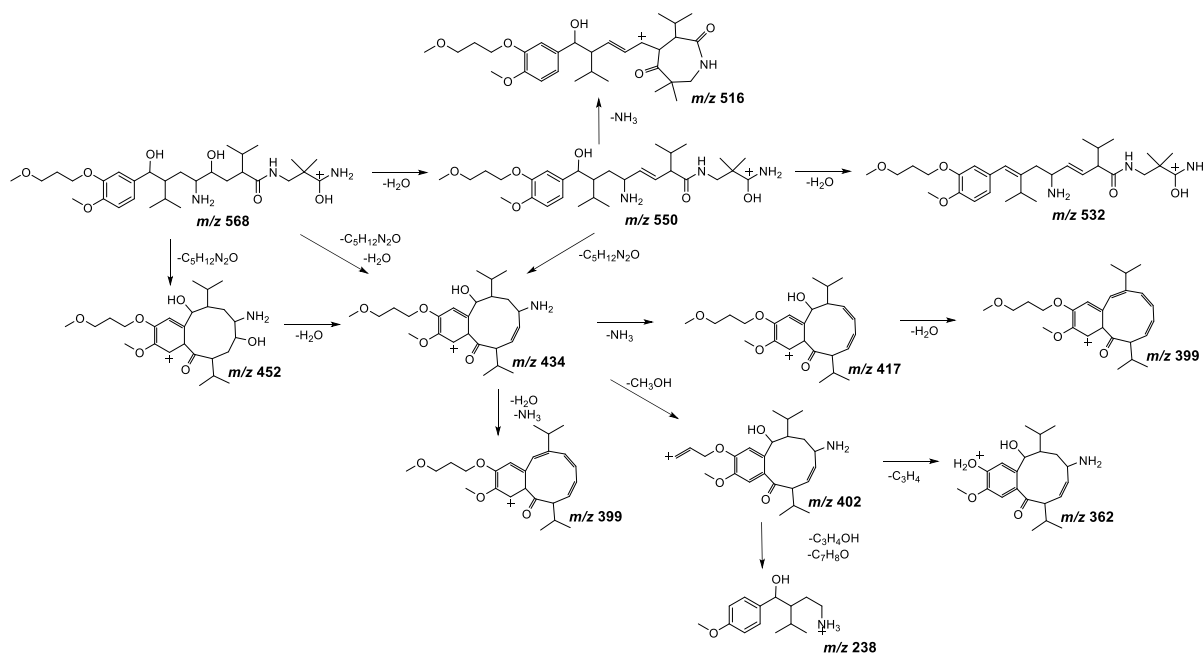


Figure S3.5. CID mechanism for the compound TP6 (m/z 568) of aliskiren

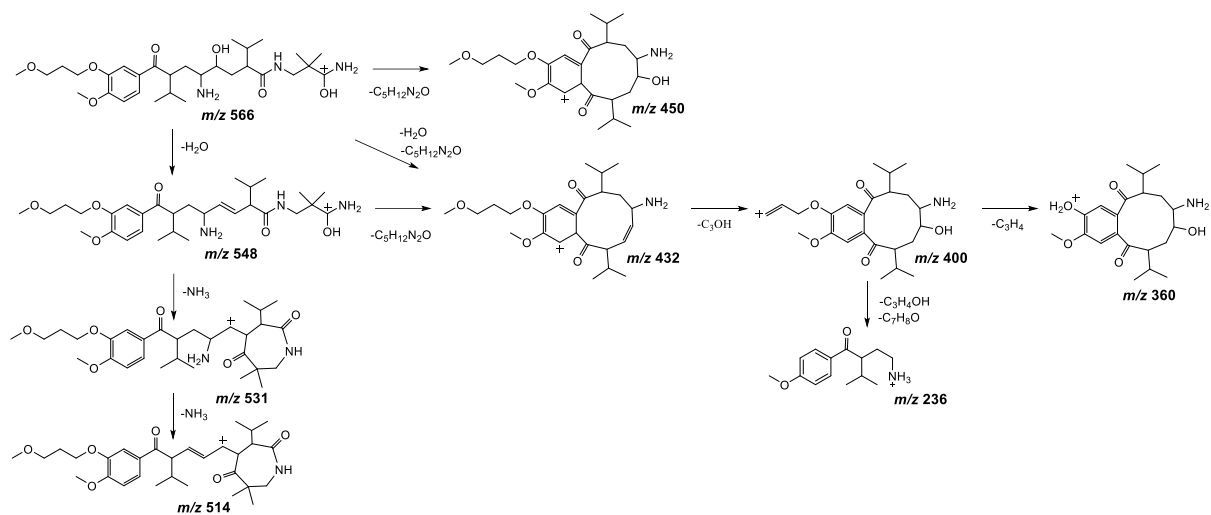


Figure S3.6. CID mechanism for the compound TP5 (m/z 566) of aliskiren

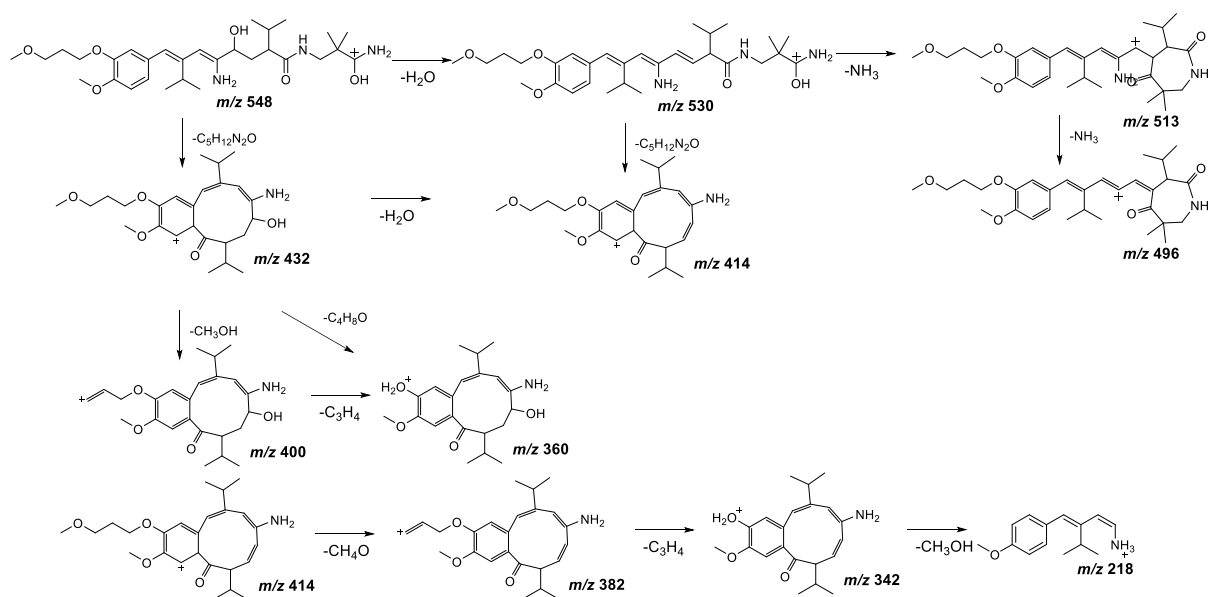


Figure S3.7. CID mechanism for the compound TP4 (m/z 548) of aliskiren

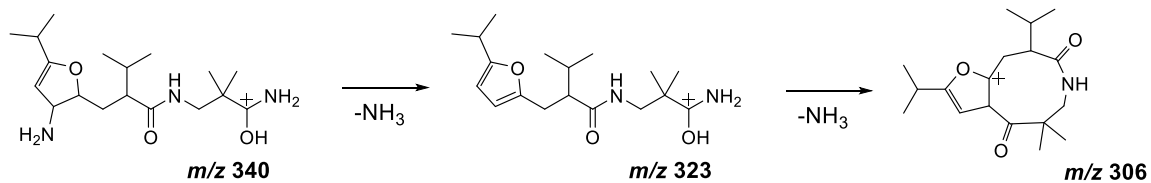


Figure S3.8. CID mechanism for the compound TP1 (m/z 340) of aliskiren

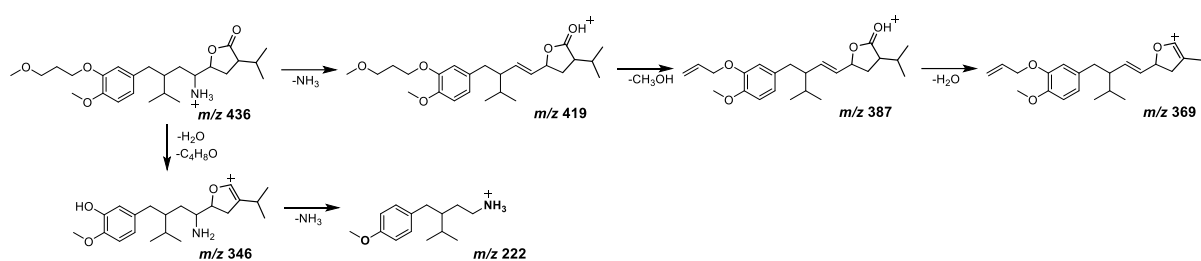


Figure S3.9. CID mechanism for the compound TP2 (m/z 436) of aliskiren

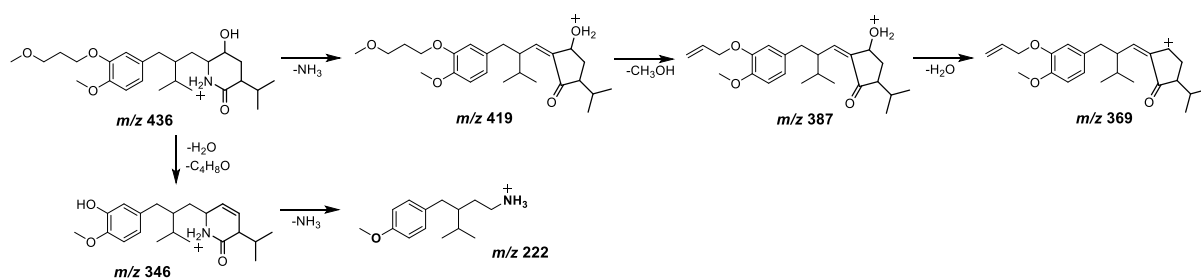


Figure S3.10. CID mechanism for the compound TP3 (m/z 436)

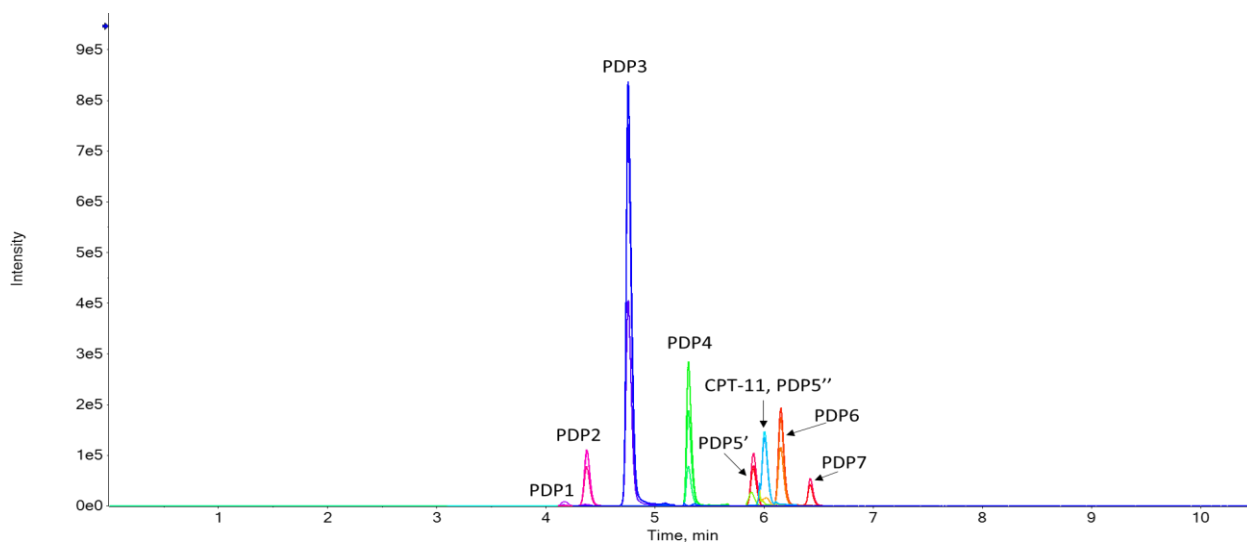


Figure S3.11. Extracted ion chromatogram of irinotecan and all PDPs in Po river water solution diluted 1/10 (v/v) and previously spiked at 10.0 mg/L with irinotecan and subjected to irradiation for 8 h.

Appendix II

g-C₃N₄/ZnWO₄ Composite Photocatalyst: Preparation and Enhanced Photocatalytic Activity

1. Introduction

This section of the Thesis details the research activities I conducted during my secondment at the Karadeniz Technical University (KTU) in Trabzon, Turkey. These works were not directly applicable to my thesis, which is why they are provided in a separate chapter as an Appendix.

The secondment research was initially planned to focus on the application of experimental design (DOE) techniques to optimize the photocatalytic degradation of CECs using graphitic carbon nitride (g-C₃N₄) doped zinc oxide (ZnWO₄) composite photocatalyst (g-C₃N₄/ZnWO₄). However, preliminary experiments devoted to the preparation of the desired catalyst, specifically determining the optimal weight ratio of g-C₃N₄ to be incorporated with ZnWO₄ in order to produce an efficient g-C₃N₄-ZnWO₄ catalyst, consumed the majority of the secondment period, and we were unable to apply DOE as anticipated. Nevertheless, we were able to produce a g-C₃N₄/ZnWO₄ composite photocatalyst with enhanced activity (as compared to the pure ZnWO₄). The model CEC selected for the photocatalytic degradation was ibuprofen (IBU). We were also interested in investigating the degradation of ibuprofen using TiO₂ and TiO₂/ZnO-based thin films; however, preliminary results were not encouraging, and time constraints prevented us from exploring further these materials. Besides, I collaborated with a researcher from the AQUALity project (ESR8 - Bethel Anucha) who had an ongoing work on the development of CuWO₄ doped TiO₂ photocatalyst for the removal of carbamazepine from water. Our collaboration was successful, and we managed to produce an article detailing the results from that effort. The article can be found at <https://doi.org/10.3390/separations8030025>.

In this chapter, the preparation, characterization, and photocatalytic activity of a g-C₃N₄/ZnWO₄ composite photocatalyst towards ibuprofen (IBU) will be summarized.

2. Background of the study

The occurrence of emerging contaminants of concern (CECs) in the environment (e.g., pharmaceuticals, per- and polyfluoroalkyl substances, personal care products, endocrine disrupting compounds, pesticides, etc.) has received great attention in recent years [1, 2]. CECs are not regulated, are not included in daily routine water analysis, and little to no information is available regarding their potential risk to aquatic biota and humans [3]. Concern over these compounds is increasing due to their persistence, bioactivity, and bioaccumulation potential, as well as their unknown harmful effects on aquatic ecosystems and human health [4-6].

Several studies have established a link between the presence of CECs in the aquatic environment and their inefficient removal from wastewater treatment plants. As a result, research has focused on developing technologies capable of managing these bio-recalcitrant chemicals and removing them efficiently [7]. Heterogeneous photocatalysis, a type of advanced oxidation process (AOP), has emerged as one of the most attractive environmental remediation technologies due to its potential to generate highly reactive oxidizing species capable of removing a wide variety of contaminants [8]. Titanium dioxide and zinc oxide have been widely recognized as the leading semiconductors for this purpose because of their high chemical and physical stability, broad adsorption range, strong electronic coupling coefficient, and photostability [9-11].

Several studies are now being conducted to identify new candidate catalysts. Among the different alternatives being researched are tungsten materials. Due to their novel structures and physico-chemical properties, tungsten materials are extremely versatile and can be used in a wide number of applications, including magnetic and fluorescent materials, optical fiber, humidity sensors, light emitting materials, and laser hosts [12]. In the realm of heterogeneous photocatalysis, ZnWO_4 is one of the most widely studied metal tungstate materials for CECs abatement [13]. However, due to the wide band gap (3.69 eV) [14], its application has been limited to a small portion of the solar spectrum and numerous experimental attempts are being made to improve the catalytic activity through morphologies, crystallinity, and doping [15].

Due to its narrow band gap (2.7 eV) and extremely high thermal and chemical stability, polymeric graphite phase carbon nitride (g-C₃N₄) has gained notable scientific interest for its applications in organic pollutants degradation [16]. Additionally, because of its huge specific surface area and 2D planar coupling structure, g-C₃N₄ can serve as a platform for anchoring different substrates; hence, the photodegradation of CECs using innovative composite photocatalysts based on g-C₃N₄ has been explored [17].

The aim of this study was to enhance the photocatalytic activity of ZnWO₄ towards CECs degradation by doping it with g-C₃N₄. The desired g-C₃N₄/ZnWO₄ photocatalysts were synthesized by hydrothermal method - a promising liquid phase preparation method that has grown in popularity in recent years. The method is simple to operate and allows for precise control of the crystal size, morphology, and agglomeration of ceramic oxides by adjusting the precursor material ratio, the pH of the reaction system, the reaction duration, and temperature [13]. The photocatalytic activity of the synthesized g-C₃N₄/ZnWO₄ composite materials was evaluated for ibuprofen degradation, and promising results were obtained.

3. Experimental section

3.1 Chemicals and reagents

Sodium tungstate dihydrate (Na₂WO₄·2H₂O; >99%), zinc nitrate hydrate (Zn(NO₃)₂·6H₂O; >99%), N,N-Dimethylformamide (DMF; ≥99.9%), Ibuprofen (>99%), ethanol, acetone, sodium hydroxide, and hydrochloric acid were purchased from Sigma Aldrich (Darmstadt, Germany). All chemicals were of analytical grade and used as purchased without further purification. Milli-Q water was used throughout the entire experiment for the photocatalytic studies.

3.2 Preparation of the g-C₃N₄/ZnWO₄ photocatalyst

The ZnWO₄ powder was prepared by co-precipitation assisted hydrothermal method described elsewhere [13]. First, 25 mL of equal molar solutions (0.1 M) of sodium tungstate (Na₂WO₄·2H₂O) and zinc nitrate (Zn(NO₃)₂·6H₂O) were prepared separately in distilled-deionized water (dd-H₂O). Each solution was magnetically stirred at room temperature (RT) for about 15 min until no more precipitation was observed. Then, both solutions were transferred slowly into a 200 mL glass beaker and mixed under magnetic stirring at RT. After vigorous stirring for 15 min, a white emulsion was formed. The mixture was transferred into a

Teflon-lined stainless-steel autoclave, heated at 150 °C for 5 h and cooled down naturally. The milky white gel was progressively washed with dd-H₂O, ethanol, and acetone and dried at 85 °C on a hot plate for 24 h. After that, the sample was ground into fine powders and then calcined at 600 °C for 2 h in air with a heating rate of 10 °C/min. The final product was a pure ZnWO₄ powder.

The **g-C₃N₄** powder was prepared as follows: First, 10 g of urea was partially dissolved in 20 mL of dd-H₂O with vigorous magnetic stirring for 1 h at RT. The colloidal suspension obtained was evaporated at 90 °C for 2 h. The resultant product was collected, and then was ground in fine powders. The g-C₃N₄ powder was calcined at 550 °C for 2 h in air with a heating rate of 10 °C/min. The resulting product was collected, finely ground, and calcined at 550 °C for 2 hours in air at a rate of 10 °C/min to obtain a pure g-C₃N₄ powder.

The **g-C₃N₄/ZnWO₄** photocatalysts were prepared as follows: The desired amount of g-C₃N₄ was completely dispersed in dimethylformamide (DMF) for 30 min under ultrasonic stirring. The as-prepared ZnWO₄ powder was then added into the g-C₃N₄ suspension and magnetically agitated at 150 °C until the solvent was completely vaporized. The obtained material was washed in ethanol and dd-H₂O. Finally, the sample was dried at 100 °C before being calcined at 300 °C for 4 h. We prepared samples with various mass ratios (i.e., 1, 2, 3, 4, 5, 6, 7, 8, 9, and 10% (w/w)), and all the g-C₃N₄/ZnWO₄ composites were referred to as CZ_x, where x denotes the weight percentage of g-C₃N₄. Photocatalytic experiments performed using all ten photocatalysts revealed that the 5% g-C₃N₄ doped ZnWO₄ (CZ5) had the best performance. As a result, this material was used for the characterization procedures along with the pristine ZnWO₄.

3.3 Characterization

The prepared photocatalyst was characterized using several techniques as detailed elsewhere [18, 19]. The crystal structures of the samples were determined by X-ray diffraction (XRD) measurements were performed on a D/Max-IIIC diffractometer (RIGAKU Corp; Tokyo, Japan) at room temperature using CuK α radiation in the 2 θ range of 10° - 70°, operating at 35 kV and 25 mA at a scan speed of 3°/min. Transmission Electron Microscopy (TEM) images were taken by using a Hitachi HighTech HT7700 Microscope. X-ray photoelectron spectroscopy (XPS) analyses were performed by Thermo Scientific K-Alpha using AlK α radiation with an energy of 1486.6 eV. Optical properties of the materials and band gap energies were obtained with UV-Vis diffuse reflectance spectroscopy (UV-Vis DRS) recorded by a Shimadzu UV-3600 Plus in the range of 300–1100 nm in absolute measurement using BaSO₄ reference plate. The Brunauer–Emmett–Teller (BET) surface area of the samples was

recorded on the nitrogen adsorption–desorption at 76 K using a Micromeritics 3 Flex version 5.00 (Micromeritics, Norcross, GA, USA). *Raman spectra* were recorded with WITech alpha 300R spectrometer (WITec Instruments Corp., Knoxville, TE, USA).

3.4 Photocatalytic experiments

The photocatalytic activity of the different photocatalysts (CZ_x) was evaluated towards the degradation of IBU under near visible light ($\lambda=365$ nm). The photocatalytic experiments were carried out in quartz cells placed under magnetic stirring. In a typical experiment, the photocatalyst (1.0 g/L) was dispersed in a 20 mL aqueous solution of IBU (10 mg/L) and allowed to reach adsorption–desorption equilibria in the dark assisted by magnetic stirring for 30 min. Next, the solutions were irradiated maintaining a sample-to-lamp distance of 30 cm. The irradiation source was composed of five 100 W UV Philips Mercury (Hg) lamps (TL-K 40W/10R ACTINIC BL REFLECTOR, Hamburg, Germany) with an intensity of 1.2 mW/cm² [20]. At certain prefixed time intervals (i.e., before dark, after dark, 0.25, 0.5, 1, 2, 3, and 4 h of exposure), about 2.0 mL aliquot was sampled and filtered using 0.45 μ m membrane syringe filters. In addition to photocatalytic experiments, the contributions of both photolysis and dark hydrolysis were evaluated.

The concentration of IBU was determined using an Agilent 1260 Infinity II LC system equipped with an Agilent G1315D Diode Array Detector (Agilent Corporation, Santa Clara, CA, USA). The analytical column was a Kinetex EVO C18 (150 \times 4.6 mm, 5.0 μ m), and the mobile phase comprised of 50 mM phosphate buffer (pH 7.5) and acetonitrile (30:70 *v/v*) at a flow rate of 1.0 mL/min. For quantitative analyses, selective detection of IBU was performed at 222 nm. Unless otherwise stated, all experimental data were the average of duplicate measurements.

4. Results and discussion

4.1 X-ray diffraction (XRD) analysis

XRD analysis was performed to determine the crystalline nature and purity of the materials. The XRD pattern of the pristine g-C₃N₄, ZnWO₄, and CZ₅ materials is shown in Fig. (i). The XRD diffraction pattern of g-C₃N₄ showed an intense broad peak at 27.8°, indexed to (002) planes due to the stacking of graphite-like conjugated triazine aromatic sheets with a 0.33 nm interlayer distance, which was consistent with the Joint Committee on Powder Diffraction Standards (JCPDS) card no. 87-1526 [21]. For ZnWO₄, the typical peaks correspond to (010), (100), (011), (110), (111), (021), (200), (121), (130), (-221) and (113) planes respectively. All the peaks were indexed and well-matched to the monoclinic wolframite ZnWO₄ (JCPDS card no. 15-0774, space group P2/c), indicating that no other impurities exist. Moreover, the strong

and sharp peaks at (111), (100), and (021) planes indicate that the as-prepared ZnWO₄ sample was highly crystalline [22]. As can be seen from the XRD pattern of the 5% C₃N₄ doped ZnWO₄, the introduction of g-C₃N₄ onto ZnWO₄ had no effect on the crystalline phase of the as-prepared ZnWO₄. There were no new crystal phases observed, and no solid-state processes were recorded.

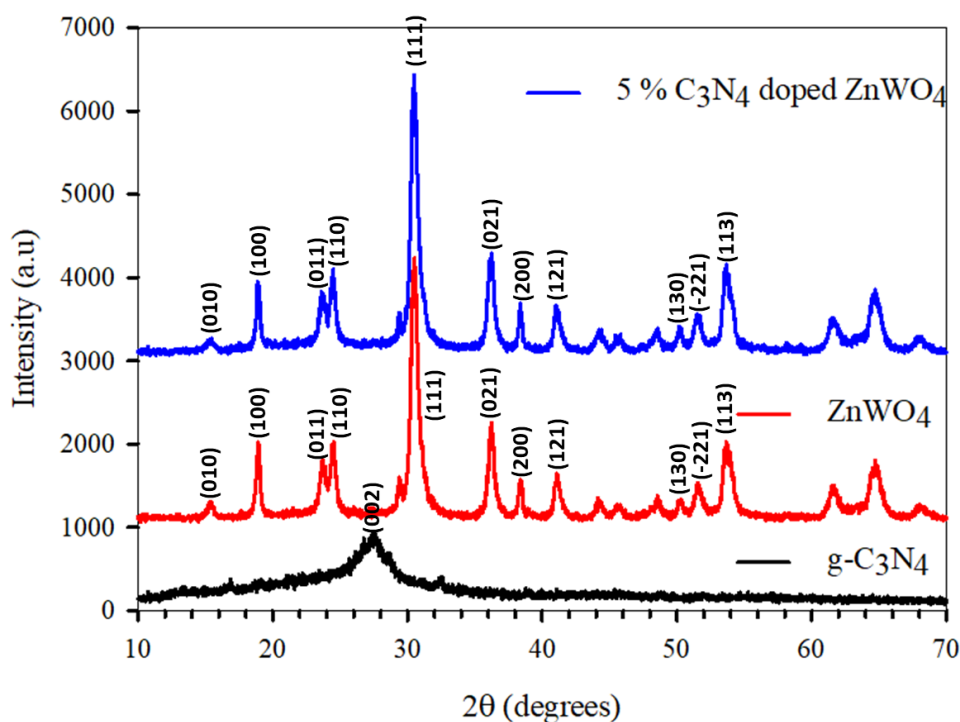


Figure (i). XRD pattern of g-C₃N₄, ZnWO₄, and g-C₃N₄/ZnWO₄

4.2 Transmission electron microscopy (TEM) analysis

The surface morphology of the synthesized materials was studied using transmission electron microscopy (TEM). In Fig. (ii), TEM images of the pure ZnWO₄ and the CZ5 composite are displayed. Fig. (ii)a shows that the pristine ZnWO₄ exhibits a consistent rod-like shape in the TEM image. Previous studies have shown that pristine g-C₃N₄ has a nanosheet-like morphology [23]. As depicted in Fig (ii)b, the g-C₃N₄ nanosheets were successfully deposited on the ZnWO₄ particles.

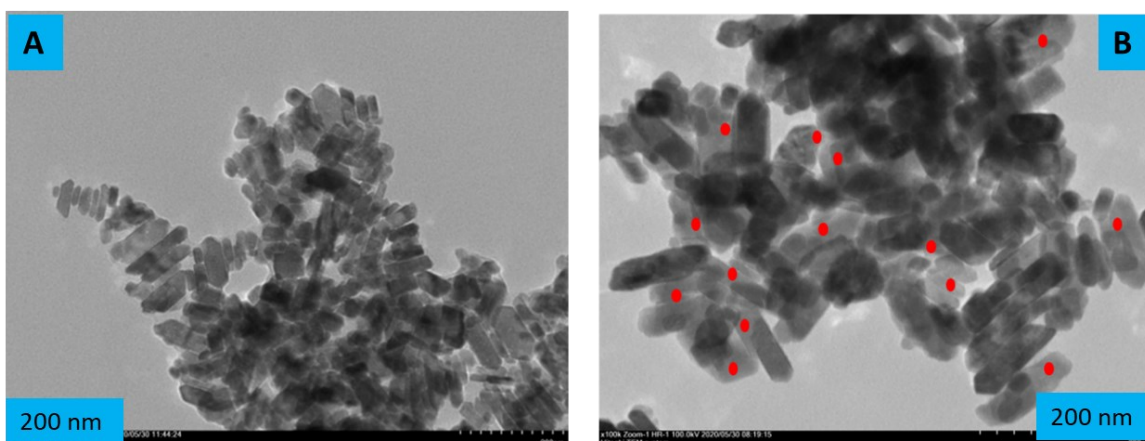


Figure (ii). Representative TEM images of (a) pristine ZnWO_4 and (b) $\text{g-C}_3\text{N}_4/\text{ZnWO}_4$

4.3 Raman spectroscopy analysis

The lattice vibration of semiconductors, which influences the energy band structure and information of the carrier, can be investigated using optical measurements obtained from the non-destructive Raman spectroscopy. According to [24], interconnected zigzag chains of deformed ZnO_6 and WO_6 octahedra, running parallel to the c -axis, provide the monoclinic wolframite-type structure of ZnWO_4 . In our work, as shown in Fig. (iii), the internal vibrations of the WO_6 octahedra of ZnWO_4 are assigned to the Raman peaks of ZnWO_4 nanoparticles at 190, 273, 343, 407, 544, 676, 707, 782, and 909.

By comparing the Raman spectra of pristine ZnWO_4 and the CZ5 composite, we can determine that all the observed Raman peaks are characteristic of the monoclinic wolframite structure ZnWO_4 [25] without any significant shift. Two prominent intense vibration modes at 909 and 343 cm^{-1} correspond to the typical W-O vibrations of the WO_6 octahedra, whereas the modes at 707 and 676 cm^{-1} involve WO_6 octahedra motions opposite to the Zn^{2+} . Bands between 500 and 600 cm^{-1} are typical of symmetric W-O-W stretching modes. The medium to strong peaks at 782, 544, 407, and 190 cm^{-1} are obtained from the symmetric stretching of ZnO_6 octahedra, while the other bands in the 400–600 cm^{-1} range are related with Zn-O stretching.

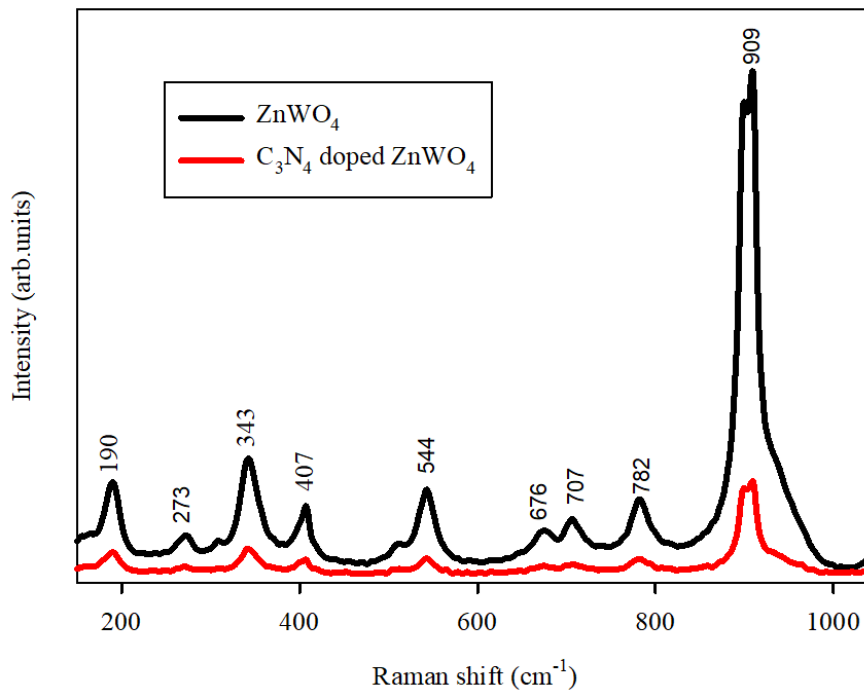


Figure (iii). Raman spectra of pristine ZnWO₄ (black line) and CZ5 (red line)

4.4 X-ray photoelectron spectroscopy (XPS) analysis

The elemental composition and valence states of CZ5 was evaluated by XPS spectra. The survey spectrum in Fig. (iv)a revealed the existence of Zn, W, and O originating from the ZnWO₄, but also the presence of C and N indicates the successful incorporation of the graphitic C₃N₄ into the composite. The high-resolution spectra of Zn 2p, W 4f, O 1s, C 1s, and N 1s are shown in Fig. (iv) b-f. In Fig. (iv)b, the Zn 2p_{3/2} and Zn 2p_{1/2} binding energies were 1020.4 and 1043.3 eV respectively, which suggests the presence of Zn²⁺ ions [26]. The doublets observed for the W 4f spectrum (Fig. (iv)c) of CZ5 with the peaks at 37.9 eV and 35.4 eV representing the W 4f_{5/2} and W 4f_{7/2} in the W⁶⁺ chemical state respectively [27]. The XPS spectrum of O 1s is presented in Fig. (iv)d, with the major peak at 531.5 eV corresponding to the lattice oxygen in ZnWO₄ and the peaks at 529.7 and 531.5 eV (green) correspond to single bond hydroxyl and adsorbed H₂O, respectively [7].

In Fig. (iv)e, the major binding energy at 287.7 eV corresponds to sp²-bonded carbon (C-C=N) and the peak at 284.6 eV can be ascribed to the C-C coordination of carbon [28]. The binding energies of C 1s at 287.7 eV of the CZ5 composite were slightly lower than those observed for the pure g-C₃N₄ (288.3 eV), which could be attributed to the interactions between g-C₃N₄ and ZnWO₄. The N 1s peak of the CZ5 composite is shown in

Fig. (iv)f. The peak 398.1 eV could be attributed to the sp^2 -bonded nitrogen in triazine rings (C–N=C) [29].

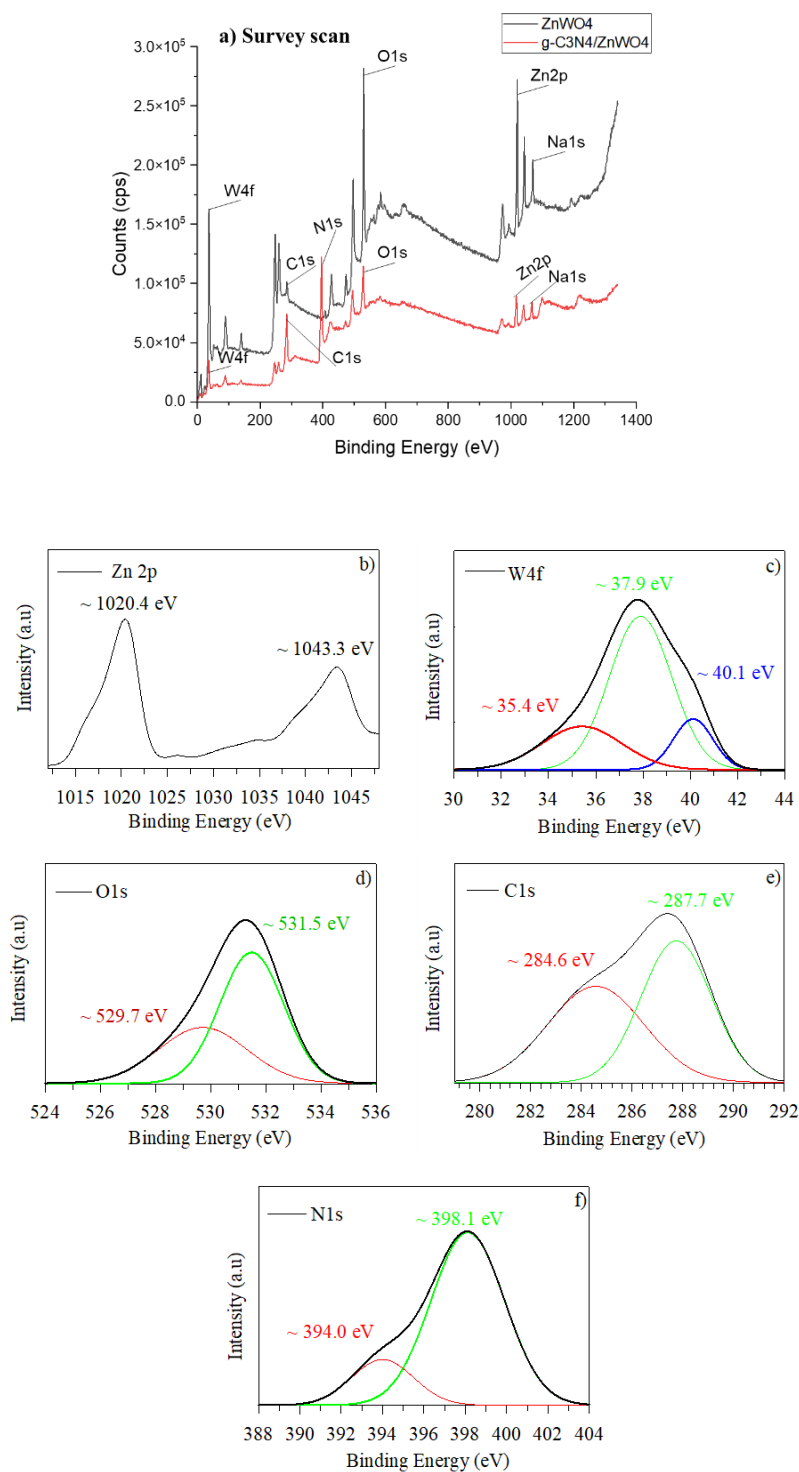


Figure (iv). XPS measurement of samples: (a) Survey spectrum of CZ5; and the corresponding deconvoluted spectrum of (b) Zn 2p, (c) W 4f, (d) O 1s, (e) C 1s, (f) N 1s.

4.5 UV-Vis diffuse reflectance spectroscopy (UV-Vis DRS) analysis

Energy band gaps of ZnWO₄ and 5%-CZ photocatalyst materials were evaluated according to the Tauc relation (Tauc 1968) using Eq. (i).

$$\alpha h\nu = A(h\nu - E_g)^{n/2} \quad \text{Eq. (i)}$$

where α , h , ν , E_g , and A represent the absorption coefficient, Planck's constant, frequency of the incident photon, bandgap energy, and a proportionality constant, respectively. As illustrated in Fig. (v), the energy band-gap (E_g) values were determined from the intercept of the extrapolated straight line to the energy axis ($ah\nu$)² curves. They were found to be 3.0 eV and 3.7 eV for g-C₃N₄/ZnWO₄ and ZnWO₄, respectively. The obtained results are consistent with previously reported values for the energy band gap of ZnWO₄ [14] and g-C₃N₄ modified ZnWO₄ nanorods [23]. The present results showed that the incorporation of the g-C₃N₄ can greatly inhibit charge carrier reunion [23] and, therefore, shift the light-response capability to the visible range.

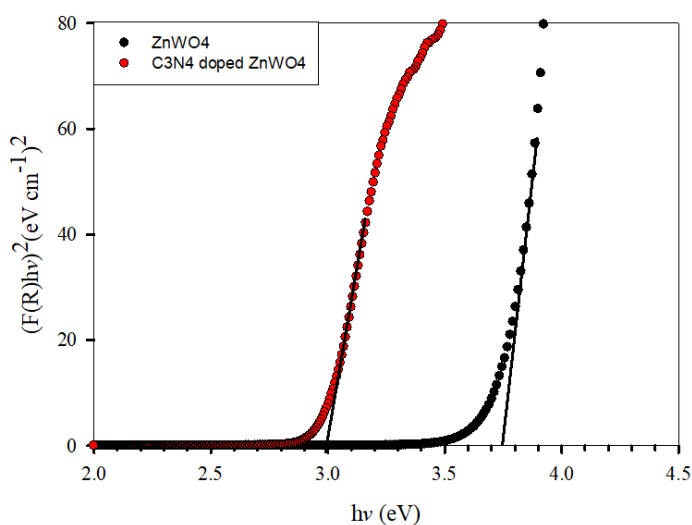


Figure (v). UV-Vis DRS plot of ZnWO₄ (black) and g-C₃N₄/ZnWO₄ (red)

4.6 Photocatalytic activity

Ten different g-C₃N₄/ZnWO₄ materials were prepared with 1, 2, 3, 4, 5, 6, 7, 8, 9, 10% of g-C₃N₄ being incorporated with ZnWO₄. The materials were designated as CZx, where x represents the % compositions.

The photocatalytic activity of each material was investigated towards the degradation of ibuprofen in water using near visible light irradiation ($\lambda=365$ nm). Besides, the photolytic

degradation without adding any catalyst was investigated. Fig. (vi) shows the degradation efficiency achieved by each material tested. The contribution of photolysis was negligible. The composite samples were all found to have higher photocatalytic activity than the pure ZnWO_4 . Compared to the pristine $\text{g-C}_3\text{N}_4$, all CZx composites except CZ1 had resulted in higher degradation performance towards IBU. Moreover, the best photocatalyst was found to be the CZ5 resulting in complete degradation of IBU after 4 h of irradiation.

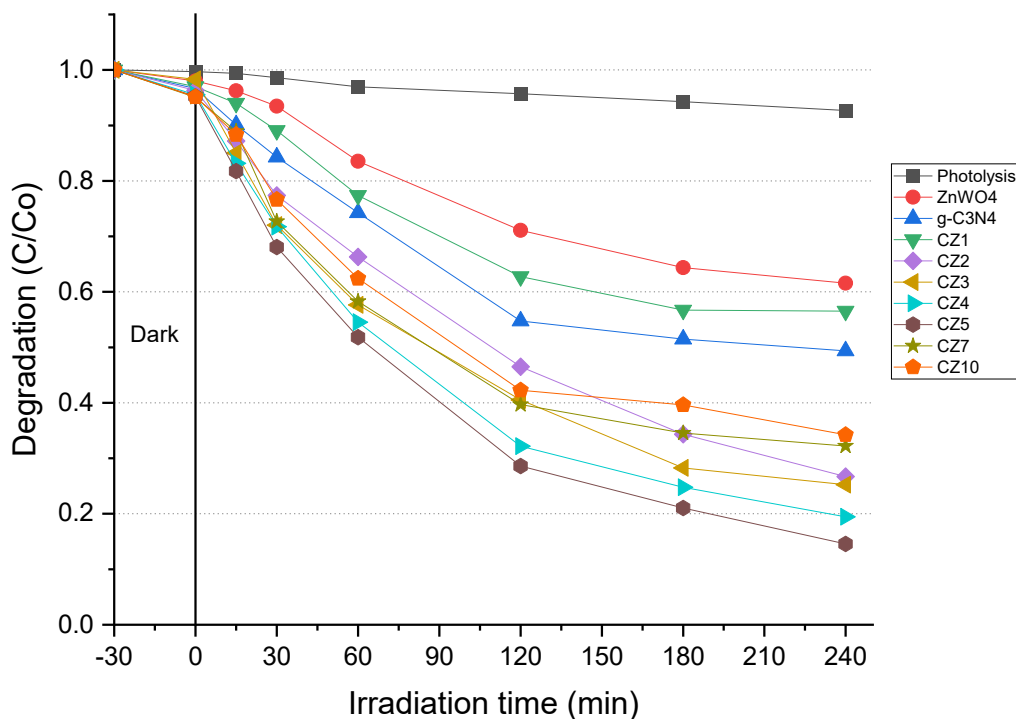


Figure (vi). Photodegradation of IBU using photolysis and all the prepared materials.

In addition, the photocatalytic performance of the synthesized photocatalysts was described using a pseudo-first-order kinetics model given by Eq. (ii), where C_0 represents the maprotiline initial concentration, C is the concentration at reaction time t , and k is the pseudo-first-order kinetic constant.

$$\ln(C) = -kt + \ln(C_0) \quad \text{Eq. (ii)}$$

The kinetics of IBU degradation for all prepared samples are depicted in Fig. (viii), and pertinent statistical values are shown in Table (i). Notably, as can be seen in Fig. (vii), the CZ5 composite demonstrated a significantly higher k value than the other materials, resulting in a rate constant of IBU degradation 5.24 times greater than pristine ZnWO_4 .

Table (i). Calculated first order kinetic parameters.

	Intercept Value	Intercept Standard Error	Slope Value	Slope Standard Error	Statistics Adj. R-Square
Photolysis	-0.0063	0.0018	-2.96×10^{-4}	1.55×10^{-5}	0.9810
ZnWO ₄	-0.038	0.019	-2.06×10^{-3}	1.60×10^{-4}	0.9594
g-C ₃ N ₄	-0.093	0.038	-2.99×10^{-3}	3.26×10^{-4}	0.9222
CZ1	-0.068	0.031	-2.48×10^{-3}	2.68×10^{-4}	0.9238
CZ2	-0.097	0.021	-5.23×10^{-3}	1.80×10^{-4}	0.9917
CZ3	-0.14	0.046	-5.70×10^{-3}	3.93×10^{-4}	0.9677
CZ4	-0.15	0.050	-6.68×10^{-3}	4.30×10^{-4}	0.9717
CZ5	-0.22	0.064	-1.08×10^{-3}	5.49×10^{-4}	0.9822
CZ7	-0.15	0.061	-4.77×10^{-3}	5.20×10^{-4}	0.9221
CZ10	-0.13	0.051	-4.39×10^{-3}	4.37×10^{-4}	0.9346

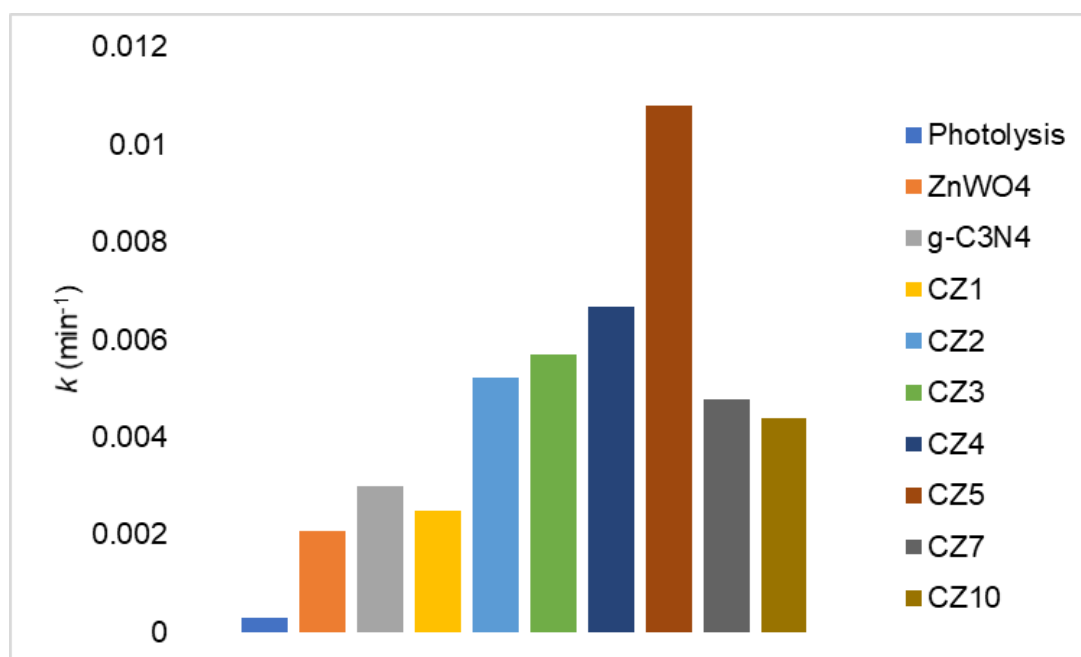


Figure (vii). Comparison of the estimated pseudo-first order model k values.

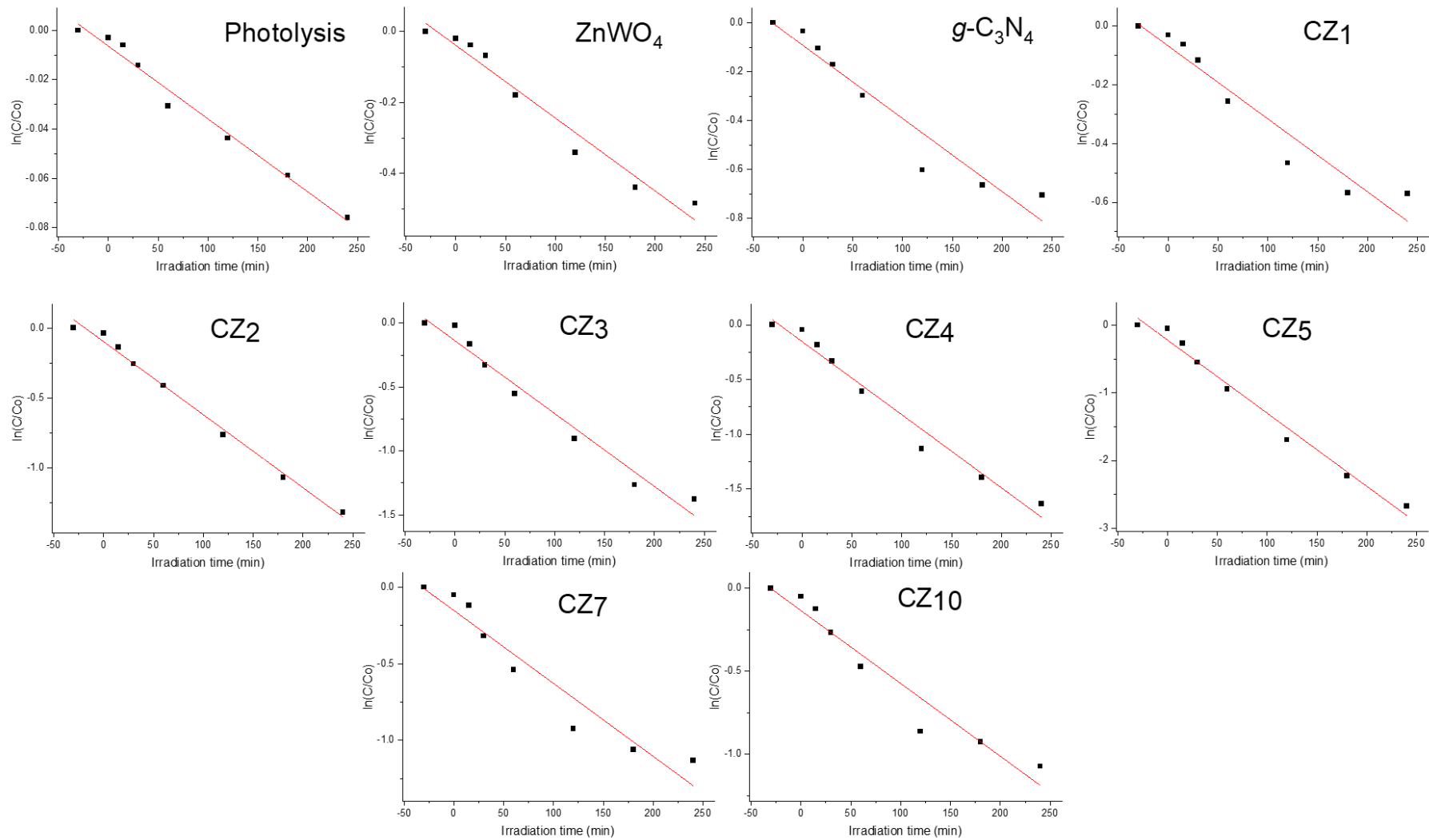


Figure (viii). Pseudo-first order kinetics of IBU degradation using photolysis and all the produced photocatalyst

5. Conclusions and forward

In this work, a g-C₃N₄/ZnWO₄ composite photocatalyst was synthesized by co-precipitation assisted hydrothermal method, homogenized in mixing under gentle mechanical agitation, and characterized for structural, morphological, and optical properties employing X-ray diffraction (XRD), transmission electron microscopy (TEM), X-ray photoelectron spectroscopy (XPS), Raman spectroscopy, and Ultraviolet-visible diffuse reflectance spectroscopy (UV-Vis DRS). Characterization studies revealed that the synthesized ZnWO₄ corresponded to the monoclinic wolframite structure. Moreover, incorporation of g-C₃N₄ into the ZnWO₄ structure resulted in a reduction in the energy band gap (E_g=3.0) compared to the unmodified ZnWO₄ (E_g=3.7). Under near visible light irradiation, the photocatalytic activity of the synthesized composite materials was investigated for the degradation of ibuprofen (IBU), and the catalyst containing 5% g-C₃N₄ (CZ5) exhibited superior performance. All degradation processes followed a pseudo-first order kinetics, with the highest rate constant recorded for CZ5 being 5.24 times higher than that of the pure ZnWO₄, suggesting that the enhanced photocatalytic activity of the catalyst.

Overall, the findings of this study were encouraging. However, we believe that by performing additional optimization experiments on the major parameters that affect the degradation efficiency (e.g., concentration of CEC, catalyst dose, pH of solution, matrix components, etc.), significant performance enhancements can be realized. We recommend the optimization of these parameters to be accomplished using experimental design (DOE) techniques to enable exploration of a broad range of the experimental domain with a small number of experiments, resulting in cost-effective and efficient experimentation. Moreover, we did not investigate the degradation mechanisms involved in the processes due to the lack of appropriate instrumentation. Thus, we recommend that future studies include mass spectrometric analysis of degraded samples to identify potential transformation products and, ultimately, the degradation mechanisms.

References

1. Patel, M., et al., *Pharmaceuticals of emerging concern in aquatic systems: chemistry, occurrence, effects, and removal methods*. Chemical reviews, 2019. **119**(6): p. 3510-3673.
2. Diamanti, K.S., et al., *Assessment of the chemical pollution status of the Dniester River Basin by wide-scope target and suspect screening using mass spectrometric techniques*. Analytical and bioanalytical chemistry, 2020. **412**(20): p. 4893-4907.
3. Dulio, V., et al., *NORMAN Prioritisation framework for emerging substances-Passive sampling interlaboratory study-data evaluation*. 2013.
4. Miller, T.H., et al., *A review of the pharmaceutical exposome in aquatic fauna*. Environmental pollution, 2018. **239**: p. 129-146.
5. Hollender, J., et al., *High resolution mass spectrometry-based non-target screening can support regulatory environmental monitoring and chemicals management*. Environmental Sciences Europe, 2019. **31**(1): p. 1-11.
6. Alygizakis, N.A., et al., *Evaluation of chemical and biological contaminants of emerging concern in treated wastewater intended for agricultural reuse*. Environment international, 2020. **138**: p. 105597.
7. He, D., et al., *Synergistic effect of TiO₂-CuWO₄ on the photocatalytic degradation of atrazine*. Environmental Science and Pollution Research, 2019. **26**(12): p. 12359-12367.
8. Byrne, C., G. Subramanian, and S.C. Pillai, *Recent advances in photocatalysis for environmental applications*. Journal of Environmental Chemical Engineering, 2018. **6**(3): p. 3531-3555.
9. Calza, P., et al., *Assessment of the abatement of acelsulfame K using cerium doped ZnO as photocatalyst*. Journal of hazardous materials, 2017. **323**: p. 471-477.
10. Gionco, C., et al., *Synthesis, characterization, and photocatalytic tests of N-doped zinc oxide: A new interesting photocatalyst*. Journal of Nanomaterials, 2016. **2016**.
11. Nakata, K. and A. Fujishima, *TiO₂ photocatalysis: Design and applications*. Journal of photochemistry and photobiology C: Photochemistry Reviews, 2012. **13**(3): p. 169-189.
12. Yan, J., et al., *Synthesis and photocatalytic properties of ZnWO₄ nanocrystals via a fast microwave-assisted method*. The Scientific World Journal, 2013. **2013**.
13. Rathi, V., A. Panneerselvam, and R. Sathiyapriya, *Graphitic carbon nitride (g-C₃N₄) decorated ZnWO₄ heterojunctions architecture synthesis, characterization and photocatalytic activity evaluation*. Diamond and Related Materials, 2020. **108**: p. 107981.
14. Lin, J., J. Lin, and Y. Zhu, *Controlled synthesis of the ZnWO₄ nanostructure and effects on the photocatalytic performance*. Inorganic chemistry, 2007. **46**(20): p. 8372-8378.
15. Pavithra, N., G. Nagaraju, and S. Patil, *Ionic liquid-assisted hydrothermal synthesis of ZnWO₄ nanoparticles used for photocatalytic applications*. Ionics, 2021: p. 1-9.
16. Yan, S., Z. Li, and Z. Zou, *Photodegradation of rhodamine B and methyl orange over boron-doped g-C₃N₄ under visible light irradiation*. Langmuir, 2010. **26**(6): p. 3894-3901.
17. Sun, L., et al., *Enhanced visible-light photocatalytic activity of g-C₃N₄-ZnWO₄ by fabricating a heterojunction: investigation based on experimental and theoretical studies*. Journal of Materials Chemistry, 2012. **22**(44): p. 23428-23438.
18. Bepalko, Y., et al., *La₂Zr₂O₇/LaAlO₃ composite prepared by mixing precipitated precursors: Evolution of its structure under sintering*. Materials Chemistry and Physics, 2020. **251**: p. 123093.

19. Trens, P., et al., *Synthesis and characterization of packed mesoporous tungsteno-silicates: application to the catalytic dehydrogenation of 2-propanol*. Applied Catalysis A: General, 2004. **263**(1): p. 103-108.
20. Anucha, C.B., et al., *Enhanced photocatalytic activity of CuWO₄ doped tio₂ photocatalyst towards carbamazepine removal under UV irradiation*. Separations, 2021. **8**(3): p. 25.
21. Ge, L., *Synthesis and photocatalytic performance of novel metal-free g-C₃N₄ photocatalysts*. Materials Letters, 2011. **65**(17-18): p. 2652-2654.
22. Fan, X. and X. Chen, *Facile synthesis of NFL-ZnWO₄ for pseudocapacitor applications*. 2019.
23. Koutavarapu, R., et al., *A novel one-pot approach of ZnWO₄ nanorods decorated onto gC₃N₄ nanosheets: 1D/2D heterojunction for enhanced solar-light-driven photocatalytic activity*. Journal of Materials Science, 2020. **55**(3): p. 1170-1183.
24. Kraus, H., et al., *Effect of Ca doping on the structure and scintillation properties of ZnWO₄*. physica status solidi (a), 2007. **204**(3): p. 730-736.
25. He, G., et al., *Synthesis, characterization and optical properties of nanostructured ZnWO₄*. Materials Science in Semiconductor Processing, 2016. **41**: p. 404-410.
26. Zhan, S., et al., *Synthesis of ZnWO₄ electrode with tailored facets: deactivating the microorganisms through photoelectrocatalytic methods*. Applied Surface Science, 2017. **391**: p. 609-616.
27. Osotsi, M.I., et al., *Synthesis of ZnWO₄-x nanorods with oxygen vacancy for efficient photocatalytic degradation of tetracycline*. Progress in Natural Science: Materials International, 2018. **28**(4): p. 408-415.
28. Tan, L., et al., *Synthesis of g-C₃N₄/CeO₂ nanocomposites with improved catalytic activity on the thermal decomposition of ammonium perchlorate*. Applied Surface Science, 2015. **356**: p. 447-453.
29. Shen, Q., et al., *gC₃N₄ nanoparticle@ porous gC₃N₄ composite photocatalytic materials with significantly enhanced photo-generated carrier separation efficiency*. Journal of Materials Research, 2020. **35**(16): p. 2148-2157.

Appendix III

(a) Secondments

From - to	Place	Tutor(s)	Description of research	Location in this Thesis
04/11/2019 – 31/12/2019	Karadeniz Technical University (KTU), Trabzon, Turkey	Prof. Emin Bacaksiz	Photocatalytic degradation of ibuprofen by g- C ₃ N ₄ /ZnWO ₄ composite catalyst: Optimization of parameters by full factorial design and response surface methodology.	Appendix II
06/01/2020 – 15/05/2020	Eurofins Environment A/S, Vejen, Denmark	Dr. Ulrich Precht and Dr. Peter Mortensen	Development and validation (ISO17025) of an online SPE-LC-MS/MS method for the simultaneous determination of 10 pharmaceutical compounds.	Chapter 3 – Part II
14/09/2020 – 18/11/2020	University of Ioannina (UOI), Ioannina, Greece	Dr. Vasilios Sakkas	Robustness studies on photocatalysis methods by exploiting experimental design and response surface methodology. Photocatalytic degradation methods already developed by other units within AQUALITY were used for this purpose.	Chapter 5
15/04/2021 – 04/06/2021	University of Turin (UniTO), Turin, Italy	Prof. Claudio Medana	Application of experimental design techniques for the optimization and the robustness study of photocatalytic degradation of emerging contaminants in water.	Chapter 5

(b) Publications

List of papers already published

1. Gosetti, F., Belay, M. H., Marengo, E., & Robotti, E. (2020). Development and validation of a UHPLC-MS/MS method for the identification of irinotecan photodegradation products in water samples. *Environmental Pollution*, 256, 113370; <https://doi.org/10.1016/j.envpol.2019.113370>.
2. Gonçalves, N. P., Iezzi, L., Belay, M. H., Dulio, V., Alygizakis, N., Dal Bello, F., ... & Calza, P. (2021). Elucidation of the photoinduced transformations of Aliskiren in river water using liquid chromatography high-resolution mass spectrometry. *Science of The Total Environment*, 800, 149547; <https://doi.org/10.1016/j.scitotenv.2021.149547>.
3. Anucha, C. B., Altin, I., Bacaksız, E., Kucukomeroglu, T., Belay, M. H., & Stathopoulos, V. N. (2021). Enhanced photocatalytic activity of CuWO₄ doped tio₂ photocatalyst towards carbamazepine removal under UV irradiation. *Separations*, 8(3), 25; <https://doi.org/10.3390/separations8030025>.
4. Papagiannaki, D., Belay, M. H., Gonçalves, N. P., Robotti, E., Bianco-Prevot, A., Binetti, R., & Calza, P. (2022). From monitoring to treatment, how to improve water quality: the pharmaceuticals case. *Chemical Engineering Journal Advances*, 100245; <https://doi.org/10.1016/j.ceja.2022.100245>.
5. Belay, M.H.; Precht, U.; Mortensen, P.; Marengo, E.; Robotti, E. (2022). A Fully Automated Online SPE-LC-MS/MS Method for the Determination of 10 Pharmaceuticals in Wastewater Samples. *Toxics*, 10(3), 103; <https://doi.org/10.3390/toxics10030103>.

List of papers in preparation

1. M.H. Belay, M. Manfredi, F. Dal Bello, S. Timo, M.C. Paganini, P. Calza, E. Marengo, C. Medana, E. Robotti, Optimization and robustness study of the photocatalysis of maprotiline by Ce-ZnO exploiting experimental design techniques.
2. M.H. Belay, F. Dal Bello, E. Marengo, C. Medana, E. Robotti, Optimization and robustness study of the photolysis of irinotecan exploiting experimental design techniques.

Position paper

1. A NORMAN & Water Europe joint Position Paper on “Contaminants of Emerging Concern in Urban Wastewater”, available on the [NORMAN website](#).

(c) Presentation in national and international conferences

Oral communications

1. M.H. Belay, D. Fabbri, "Prioritization and evaluation of contaminants of emerging concern in water", NIS Colloquium, 16 May 2019, University of Turin, Italy.
2. M.H. Belay, F. Gosetti, E. Marengo, E. Robotti, "Development and Validation of A UHPLC-MS/MS Method for the Identification of Irinotecan Photodegradation Products in Water Samples", XXVIII Congress of the Analytical Chemistry Division, 22-26 September 2019, Bari, Italy.
3. M.H. Belay, F. Gosetti, E. Marengo, E. Robotti, "Photodegradation study of irinotecan and identification of transformation products in water samples by UHPLC-MS/MS", the 3rd Summer School of the European PhD School on Advanced Oxidation Processes, 3-7 June 2019, Polytechnic University of Valencia – Alcoy Campus, Spain.
4. M.H. Belay, U. Precht, P. Mortensen, E. Marengo, E. Robotti, A fully automated online SPE-LC-MS/MS method for the determination of 10 pharmaceuticals in wastewater samples, The XVIII Chemometrics in Analytical Chemistry Conference, XX-XX 2021, Courmayeur (IT), postponed, planned.
5. PhD research progress has also been presented in 7 periodic meetings of the AQUAlity project.

Poster presentations

1. M.H. Belay, F. Gosetti, E. Marengo & E. Robotti, "Photodegradation study of cytotoxic drugs", *6th European Conference on Environmental Applications of Advanced Oxidation Processes (EAAOP-6)*, 26-30 June 2019, Portoroz, Slovenia.
2. F. Gosetti, M.H. Belay, E. Marengo & E. Robotti, "Sunlight photodegradation of cytotoxic drugs. Identification of photodegradation products by UHPLC-MS/MS in water samples", *XXVIII Congress of the Analytical Chemistry Division*, 22-26 September 2019, Bari, Italy.
3. M.H. Belay, F. Gosetti, E. Marengo & E. Robotti, "Photodegradation study of irinotecan and identification of transformation products in water samples by UHPLC-MS/MS", *Eurachem Workshop 2019*, 20-21 May 2019, University of Tartu, Estonia.
4. M. H. Belay, F. Gosetti, E. Marengo, E. Pisano, J. Luisetti, E. Robotti, "A validated UHPLC-MS/MS method for the identification of aliskiren photodegradation products in water", *68th ASMS Conference presented virtually as ASMS Reboot 2020*, 1–12 June 2020.

5. Nuno P. F. Gonçalves; Masho Hilawie Belay; Elisa Robotti; Claudio Medana; Alessandra Bianco Prevot; Paola Calza, “Elucidation of environmental fate of Maprotiline and Aliskiren drugs in natural waters: Identification of degradation products via HPLC-HRMS”, *68th ASMS Conference presented virtually as ASMS Reboot 2020*, 1-12 June 2020.
6. M.H Belay, E. Robotti, M.C. Paganini, C. Medana, F. Dal Bello, M. Manfredi, S. Timo, P. Calza, E. Marengo, “Application of experimental design techniques for the optimization and the robustness study of photocatalytic degradation of emerging contaminants in water”, *XXVII Congresso Nazionale della Società Chimica Italiana*, 14-23 September 2021.

(d) Outreach activities

Activity	Date	Place
European Researchers Night 2018	28/09/2018	UPO, Alessandria, Italy
European Researchers Night 2019	27/09/2019	UPO, Alessandria, Italy
AQUALity lab to upper secondary school students	28/01/2019 – 06/02/2019	UPO, Alessandria, Italy
AQUALity lab to primary and lower secondary school students	07 & 20 February 2019	UniTO, Turin, Italy
European Researchers Night 2020 (Virtual)	27/11/2020	UniTO, Turin, Italy

(e) Co-advising undergraduate and graduate students

Student's name	Thesis type	Status (Year)
Edoardo Pisano	Master's Thesis	Completed (2018/19)
Jessica Luisetti	Master's Thesis	Completed (2018/19)
Riccardo Magagnato	BSc Thesis	Completed (2019/20)
Alessia Fabbris	BSc Thesis	Completed (2020/21)
Flavia Repeto	BSc Thesis	Completed (2020/21)
Arianna Ghignone	BSc Thesis	Completed (2020/21)
Eleonora Goggi	BSc Thesis	In progress

(f) PhD courses and trainings attended

Year	When	Where	Title of the event	Type	Unit	Qty	CFU
2017/ 18	27-28/08/2018	Aalborg (Denmark)	The 2nd AQUALity symposium meeting	Symposium	h	16	0.4
	29-31/08/2018	Aalborg (Denmark)	International Summer Course on “Micropollutant Analysis and Emerging Technologies for their Abatement”	Summer School	h	24	3
	28/09/2018	Alessandria (Italy)	Notte dei ricercatori 2018 - Dissemination of research work to the public	Dissemination	h	16	1
	6-9/11/2018	Rimini (Italy)	Ecomondo - The Green Technologies Expo	Seminars	No	2	0.2
Annual Total							4.6
2018/ 19	10/2018 - 02/2019	Turin (Italy)	Innovation for the Circular Economy	PhD course	h	48	3
	01/2019 - 02/2019	Turin (Italy)	Interactive laboratory to stimulate an attitude to outreach activities on basic physico-chemical phenomena	PhD course	h	48	3
	28/01/2019- 06/02/2019	Alessandria (Italy)	'Aquality lab' for secondary school students (17 secondary school students of the third year and 1 teacher)	Dissemination	h	24	1.5
	20/02/2019	Turin (Italy)	'Aquality lab' for secondary school students (60 secondary school students of the third year and 1 teacher)	Dissemination	h	8	0.5
	4-5/03/2019	Palaiseau (France)	3rd AQUALity symposium meeting	Symposium	h	16	0.4
	06/03/2019	Palaiseau (France)	International Winter School on Mass Spectrometry	Winter School	h	48	3
	7-8/03/2019	Palaiseau (France)	Prioritization of emerging contaminants in Urban Wastewater	Workshop	h	8	1
	15-16/03/2019	Turin (Italy)	Patenting and Knowledge Transfer	Workshop	h	8	1
	15-16/03/2019	Turin (Italy)	Lean thinking	Workshop	h	8	1
	16-17/05/2019	Turin (Italy)	NIS Colloquium	Colloquium	No.	32	2
	20-21/05/2019	Tartu (Estonia)	Eurachem Workshop 2019	Inter. Workshop	h	16	0.6
3-7/06/2019	Alcoy (Spain)	III Summer School of the European PhD School on Advanced Oxidation Processes	Summer School	h	48	3	

	26-30/06/2019	Portoroz (Slovenia)	6th European Conference on Environmental Applications of Advanced Oxidation Processes (EAAOP-6)	International conference	h	40	1.5
	2-3/09/2019	Trabzon (Turkey)	4th AQUAlity symposium meeting	Symposium	h	16	0.4
	4-6/09/2019	Trabzon (Turkey)	Inter. Conference on Chemical Energy and Semiconductor Photochemistry (Cescop 2019)	Inter. conference	h	24	0.9
	22-26/09/2019	Bari (Italy)	XXVIII Congress of the Analytical Chemistry Division of the Italian Chemical Society	Conference	h	16	0.4
	27/09/2019	Alessandria (Italy)	Notte dei ricercatori 2019 - Dissemination of research work to the public.	Dissemination	h	16	1
Annual Total							24.2
2019/ 20	06/02/2020	Eurofins (Denmark)	HPLC Troubleshooting organized by Phenomenex	Workshop	h	4	0.25
	15-17/02/2020	Alessandria (Italy)	Safety in Chemical and Biological Laboratories for Workers	Training course	h	8	0.5
	29/04/2020	Webinar	"Oh no! Not another boring webinar on column lifetime?"	Webinar	No	1	0.1
	06/04/2020	UPO (Italy), Online	5th AQUAlity symposium meeting	Symposium	h	8	0.2
	21/05/2020	Sciex University (Online)	Method Development: Mobile phase	Webinar	No	1	0.1
	22/05/2020		Front end cleaning of Sciex Triple Quadrupole and QTRAP systems	Webinar	No	1	0.1
	26/05/2020		Intro. to LC-MS/MS Operation Series for SCIEX X-Series QTOF Systems	Webinar	No	1	0.1
	26/05/2020		Non-target screening workflow using Sciex X500R QTOF system	Webinar	No	1	0.1
	27/05/2020		High-Resolution MRM HR Workflow Using SCIEX X500R QTOF System	Webinar	No	1	0.1
	20-24/06/2020	SMAT, Turin (Italy)	Sciex X500R QTOF System	Training course	h	8	0.5
	01-12/06/2020	Houston (Texas), Online	68th ASMS Conference (ASMS 2020 Reboot)	Inter. conference	h	40	1.5
	15-16/06/2020		LC-MS: Advanced Techniques and Applications	Training course	h	16	1
	17-18/06/2020		Practical LC-MS Troubleshooting	Training course	h	16	1

	22/09/2020	UPO (Italy), Online	6th AQUAlity symposium meeting	Symposium	h	8	0.2
	23-24/09/2020	UPO (Italy), Online	Introduction to Basic Statistical Tools and Data Analysis in Research	Summer School	h	32	2
Annual Total							7.8
2020/ 21	December 9, 2020	UPO (Italy), Online	Towards Horizon Europe (Agency for the Promotion of European Research in Italy (APRE) and UPO	Workshop	h	3	0.2
	January 18, 2021		EU versus Italian Water Management (organized by SMAT, Turin (Italy))	Seminars	No	7	0.7
	January 27, 2021		Preparation and characterization of photocatalysts for environmental applications (IPS-AOP webinar organised by UPV-CSIC, Universitat Politècnica de Valencia (Spain))	Training course	No	1	0.1
	13 April 2021		Online QSAR Modelling Hackathon by Easy Access to Jaqpot: Deploy your model as a web service in a few minutes (organized by University of Birmingham, UK))	Training course	h	4	0.25
	01-02/03/2020		7th AQUAlity symposium meeting	Symposium	h	16	0.4
	03/2021- 06/2021		Statistica con R	University course	h	32	2
	06-07/07/2021		7th AQUAlity symposium meeting	Symposium	h	16	0.4
	13-24/09/2021		XXXII Congresso Nazionale Della Società Chimica Italiana (SCI2021)	Conference	h	16	0.4
Annual Total							4.4

The
End